AD
A090 980

MICROCOPY RESOLUTION TEST CHART
NATIONAL BUREAU OF STANDARDS 1963-A

PHOTOGRAPH THIS SHEET

LEVEL

INVENTORY

FTD-ID(RS)T-1163-79, Part 1 of 2

DOCUMENT IDENTIFICATION

DISTRIBUTION STATEMENT

ACCESSION FOR	
NTIS GRA&I	☒
DTIC TAB	☐
UNANNOUNCED	☐
JUSTIFICATION	

BY

DISTRIBUTION /
AVAILABILITY CODES

DIST	AVAIL AND/OR SPECIAL
A	

DISTRIBUTION STAMP

AD A090980

DTIC ACCESSION NUMBER

DTIC
ELECTE
OCT 3 1 1980

D

D

DATE ACCESSIONED

DATE RECEIVED IN DTIC

PHOTOGRAPH THIS SHEET AND RETURN TO DTIC-DDA-2

DTIC FORM 70A
OCT 79

DOCUMENT PROCESSING SHEET

AD A090980

FOREIGN TECHNOLOGY DIVISION

DE-ICING SYSTEMS OF FLIGHT VEHICLES. BASES OF
DESIGN METHODS FOR TESTING

by

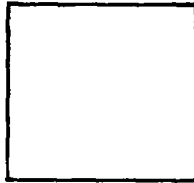R.Kh. Tenishev, B.A. Stroganov, et al

80 6 25 069

UNEDITED MACHINE TRANSLATION

FTD-ID(RS)T-1163-79   7 September 1979

MICROFICHE NR: *FTD - 79 - C -001215*

DE-ICING SYSTEMS OF FLIGHT VEHICLES. BASES OF
DESIGN METHODS FOR TESTING

By: R.Kh. Tenishev, B.A. Stroganov, et al

English pages: 681

Source: Protivoobledenitel'nyye Sistemy
Letatel'nykh Apparatov. Osnovy
Proyektirovaniya i Metody Ispytaniy,
Izd-vo "Mashinostroyeniye", Moscow,
1967, pp. 1-320

Country of origin: USSR
This document is a machine translation
Requester: AEDC
Approved for public release; distribution unlimited.

Table of Contents

U. S. BOARD ON GEOGRAPHIC NAMES TRANSLITERATION SYSTEM

Block	Italic	Transliteration	Block	Italic	Transliteration
А а	*А а*	A, a	Р р	*Р р*	R, r
Б б	*Б б*	B, b	С с	*С с*	S, s
В в	*В в*	V, v	Т т	*Т т*	T, t
Г г	*Г г*	G, g	У у	*У у*	U, u
Д д	*Д д*	D, d	Ф ф	*Ф ф*	F, f
Е е	*Е е*	Ye, ye; E, e*	Х х	*Х х*	Kh, kh
Ж ж	*Ж ж*	Zh, zh	Ц ц	*Ц ц*	Ts, ts
З з	*З з*	Z, z	Ч ч	*Ч ч*	Ch, ch
И и	*И и*	I, i	Ш ш	*Ш ш*	Sh, sh
Й й	*Й й*	Y, y	Щ щ	*Щ щ*	Shch, shch
К к	*К к*	K, k	Ъ ъ	*Ъ ъ*	"
Л л	*Л л*	L, l	Ы ы	*Ы ы*	Y, y
М м	*М м*	M, m	Ь ь	*Ь ь*	'
Н н	*Н н*	N, n	Э э	*Э э*	E, e
О о	*О о*	O, o	Ю ю	*Ю ю*	Yu, yu
П п	*П п*	P, p	Я я	*Я я*	Ya, ya

*ye initially, after vowels, and after ъ, ь; e elsewhere.
When written as ё in Russian, transliterate as yё or ё.

RUSSIAN AND ENGLISH TRIGONOMETRIC FUNCTIONS

Russian	English	Russian	English	Russian	English
sin	sin	sh	sinh	arc sh	$\sinh^{-1}$
cos	cos	ch	cosh	arc ch	$\cosh^{-1}$
tg	tan	th	tanh	arc th	$\tanh^{-1}$
ctg	cot	cth	coth	arc cth	$\coth^{-1}$
sec	sec	sch	sech	arc sch	sech^{-1}
cosec	csc	csch	csch	arc csch	csch^{-1}

Russian	English
rot	curl
lg	log

DE-ICING SYSTEMS OF FLIGHT VEHICLES.

BASES OF DESIGN METHODS FOR TESTING.

R. Kh. Tenishev, B. A. Stroganov, V. S. Savin, V. K. Kordinov, A. I.
Teslenko, V. N. Leont'yev.

Edited by Cand. of the tech. sciences R. Kh. Tenishev.

Page 2.

In the book are presented theoretical bases and practical
methods for calculation and testing of the de-icing systems (POS) of
aircraft and helicopters.

On the basis of the generalization of the results of
experimental investigations are shown the meteorological conditions,
under which is possible the aircraft icing and power plant and are
prescribed/assigned the conditions, which can be accepted as
calculated for design of POS.

Is shown the adverse effect of different forms and forms of
icing on stability and aircraft handling and operation of engine. Are
given the approximation methods of sizing of the icing up zones.

Are briefly examined contemporary mechanical, physicochemical
and thermal deicers and are proposed criteria according to their
evaluation during design of POS. Primary attention is given to the
thermoelectric and air-heat systems, for which are given the detailed
procedures of thermal designs.

Are described methods and the tests technique of POS under the

actual and artificial conditions or icing and are noted the special
features/peculiarities of tests with the imitators of icing.

The book is intended for the engineers of the aircraft industry,
instructors and students of aviation VTUZ [higher technical
educational institution].

Page 3.

Preface.

For contemporary aviation transport the task of reducing to the
minimum of the effect of meteorological conditions on the regularity
of flights is extremely urgent. In its solution one of the
fundamental places occupies the protection of aircraft and
helicopters from icing.

On this question there is a sufficiently large number of foreign
and Soviet works, but some of them became obsolete, and others either
were dedicated to separate problems or represent only the
descriptions of the constructions/designs of de-icing systems. O. K.
Trunov's recently published book [58] is the most complete work, in
which are generalized many materials on existing means of defense

from icing; however, in it are insufficiently represented the practical methods for calculation and testing of de-icing systems.

At present most effective are thermal methods of the protection of flight vehicles from icing. They require the expenditure of the very considerable power whose selection of engines in many instances noticeably affects the flight characteristics of flight vehicle. Therefore the creation of sufficiently effective and at the same time economical protective systems in many respects depends on how are correctly selected their design and thermal parameters. Specifically, to these questions - to the calculation of thermal deicers, to the criteria of the selection of their optimum parameters and to the methods for testing de-icing systems - is given primary attention in this book.

The authors express deep gratitude to N. G. Shchitayev, who wrote Section 2 of chapter II, O. B. Buslayev for the participation in writing Section 1 of chapter VIII, and also L. L. Kerber, V. A. Krupenikova, A. F. Polomeyev and T. P. Meshcheryakova for valuable observations about the manuscript and V. V. Yegorova, L. P. Pestova, L. F. Vinogradova and other colleagues for large by aid for the creation of the book.

The authors express their gratitude to Cand. of tech. sciences,

docent A. S. Zuyev whose recommendations regarding the number of questions of calculation and investigations of protective systems of flight vehicles from icing are used in the bock.

Page 4.

PRINCIPAL NOTATIONS AND UNITS OF MEASUREMENT. (remaining designations are given in text).

Mechanical values.

b - size/dimension of chord m;

C - profile thickness m;

D, d - diameter m;

H - flight altitude m;

R, r - radius m;

S - size/dimension on the enclosure of profile/airfoil m;

x - projection of size/dimension on chord direction m;

δ - thickness of the layer m;

F - area in the m²;

a - speed of sound in m/s.

I_n —- speed of the growth of ice in m/s;

V - true airspeed in m/s;

g - acceleration of gravity in m/s²;

w - water content of clouds (mass of drop-forming water into 1 m³ of air) in kg/m³;

ρ - density in kg/m³;

G - mass flow rate per the unit of area in kg/s•m²;

p - specific pressure in N/m²;

Δp - drop/jump in the specific pressures in N/m²;

$p_{4.8}$ — partial pressure (elasticity) of the saturated water vapor in N/m^2;

$e'_{14.1}$ — elasticity of vapor at equilibrium temperature of surface in N/m^2.

v — kinematic modulus of viscosity in m^2/s;

μ - coefficient of dynamic viscosity in $N \cdot s/m^2$;

α - angle of attack into rad;

χ —- sweep angle into rad;

ω - the angular rate of rotation in rad/s;

n - rotational speed in rad/s.

Values of heat- and mass exchange, energies and powers.

T - temperature in deg. K;

t - temperature in deg. S;

$t_{in}^{'}$ — equilibrium temperature of moist surface in deg. K;

ΔT, Δt - the temperature differential in deg.;

Q - heat flux, in W/m;

q - heat-flux density (density of heating) in W/m^2;

λ - coefficient of thermal conductivity in W/m•deg;

K - coefficient of heat transfer in W/m^2•deg;

α - heat-transfer coefficient in W/m^2•deg;

a - coefficient of thermal diffusivity in m^2/s.

Page 5.

c - coefficient of heat capacity in J/kg•deg;

c_p — coefficient of heat capacity of the air at a constant pressure in J/kg•deg;

R - the gas constant of air in J/kg•deg;

$L_м$ -- latent heat of evaporation in the J/kg;

$L_я$ - specific heat of fusion of ice in the J/kg;

$L_т$ - specific heat of combustion of fuel/propellant in J/kg.

Electrical values.

E - electromotive force in V;

U - voltage (potential difference) in V;

I, i - current in metering circuit in A;

R - resistance in ohm;

$C_{эл}$ -- capacity/capacitance in f;

a_R -- temperature drag coefficient in Ω/deg;

γ - mutual conductance of sensor (instrument) in mv/deg.

Dimensionless quantities.

E - general/common/total (integral) interception coefficient of the drops;

ε — local interception coefficient;

η_m — cyclic recurrence (relation to cycle time to the time of heating one section);

π_κ — pressure ratio in the compressor;

ξ_π —— coefficient of freezing ice;

$\xi_{\text{B}\pi}$ —— coefficient of the humidity of the surface;

r* - temperature recovery factor;

ψ — parameter of the relative size/dimension of the drops;

M - Mach number (relative speed) of the flight;

∮ - relative air humidity (o/o).

Fundamental indices.

1 - boundary layer edge;

ad - adiabatic;

v - water, and also "internal";

v1 - moist, moist surface (p. vl. - surface moist);

v. p - water vapor;

g - to the characteristics of galvanometer (and also millivoltmeter, tail, etc.);

gd - hydraulic;

gf - corrugation;

din - dynamic (to the pressure of flow);

i - evaporation.

iz - insulation/isolation;

k - drop of the water;

kr - critical;

l - ice;

n - heating, heated, and also "external";

o - the undisturbed flow.

p - surface;

pl - film of water on the surface;

pn - complete;

pr - instrument, and also "given";

rasch - calculation, calculated value;

st - statistical (to the pressure of flow);

t.n - "thermal knife".

Page 6.

ul - zone of the catching;

z - zone of the flowing in of water on the surface;

e - heating element;

ekv - equivalent;

ef - effective;

α - to the convective heat exchange;

β - to the values, connected with the intensity of mass transfer (evaporation);

c - to the parameters of th saturated water vapor;

E - to a total quantity cf absorbed by water (on an entire region of

catching);

τ · to a local quantity of the absorbed by water;

Σ - to the total value of quantity.

Superscripts.

* - to equilibrium temperature or stagnation air flow;

$^{-}$ - relative value (dimensionless);

$^{\sim}$ - average/mean value of quantity.

Page 7.

Part one.

CALCULATION AND IDENTIFICATION OF THE PARAMETERS OF DE-ICING SYSTEMS.

Chapter I.

Meteorological and design conditions of icing[1].

FOOTNOTE [1]. Section 1.1-1.3 were written by B. A. Stroganov, Section 1.4 - A. I. Teslenko. ENDFOOTNOTE.

1.1. Fundamental information about clouds.

Aircraft icing connected with the presence in the atmosphere of water in the drop-forming state with negative temperature and in the overwhelming majority of the cases occurs during flights in clouds. In meteorology accept following division of clouds into classes or forms: cirrocumulus and cirrostratus, altocumulus and altostratus, laminar, stratocumulus and nimbostratus, cumulus and cumulonimbus. The fundamental characteristics of the clouds of various forms are represented in Table 1.1. However, in the examination of clouds from

the point of view of icing it is possible to be restricted by their unification into two groups: stratus and cumulus clouds, moreover the first include altostratus, stratus, stratocumulus and nimbostratus clouds, and to the second - altocumulus, cumulus and cumulonimbus.

1.2. Fundamental meteorological parameters of icing.

The fundamental meteorological parameters on which depends the icing, they are:

a) the quantity (mass) of water in the form of drops, which is contained per unit of volume of cloud (water content);

b) the temperature, with which occurs the icing;

c) the size/dimension of the water drops;

d) the extent of cloud on the vertical line and the horizon/level.

Icing is connected with the defined set of parameters indicated above, but from the point of view of recurrence in the flights of it can be considered as the phenomenon random.

Pages 8-9.

Therefore during the design of de-icing system the design conditions
of icing must be defined from that how frequently they are
encountered in practice and as is dangerous their effect on flight
aircraft characteristics. Are known cases [77] when icing was
encountered at very low (-65--70°C) temperatures or with extremely
high (5-10 g/m³) water content; however, hardly this can serve as
base/root for the selection of such conditions for initial ones
during the calculation of de-icing systems, if are encountered they
very rarely. The selection of design conditions must be produced by
processing sufficiently vast weather data by the methods of
mathematical statistics. From this point of view we analyze the
values of the temperature, water content and size/dimension of drops
with icing in flight.

Temperature of clouds with icing.

As already mentioned above, icing obuslovlivaets4 on the
presence at minus temperatures of the supercooled drops of water. The
ability of water to remain in the liquid state, without being
crystallized, depends on a whole series of the factors, including
such, which do not yield to sufficiently precise evaluation as, for
example, the contamination of water by salts or the presence of the

mechanical crystallization nuclei.

But numerous experiments [3], [4], [40], [49] show that at first at relatively small minus temperatures (-10--15° C) the drops stable are retained in the liquid state and do not freeze.

Table 1.1.

Brief Cloud Characteristics.

	(1) Форма облаков	*(2)* Высота нижней границы, км	*(3)* Толщина	*(4)* Протяженность по горизонту	*(5)* Средняя водность г/м²
(11) Верхний ярус	Перистые *(12)* Перисто-кучевые Перисто-слоистые	7÷10 6÷8 6÷8	От сотен метров до нескольких (5÷7) километров *(13)*	200÷600 км по нормали к фронту и 1000 км и более вдоль фронта *(14)*	—
(7) Средний ярус	*(8)* Высоко-кучевые Высоко-слоистые *(9)*	2÷6 3÷5	Несколько сотен метов От 1 до 2 км *(20)*	*(31)* — 500÷900 км по нормали к фронту и 1000 км и более вдоль фронта	0.08 0.17
(26) Нижний ярус	*(27)* Слоисто-кучевые *(28)* Слоистые Слоисто-дожде-вые *(29)*	0.6÷1.5 0.1÷0.7 0.1÷1	0.2÷0.8 км *(30)* 0.2÷0.8 км *(30)* До нескольких километров *(31)*	200÷400 км по нормали к фронту и 1000 км и более вдоль фронта *(32)*	0.19 0.18 —
(37) Вертикального развития	*(38)* Кучевые Кучево-дожде-вые *(39)*	0.8÷1.5 0.4÷1	От сотен метров до нескольких километров (иногда до тропопаузы) *(40)*	До 20÷30 км (идут вдоль фронта грядами в зоне 30÷100 км от фронта) *(41)*	— 0.36

Table 1.1 (cont.)

(6) Микроструктура	(7) Среднеарифметический радиус капель мк	(8) Вероятность обледенения при отрицательной температуре %	(9) Средняя скорость льдообразования мм/мин	(10) Внешний вид
Кристаллическая (15)	—	—	—	(16) Белые или голубоватые, обычно очень тонкие и прозрачные, имеют вид волнистой или волокнистой пелены
Преимущественно капельная Смешанная (22)	5÷7 (с колебаниями от 3 до 20) (23)	60 / 30	0.4÷0.8 (наибольшая у верхней границы облака) (24)	Белые или серые в виде волн или пелены, как правило, закрывающей все небо (25)
(30)Капельная Преимущественно капельная (32)Смешанная	5÷10 (с колебаниями от 1 до 60); 2÷5 (с колебаниями от 1 до 29); 7÷8 (с колебаниями от 2 до 72) (34)	85 / 85 / 60	до 1÷2 (наибольшая у верхней границы облака); 0,5÷0,6 (наибольшая в нижней части облака) (35)	Серые или темносерые, в виде сплошного иногда волнистого или слоистого покрова, часто закрывающего все небо (36)
(33)Капельная Смешанная (42)	0÷12	50÷65 / 65÷75	1.1÷2 (наибольшая в верхней части); 2÷3 (до 5) (наибольшая в верхней части) (43)	Плотные белые в виде башен или куполов с сероватым или темным основанием (44)

Key: (1). Cloud form. (2). Height/altitude of lower boundary, km.
(3). Thickness. (4). Extent on horizon/level. (5). Average/mean water
content g/m³. (6). Microstructure. (7). Mean arithmetic radius of
drops μ. (8). Probability of icing at minus temperature. (9). Average
speed of ice formation mm/min. (10). Appearance. (11). Upper deck.
(12). Cirrus. Cirrocumulus. Cirrostratus. (13). From hundreds of
meters to several (5-7) kilometers. (14). 200-600 km along the normal
to front and 1000 km and more along front. (15). Crystal. (16). White
or bluish, usually very thin and transparent, take form of undulating
or fibrous film. (17). Average/mean deck. (18). Altocumulus. (19).
Altostratus. (20). Several hundred meters. From 1 to 2 km. (21).
500-900 km along the normal to front and 1000 km and more along
front. (22). Predominantly drop. Mixed. (23). (with
oscillations/vibrations from 3 to 20). (24). (greatest in upper cloud
boundary). (25). White or gray in the form of waves or film, as a
rule, closing entire sky. (26). Lower deck. (27). Stratocumulus.
(28). Laminar. (29). Nimbostratus. (30). km. (31). To several
kilometers. (32). 200-400 km along the normal to front and 1000 km
and more along front. (33). Drop. (34). 5-10 (with
oscillations/vibrations from 1 to 60) 2-5 (with
oscillations/vibrations from 1 to 29) 7-8 (with
oscillations/vibrations from 2 to 72). (35). to 1-2 (greatest in
upper cloud boundary) 0.5-0.6 (greatest in lower part of cloud).
(36). Gray or dark gray, in the form of continuous sometimes fibrous

or laminar deposit, which frequently closes entire sky. (37).
Vertical development. (38). Cumulus. (39). kucevno-rain. (40). From
hundreds of meters to several kilometers (sometimes to tropopause).
(41). To 20-30 km (they go along front by banks in zone 30-100 km
from front). (42). Mixed. (43). 1.4-2 (greatest in upper part) 2-3
(to 5) (greatest in upper part). (44). Dense white in the form of
towers or canopies with greyish or dark base/root.

Page 10.

Then begin to freeze major drops, but crystallization occurs the
majority of drops it nonintensively and remains nonfrozen. So, at
temperatures it is above - 36° C was noted crystallization only by
20c/o of drops with a diameter or 20-50 μ. Upon reaching of the
specific temperature is observed a sharp (spontaneous) increase in
the number of freezing drops and in practice occurs complete
crystallization. The temperature of spontaneous crystallization
depends on the size/dimension of drops, rate of cooling, presence of
admixtures/impurities, etc., and on the investigations of different
authors it has somewhat distinct values. The majority of the data
obtained by them tells about the fact that virtually the limit of the
existence of supercooled water in the drop-forming form is the
temperature of approximately -40° C, although sometimes were obtained
the supercooled drops even at -72° C.

Fig. 1.1. depicts the dependence of the temperature of crystallization $t_{кр}$ on the size/dimension of drops according to the data of the studies, carried out by different authors. In spite of certain disagreement, is distinctly visible the general/common/total tendency of a decrease in crystallization temperature with the decrease of size of drops.
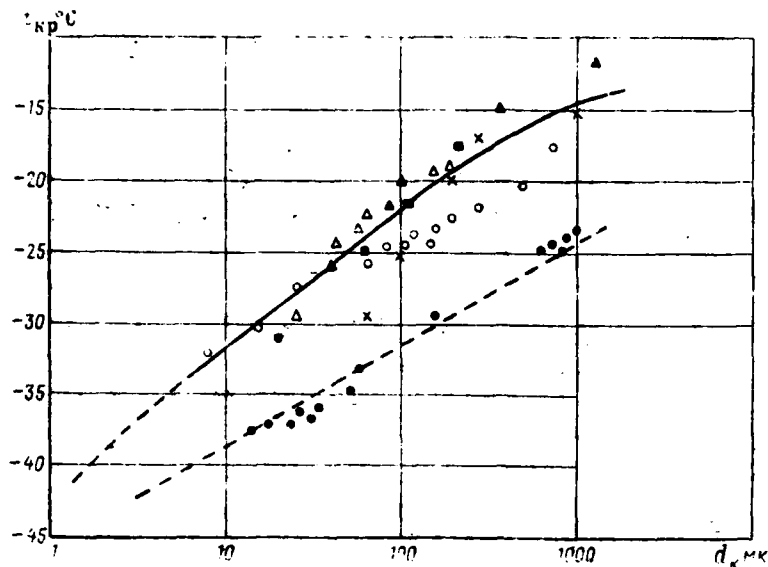
Fig. 1.1. Dependence of tae temperature of crystallization $t_{кр}$ of the drops of water on their sizes/dimensions.

data: × - Haverly;   · - Hosler;   o - Dorsh and Hecker;   ● - Bigg;

▲ - Zak and Malkinoy;   ■ - Lafarg.

Page 11.

However, the maximum temperature or the crystallization of drops is substantially lower than the maximum temperature of icing, since a quantity and sizes/dimensions or nonfrozen drops at sufficiently low temperatures of surrounding air are very low, icing intensity insignificant and it is encountered rarely.

So, on the investigations of Pepler, who analyzed the results of 9000 aircraft soundings in Germany, icing at temperature is below - 8° C were noted only into 22o/o of cases. True, the investigations of Pepler are related to the 1930th one-year; however, data on the tests, carried out much later, confirm this law. Table 1.2 gives the statistical data about the recurrence of temperatures at icing, obtained in the USA, England and USSR in in the period from of 1955-1960 to [58], [70], [108], [124], [132]. They also show that a number of cases of icing at low temperatures sharply is decreased and the overwhelming majority of the cases of icing occurs in the range of temperatures from 0 to -15° C.

Table 1.2. Recurrence of different temperatures at icing.

(1) Температура наружного воздуха °C	(2) Северная Америка		(3) Англия		(4) Европейская территория Союза	
	(5) число случаев	(6) % от общего количества случаев	(9) число случаев	(6) % от общего количества случаев	(5) число случаев	(6) % от общего количества случаев
0÷—5	142	25,4	18	25,0	69	7,8
—6÷—10	215	38,4	40	55,6	426	48,0
—11÷—15	122	21,8	13	18,0	213	21,0
—16÷—20	51	9,1	1	1,4	122	13,8
—21÷—25	21	3,7	—	—	50	5,6
—25÷—30	8	1,4	—	—	4	0,5
—30÷—35	1	0,2	—	—	2	0,2
—35 и ниже (7)	—	—	—	—	1	0,1

Key: (1). Temperature of surrounding air of °C. (2). North America.

(3). England. (4). European territory of union. (5). number of cases.

(6). o/o from total quantity of cases. (7). and it is below.

Page 12.

Water content of clouds with icing.

From water content, or more precisely speaking, from the
combination of water content and sizes/dimensions of drops in essence
depends a quantity of ice, which is formed on lifting surfaces of
flight vehicle with icing.

To the investigation of water content in clouds is devoted a
large number of works [25], [36], [37], [41], [50], [58], [63], [80],

[82], [148], and the data accumulated at present make it possible to sufficiently accurately rate/estimate its numerical value in clouds depending on temperature.

The maximum value of water content in clouds can be obtained on the basis of the theoretical calculation of the condensation of water during the adiabatic process or heat exchange in dependence on height/altitude and temperature. Fig. 1.2, borrowed from [40], depicts changes in the value or the concentration of liquid water during its condensation under varied conditions.

This figure is interesting because it makes it possible to rate/estimate the relationship/ratio of water content for clouds in different geographical areas (tropics, temperate zone and polar climate) according to the temperature of cloud base.

The theoretical values or concentration represented in Fig. 1.2, apparently, even if they are encountered in practice, then only in very powerful/thick clouds. The real values of water content depend on many factors (for example, from the time of the "life" of the clouds), which cannot be taken into consideration during theoretical calculation; therefore for the sufficiently precise evaluation of water content are represented more reliable statistical data on the measurements of water content or clouds in flight.

Such investigations were carried out by a number of organizations both in the USSR (central aerological observatory, State NII [Scientific Research Institute] of civil aviation) and abroad - in the USA (NACA), England (ARC), etc. Most completely these investigations are reflected in works [37], [56].
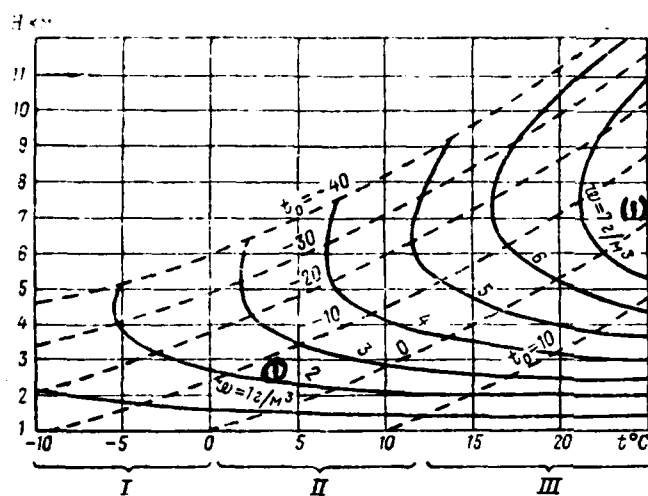
Fig. 1.2. The limiting concentration of liquid water (g/m³) during the adiabatic process of heat exchange depending on height/altitude and temperature.

The climate: I - polar; II - moderated: III - tropical.

Key: (1). g/m³.

Page 13.

The recurrence of the different values of water content in the clouds of laminar forms at minus temperatures in middle latitudes is represented in Table 1.3.

For the clouds of other forms is retained the analogous relationship/ratio between water content and temperature, namely: with a decrease in the temperature of cloud decreases the water content and is decreased the probability of the rendezvous of this water content with icing. However, the absolute values of water content at one and the same temperatures of air in the clouds of various forms will be substantially distinct. Thus, for instance, mathematical expectation of the value of water content, designed according to the data of NACA [82], composes in cumulus clouds 0.4 g/m^3, and into laminar ones only 0.23 g/m^3.

A change in the water content in height/altitude in different types clouds is not equal. In the clouds of laminar forms the water content grows/rises with height/altitude, beginning from lower cloud base, it reaches maximum in upper third and sharply it falls about its upper boundary. For frontal clouds as a result of the precipitation of water the water content in their upper parts is decreased, and in lower ones it grows/rises; therefore the maximum of water content is equally probable in an entire thickness of cloud.

Table 1.3. Recurrence of the different values of water content in the clouds of laminar forms at minus temperatures in middle latitudes.

(1) Температура, °C / (2) Водность, г/м³	−0,1÷−5,0	−5,1÷ −10,0	−10,1÷ −15,0	−15,1÷ −20,0	−20,1÷ −25,0
	(3) Повторяемость в %				
0,05÷0,15	17,88	19,08	11,26	3,95	1,21
0,16÷0,25	11,97	7,71	3,75	0,88	0,18
0,26÷0,35	6,13	3,77	1,63	0,32	0,11
0,36÷0,45	3,15	1,28	0,44	0,08	0,03
0,46÷0,55	1,49	0,59	0,15	0,04	—
0,56÷0,65	1,07	0,28	0,12	—	—
0,66÷0,75	0,26	0,11	0,05	—	—
0,76÷0,85	0,53	0,03	—	—	—
0,86÷0,95	0,19	0,01	0,01	0,01	—
0,96÷1,05	0,08	0,04	—	—	—
1,06÷1,15	0,06	—	—	0,01	—
1,16÷1,55	0,06	—	—		—
(4) Число случаев	3385 (5) или 42,87%	2600 (5) или 32,9%	1375 (5) или 17,41%	418 (5) или 5,29%	121 (5) или 1,53%

(6) Всего число случаев
(100%) 7899

Key: (1). Temperatures. (2). Water content, g/m³. (3). Recurrence in o/o. (4). Number of cases. (5). or. (6). Entire number of cases.

Page 14.

In cumulus clouds the water content grows/rises from lower boundary to the middle of cloud, and then is depressed to upper boundary and, thus, the maximum value of water content is reached in the center section of the cloud.

Should be noted close agreement of the results of the
measurements of water content in moderate band of the Soviet Union,
USA and Canada [4], [37]. So, in the clouds of laminar forms at minus
temperatures the maximum of recurrence falls at the value of water
content in the USSR and Canada to 0.1 g/m^3, tc the USA to 0.19 g/m^3.
In this case the maximum of water content is considerably above
(order 1.5-2 g/m^3), but according to latter/last data in cumulus
congestus clouds was noted the water content of more than 40 g/m^3.

The majority of measurements indicated above of water content
was made with the aid of ice-depositing cylinders which average the
measured water content on the distance of 5-10 km. Therefore one
should to assume that these data are related in essence to this
extent of the zone of icing. The investigations of a change in the
water content in the horizontal extent of cloud in sufficient space
it was not produced; therefore information on this question tears
tentative character. So, Fig. 1.3 shows a change of the average/mean
water content in dependence on the extent of zone L of icing,
borrowed from [37] which is constructed on the basis of the
distribution of water content in frontal clouds. In Fig. 1.3 points
additionally plotted/applied Lewis's data on the investigation of
icing above North America.

In meteorology during processing of the results of soundings of

the atmosphere frequently the measurments of water content
divide/mark off over temperature ranges (0-5° C; -5--10° C, etc.) and
is examined the recurrence or water content independently in each
range. This processing although does not give the
general/common/total evaluation of the recurrence of water content
and temperature in clouds, it is very convenient for the analytical
expression of the dependence of water content on temperature and
recurrence of water content at this temperature. In analogy with the
concept of conditional probability accepted in mathematics which
determines the probability of event A (in our case the specific water
content) when the event B (in our case the specific temperature)
already began, this recurrence should be called conditional
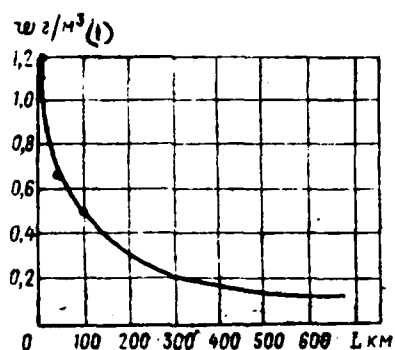recurrence, or recurrence of water content.

Fig. 1.3. The dependence of average/mean water content on the extent
of the zone of the icing (points plotted/applied Lewis's data).

Key: (1). g/m^3.

Page 15.

Some authors [37], [58], [82] use the quantile of the recurrence
of the specific water content, under which is understood not only a
number of cases, in which this water content was observed at this
temperature, but also all cases, in which the water content was less
than the given. So, 90o/o quantile mean that the water content into
90o/o of cases at this temperature was less or equal to the given,
but in 10o/o of cases it was more than it.

On the basis of the analysis of statistical data on water
content in the clouds of I. P. Mazina's laminar forms [36] it

proposed the empirical formula which gives the dependence between the water content, temperature and quantile of the recurrence of water content at the prescribed/assigned temperature:

$$w_n = \frac{w_0(t)}{\lg e}\, [2 - \lg(100 - n)] + w_{min}. \qquad (1.1)$$

where w_n - the value of water content, which corresponds no/o to the quantile of recurrence at this temperature;

$w_0(t)$ - the value of water content, which corresponds to 63o/o of quantile of recurrence, which accept during calculation as the initial;

e - Naperian base (e=2.7183);

w_{min} - minimum value of water content which it can be fixed at present by the instruments used.

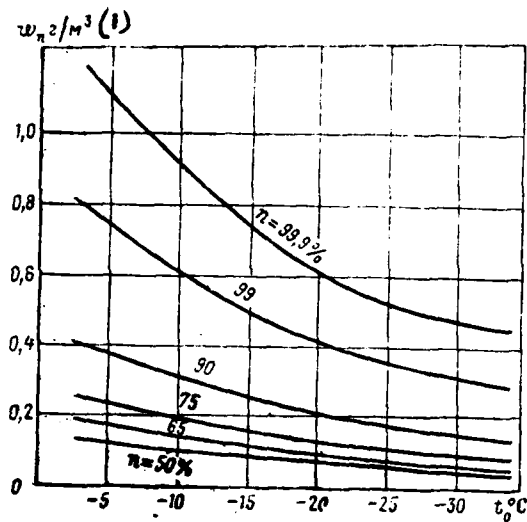Fig. 1.4. Dependence of water content w_n on ambient temperatures t_0 with different quantiles of water content.

Key: (1). g/m^3.

Page 16.

Value $w_0(t)$ is determined from the empirical formula

$$w_0(t) = 52,5 \frac{e^{0.04t_0}}{273 + t_0} \; g/m^3 \qquad (1.2).$$

where t_0 — temperature of air in °C.

Value w_{min} is equal to 0.02-0.04 g/m^3 and during calculations can be omitted.

Dependences w_n calculated by this formula cn t_0 for different

no/o are shown in Fig. 1.4. They virtually coincide with the

dependences for the quantiles of water content, given in work [58].

From the point of view of providing flight safety during the

calculation of de-icing systems to more conveniently use not the

quantiles of the recurrence of water content, but by the recurrence

of the rendezvous of conditions heavier than calculation. It is not

difficult to see that if at this temperature is selected water

content w_n, which corresponds to n o/o of quantile, then the

recurrence of the rendezvous of water content $w > w_n$ comprises

(100-n) o/o.

If we (100-n) o/o designate through $P_w\%$, then, by

throwing/rejecting w_{min} and by substituting lg e=0.434, we will obtain

the following calculation formula:

$$w_n = 2,3 w_0 (t) [2 - \lg P_w],\qquad (1.3)$$

in which P_w - a recurrence of rendezvous at this temperature t^o C of

water content, which exceeds water content w_n.

Size/dimension of drops with icing.

Cloud is polydispersa aerosol, in which are contained the drops

of different sizes/dimensions from several microns to several ten,

and with rain - even hundreds of microns. The distribution of drops
in cloud according to sizes/dimensions depends on many reasons
(duration of the "life" of cloud, the temperature of surrounding air,
the character of the formation/education of cloud and its type, etc.)
[3], [37], [40], [49], [66]. In Fig. 1.5, borrowed from [107], are
shown comparative relative sizes/dimensions of different atmospheric
drops. in the different authors it is possible to find the various
forms of the law of the distribution of cloud drops, obtained
empirically or derived with the specific assumptions.

Page 17.

Thus, for instance, the law of Khirgian - Mazin takes the form

$$n(x) = ax^2 \exp(-bx), \qquad (1.4)$$

and Palmer's law

$$n(x) = a \exp(-bx) \qquad (1.5)$$

and both are special cases of the distribution, obtained by L. M.
Levin [32] on the base of Kolmogorov theorem about the random process
of the fragmentation:

$$n(x) = \frac{1}{\gamma \sqrt{2\pi x}} \cdot \exp\left[-\frac{\left(\ln \frac{x}{x_0}\right)^2}{2\delta^2}\right]. \qquad (1.6)$$

In these formulas by x is understood diameter of drop, a in
question, b, γ - empirical coefficients.

In addition to this, is a series/row of dependences (Schumann, Best, Langmuir, etc.), the drops linking distribution with water content or time whose examination does not enter into our task.

However, it is necessary to note that for the characteristic of the sizes/dimensions of drops in clouds they usually use the values of "average/mean" radii or diameters which frequently have different value, depending on that, from what point of view is rated/estimated the spectrum of drops. So is distinguished:

- the mean arithmetic radius, equal to the sum of radii of all drops, divided into their total number;

- mean modal radius, which corresponds to the most frequently encountered radius of the drops;

- semieffective, i.e. giving maximum contribution to the water content;

- mean median, i.e. radius with which one half an entire water content falls to more major drops, and the other - to small/finer.
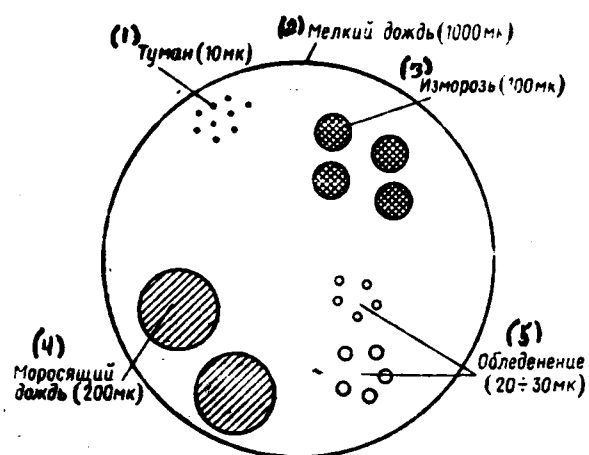
Fig. 1.5. Comparative relative sizes/dimensions of different atmospheric drops.

Key: (1). Fog (10 μ). (2). Small/fine rain (1000 μ). (3). Hoarfrost (100 μ). (4). Drizzling rain (200 μ). (5). Icing (20-30 μ).

Page 18.

For the characteristic of clouds from the point of view of icing
greatest interest are of two latter/last values of mean radius, since
they are directly connected with water content of clouds. In their
absolute values they are close to each other, and for the symmetrical
spectra their values coincide, but at the same time they are
substantially different from other mean radii. So, for a law
Khrgian-Mazin the mean-median radius, for example, is obtained 1.83
times of more than mean aritnmetic. Therefore during the analysis of
the meteorological conditions of icing, examined/considered by
different authors, should be focused attention on what concept of
mean radius it is accepted for that being determining.

On the study of the sizes/dimensions of drops, just as water
content in the clouds of various forms, is a large number of works:
therefore we will be restricted to indication that in the opinion of
authors' majority the semieffective diameters of drops in stratus are
within the limits of 20-25 μ, and in cumulus clouds 30-40 μ.

Water content of ice clouds and fog.

Usually in ice clouds icing does not occur, but under specific conditions (on the heated surface) can occur sufficiently intense icing. So, a whole series of shutdowns of engines "Proteus" on aircraft "Britain" [76] and [129], as it seemed, was caused by the accumulation of the crystals of ice in the air channel of engines.

In connection with the fact that the crystalline ice in the atmosphere is obtained as a result of the gradual crystallization of the drops of water with a temperature decrease, the general/common/total water content (drop and crystal) of clouds even at low temperatures is very large [83], [120] and Table 1.4.

Table 1.4. Maximum general/common/total water content of clouds.

(1) Диапазон темпе-ратур °C	(2) Диапазон высот м	(3) Водность г/м³	(4) Протяженность км
0 ÷ —20	3000÷9000	8,0 5,0 2,0 1,0	1 5 80 (5) 150 и более
—20+ —40	5000+ 12 000	5,0 2,0 1,0 0,5	5 15 80 (5) 150 и более

Key: (1). Temperature range. (2). Altitude range. (3). Water content g/m³. (4). Extent. (5). and more.

Page 19.

With icing in fog we encounter in essence with the operation of engines on the earth/ground.

The value of water content in fog for the different values of a mean arithmetic radius of drops r_k is given in Table 1.5, borrowed from work [63].

1.3. The design conditions or icing[1].

FOOTNOTE [1]. Conditions, assigned for the calculation of the parameters of POS. ENDFOOTNOTE.

Above were separately examined the recurrence of icing and the
recurrence of the value of water content at different temperatures of
air which in the first approximation, subsequently let us accept for
the probability of the rendezvous of icing and value of water content
at these temperatures. Let us designate the probability of the
rendezvous of icing at temperature t through P_t and the probability
of rendezvous at this same temperature of the value of water content,
greater than certain computed value w_p, through P_w. Then the
probability of the joint rendezvous of the conditions of icing at
temperature t ace by water content $w > w_p$ is equal to the product of
the probabilities of the events indicated:

$$P_0 = P_t \cdot P_w. \qquad (1.7)$$

Utilizing the data examined above (see Table 1.2 and 1.3)
through the recurrence of icing and water content, we find value P_0
at different temperatures, then according to the formula, analogous
(1.3), we determine the value of water content w_p. The results of
calculations, represented in the form of function w_p from the
temperature of air for different P_0, are given in Fig. 1.6.

This form of the assignment of the calculated values of water
content is most substantiated, since it, in the first place,
sufficiently clearly shows, with what probability should be expected

the rendezvous of the conditions or icing more heavily in the sense
of larger water content than those, to which is designed protective
system, and, in the second place, is assumed this probability of
identical in entire temperature range of icing, which is important
from the point of view of providing flight safety.

Table 1.5. Water content of fog.

(1) Вид тумана	(2) Горизонталь-ная видимость L м	(3) Радиус капли $r_к$ в мк		
		$r_к = 3$	$r_к = 5$	$r_к = 9$
		(4) Водность в г/м³		
Густой туман (5)	50	0,39	0,65	1,05
Слабый туман (6)	1000	0,020	0,033	0,052
Дымка (7)	2000	0,010	0,016	0,026

Key: (1). Form of fog. (2). Horizontal visibility. (3). Radius of drop $r_к$ in μ. (4). Water content in g/m³. (5). Dense fog. (6). Haze. (7). Mist.

Page 20.

To avoid misunderstanding should be again focused attention on the fact that probability P_0 of the joint rendezvous of water content and temperature is related to the recurrence of the specific meteo-climatic parameters at the presence of icing. If it is necessary to indicate the probability of the rendezvous of these parameters generally to one flight, that for this it is necessary to still consider the probability of rendezvous in flight of clouds and the probability of icing in them. The probability of the rendezvous of clouds is determined in essence by meteo-climatic characteristics of the geographical area, above which is fulfilled flight [48]. For the territory of the Soviet Union the recurrence of clouds at minus

temperatures is examined, for example, in work [16].

As far as computed value is concerned of probability P_0, then it can be selected by designer according to agreement with client or be standardized in state order. The calculated values of water content (unbroken curve in Fig. 1.6) accepted in the Soviet Union in the range of temperatures to $-25°C$ correspond to probability $P_0 \approx 0.5 o/o$.
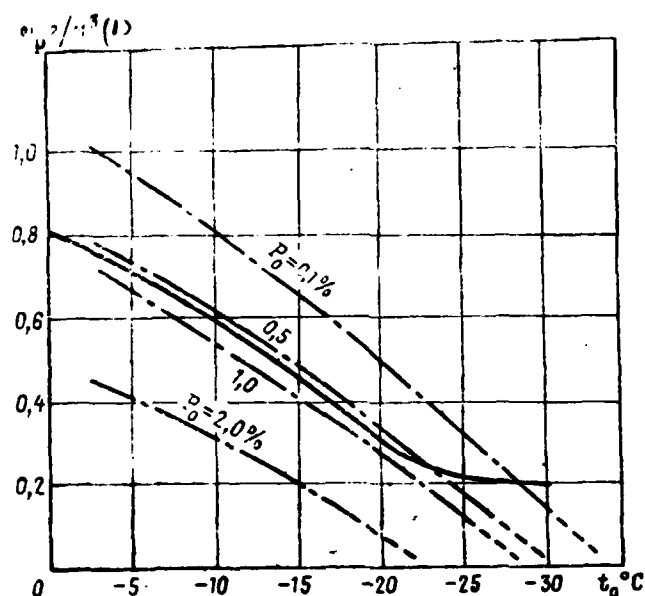
Fig. 1.6. Dependence of the value of water content on ambient temperature at different values of probability P_0.

Key: (1). g/m^3.

Page 21.

In the range of temperatures of $-25-30°C$ data in the values of water content are statistically confirmed insufficiently; therefore for increasing the flight safety the values of the probability of the rendezvous of the off-design conditions of icing P_0 are accepted somewhat smaller (consequently, the calculated values of water

content ω_p - large).

The calculated diameters of drops can be accepted: 20 μ - for prolonged icing and 30 μ - for short-term.

Tables 4 and 5 and in fig. 6-9 applications/appendices give the English and American design conditions of icing [74], [86], [120].

1.4. Air humidity, condition for condensation and sublimating the moisture.

In atmospheric air always is contained certain quantity of water vapor. As is known, a quantity of vapor in air is characterized by its absolute and relative humidity. **Absolute humidity** - quantity (mass) of vapor per 1 m^3 or humid air ($M_{\text{в.п}}$ in kg/m³). Calculations the absolute humidity of air to usually more conveniently express as **partial pressure** $p_{\text{в.п}}$ (elasticity) of vapor:

$$M_{\text{в.п}} = \frac{R}{R_{\text{в.п}}}\frac{p_{\text{в.п}}}{\rho U} = 0.622 \frac{p_{\text{в.п}}}{RT} = \frac{2.17 \cdot 10^{-3} p_{\text{в.п}}}{T}\ \frac{(1)}{\text{кг/м}^3}. \quad (1.8)$$

Key: (1). kg/m³.

Here R and $R_{\text{в.п}}$ - gas constants of air and water vapor; p and $P_{\text{в.п}}$ - partial vapor pressures respectively of air and water T - absolute temperature of air-steam mixture.

At this temperature air can contain the completely specific maximum (saturated) quantity of vapor $M_{\mathfrak{n}}$, having completely specific elasticity e. Relation $M_{\mathrm{B}\,\mathfrak{n}}$ to M_{ℓ} or with respect to elasticity of vapor $p_{\mathfrak{s}.\mathfrak{n}}$ to elasticity e of the saturated steam is relative humidity ϕ:

$$\varphi = \frac{M_{\mathfrak{a}.\mathfrak{n}}}{M_{\ell}} \cdot 100\%, \qquad (1.9)$$

or

$$\varphi = \frac{p_{\mathfrak{a}.\mathfrak{n}}}{\ell} \cdot 100\%. \qquad (1.10)$$

During cooling of air by saturated steam occurs the isolation/liberation of moisture either in liquid form - condensation or settling to any surface with the minus temperature in the form of ice (passing liquid phase) - sublimation. These critical values of temperature are called the point of dew - in the case of condensation and hoar-frost point - in the case of sublimation.

Page 22.

In other words, the point of dew or hoarfrost - this of the temperatures to which it is necessary to cool humid air so that it would become saturated by water vapor. Saturation vapor pressure relative to ice somewhat less than the saturation vapor pressure relative to water (see Table 1 of application/appendix); therefore

saturation must by ice occurs at smaller values of relative humidity
on psychrometer, than for water [56]. Consequently, the cooling air
will achieve saturation before must by ice and it is later with a
larger decrease in the temperature - above supercooled water. At
temperature of 0°C points coincide, in proportion to a temperature
decrease the difference between them grows/rises (see Table 1.6).

The comparison of the point or dew or of hoar-frost point with
the temperature of air makes it possible to judge about the degree of
the proximity of air to saturation by vapor and, consequently, also
about the possibility of icing as a result of condensation or
sublimating the moisture.

Example 1.1. To determine a quantity of that condensing per 1 m^3
of water with a decrease in the temperature to 0°C, if it is known
that at +15°C ϕ=60o/o.

In *T*able 1 of application/appendix through temperature of +15°C
we find saturation pressure $e_{(+15)} = 1720$ **N/m²**, and then according to
formula (1.10) we determine partial vapor pressure (elasticity) of
the water

$$P_{\text{n. n}(+15)} \quad \frac{\varphi \cdot e_{(+15)}}{100} = \frac{60 \cdot 1720}{100} = 1032 \, \overset{(1)}{\text{N/m}^2}.$$

Key: (1). **N/m².**

The dew point for this value of elasticity on Table 1 of application/appendix composes +7.5°C.

Consequently, a quantity of condensing water under given conditions will be

$$M_{e\ (+7.5)} - M_{e\ (0)} = 2.17 \cdot 10^{-3} \left(\frac{1032}{280.5} - \frac{610}{273} \right) = 3.14 \ \binom{1}{g/m^3}.$$

Key: (1). g/m³.

Table 1.6. Temperatures ot points increases also in the hoarfrost.

(1)Точка росы °C	—5	—10	—15	—20	—25	—30	—40	—50
(2)Точка инея °C	—1.4	—8.9	—13.4	—18.0	—22.5	—27.2	—36.5	—46.1

Key: (1). The dew point. (2). Hoar-frost point.

Page 23.

Chapter II.

Icing of the parts of the aircraft[1].

FOOTNOTE [1]. Section 2.2 is written by N. G. Shchitayev, Section 2.3 -
A. I. Teslenko, others - by B. A. Stroganov and by R. Kh. Renishev.
ENDFOOTNOTE.

2.1. Forms and forms of ices formation.

The forms of ices formation are very different and depend on the
effect of many random factors which cannot be evaluated with
sufficient certainty. Strongest effect on the form of ice formation
have the temperature of surrounding air and flight speed. Authors'
majorities isolate two characteristic forms of ice: channel-like (in
cross section horn-shaped) and tapered ice (Fig. 2.1).

Channel-like ice is formed at relatively small temperatures of
surrounding air (usually 0--7°C) and its form is explained by the
fact that at temperatures of surface, close to 0°C, the drops of
water freeze not immediately, but somewhat spread over surface. As a

result on surface appear VA of the ice ones of barrier, which gradually form the horn-shaped built-up edges, which strongly distort profile/airfoil.

Tapered ice is formed at low temperatures of order of $-10--15^\circ$C and it is below. This form of ice is explained by the fact that the temperature of surface is low and the drops of water, which fall to it, freeze instantly. Between the freezing drops remain air cavities; therefore such an ice frequently has dull milk-white color. The sizes/dimensions of tapered ice are usually limited and it occupies small, surface along chord.

In the range of the temperatures of surrounding air of $-7--12^\circ$C is possible the ice formation both of that and other form. In this case the intensity of ice formation remains sufficiently high, and the sizes/dimensions of the generatrix of ice are considerable.
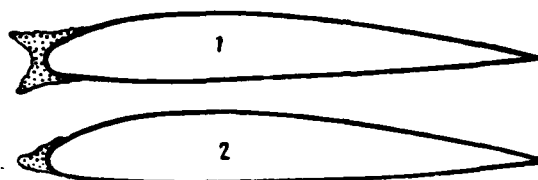
Fig. 2.1. Diagrammatic representations of the forms of ice formation on the aircraft profiles/airfoils: 1 - channel-like (horn-shaped); 2 - tapered.

Page 24.

Ice at these temperatures is formed solid and with great difficulty is removed from surface, but in the case of department/separation from surface it can apply the essential damages to elements/cells of construction/design.

Some authors isolate into the special variety of icing the formation/education of hoarfrost on surface with a sharp reduction/descent in the aircraft from high altitudes. Hoarfrost is formed as a result of sublimating water vapors on cold surface. Usually it rapidly disappears, as soon as the temperature of surface it will be equalized with ambient temperature. From the point of view of a deterioration in aerodynamics of the profile/airfoil of construction/design such an ice or high value does not have, but, being formed on sight glass, it can cause the short-term loss of

visibility for a pilot with all escape/ensuing from this consequences.

The effects of flight speed on icing it is developed in a two-fold manner. On one hand, an increase in the speed raises the intensity of ice formation as a result of an increase in the quantity of air, which encounters to surface per unit time, and increase in the interception coefficient (see Chapter IV). On the other hand, an increase in the speed causes the amplification of aerodynamic heating. As a result the temperature of surface grows also upon reaching of the values, which exceed 0°C, icing becomes impossible. With this phenomenon is connected the fact that frequently at relatively small minus temperatures (5°C it is above) occurs ice formation in the form of protuberances/prominences or barriers on the surface of profile/airfoil after the critical point (temperature at the critical point where the braking complete, is always higher than on lateral surface). At flight speeds is above 700-750 km/h the icing possibly in very rare cases, since the hit probability under the conditions of icing with extremely low temperatures, as follows from the preceding/previous chapter, is low.

2.2. Effect of icing on the aerodynamic characteristics of aircraft.

Great effect on flight characteristics, stability and

controllability exerts the icing of wing and tail assembly of
aircraft. With icing is distorted the form and appear inequalities at
the surface of the nose section of the profile/airfoil the character
of the flow of which substantially affects the lift and wing drag. In
pure/clean (uniced) wing at subsonic speeds at low angles of attack
in the nose section of the profile/airfoil is retained laminar flow
in boundary layer. In this case the position on the profile/airfoil
of the transition point of this flow into turbulent depends on the
smoothness of surface (by evaluated medium altitude of the
protuberances/prominences of roughness), Reynolds number and special
features/peculiarities of the form of the nose section of the
profile/airfoil.

Page 25.

At medium altitude of the protuberances/prominences of roughness
on the order of 5-10 μ in the favorable cases the flow is retained
laminar to numbers Re=$15 \cdot 10^6$-$20 \cdot 10^6$, whereas roughness in 20-30 μ
shifts boundary layer into turbulent state already with numbers
Re=$1 \cdot 10^6$-$1.5 \cdot 10^6$. During turbulent flow the frictional resistance
grows/rises 5-10 times. The distortions of the form of
profile/airfoil and the roughness, called by icing, lead to the
complete disturbance/breakdown of laminar flow and the onset of the
local separations of flow, which substantially increase boundary

layer thickness. As a result considerably grows/rises resistance and somewhat is decreased lift. Most considerably grows/rises resistance with channel-like icing.

The wing profiles of supersonic aircraft have smaller thickness ratio and more pointed leading edge, than the wing profiles of subsonic aircraft.

The climb regimes and gliding/planning of such aircraft lie/rest at velocity band, at which on the surfaces of wing and tail assembly appear local supersonic the zones and shock waves [40], [45]. These profiles/airfoils are especially sensitive to the icing whose effect is developed in an increase in the resistance, the lift convergence and angle of attack, at which begins flow separation.

In an overall drag increment of aircraft with icing the portion of wing and tail assembly comprises to 70-80o/o. In the case of icing (Fig. 2.2) not only grows/rises the resistance of aircraft, but also substantially is decreased the value of the coefficient of maximum lift $c_{y max}$. The latter occurs as a result of the onset of flow separation at smaller than without icing, angles of attack. The especially considerable decrease of critical angle of attack occurs during the deposits of channel-like ice. It is logical that this decrease is determined by icing intensity, by sensitivity of
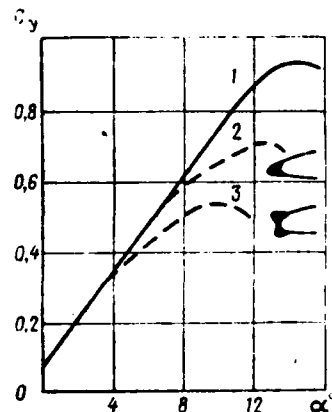
Fig. 2.2. The character of the effect of icing on c_y and on the angle of attack of the beginning of flow separation: 1 - there is no icing; 2 - tapered ice; 3 - channel-like (horn-shaped ice). Page 26.

It is essential to note that in the presence of icing the critical angle of attack and value $c_{y\,max}$ considerably are decreased, but the linear character of curve $c_y(\alpha)$ is disrupted long before achievement $c_{y\,max}$. The latter is explained by the fact that local flow separations on the iced over wing (tail assembly) appear at considerably smaller angle of attack, than $\alpha_{кp}$ pure/clean wing, and they decrease the angle of the slope of curve $c_y(\alpha)$. The onset of local flow separations is usually accompanied by the buffeting of aircraft and entails a change in the curve of the dependence of hinge moments on the elevator angle.

profile/airfoil to the distortions of the form of its nose section,

by form of wing (tail assembly) in **plan/layout**, by its effective

aspect ratio. The dependence of **value** c_y **given in** Fig. 2.2 from angle

of attack makes it possible to **rate/estimate a** change in the lift of

the iced over wing (tail assembly) in comparison with pure/clean.

The decrease of thickness and radius of curvature of nose/leading edge usually increases the sensitivity of profile/airfoil to icing, i.e., is caused flow separation at smaller angle of attack.

With aircraft icing is disrupted the evenness of the flow around its parts, on which was formed ice, descends the thrust of power plant, substantially deteriorate flight characteristics of the aircraft: is decreased the vertical rate of climb, descend ceiling and maximum speed of flight, increase the fuel consumption and required power (thrust) for flight at given speed.
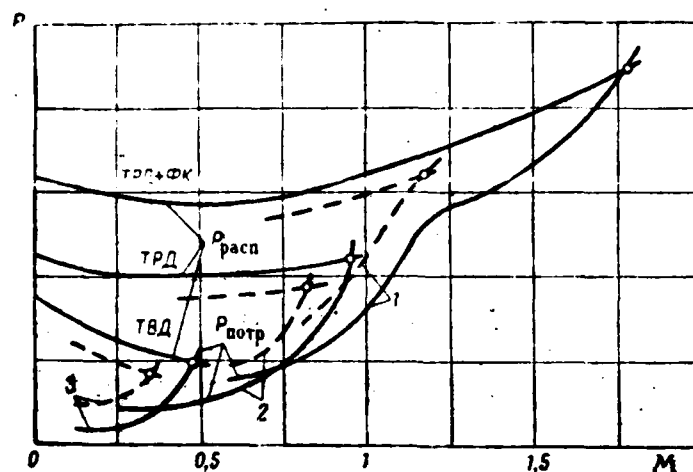
Fig. 2.3. The character of change in Mach number of required for level flight and available thrusts of uniced and iced over (dotted line) aircraft with the turboprop engines (TVD), turbojet (TRD), and TRD, equipped with afterburner (TRD+FK): 1 - supersonic aircraft; 2 - subsonic aircraft with TRD; 3 - aircraft with TVD.

Page 27.

The results of the special tests, carried out on contemporary passenger aircraft, show that even the moderate icing (with switched off deicers) with the thickness of channel-like (horn-shaped) icing on wing and tail assembly on the order of 10-12 mm leads to a noticeable reduction/descent in the instrument flight speed during the stable operation of engine [58].

The variety of the forms of icing and the complexity of obtaining in flight of the necessary information about rate of icing of aircraft on make it possible to sufficiently reliably rate/estimate its effect on aircraft performance during flight tests. This effect qualitatively can be rated/estimated in the examination of the curves of the dependence or required $(P_{потр})$ for level flight and arranged/located $(P_{расп})$ of thrusts on flight speed (Fig. 2.3). Under conditions of icing grows/rises the required thrust and falls the available thrust as a result of the icing of the elements/cells of inlet duct of power plant. As a result reserve thrust $P_{изб}$ significantly is decreased. Comparing $P_{потр}$ and $P_{расп}$, it is possible to note, in particular that the supersonic aircraft, even with the moderate icing, must very considerably lower flight speed. During the explanation of the need for installation on the supersonic aircraft of anti-icing protection should be refined the probability of its icing, on the basis of the heights/altitudes adjustable for it and flight conditions, and considered also the possibility in the pilot of combating icing by an increase in speed or change in the flight trajectory.

During the design of air-heat POS one should consider that they with work select/take a considerable quantity of air from the

compressors of engines, which leads to certain reduction/descent in
the engine thrust, and consequently, to a deterioration in the
aircraft performance. This deterioration must be evaluated by
calculations and it is refined by flight tests.

The decrease of the critical angles of attack of wing and tail
assembly with icing can represent extreme danger at the low speeds of
flight, especially during landing. Here one should recall that a
decrease in the velocity of the gain of altitude, level flight and
gliding/planning is connected with the considerable increase of the
angle of attack of wing. As a result on the iced over aircraft flow
separation on wing can arise unexpectedly for a pilot, namely on such
speeds and g-forces which without icing are considered safe (Fig.
2.4). For providing of safety in this case it is necessary that the
minimum allowable speed would be not less than 1.3 times more than
the speed of disruption/separation in the absence of icing. However,
in this case should be considered the limitation of flight speed with
the let-down flaps from the condition of warning/preventing flow
separation on iced over stabilizer [28].

Page 28.

The angle of deflection (setting) of stabilizer is determined by
the moment/torque of horizontal tail assembly necessary for

longitudinal balance, by the downwash angle, by the position of
stabilizer by height/altitude relative to wing, also, to a
considerable degree by the flap angle of wing. On contemporary
aircraft with the high degree of the high-lift device of wing
horizontal tail assembly at takeoff and landing speeds usually flows
itself at negative angles of attack.

The icing of stabilizer, decreasing the critical angle of attack
with relatively greater flight speed and low g-force, can lead to
flow separation at sufficiently small negative angles of attack (Fig.
2.5, I). Further decrease of the angle of attack of stabilizer with
an increase in the speed or a decrease of g-force conducts to
complete flow separation on its lower surface, what causes "peck" -
the sharp uncontrolled lowering of the nose of aircraft, which pilot
not in state to parry without retraction of flaps, in connection with
which occurs the considerable loss of height/altitude.

Thus, flight with the let-down flaps under conditions of icing
both on excessively low and at excessively large speed can lead to
flow separation in the first case on wing, the secondly - on the
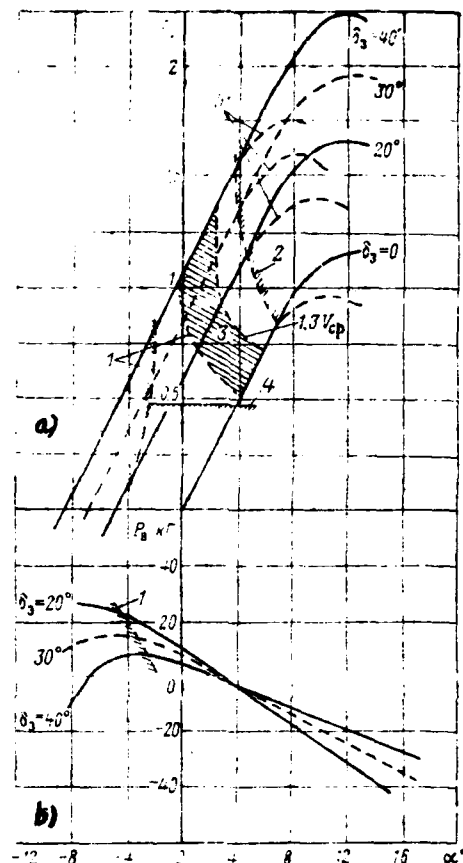lower surface of stabilizer.

Fig. 2.4. the boundary of the beginning of separation of flow and region of the most safe flight conditions on angle of attack during icing at different angles δ_3 of the flap deflection: a) dependence c_y on α; b) the dependence of balancing efforts P_s on α: 1 - possible boundary of the beginning of flow separation for the lower surface of the stabilizer; 2 - possible boundary of the beginning of flow separation on the wing; 3 - region of most safe ones c_y and the angles of attack of the level flight; 4 - value c_y corresponding to

the speed of limitation in flight with the released high-lift device of the wing; 5 - with the icing (position of boundaries of 1 and 2 depends on rate of icing).

Page 29.

The boundaries of the dangerous zones of output to the inadmissible angles of attack under conditions of icing are given on the curves of dependence c_y and effort/force on elevator P_s on angle of attack α (see Fig. 2.4). Usually in the absence of icing these dependences are close to linear ones [45]. Icing causes a considerable incidence/drop in the efforts/forces from elevator with the decrease of g-force (angle of attack) after the onset of local flow separation on the lower surface of stabilizer (in the zone of elevator). An incidence/drop in the efforts/forces with sharp evolutions of aircraft can lead to the creation of low g-force or even cause the throw/excess/overshoot of control to end lower position - with the subsequent sharp "peck" of aircraft. The decrease of the angle of extension of flaps significant improves the character of balancing curves which is explained by decrease in this case of the downwash and angle of flow separation in the zone of axial balancing of control surfaces of height/altitude. Analogous effect exerts the decrease of the power of the turboprop engines, which blow out/blow off wing by the air, rejected by screws/propellers. The

analysis of the effect of the form of the icing of stabilizer on
longitudinal stability is shown (see Fig. 2.6) that here also are
confirmed the general/common/total tendencies - great destabilization
is developed with channel-like icing, somewhat smaller - with the
tapered (still smaller - with the formation of barrier ice on the
boundary of the warmed zone of the nose/leading edge of stabilizer
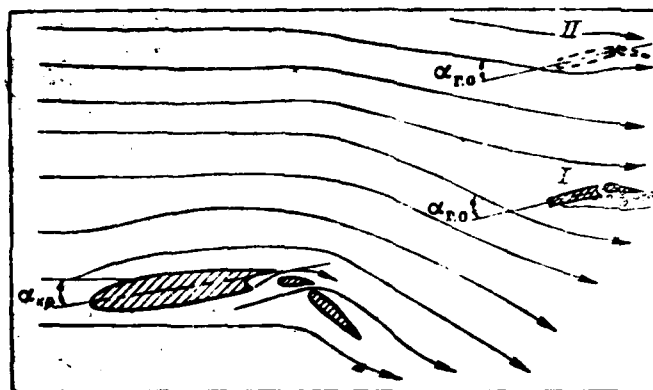with the working deicer).

DOC = 79116302   PAGE

Fig. 2.5. The diagram of the onset of flow separation on stabilizer at the small (negative) angles of attack of the wing: I - stabilizer in the zone of large downwashes with the deflected high-lift device of the wing; II - stabilizer is carried out of the zone of large downwashes.

Page 30.

After the onset of local flow separation on the lower surface of the stabilizer, which calls an incidence/drop in efforts/forces $P_в$, the elevator-effectiveness derivative usually is retained in the sufficiently broad band of low g-forces, which allows with the aid of springs in the control system to improve balancing curves $P_в = f(n_y)$ and to raise flight safety. However, more rational are the measures, directed toward an increase in the negative critical (on disruption/separation) angle of attack of stabilizer, an improvement

in the effectiveness of anti-icing means and an increase in the
reserve of the angle of attack of stabilizer from
disruption/separation. The latter, in particular, can be
achieved/reached by a decrease in the velocity of flight under
conditions of icing with the let-down flaps under the condition of
guaranteeing a sufficient reserve of angle of attack from
disruption/separation on wing. Should be noted the utilized sometimes
structural/design measures, directed toward the decrease of the
danger of disruption/separation at the low angles of the attack of
aircraft with the icing of the stabilizer: an increase in its area
and arm of lift, the use/application of the more carrying
(unsymmetric) profiles/airfoils, the shaping of slots on the
stabilizer before the control, the carrying out of stabilizer from
the zone of intense wing downwash (see Fig. 2, 5, II) and the
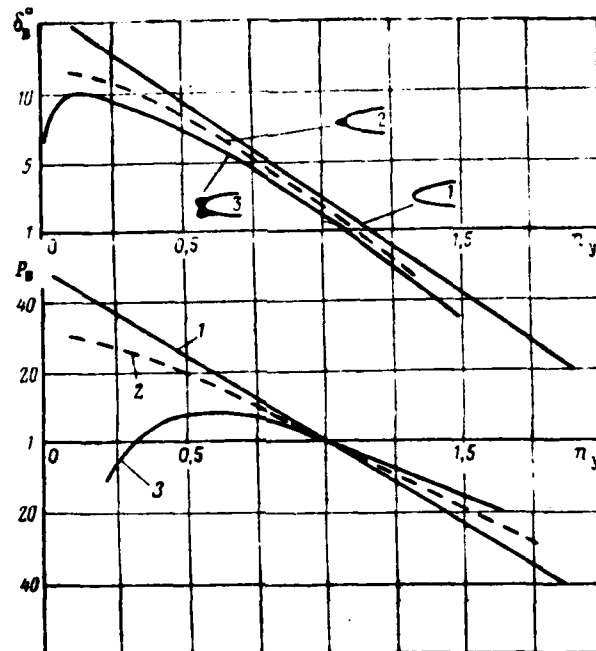decrease of effective aspect ratio of stabilizer.

Fig. 2.6. **Balancing curves of aircraft with flaps lowered to** landing
position: 1 - uniced aircraft; 2 - tapered icing; 3 - channel-like
(horn-shaped) icing.

Page 31.

However, all these measures with high rate of icing can prove to be
insufficient and decisive importance in providing of safety acquires
effective de-icing system.

The important value in providing of safety with icing has the

correct selection of gliding speeds, duration of extension of flaps
and angles of their deviation.

Selective gliding speeds must provide the
approximately/exemplarily identical reserve of angle of attack (see
Fig. 2.4) from disruption/separation both on the wing and on
horizontal tail assembly with the retention/preservation/maintaining
of acceptable controllability both before beginning issue and with
the let-down flaps. The duration of the issue of highly efficient
mechanization/lift-off device must be such that would not arise the
need for sharp action of control surface for the retention of
aircraft on the prescribed/assigned glide path, since a change in the
g-force (decrease or increase) significantly decreases the reserve of
angle of attack from disruption/separation either on wing or by the
lower surface of stabilizer. Under conditions of icing the extension
of flaps is fulfilled gradually, which facilitates pilot
retention/preservation/maintaining during gliding/planning constant
g-forces and flight path angle with consecutive deceleration in such
a way that the flight would be completed in the region of safe angles
of attack (see Fig. 2.4, zone 3). With the presence of ice on tail
assembly and the wing, it are allowed the sizes/dimensions of takeoff
and landing strip, is expedient accomplishing landing at the reduced
flap angles of wing.

The provision of a sufficient speed range of flight and safety of the latter under conditions of icing is by and blown out/blown off by screws/propellers straight wing especially necessary for aircraft with the highly efficient high-lift device of wing. The introduction of boundary layer control systems and the increase connected with them of the downwash angles in the region of stabilizer will cause supplementary difficulties in providing of flight safety with icing on aircraft both with the straight line and by sweptback wings. In this case also can be applied the named above structural/design measures.

The icing of the leading edges of tail assembly and wing, causing decrease of critical angles of attack and local flow separations, deranges rudders and ailerons. Disturbances/breakdowns are developed, in the first place, in decrease sometimes to zero hinge moments/torques with the low deflections of controls as a result of the onset under the effect of the icing of the turbulent boundary layer of considerable thickness.

Page 32.

Flow separation on one of the surfaces of tail assembly, in the region of aerodynamic balancing of control surfaces, causes the decrease of hinge moment with the deflection of control and it can

DOC = 79116302   PAGE 74

lead to the throw/excess/overshoot of control to end position.

Aerodynamic forces and moments/torques of them relative to the
center of gravity, called by the deflection of control (aileron), to
a considerable degree are determined by the redistribution of
pressure on the surfaces or tail assembly or wing. The insignificant
icing of the latter virtually does not cause the redistribution of
pressure with the deflection of control and, consequently, also does
not affect the effectiveness of control, evaluated by an increment in
the aerodynamic moment with the deflection of control of one degree.

With considerable icing and considerable reduction/descent
connected with it in the critical angle of attack of tail assembly or
wing the deflection of control increases camber and it leads to the
onset of disruption/separation or the increase of its intensity,
which decreases the effectiveness of control and can cause the loss
of control of aircraft.

The icing of the leading edges of controls, the freezing of
moisture in the joints or the sections of slats, the slots of the
joints of mobile stabilizer, flaps, flaps, mechanisms of locks can
lead to their wedging in flight and failure. Here it should be noted
that similar type failures as a result of the freezing of moisture
can lead to extremely serious consequences. The incidence/impingement

of moisture in the form of rain, sprays, wet snow to the named
elements/cells with the subsequent freezing can occur at rest,
taxiing of aircraft and in flight.

Therefore the guarantee of a drainage of construction/design,
the possibility of its convenient inspection before flight and
preservation from the incidence/impingement of moisture during
taxiing, on takeoff/run-up and landing run into mechanisms and
systems together with the guarantee of anti-icing means is the
measure, directed toward an increase in the flight safety.

High value has protection from the icing of the receivers of
speed indicators, height/altitude and angle of attack, since their
failure or malfunction as a result of icing can lead to involuntary
conclusion by the pilot of aircraft to dangerous modes/conditions.

2.3. Icing of air intakes and engines.

Efficiency of power plant under conditions of icing is
determined by layout, effectiveness of de-icing systems and by
strictest observance of the commands, which foresee the need for the
start of deicers in advance, with the least threat of icing.

Icing of air intakes.

The icing of air intake, as it was already said, is fraught with the danger of the damage of engine.

Page 33.

According to the achievement of the specific sizes/dimensions ice under the action of the vibrations of construction/design or fluctuations of air flow is thrown off into the air duct of engine, strikes the guiding device, the blades of the inlet compressor stage or other elements of the construction/design of engine it leads to the damage of these elements/cells and, consequently, also to the early replacement of engine.

Ice formation on air intake distorts air flow at the engine inlet. The distortion of the form of entering lip and other inlet components causes disruptions/separations and turbulence of flow, which can lead to surge or even to shutdown of engines [73].

Finally, comparatively it is recently established/installed [58], that the incidence/impingement of the specific quantity of ice into the compressor of some types of gas turbine engines leads to their spontaneous disconnection as a result of flameout in combustion.

chambers.

Icing of input devices of aircraft engines.

Ice hazards are especially subjected gas turbine engines with axial-flow compressors.

The existing aircraft engines with axial-flow compressors have several versions of the layout of the input devices, bases of which are shown in Fig. 2.7. All these elements/cells of inlet duct of the gas turbine engine: fairing, struts of housing or intake adapter, blade of input guide ring, rotor blades of first stage (rotor), rectifying blades of first stage, which appear into the flow of surface, and other inequalities become the seats of deflection of ice.

Ice accumulations on struts are analogous to ice built-up edges on wing or tail assembly, but have relatively larger sizes/dimensions (Fig. 2.8a).
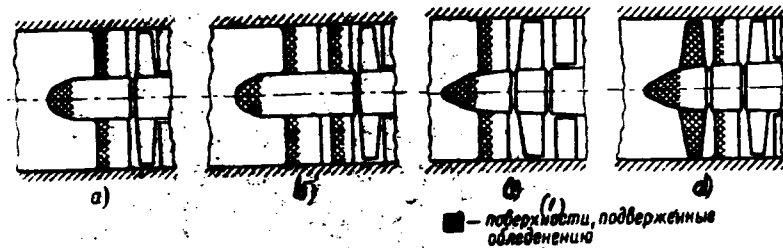
Fig. 2.7. The basic versions of the input devices of the axial-flow compressors of the engines: a) VNA is absent, fairing and struts are fixed; b) VNA, fairing and struts are fixed; c) VNA is power (it replaces struts), fairing is fixed; d) VNA and strut are absent, fairing rotates.

Key: (1). the surfaces, subjected to icing.

Page 34.

Stator blades as a result of relatively low sizes/dimensions ice up more intensely than strut, moreover in certain cases ice can build up on an entire concave surface of the blade (see Fig. 2.8b).

However, the possibility of the icing of the subsequent steps/stages of aligning compressor blades considerably smaller, since already its first step/stage noticeably raises the temperature of air.

Pressure ratio, necessary for the prevention of the icing of the pre-rotation blades of the second step/stage, can be determined from the relation

$$\frac{p_2}{p_1} = \left(\frac{T_2}{T_1}\right)^{\eta_K \frac{k}{k-1}},\qquad(2.1)$$

where p_1, T_1, p_2, T_2 - pressure and temperature of air at the inlet into first and second stages;

η_K- stage efficiency of the compressor;

k - adiabatic index.

For example [56], assuming that T_2 must be order of +3°C, then with t_0=-30°C, M=0.6 and $\eta = 0.82$ is sufficient to have pressure ratio of first stage a total of of approximately 1.18.

The icing of the blades of first stage of compressor rotor can be sufficiently intense, especially in the absence of guiding device. Although the rotating blades to some degree have a self-defense from icing as a result of large centrifugal force, being separated before ice can reach considerable thickness (especially with the lowered/reduced engine revolutions). Furthermore, the spontaneous

disruption/separation of ice from blades occurs usually unevenly and this asymmetric icing of rotor blades leads to the disbalance of rotor and the appearance of vibrations.

The operation of engine with considerable disbalance on rotor can lead to service failure or spin bearings.
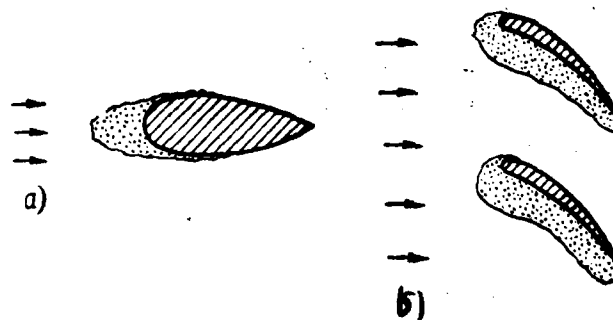
Fig. 2.8. **Icing of the input devices** of the engine: a) the strut; b) blade VNA.

Page 35.

The asymmetric icing of stator blades can lead to the nonuniformity of temperature field at the entry into turbine and in jet nozzle.

Ice accumulation on blades changes profile/airfoil and sharply makes their lift-drag ratios worse. Furthermore, the gap/interval between adjacent blades is decreased, which leads to the considerable decrease of flow area.

Ice accumulation on the leading edges of moving vanes can lead to the fact that the ice built-up edges will interfere the trailing edges of stator blades.

On some aircraft with the low location of engines under wing, especially when air intakes are located behind front/nose wheel, for preventing the incidence/impingement into the engine of foreign objects on the engine inlet are established/installed shielding grids/cascades. But in flight in zones favorable for icing these grids/cascades become the most vulnerable element/cell of inlet duct in the relation to icing. Grid/cascade can greatly rapidly be covered with ice and close the significant part of the flow area of inlet duct, which will lead to the decrease of the weight flow rate of the air through compresses. If grid/cascade is not warmed, then retention time in the zone of icing for aircraft with such engines must be will be limitedly, otherwise raised the temperature of the gases before the turbine, which in turn, can create the danger of the rapid superheating of the blades of turbine and destruction. Virtually this danger can be eliminated only by year down of engine, but this will involve the decrease of thrust with all resultant consequences.

It is possible to rate/estimate the value of an increase in the turbine inlet gas temperature, assigned by the decrease of expenditure/consumption of G of the air through the compressor. From the equation of heat balance [54] with the combustion of fuel/propellant we have

$$G_r L_r \eta_r = G c_p (T_3 - T_2) + G_r c_p T_3 - G_r i_r \qquad (2-2)$$

where G_τ - a fuel consumption in the kg/s;

L_τ - fuel heating value in the J/kg;

η_r - combustion efficiency (can be accepted $\eta_k = 0.99$);

T_2 - inlet temperature into combustion chamber;

T_3 - inlet temperature into the turbine;

i_s - the specific enthalpy of fuel/propellant in the liquid state at temperature T_2.

Page 36.

Disregarding value $G_\tau i_s$ or insignificant in comparison with other terms, after the conversion of formula we obtain

$$\frac{L_\tau \eta_r}{c_p} = \frac{T_s - T_s}{f} + T_s = \frac{T_s(1+f)}{f} = \frac{T_s}{f}$$

(2. 3)

or

$$T_s = \frac{1}{\frac{1}{f}+1}\left(\frac{L_\tau \eta_\tau}{c_p} + \frac{T_s}{f}\right),$$

(2. 4)

where $f = \dfrac{G_\tau}{G}$ - a relative fuel consumption.

If we use formula (2.4), then for TRD with n=14000 r/min, at height/altitude H=9000 m, T_0=228°K, T_2=400°K and by the initial T_3=980°K with the decrease of the air flow rate through the compressor by 10o/o temperatures T_3 are raised approximately/exemplarily by 60°C, but with the decrease of expenditure/consumption to 20o/o - increase T_3 is about 140°C.

It is necessary to focus attention on the special feature/peculiarity of the icing of the input devices of engine, which is connected with a change in temperature and water content of air in inlet duct as a result of a change in it of the temperature of the entering airflow. If the external surfaces of aircraft at temperatures of higher than 0°C do not ice up, then the elements/cells of inlet duct can undergo icing at temperatures to +5°C and even somewhat above. This phenomenon can be observed in the case of expanding (lowering the pressure) the airflow during its motion along the inlet duct of engine, since in this case occurs the decrease in its temperature, which depends on the layout of channel and on air speed at the inlet into the compressor (the higher this speed, the more considerable the temperature decrease). Conditions favorable for this phenomenon usually occur with the operation of engine on the earth/ground, and also in flight of aircraft with small

speed, but with high engine revolutions (climb). In these modes/conditions even at positive temperatures of surrounding air the inlet temperature into compressor can fall to negative value and as a result of the condensation of moisture, especially with the increased air humidity, can occur the icing of the intake parts of the engine (method of calculation of the temperature of humid air in inlet duct is given in Section 5.7).

Therefore with purpose of an increase in the flight safety in the inlet ducts of engines should be had the individual signaling of icing independent of the presence of signal indicator on board aircraft and effecting it is separate with it.

It is necessary to keep in mind that during engine starting under conditions favorable for icing its intake elements/cells in the case of heating with their air can begin to ice up before their heating surfaces will be heated to the necessary temperature, since air itself from compressor is at first still insufficiently heated, especially under conditions of idling. Therefore this transfer mode/conditions under such conditions should be passed into the shortest possible time interval.

Page 37.

2.4. Icing of propellers.

Icing of aircraft screws/propellers.

The small sizes/dimensions of propeller blades along chord and high peripheral speed lead to the fact that the interception coefficient of water drops in screw/propeller is considerably more than in wing, tail assembly or other elements of the construction of the aircraft.

On the other hand, large centrifugal forces are natural protection from ice and provide its periodically spontaneous jettisoning. However, this phenomenon always does not have positive results. Are known the cases, when the pieces of ice, flying from blades/vanes, broke down fuselage covering or damaged other elements of construction/design. Furthermore, icing, as a rule, leads to the unbalancing of screw/propeller, the appearance of vibrations and sometimes even to the destruction of the radial bearings of propeller shaft.

Forms and forms of ices formation on propeller blades differ little from ices formation on wing and tail assembly, with exception of the fact that under identical conditions the region of the catching of water drops in blades/vanes usually is more and can reach

along chord to 25-27o/o.

The icing of blades/vanes can stretch all their over length, but on tail pieces ice usually is thrown off under the action of centrifugal forces and vibrations, which leads to the appearance of a disbalance and the buffeting or screw/propeller.
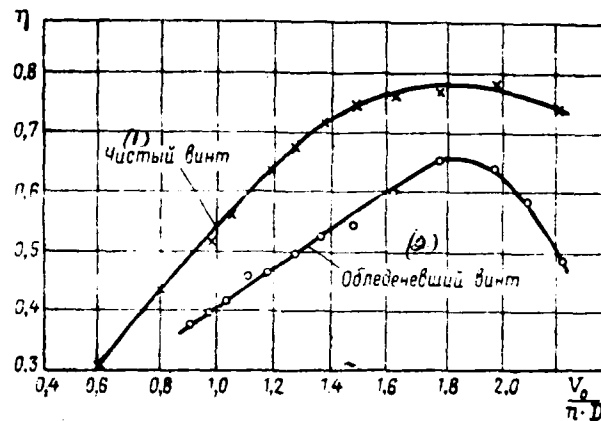
Fig. 2.9. Effect of icing on propeller efficiency (testing with the imitators of ice).

Key: (1). Pure/clean screw/propeller. (2). Iced over screw/propeller.

Page 38.

Fig. 2.9 shows a change efficiency in the iced over screw/propeller in comparison with uniced, obtained during tests with the imitators of ice - the horn-shaped form, which reached along chord 27o/o. The decrease of efficiency to 12-16o/o corresponds to a decrease in the velocity of flight (only due to the icing of screw/propeller) to 20-30 km/h [110].

The powerful/thick "accumulator/storage" of ice is also

propeller spinner. If he is not shielded or shielded insufficiently, on it are formed the large masses of ice, which, blowing away, can deposit the essential damages to engine or elements of the construction of the aircraft.

Fig. 2.10 shows the damage to propeller blade, obtained as a result of jettisoning ice from cook. After being hammered against blade/vane and after applying to it such imposing damages, ice it was rejected/thrown by blade/vane to the side of fuselage and broke the illuminator, which was located at a distance more than one meter from screw/propeller [80].

Icing of helicopter screws/propellers.

Special peculiarity is characterized by the icing of the blades/vanes of the helicopter screws/propellers the speed of flow around which they change between very wide limits, up to negative values in the zone of reverse/inverse flow[1].

FOOTNOTE [1]. Zone in the root part of the blade/vane in limits of which it moves with trailing edge forward. ENDFOOTNOTE.

The picture of icing along the length of blades/vanes to a considerable extent depends also on ambient temperature. At low

temperatures (usually order of -10°C it is below) of the blade/vane

of rotor the majorities of helicopters ice up all over length. If

helicopter in this case has forward velocity, then along the length

of blade/vane it is possible to observe three zones of icing. In the

zone of reverse/inverse flow as a result of the fact that the icing

occurs only during of the part of the revolution, and the speed of

flow is low, the intensity of ice formation very small and only

slightly it grows/rises along blade/vane (dotted line in Fig. 2.11).

Further it begins sufficiently rapidly to build up and even when with

certain radius and to blade tip it grows/rises

approximately/exemplarily proportional to distance from screw axis.

With respect to the speed of flow changes the region of the catching:

in the first zone it is sufficiently low, then toward the end of the
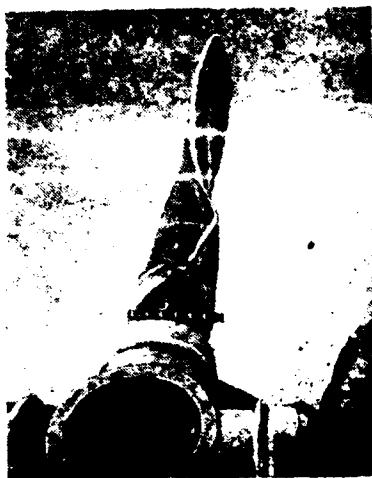
blade/vane it grows/rises.

Fig. 2.10. Damage to propeller blade by ice, discarded frcm propeller spinner.

Page 39.

With large water content and, especially, majcr drops in root of the blade/vane ices up trailing edge and certain part of the upper surface (Fig. 2.12). Furthermore, icing undergo the sleeve and all parts of control of screw/propeller, which are located in flcw.

under conditions of the hovering of the described picture, naturally, it is not observed; the intensity cf ice formation in this case all over length of blade/vane grows/rises approximately/exemplarily proportional to distance from screw axis
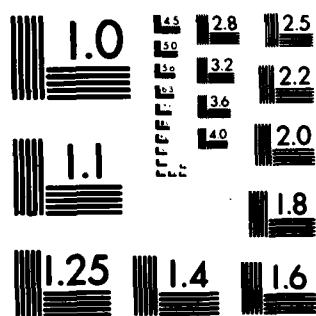
MICROCOPY RESOLUTION TEST CHART
NATIONAL BUREAU OF STANDARDS 1963-A

(see Fig. 2.11).

Higher than certain maximum temperature of air tail pieces of the blades/vanes as a result of the high-speed/velocity heating (for greater detail, see Section 5.4) cease to ice up first on leading edge, and thereupon on entire enclosure of nose/leading edge, the value of this maximum radius of the icing of blades/vanes sufficiently strictly following the ambient temperature.

As a result of the joint effect of the temperature of air and speed of flow ice built-up edges along the length of blade/vane can take the most diverse forms.

To the form of ice built-up edge have also effect different inequalities, available on surface, since they serve as the centers of the ices formation, during which the increase of ice occurs more intensely than on remaining surface (besides leading edge). The degree of the effect of inequalities on the form of ice built-up edge in proportion to an increase in the temperature of air is decreased.

Helicopter screws/propellers are considerably more sensitive to icing than aircraft.

The first signs/criteria of the icing of propeller - appearance

of the vibrations which appear as a result of the nonuniform
splitting of ice from blades/vanes, and in helicopter screw/propeller
this is aggravated even and by an increase in flow separation on the
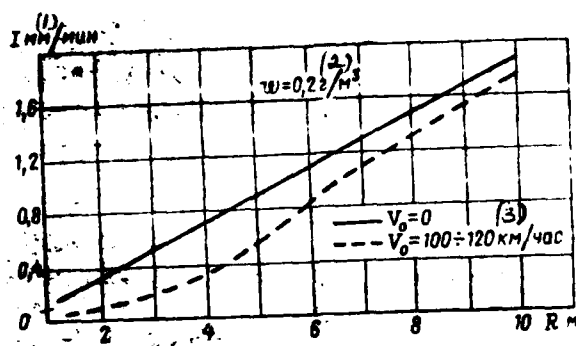returning blade/vane during progressive/forward flight.

Fig. 2.11. Speed of ice formation along the leading blade edge of helicopter rotor.

Key: (1). mm/min. (2). g/m³. (3). km/h.

Page 40.

After the appearance of vibrations and onset of the driving of control stick/knob/column (with boosterless control) usually deteriorates the controllability and finally can begin the loss of stability of helicopter. As is known, flow separation on blades/vanes in large measure depends on the degree of the roughness of the surface of blades/vanes. The speed of helicopter is limited to the permissible value of disruption/separation on the returning blade/vane. However, with icing sharply deteriorate both surface condition and the form of profile/airfoil itself, this leads to the considerable decrease of critical angle of attack and flow separation

can exceed the permissible value even at comparatively low flight velocities.

Even with icing on stand is observed a sufficiently noticeable increase in the buffeting in comparison with the general/common/total level of the vibrations of helicopter. With icing on the stand of the helicopter of Mi-4 this increase in the buffeting occurred usually in 1-1.5 min after the beginning of icing, further during several minutes its level somewhat increased and then more or less it was stabilized.

In flights with natural icing, and also in flights with the preliminary artificial icing of the screw/propeller of Mi-4 with the thicknesses of ice on the end halves blades/vanes to 7 mm were observed the vibrations somewhat smaller intensity, but in this case control of helicopter became slack, deteriorated the maneuverability of apparatus and after certain time after the beginning of icing appeared the driving and jerks/impulses[1] on control stick/knob/column.

FOOTNOTE [1]. In flight with natural icing the jerks/impulses were observed predominantly lengthwise. ENDFOOTNOTE.
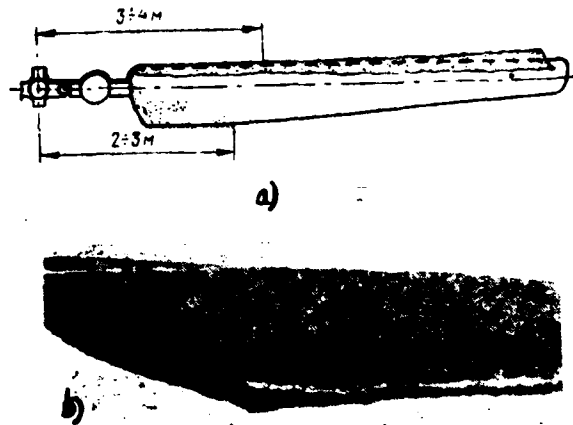
Fig. 2.12. Icing of helicopter rotor during the progressive/forward flight: a) the schematic figure of the icing; b) the icing of trailing edge and upper surface of the blade/vane of the model of screw/propeller under artificial conditions.

Page 41.

Especially strongly icing affects the light helicopters with the piston engines which usually have the small power reserve. For maintaining the revolutions of this helicopter while hovering with the artificial icing (the average speed of ice formation was 1.5-2 mm/min) it was required to sufficiently intensely increase the supercharging/pressurization of engine. In spite of this, approximately/exemplarily through the minute helicopter began to lose altitude and hovering it ceased [154], [58].

Icing of coaxial propellers.

The interesting phenomenon is observed with the icing of the coaxial propellers of aircraft. Water content in the jet, rejected by the first screw/propeller, is less than water content of clouds before it, since due to an increase in the speed of the rejected air the distance between drops increases and cloud in the direction of the motion of jet becomes seemingly more rarefied (Fig. 2.13). Tentatively it is possible to consider that the water content in jet varies in proportion to to the relation to air speed V_1 before the plane of screw/propeller [1] to speed V_2 after the plane of the screw/propeller

$$\omega_2 = \omega_1 \frac{V_1}{V_2}. \qquad (2.5)$$

FOOTNOTE [1]. It is logical that the described phenomenon does not affect noticeably the icing intensity of the stationary parts, washed by flow from screw/propeller, since the total quantity of drops of water, sucked through the screw/propeller, barely changes, but only it moves with larger speed. True, certain quantity of water recovers by the first screw/propeller, but it is relatively very small. ENDFOOTNOTE.

As a result the icing intensity or front/leading screw/propeller
proves to be above.

Similar pattern is observed also for the coaxial propellers of
helicopter. So, during investigation the already mentioned above
light helicopter under conditions of artificial icing on hovering the
icing intensity of the lower screw/propeller was obtained on the
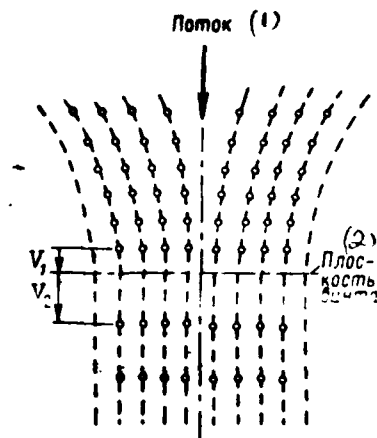average along the length of blade/vane 1.3-1.5 times lower than upper
one.

Fig. 2.13. **Rarefaction/evacuation** of cloud in slipstream.

Key: (1). Flow. (2). Plane of screw/propeller.

Page 42.

2.5. Icing of the air-pressure heads and nozzles of thermometers.

Receivers and air intakes or air flow in contrast to other
exteriors are subjected not only usual icing in supercooled clouds,
but also "forcing" by ice in ice clouds.

This "forcing" occurs up to the temperatures of air,
considerably lower (to -40 - -50°C and lower), than with usual icing,
which substantially raises the specific power required for their
heating, in comparison with other heating surfaces.

The usual icing of pressure units also has its of the special
feature/peculiarity: in proportion to the increase of ice the inlet
of receiver is decreased and, when it stops by the area of the same
there occurs a sharp decrease in dynamic pressure and
order as drain holes, in intake chamber respectively also readings
(Fig. 2.14). But if this is the nozzle of the thermometer of braking,
then changes the recovery factor of instrument. Furthermore, the
temperature of nozzle is decreased due to the evaporation of ice. As

a result an error in the thermometer can reach tens of percent.

Even air intakes of the engines, in which the flow is turned to
the angle of more than 90°, with the large water content of ice
clouds can be driven in completely by ice or snow, as this occurred,
for example, on aircraft "Britain" with engines "Proteus" in flight
in the tropical areas of Atlantic Ocean [76], [129].
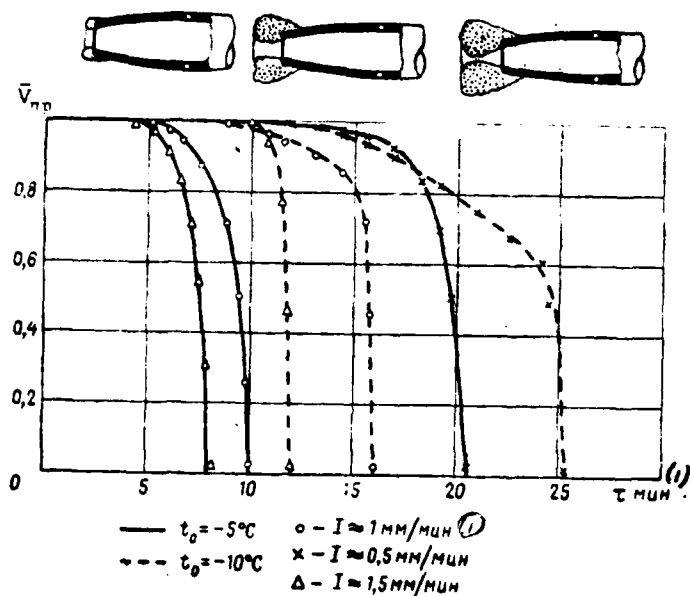
DOC = 79116303   PAGE 102

Fig. 2.14. Change in the readings (speed indicator) in relative unity
with icing PVD (under artificial conditions). Above - the process of
backlash by ice of opening/aperture.

Key: (1). min.

Page 43.

Chapter III.

Methods and protective systems of flight vehicles from icing[1].

FOOTNOTE Section 3.1-3.4 and 3.6 are written by R. Kh. Tenishev,
Section 3.7 - by V. S. Savin; Section 3.5 is written by V. S. Savin,
V. N. Leont'yev and A. I. Teslenko. ENDFOOTNOTE.

Should be distinguished the methods of deicing and the deicers,
based on these methods.

Are at present known the following methods of deicing:

- mechanical;

- physicochemical;

- thermal.

Protection can be accomplished/realized either by the prevention
of the icing of surface or by the periodic removal/distance of the

generatrix of ice.

Mechanical methods are based only on the removal/distance of ice
with the aid of any mechanical effect (strain or vibrations of
surface, aerodynamic, centrifugal or other external forces).

The physicochemical methods are based on the use of liquids or
compositions, which dissolve ice and depressing the freezing point of
water, i.e., they in principle can be used both for prevention and
for the removal of ice. The removal/distance of ice can occur either
by its complete dissolution, or dissolution only of the thin layer,
which is contacted with surface, after which ice build-up it is
thrown off by external forces.

Thermal methods are based either on the permanent heating of the
shielded surface to the positive temperature with which ice formation
becomes impossible (prevention of icing), or on the periodic melting
of ice, jettisoned then by external forces (removal/distance of ice).

Page 44.

On examined safety methods from icing are based aviation
also
deicers, which can be rather   complicated on-board systems
and comparatively simple devices/equipment.

Abroad of means of defense, preventing ice formation on the shielded surface, are known by the name "deicers" (anti-icing, antigivrage), the means cf the periodic jettisoning of ice from surface - by the name "deicers" (de-icing, degivrage). In this book we will use the more taken term "deicers" to all systems and devices/equipment, used for the protection of flight venicles from icing, isolating the deicers of permanent action (preventing icing) and the deicers of cyclic action (removing ice).

In the space of this chapter it is not the possible in any detail to stop at the device/equipment of deicers known at present, especially because description it is possible to find them in the appropriate literature (in particular, sufficiently detailed information they are contained in [58]).

Therefore we will be restricted to the short examination of the fundamental types of deicers, after paying main attention to thermal systems.

3.1. Mechanical deicers.

Pneumatic deicers.

The operating principle of this deicer consists of the following. To the shielded surface is fastened the thin rubber protector, made in the form of the oblong elastic chambers/cameras, closely fitted to surface. Upon the start of deicer the chambers/cameras under the pressure of the compressed air periodically are inflated and is broken open the incrustation of ice forming on them. Along the length (spread/scope) of the shielded surface the protectors usually consist of several sections. Such deicers sufficiently widely were applied during the years 1930-1940 for the protection of wing and tail assembly. With the advent of aircraft with gas turbine engines they yielded the place for thermal systems, but on some foreign aircraft, predominantly with piston engines, they are applied up to now. Moreover, recently appeared tendency toward the expansion of the range of their use, that it is possible to explain by the improvement of construction/design and by an increase in the reliability of protectors. Fair results in this it achieved, for example, English firm "Palmer", producing several versions of pneumatic deicers [128]: with longitudinal (on the wingspan) and transverse chambers/cameras, with successive and joint action of chambers/cameras (Fig. 3.1).

Page 45.

According to the data of firm the total specific gravity/weight of deicer composes 3-3.5 kg/m², expenditures/consumptions of the compressed air - about 0.4 kg/min.

Pneumatic deicers can be used also for the protection of such parts as the radio-transparent fairings about the radar antennas (Fig. 3.2), in which the use/application of thermal methods is impossible or is very hindered/hampered, and physicochemical methods are ineffective. The effect of such deicers on aerodynamics of the flight vehicle (which limits the possibility of their use/application on the lifting surfaces of high-speed/velocity of aircraft) will be insignificant.
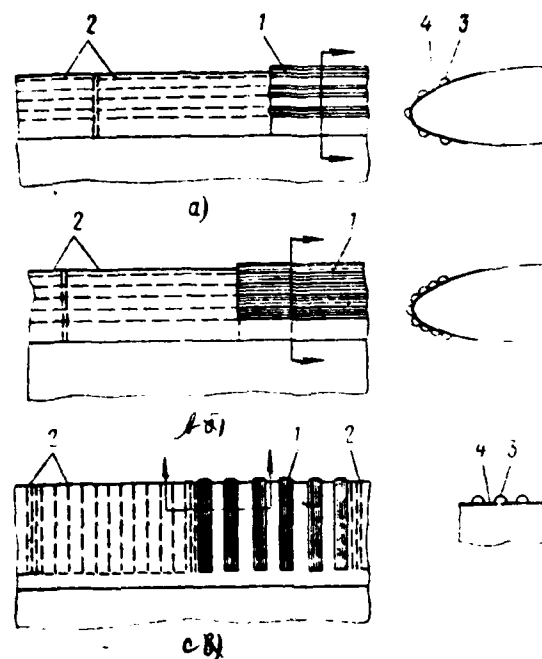
a)

б)

в)

Fig. 3.1. The pneumatic anti-icing protectors: a)with the longitudinal alternately filling chambers/cameras; b) with longitudinal simultaneously by the filling chambers/cameras; c) with the transverse chambers/cameras; 1 - working sections; 2 - inoperative sections; 3 - filled chamber/camera; 4 - unfilled chamber/camera.
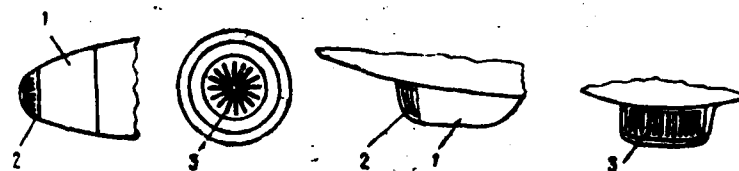

Fig. 3.2. Use of pneumatic deicers for protection of radomes: 1 -

fairing; 2 - protector; 3 - chamber/camera of protector.

Page 46.

Vibration deicers.

In principle are possible two versions of such deicers. The first is based on the fact that under the effect of the ultrasonic oscillations/vibrations, created by special siren and directed against flow, the supercooled drops of water must be crystallized; but crystals, reaching surface, will be blown away by flow. However, this method requires experimental check, the effectiveness of it thus far is doubtful and it, apparently, will require the expenditure of considerable energy. Therefore its to use most likely will be only for the protection of the separate small parts for which other methods on any reasons will prove to be unsuitable.

The second version is based on the use of the special vibrators which periodically shake the sections (sections) of the protected surface by short series of high-frequency pulses and in this way break up ice crust. The duration of series can be very short, and periodicity - as in usual cyclic deicers.

However, for the evaluation of the possibility of the practical

realization of method will be required the serious studies both of
the point of view of the effectiveness of the removal/distance of ice
and structural strength of the shielded parts.

Hydrophobic coatings.

The idea of the use of hydrophobic (not wet) coatings for
protection from icing consists in obtaining of this decrease of the
cohesive force of ice with the shielded surface, so that it would be
thrown off by the external forces, without having had time to achieve
undesirable sizes/dimensions. This means could actually serve as the
deicer of mechanical operating principle with the periodicity of the
removal/distance of ice, which was being arbitrarily
established/installed in dependence on the conditions of icing, the
flight conditions, etc. Unfortunately, up to now it was impossible to
find this substance for coating, which would satisfy the necessary
requirements. Experiment or the numerous investigations, which were
being carried out by the author [1], with teflon coatings on the
helicopter of Mi-1 [154] and with the series/row of other coatings on
special spiral stand shows that even on the rotating parts the
thickness of ice before jettisoning reaches the significant
magnitude.

FOOTNOTE [1]. Investigations were conducted together with L. F.

Vinogradovoy. ENDFOOTNOTE.

Page 47.

Jettisoning itself occurring unevenly and very unsymmetrically, which leads to the sufficiently strong buffeting of screw/propeller.

Only on the fast-turning parts (blade of compressor rotor), equipped with such coatings, ice is thrown off with considerably smaller thickness; however, coatings themselves usually rapidly are worn as a result of their insufficient mechanical durability.

From the aforesaid it follows that the coatings known at present cannot be used as any reliable means of defense from the icing of the parts of the flight vehicles in flight and in particular - not rotating (it is possible, sometimes they will be useful as booster agent in combination with mechanical or thermal methods).

Numerous unsuccessful "inventions" and fruitless attempts at the use of different coatings, undertaken in the hope for the very tempting resolution of the problem of the protection of flight vehicles in flight without expenditure of energy or without the flow rate of any anti-icing substance, should be explained that fact that the mechanism of wetting and freezing of the small/fine supercooled

cloud drops, brought to surface in by large speed in terms of airflow, differs significantly from the phenomenon of the wetting cf the cooled hydrophobic surface in ground-based conditions with the more major, freely draining drops of water (tc say nothing of the case of the wetting of this surface it is simple with water jet).

Furthermore, investigations snow that in spite of the excellent hydrophobic properties or hard-surfaced pavements the cohesive force of them with ice in the atmosphere proves tc be sufficiently large [142]. In other words, for decreasing the cohesive force of ice with the shielded surface with the aid of the undissolved solid coatings hydrophobicity is, apparently, tne necessary, but completely insufficient property.

Should be again focused attention on the fact that in many instances the erroneous conclusions about the applicability of the coatings in question are done on tne basis of investigations with the freezing of water for such coatings under laboratory conditions. During such experiments actually/really the cohesive force of frozen ice frequently is obtained by several orders lower than under the atmospheric conditions of icing.

Page 48.

3.2. Deicers, based on the physicochemical methods.

For surface protection from icing can be used two physicochemical methods: one is based on the use of the soluble anti-icing coatings (chloride of sodium or calcium, nitric acid sodium, etc.) - by the second - on the wetting of surface with anti-icing liquid (glycol compositions, ethyl alcohol, alcohol glycerin mixtures, etc.).

Soluble anti-icing coatings.

In contrast to hydrophobic (not wet and, therefore, not dissolved) coatings the operating principle of the soluble physicochemical active coatings consists in the fact that the drops of water, interacting with the substance of coating, form the solution/opening which has the lowered/reduced freezing point and is capable to dissolve ice. Although, as shows experiment, forming ice does not manage to be dissolved completely (with exception of extremely weak icing), it loses cohesive force with surface and from time to time is thrown off by external forces.

During the use of soluble (active) of coatings their substance in the process of icing sufficiently intensely is expended/consumed, furthermore, coatings are destroyed under the effect of atmospheric

conditions, mainly rain and humid air. As a result of the
shortcomings indicated this method did not find practical
use/application, although sometimes it can be useful, for example for
the flight vehicles of the very short-term or single action, on which
the use of other methods is inexpedient.

Liquid deicers.

Were applied several varieties of the liquid deicers which are
characterized by the method or the supply of anti-icing liquid to the
shielded surface.

To blade/vane of aircraft screws/propellers and frontal glasses
the liquid is fed/conducted usually with the aid of tube from face
and then under the effect or centrifugal forces or airflow it spreads
over surface. This method is applicable for relatively small
surfaces, so in this case is not provided the uniformity of the
wetting of surface and the significant part of the liquid is expended
for nothing.

On helicopter rotors the liquid is supplied usually all over
length of the blade/vane through openings/apertures or slots in the
fcre- PART   of the tipping. Thus are made, for example,
anti-icers of the helicopter rotors of Mi-1 and Mi-4, experimental

anti-icer of the English helicopter "Vessex" and deicer of the American helicopter YVH-1D. Main disadvantage in the deicers with openings/apertures is nonuniform and is insufficient wetting of surface.

Page 49.

As a result, in spite of continuous feed to liquid, ice between openings/apertures nevertheless builds up, after which liquid begins leak only on the grooves, formed by it in ice, and at enhanced intensity ice gradually involves/tightens the large part of the surface. This phenomenon especially strongly manifests itself upon the overdue start of system.

On lifting surfaces the supply of liquid is sometimes accomplished/realized from within through porous diaphragm, which must ensure the uniform wettability of an entire surface.

From such deicers is of interest the system of the cyclic action of the English firm TKS [140], used for the protection of the lifting surfaces of the series/row of piston-engine aircraft. The principle of device/equipment their following: the shielded skin/sheathing it is made from porous metal, at certain distance from it is arranged/located usual lower covering. In this slot cavity is

supplied periodically the anti-icing liquid as which is utilized

usually the glycol liquid R-328. For the more even distribution of

liquid according to surface and guarantees of necessary in this case

of its low flow rate under porous skin/sheathing is a layer from

porous elastic material. According to the information of firm TKS the

system provides the sufficiently effective removal/distance of ice

with the very small fluid flow rates of the order of several ten

cubic centimeters per minute to the square meter of the shielded

surface.

This system has even some advantages before thermal consisting

in the fact that in it is absent the spreading of water, that leads

to the formation of barrier ice, and the zone of protection,

therefore, can be minimum and, furthermore, in contrast to the

thermal system, for which is required considerable time to the

heating to surface, the action of the liquid practically begins

immediately after its supply and continues still for a while under a

layer of ice after the cessation of supply, i.e., ice built-up edge

does not freeze again to the surface after the disconnection of the

section (as with thermal method when ice does not manage to fly off

for cycle time).

Deicers with porous diaphragm can be used, also, for the

blades/vanes of helicopter screws/propellers, but in this case, as

showed experiment of the investigations of firm TKS, into blades it
is necessary to feed/conduct not liquid, but its froth (for
decreasing the effect of the centrifugal force, displacing liquid
unevenly along the length of blade/vane), which is extruded through
porous diaphragm by the compressed air.

In the examination of the possibility of using the deicers with
porous diaphragm the most important factor is the guarantee of the
retention/preservation/maintaining the filtering properties of porous
skin/sheathing in operation, since otherwise, naturally, the
effectiveness of this deicer turns out to be completely
unsatisfactory.

Page 50.

3.3. Special features/peculiarities of thermal deicers.

For the protection of contemporary flight vehicles from icing in
the overwhelming majority of the cases are applied the thermal
deicers, which are subdivided into two basic groups: electrical and
air-heat. Furthermore, sometimes, mainly for the protection of the
parts of the inlet ducts of engines, are applied the deicers, which
use hotter oil from engine.

Electrical POS of such large/coarse parts as wings and tail
assembly of aircraft and helicopter rotors, are applied almost
exclusively cyclic action, since the power, required for the
permanent heating of these parts, reaches hundreds of kilowatts. The
cyclic protection of the icing up surfaces lies in the fact that they
are divided/marked off into several sections which periodically they
are heated and they are cooled, allowing/assuming in this case ice
formation of certain safe thickness which is thrown off during the
next heating of section.

Air-heat POS until recently, as a rule, were permanent action.
However, the high required flow rates of hot air, leading to the
noticeable decrease of the thrust of some types of engines, force to
resort to air-heat POS of cyclic action, in spite of of certain
complication of construction/design.

When selecting of the diagram of cyclic POS one should consider
that to increase a quantity of sections is expedient only to a
definite limit whereas higher than which the general/common/total
savings of power becomes very small (Fig. 3.3), the complexity of
system and, consequently, also its weight they grow/rise very
considerably, especially in the air-heat system. An optimum quantity
of sections is determined for each concrete/specific/actual
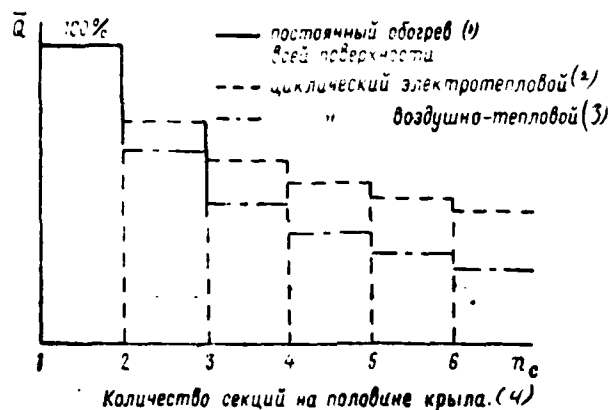construction/design of deicer.

Fig. 3.3. Decrease of the required power of cyclic POS in comparison with POS of permanent action $(n_c = 1)$

Key: (1). the permanent heating of an entire surface. (2). cyclic of thermoelectric. (3). air-heat. (4). Quantity cf sections on half wing.

Page 51.

Permanent heating of surface.

With permanent heating drops of water, falling to the surface heated to positive temperature, without freezing, spread on it, gradually evaporating and partially blowing away by airflow. If the extent of the warmed zone proves to be insufficient for complete

drainage, then the latter freezes on the boundary of heating in the form of barrier ice, which distorts the ducts/contours of the streamlined body (Fig. J.4).

It is logical that the intensity of the formation of barrier ice on one and the same of heating surface depends on its temperature and conditions of the icing: in some conditions the water will be completely removed, in other heavier - it will not be, then also is formed barrier ice.

Exists two varieties of the deicers of the permanent action:

- so called "de-icer of complete evaporation", which is previously designed in such a way that in entire required range of the conditions of icing would be provided complete drainage from surface, in other words, the deicer, not allowing/assuming the formation of barrier ice under the prescribed/assigned conditions of the icing:

- the "deicer of incomplete evaporation", which was not designed for complete removal/distance of the water (i.e. the deicer, allowing/assuming the formation of barrier ice) spreading over surface.

Outside boundary these varieties are known by the name "dry anti-icing system" - system with the dry surface (it corresponds to complete drainage from surface) and "wet anti-icing system" - system with the moist surface (allows/assumes the formation/education of the barrier flows of ice).

The use/application of deicers of complete evaporation requires the increased heat expenditure and is connected usually with the need for the protection of sufficiently large areas, in particular, if heating is designed for the guarantee only of a minimum (i.e. equal to 0°C) temperature of heating surface, as shown in examples 5.4-5.6 Ch. V. Therefore them are applied for the protection only of those parts, on which is inadmissible the formation of barrier ice. In the remaining cases they are limited to the deicers of the incomplete evaporation (taking into account that the real probability of forming the large barriers of ice is usually small).
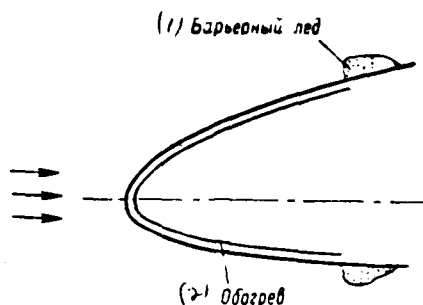
Fig. 3.4. Barrier ice, which appears under the effect of the system of incomplete evaporation.

Key: (1). Barrier ice. (2). heating.

Page 52.

Cyclic heating of surface.

As it was said, with this method on the protected surface is formed a layer of ice which during the next heating of section must be thrown off. However, if periodically is heated and is cooled entire/all icing up forepart/nose surface, then ice built-up edge, in spite of its slight melting on the boundary of contact with the heated surface, it is pressed against it by flow and is not thrown off (Fig. 3.5a). During the next cooling of surface it again freezes and, thus, it gradually reaches the undesirable sizes/dimensions

(aforesaid is related to the nonrotating parts).

It is possible to avoid the similar phenomenon via the permanent heating of narrow band in the limits of leading edge, i.e., by the use/application of the so-called "thermal knives", which seemingly are cut the ice build-up into two parts (see Fig. 3.5b). In certain cases "thermal knives" apply also at the joints of the sections of deicer, if the width of these sections is sufficiently great. At first of the use of cyclic deicers there was an opinion that for swept carrying surfaces "thermal knives" they are not required. However, experiment of the Soviet and foreign investigations of latter/last years shows that up to the sweep angle of 50-60° effective removal/distance of ice without "thermal knives" is not provided.

a)

(1) Зона циклического нагрева

б)

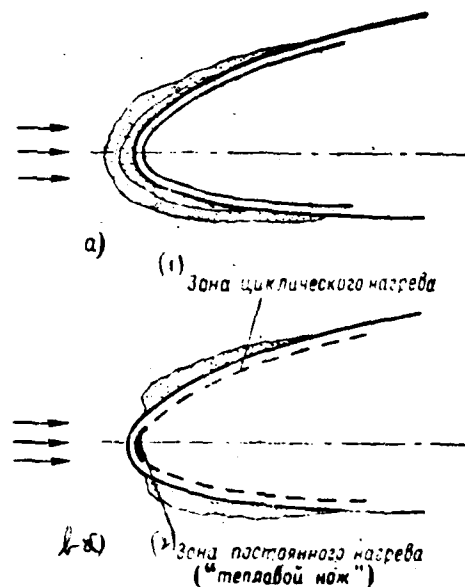(2) Зона постоянного нагрева ("тепловой нож")

Fig. 3.5. Ice built-up edge on the leading edge of an airfoil profile: a) without "thermal knife"; b) in the presence of "thermal knife".

Key: (1). Zone of cyclic heating. (2). Zone of permanent heating ("thermal knife").

Page 53.

Another special feature/peculiarity of cyclic heating is connected with the following contradictory fact: in order to ensure the work of deicer despite all prescribed/assigned temperatures of

icing, its specific power is determined on the basis of lowest
calculated temperature. It is obvious that despite all higher
temperatures of surrounding air heating surface proves to be
excessive, i.e., the surface already after jettisoning of ice
continues to remain heated and the longer, the higher surrounding
temperature (Fig. 3.6). On it, naturally, it occurs the spreading of
water, and, as follows from Fig. 1.6 chapter I, that in a larger
quantity, the higher the temperature of icing. As a result from one
cycle to the next is formed barrier ice, which with prolonged icing
can reach significant values. For eliminating (or decrease) this
phenomenon it is necessary to considerably increase zone heating and
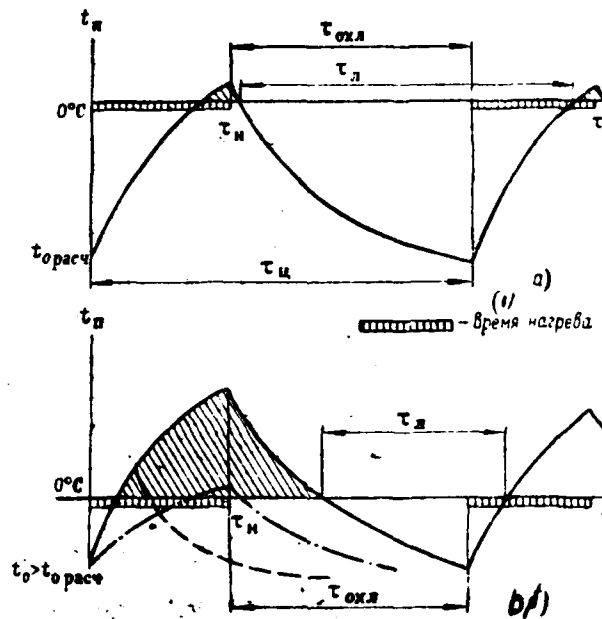thereby it is inexpedient to expend/consume large energy content.

Fig. 3.6. The cyclic heating of the surface: ——— - the unregulable (fixed/recorded) cycle (a - with t_o, by close to the calculation; b - with t_o, higher than calculation); - - the cycle, adjusted on the time; —·- cycle, adjusted according to power.

Key: (1). Heating time.

Page 54.

To decrease the possibility of the formation of barrier ice of deicer with the fixed/recorded cycle of work is possible also by shortening

the heating time, thanks to which the water will not manage to spread
in large ones quantity. However, as a result of the fact that in this
case is required the corresponding increase in the specific power
(see Chapter VI), to apply too short a heating time is also
inexpedient.

Another, less essential shortcoming in unregulable POS is
connected with the fact that the duration of cycle is limited to
permissible thickness $h_{\text{л.доп}}$ of ice which manages build up on surface
for the time of cooling[1]

$$\tau_{\text{охл}} < \frac{h_{\text{л. доп}}}{l_{\text{л}}} = f(w).$$

FOOTNOTE [1]. It is more precise, for the time of ice formation $\tau_{\text{л}}$
which can be both less and is more than $\tau_{\text{охл}}$ (see Fig. 3.6).
ENDFOOTNOTE.

At calculated (most low in calculated range) temperature $t_{\text{o. рас}}$
water content and, consequently, also $l_{\text{л}}$ are small; therefore the
condition indicated is satisfied. However, at more high temperatures
it ceases to be satisfied, i.e., the thickness of ice for cycle time
begins to exceed permissible value $h_{\text{л}} > h_{\text{л.доп}}$ and, consequently, flight
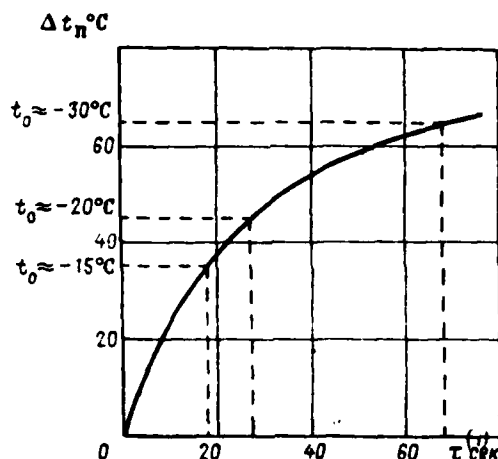safety cannot be guaranteed.

Fig. 3.7. Expansion of the range or the effective work of cyclic deicer by timing of heating.

Key: (1). s.

Page 55.

From the aforesaid follows that for guaranteeing the protection necessary for effectiveness from icing, and also increase in the flight safety the time (or the specific power) of heating by cyclic POS must change in dependence on the temperature of surrounding air and flight conditions, but the time of cooling - in dependence on icing intensity, in other words, is necessary system with the adjustable cyclic recurrence. This system will almost completely

avoid the formation of barrier ice, without considering that it will have optimum efficiency in entire range of ambient conditions. As a result the power necessary for heating can be substantially reduced - at low temperatures the required temperature drop can be achieved/reached at the considerably smaller specific power due to an increase in the time of heating (Fig. 3.6 and 3.7), which during the fixed/recorded cycle is unacceptable (due to the danger of the formation of barrier ice for the time of heating and inadmissible thickness of ice for the cooling time at higher temperatures of air).

Methods of regulating the cycle.

Simplest and available method is the manual switching which is applied in series/row foreign and some Soviet aircraft and helicopters. It consists in the fact that with the the low t_0 is included the prolonged cycle, with less low ones - the cycle is shortened, that also corresponds to the standard curve of the water content (see Chapter I). In this case most frequently is applied proportional decrease τ_{H} and τ_{oxn}, when cyclic recurrence, i.e., relation τ_{o}/τ_{H}, remains constant/invariable. However, this system has sufficiently coarse control (usually it is applied no more than 2-3 switchings in entire temperature range) and distracts crew's attention under difficult conditions for the flight when the latter

even without that is sufficiently stressed. Therefore this switching
is used by crew especially not willingly and fairly often (just in
case) system it is included to the maximum duration of cycle even at
mean temperatures of surrounding air.

Considerably more effectively must be the system, controlled by
the special automatic machine which depending on the temperature of
surrounding air would continuously change the time (or power) of
heating, also, depending on actual icing intensity in datum
moment/torque - cooling time, which can be realized with the aid of
the ratemeter of icing, constructed, for example, on the principle of
radioactive or thermoelectric ice-indicating equipment.

Page 56.

For increasing the flight safety in system can be provided for
the signaling for the case of incidence/impingement under the
off-design conditions of icing, moreover there can be two signal
aspects of the danger: if system in time does not manage to dump ice
(i.e. ice with next section is thrown off already after it will exceed
the permissible thickness), then in this case must be given out
"danger signal" in the intensity; but if intensity is small, but the
temperature of air lower than calculation and therefore heaters it is
simple not in state to heat surface to the positive temperature,

necessary for slight melting of ice, then must be "danger signal according to the temperature of air". Virtually on the panel for pilots both signals can be united into one.

If it is required to include/connect POS prior to the entry into cloudiness, i.e., prior to the beginning of icing, then for this must be provided for the possibility of the manual start of system. After obtaining of the signal of the beginning of icing the pilot can switch system to the mode/conditions of automatic regulation.

Is of interest one additional system (its mock-up was investigated by the author under laboratory conditions) whose fundamental difference from preceding/previous is in the fact that the successive switching of the sections of deicer is fulfilled not by distributor gear, but with aid of the thermosensitive elements[1], established/installed in the heaters of the surface of the sections: when temperature of skin/sheathing of next section reaches the assigned magnitude (somewhat higher than 0°C), signal from the thermosensitive element through the sensitive diagram switches heating in the following section.

FOOTNOTE [1]. As such thermosensitive elements can be used the same sensors which are used for the protection of skin/sheathing from superheating, for example, in the deicers of the firm of "Nepir"

[58], firm "Lockheed" [125] and the series/row of others.
ENDFOOTNOTE.

Therefore the heating time automatically changes in dependence on the
ambient temperature and the mode/conditions of flight, i.e., in all
cases is maintained/withstood the optimum mode of operation of
deicer. Thus, switching sections continues, until terminates icing.

In the case of off-design water content or temperature of air
for such a system can be provided for the same "danger signals" as
for preceding/previous, for which the system also must have a
ratemeter of icing.

It is obvious that a similar system despite all ambient
conditions will automatically protect skin/sheathing from
superheating, furthermore, upon the start of system on the
earth/ground skin/sheathing will be heated not more than to several
degrees of higher than zero, which will allow conveniently and
without the danger of superheating to carry out the preflight check
of system.

Page 57.

3.4. Thermoelectric deicers.

Standard diagrams of thermoelectric POS, used usually for the protection of wing and tail assembly, propellers and sometimes air intakes, consists of following basic parts (Fig. 3.8): heating elements, switchboard, included by hand by crew or it is automatic by the signal indicator of icing simultaneously with application of voltage on the power bus or heaters, thermosensitive elements for the protection of heating elements from superheating and network/grid of electric power supply (power and controlling/guiding wires/conductors, switches, contactors, etc.).

Heater (heating bundle) (Fig. 3.9) consists of the heating element, embedded between external and interior layers of insulation/isolation, which on carrying and some other parts of subsonic aircraft, which have comparatively thin skin/sheathing, is arranged/located either under skin/sheathing (a), or from its face (b), or for an increase in the rigidity of entire bundle it is installed between two thin skins/sheathings (c). During thick-walled or continuous constructions/designs as, for example, propeller blades, struts, and also sharp edges of the parts of the supersonic aircraft, etc., heaters are established/installed outside (d).
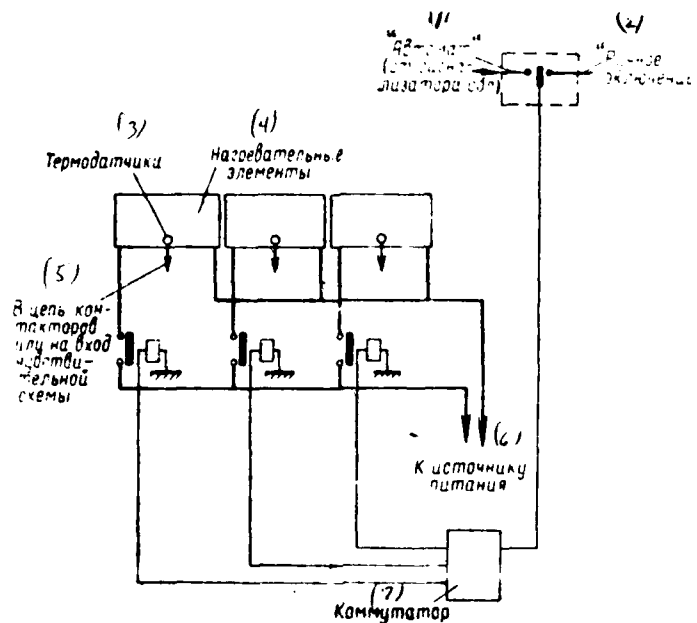
Fig. 3.8. Standard diagram of thermoelectric cyclic POS.

Key: (1). "Automatic machine" (from signal indicator reg.). (2). "Manual start". (3). Thermosensitive elements. (4). Heating elements. (5). In circuit of contactors or to entry of sensitive diagram. (6). To power supply. (7). Switchboard.

Page 58.

In this case they have protective layer in the form of thin metallic tipping or anti-abrasive coating.

Heating elements can be most varied: from the series/row of parallel thin wires, from metal foil of zigzag layout, from different current-conducting compositions, current-conducting fabrics, etc.

So, heating elements of the type "Spraymat" of the English firm of "Nepir" [107] are fulfilled from the alloy of metal (usually copper, manganese and magnesium), applied by the method of the flame-spraying method to the specially prepared layer of insulation/isolation. The current-conducting element/cell will be deposited in the form of the bands with a width of 20-30 mm which are connected on ends/faces by the copper cross connections spray-coated above them. The outside current-conducting layer is covered/coated with the layer of insulation/isolation, above which will be deposited anti-abrasive coating, and on the blades/vanes of rotors, on their end half, outside adheres another tipping made of stainless steel, since anti-abrasive coating itself sufficiently brittle and that the impact/shock of solid particles is cracked.

Elements/cells "Spraymat" possess a comparatively small thermal inertness, since they will be deposited outside. They can be deposited to the surface of any of intricate shape (Fig. 3.10), without any difficulties they allow in the limits of one heating element to obtain sections with different specific power and to accomplish/realize the current supply of different voltage, and also by three-phase current.
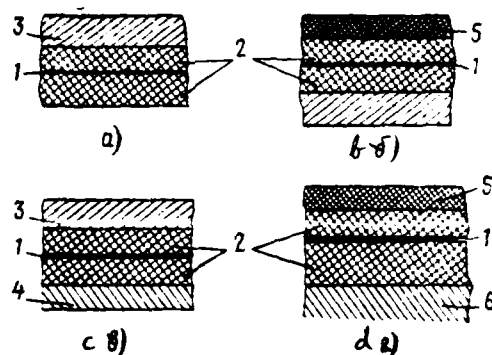
Fig. 3.9. The versions cf the construction/design of the heating bundles: 1 - heating element; 2 - insulating layer; 3 - outer skin; 4 - the lower covering; 5 - protective layer (tipping); 6 - thick-walled or continucus body.

Page 59.

A shortcoming in these coatings is their comparatively complicated technology, which requires the large space of manual labor. However this difficulty in proportion to for improvement and automation of producticn can be to a considerable extent overccme.

Should be focused attention on some special features/peculiarities cf heating elements. In the frequently used elements/cells of zigzag form, cut usually made of the thin sheet stainless steel, in internal angles (Fig. 3.11a) the current density

and, consequently, also heating are very increased, whereas external
angles almost in no way are heated. This leads frequently to the
burning out of insulation/isolation in places with the increased
heating and, on the other hand to decrease in the effectiveness of
heater due to the non-heating sections.

For decreasing this undesirable phenomenon are best anything and
sections to copperplate or, at least, to make in internal angles of
the cutting out (see Fig. 3.11b), and to also apply the
current-conducting tapes of small width.

Interesting special feature/peculiarity have the elements/cells,
made in the form of the continuous layer; their current-conducting
properties can be characterized by the resistance of the
element/cell, which has square form, which does not depend on the
size/dimension of square, since a change of the width of the square
in equal of degree changes its length. This specific resistance is
expressed in ohms to square (Ω/kV).

The resistance of right-angled element/cell is determined from
the relationship/ratio

$$R_{ЭЛ} = R_{КВ} \frac{l_{ЭЛ}}{B_{ЭЛ}},\qquad\qquad (3.1)$$

where $R_{КВ}$ - a resistance of square in the Ω/kV; $B_{ЭЛ}$ - width of

element/cell (of busbars of reed/supply equal to length); l_n -
length of element/cell (in the direction of the flow of current).

The switchboard of thermoelectric POS during the fixed/recorded
cycle acts with constant velocity, alternately connecting contactors.
A change in the duration of cycle with constant/invariable cyclic
recurrence is accomplished/realized by simple change in switching
rate of switchboard or by switching a multiple quantity of contacts
in mechanism.

Fig. 3.10. Plotting heating element "Spraymat" to shielded surface.

Page 60.

As thermal switches intended for the protection of heater and
skin/sheathing from superheating, they are most frequently applied by
thermorelay with thermistors (usually by the thermistors), with the

aid of which upon reaching of the specific temperature of heater is
disconnected the electric power supply of the corresponding section
of deicer.

Sometimes are applied also bimetallic thermoswitches, connected
in series in the feed circuit of welding contacts. However, they have
too great a thermal inertia and therefore for the target indicated
they are recommended to be they not can (such switches can be used
only in the air-heat systems, since they react well only to the
temperature of the air, which washes directly bimetallic plate).

Special features/peculiarities of the electrical heating of glasses.

On flight vehicles the heating of glazing is applied mainly for
two targets: protection from the icing of frontal glasses of flight
deck and defogging of glasses, illuminators, canopies of cockpits,
etc. Furthermore, it is established/installed, that preheating
frontal glass to a considerable extent increases its durability
against destruction during collision with birds apparently due to an
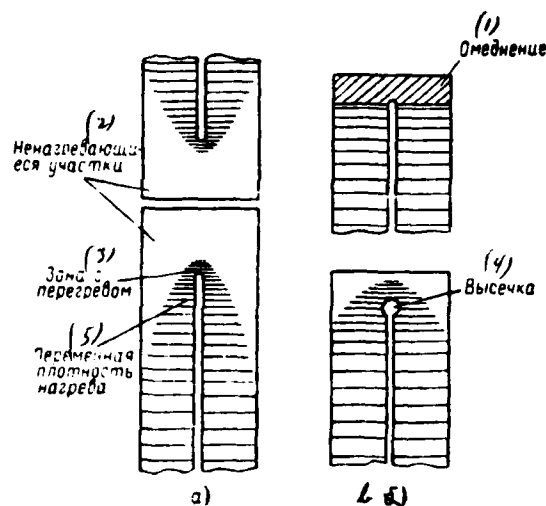increase in the elastic deformation of layers.

Fig. 3.11. Heater of zig-zag form: a) the nonuniform density of the heating; b) the methods of decreasing the nonuniformity.

Key: (1). Copper coating. (2). Non-heating sections. (3). Zone with superheating. (4). Cutting out. (5). Variable/alternating density of heating.

Page 61.

Electric heating glass consists of the following layers: external and internal, glued/cemented between themselves by elastic layers¹, for example from polyvinyl butyral, and the most current-conducting film, which cr dependence cn the fundamental

designation/purpose of glass will be deposited to one or another
layer: for protection from icing - to the internal surface of
external glass (Fig. 3.12a); ror defogging - to internal glass (see
Fig. 3.12b).

FOOTNOTE ¹. For increasing in the impact strength, decrease cf
thermal stresses frontal glasses sometimes are made more than
three-layered ones. ENDFOOTNOTE.

The glasses utilized at first with wire heaters did not find
application due to the diffraction phenomena during landing in night
time.

The skin of frontal glasses is fulfilled from silica glass,
internal - both of the silicate and from organic. In the latter case
for increasing abrasive resistance of internal surface frequently is
applied a supplementary layer of silica glass.

As the current-conducting element/cell are applied or the oxide
films (for example, from oxide of tin) or films from metals (for
example, gold). Oxide and some metallic films will be deposited to
glass by pulverization/atomization at eleyated temperatures on the
order of 550-650°C. This fact blocks their use/application on organic
glass.

Abroad at present they are applied in essence four types of electric heating glasses [156]: "Neza", "Electrapane", "Triplex" and "Sayrecoat".

In the first two types is utilized the tin oxide film, in "Triplex" - the combination of film from metallic gold and bismuth, moreover these films are applied with silica glass. Is of interest the current-conducting film "Sayrecoat-3", developed by the firm of "Sayresin Corporation", and at present manufactured also with firm "Nepir" that has license for its manufacture. It is the oxide-free metallic film which is settled to glass by the method of evaporation in high vacuum at temperature, considerably less than for the oxide films, manufactured with the method of pulverization/atomization [94].
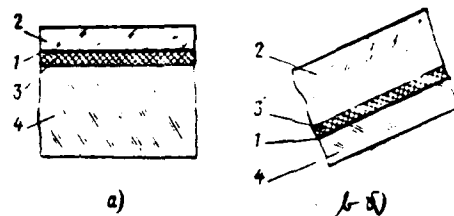
Fig. 3.12. The electrical heating of the glasses: a) for the protection of frontal glass from the icing; b) for defogging of lateral glasses or lamps/canopies: 1 - current-conducting film; 2 - external glass; 3 - elastic layer; 4 - internal glass.

Page 62.

Therefore the film can be deposited on many plastic transparent materials, technology of plotting virtually providing the absence of the so-called "hot spots" - the sections with the increased heating, which lead to large local stresses, bubbling interlayers and even destruction of glass.

The specific power (power, per unit surface area), necessary for the protection of glass from icing, according to the data of the firm of "Sayresin" [94], is represented in function of flight speed in Fig. 3.13.

Are been commonly used films with the specific resistance (see page 59) from 6 to 40 Ω/kV. In this case the color of films in straight/direct light/world is obtained pale- straw, and transparency oscillates in limits of 70-850/o. There is an assumption that the straw hue of glazing even is favorable for decreasing the luster in cabin/compartment, the film not producing polarizational or interference effects. Furthermore, it possesses property to reflect infrared radiation, which is important for protection from solar radiation at high altitudes, and also for high-speed/velocity aircraft. For example, with the thickness of the film, which corresponds to 5 Ω/kV, it is reflected to 45-70o/o, with more thin films, on the order of 25 Ω/kV, to 20-40o/o of radiation/emission.

Possibility of applying a film of the type "Sayrecoat-3" on organic glasses made it possible to prepare all frontal glazing from organic glass, as a result of which increased its durability against impact loads and against lamination during temperature variations.
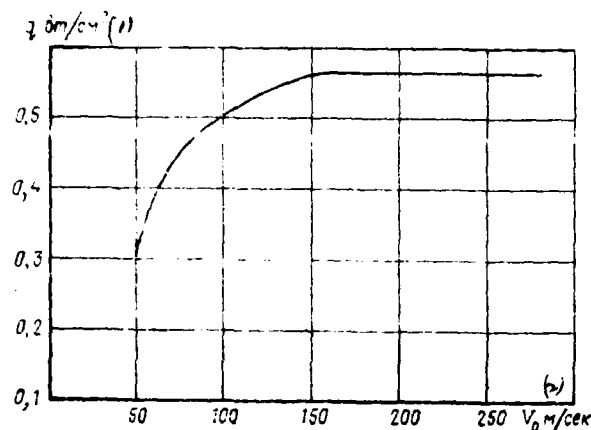
Fig. 3.13. The required specific power for protection from the icing glasses, covered with film "Sayrecoat".

Key: (1). W/cm². (2). m/s.

Page 63.

As an anti-abrasive layer is applied the specially developed polyester plastic "Sayresin-900" and of its varieties which many times are more stable against scratches, than other transparent plastics. Furthermore, are developed the methods of the restoration of glasses from solid plastics via the polishing of small/fine scratches or with the replacement of entire exterior layer.

Feed of the electrical heating of glasses is

accomplished/realized by alternating current 400 Hz. The oxide films, which possess the high specific resistance, require the increased voltage which is obtained usually with the aid of the autotransformer, which has several conclusion/output with different voltage so that in proportion to "aging" of film (increase in the resistance) it would be possible to raise the supply voltages. Metallic films ("Triplex", "Sayrecoat") have considerably smaller resistance and require therefore smaller voltage, film "Sayrecoat" moreover, is very stable in time, thanks to which the need in autotransformer for its feed/supply can generally fall.

For the protection of glass from superheating are applied the automatic machines of heating with sensors from the semiconductor (thermistors) or wire thermistors, installed into connecting/cementing layer under heating element. Upon reaching on the sensor of the prescribed/assigned temperature the automatic machine disconnects the contactor of feed/supply of electric heater.

Upon the inclusion of heating in glass appear considerable mechanical stresses. For their decrease frequently is applied the step connection of heating, at first to smaller power or smaller temperature, then in proportion to heating of glass - to complete.

However, more promising is the method of heat control by a

steady change in the power as this, for example, is
accomplished/realized by a firm or "Nepir" [107]. It consists in the
fact that the part of the sinusoid of alternating current with the
aid of the controlled semiconductor rectifier is shorn with phase
displacement, which are changed in accordance with the temperature of
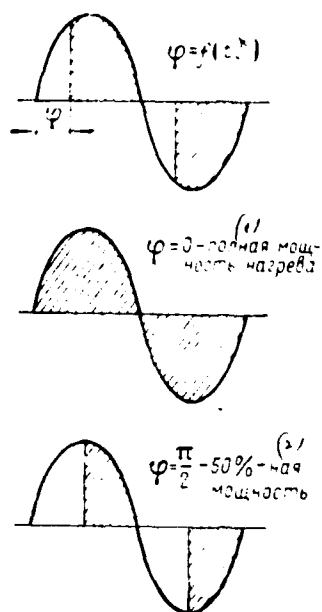external medium, as shown in Fig. 3.14.

Fig. 3.14. Regulation of the power of heating via the cut-off of the part of the sinusoid of alternating current in accordance with the conditions of icing.

Key: (1). the total power of heating. (2). power.

Page 64.

Use of high-frequency heating.

As is known, some engines can be very sensitive to the icing of the blades of rotor. However, the protection of moving vanes by usual methods represents complex problem both in the relation to the device/equipment of heaters themselves and in the relation to the supply to them of energy. In this connection is of interest the method[1] of the protection of steel compressor blades, and also some other parts, based on the use of high-frequency heating.

FOOTNOTE [1]. Method was investigated in 1958 on laboratory installations by engineer M. G. Lapshin together with the author of present chapter. ENDFOOTNOTE.

On compressor casing in the plane of the rotation of the shielded series/row of blades are established/installed the pole pieces, magnetized from the electromagnet (possible the permanent magnet) (Fig. 3.15a). With the passage of the steel blades through the

magnetic field of caps they are heated as a result of the onset in
them of eddy currents and hysteresis losses. The necessary intensity
of heating can be reached via the selection of a necessary number of
magnets and their power.

More rational version is the combination of device/equipment for
heating of blades with the generator of electrical high-frequency
current. For this the pole pieces are fulfilled all over
circumference in the form of the stator of electrical machine with
the slots/grooves, into which is inserted the winding (see Fig.
3.15b). In other words, is obtained induction type electric
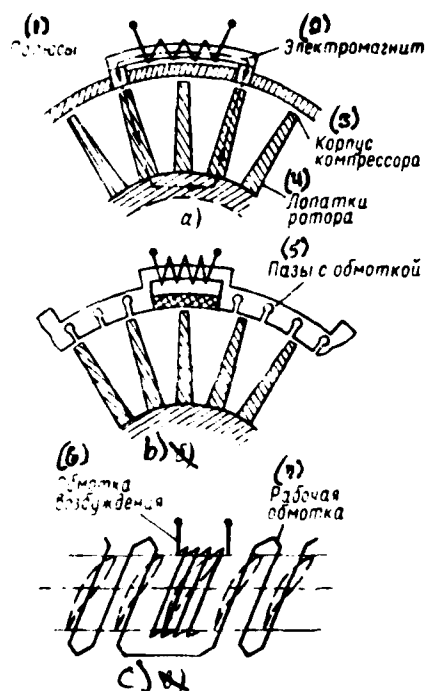generator.

Fig. 3.15. Use of the high-frequency heating:

a) the protection of the blades of the rotor; b) - deicer-generator; c) - the winding diagram of generator.

Key: (1). Poles. (2). Electromagnet. (3). casing. (4). Blades of rotor. (5). Slots/grooves with winding. (6). Excitation winding. (7). Inducing winding.

Page 65.

As a result of the large speed or rotation of the rotors of aircraft
engines and considerable number of their blades the frequency is
obtained the order of several kilohertz, but the intense cooling of
the inlet compressor stage makes it possible to allow high current
density in winding therefore the weight of this deicer- generator it
can be insignificant. The obtained high-frequency current can be
successfully utilized for the heating of other parts of the flight
vehicle and engine. In particular, if we make housing (core) of
stator blade from magnetoconductive material, and external
duct/contour it to fulfill made of the thin stainless steel, then
with the transmission through the core of alternating magnetic field
external duct/contour will be heated as short-circuited secondary
winding of transformer. In this case automatically is provided
heating an entire surface of blade and, furthermore, it is
sufficiently simple to carry out redistribution of heat-flux density
over the surface (which during air heating is extremely difficult).
For this the sections of skin/sheathing of blade on the duct/contour
of the cross section on which it is required to obtain more intense
heating, one should make thinner (by etching), and sections with the
lowered/reduced heating it is possible to coat with copper. The same
construction/design can be utilized for the heating of sharp edges.

As far as lifting surfaces are concerned large, then with
heating by their high-frequency current is a possibility, besides the

ohmic heating of a quite heating layer, to obtain supplementary effect from the induction heating of directly outer covering. For this it must be made from the thin sheet of magnetoconductive material, and the conductors of heating element are lined in a special manner in order to enforce the forming magnetic flux (for example, in the form of flat/plane spiral). The obtained in this case effect substantially raises the rate of heating the outer covering, especially in initial heating-up period, which is very important for a cyclic deicer. According to the results of the investigations, which were being carried out under laboratory conditions, the rate of heating heating element with thin outer covering made of magnet steel grew/rose approximately/exemplarily from 0.03 1/s with the feed/supply by direct current approximately/exemplarily to 0.06 1/s with the current supply of the high frequency of 5 kHz. From the comparison of the corresponding curves of the dimensionless temperature of heating (see Fig. 5 application/appendix) it is possible to see that this method would make it possible to noticeably decrease the required power or the time of cyclic heating.

Page 66.

3.5. IR-heat deicers.

The standard schematic diagram of the air-heat de-icing system

based on the example of aircraft with two jet engines is shown in Fig. 3.16. Hot air is selected/taken from compressor and is fed/conducted to the aircraft components, shielded from icing (wing, tail assembly, air intakes, glasses, etc.). For limiting the air bleed from engines are utilized the limiters of flow rate (reduction valves, washers, etc.), control or the supply of hot air into one or the other part of the system is accomplished/realized with the aid of remote locking devices/equipment. In the bleed line of air are established/installed the check valves, which prevent the overflowing of the selected/taken air of one engine in another and provide the operation of de-icing system in the case of failure of one of the engines.

The temperature of the hot air, applied into deicer, for reasons of strength must not exceed certain permissible value (for duralumin alloys - not more than 180-200° C). For a decrease in the temperature of the air before supply in deicer are applied the ejectors, in which to hot air is mixed cold. Another method of a decrease in the temperature of air is simultaneous air bleed from low-pressure and high-pressure compressor stages with the subsequent mixing.
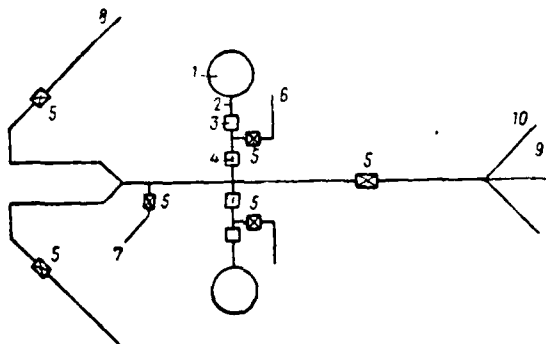
Fig. 3.16. The schematic diagram of the air-heat de-icing system of the aircraft:

1 - compressor of the engine; 2 - air extraction manifold; 3 - limiter of the flow rate; 4 - check valve; 5 - locking device/equipment; 6 - deicer of the engine; 7 - deicer of the glasses; 8 - deicer of the wing; 9 - deicer of the fin; 10 - deicer of stabilizer.

Page 67.

Diagram of deicers.

The diagrams of the existing air-heat deicers can be presented in the form of the following basic versions (Fig. 3.17). Most simple is the first diagram (see Fig. 3.17a). hot air enters the longitudinal air duct A, formed by outer covering 1 and wall (or

longeron/spar) 2, and is heated the shielded surface to the prescribed/assigned temperature. This construction/design usually is applied for the protection of the small aircraft components or helicopter, for example struts, compressor blades and guiding device, blades/vanes of helicopter, etc. Sometimes on this diagram is fulfilled the construction/design of the deicer of nose/leading edge of air intake of engine.

In other version (see Fig. 3.17b) is applied the longitudinal-transverse distribution of hot air. As in the first case, hot air enters the longitudinal air duct A and then it is opened into transverse channels which are fulfilled with the aid of the fluted or dual skin/sheathing. For the creation of the necessary pressure differential along transverse channel wall 2 is made by hermetically sealed. Another longitudinal air duct B, into which enters the exhaust air, has special openings/apertures ("louver") for the outlet of this air in the atmosphere. This diagram received wide distribution and it is applied in the construction/design of the deicers of wing, tail assembly and air intakes of engines.
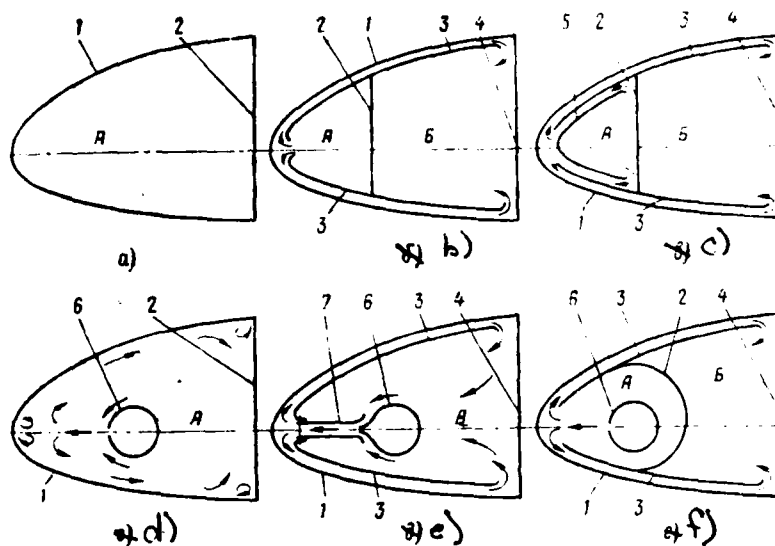
Fig. 3.17. The standard diagrams of the air-heat heaters of the surface:

1 - skin/sheathing; 2 - wall (or longeron/spar); 3 - corrugation; 4 - longeron/spar; 5 - shield; 6 - manifold "piccolo"); 7 - flat/plane mixing chamber.

Page 68.

The variety of the preceding/previous diagram is the diagram, given in Fig. 3.17c. The special feature/peculiarity of this version is the presence of special shield 5, which serves for increasing the heat efficiency of hot air in channel A. Shield usually is fulfilled from nonmetallic material (for example, fiberglass laminate). It

should be pointed out that the introduction of this shield very insignificantly raises the effectiveness of deicer, and therefore this diagram did not receive wide distribution.

In three latter/last versions the longitudinal distribution of hot air is accomplished/realized with the aid of the so-called tubes "piccolo" which have a series/row of small openings/apertures (on the order of 1.5 mm) along frontal generatrix. These diagrams make it possible to decrease the unproductive heat expenditures in channel A and to ensure the even distribution of hot air along the length of deicer. The simplest version of this heater is shown in Fig. 3.17l. Hot air escape/ensues from the openings/apertures of tube "piccolo" with speed, close to sonic, and then it moves over channel A, heating skin/sheathing to the prescribed/assigned temperature. Due to the ejection, created by the jet of hot air which escape/ensues from openings/apertures, occurs the circulation of exhaust air in the cross section of channel. Given construction/design has some advantages according to thermal characteristics in comparison with diagram in Fig. 3.17a.

The more advanced version of such heaters is the diagram in Fig. 3.17e, which was called "micro-ejector". Hot air is fed/conducted into manifold 6, established/installed along the span of wing or tail assembly, and it is supplied into the flat/plane mixing chamber by 7

through the small nozzles, arranged/located with the specific space
(about 10 mm) on manifold. During the outflow of hot air behind
nozzle occurs the draining of air from channel A. The flat/plane
mixing chamber smoothly passes into corrugation on upper and pressure
sides of profile [125].

Is of interest the sixth diagram (see Fig. 3.17f), which has
much in common with "micro-ejector" diagram, but by
construction/design somewhat simpler. The essential difference for
this diagram from preceding/previous is the presence of pressure
chamber, which is formed by skin/sheathing 1 and hermetically sealed
wall 2. In this chamber/camera is created the overpressure of hot air
for its "extrusion" through the transverse channel of a small height
(on the order of 1.5 mm). It is obvious that in this heater it does
not occur the supplementary draining of exhaust air (as it takes
place in micro-ejector system).

It is necessary to note that the air-heat heaters, made on one
of the three latter/last diagrams, most effectively work when all
over length of distributing pipe (tube "piccolo") is provided
supercritical pressure.

Page 69.

The transverse channels of the air-heat deicer can have
different construction/design. The possible versions of the design of
these channels are shown in Fig. 3.18. The first three
constructions/designs are fulfilled by stamping the lower covering
along the prescribed/assigned profile/airfoil with its further
riveting to the outer covering. The dual channel, formed by the
corrugated covering and the plate (see Fig. 3.18b), was planned with
purpose of the elimination of the badly/poorly warmed zones in area
of riveted joints of the outer covering from internal. However,
practice shows that this construction/design of channels does not
give any considerable advantage before the single channel (see Fig.
3.18a), so KAI has the supplementary thermal resistance, due to which
in the places of contact of both skins/sheathings it does not occur
the expected increase in the temperature of the outer covering. For
decreasing the unheated zones can be used transverse channels with
the lower covering, in which are made the punch-outs under riveted
joints (see Fig. 3.18c). Transverse channels can be done permanent
and variable/alternating cross section (on height/altitude) along the
length of channel on the enclosure of profile/airfoil.

Three recent designs of transverse channels are fulfilled by
mechanical or chemical milling. Version in Fig. 3.18d is simplest
from the point of view of manufacture; however, the structural weight
can be considerable. The most modern construction/design of

DOC = 79116304   PAGE 161

transverse channel is the version (see Fig. 3.18f), in which the
connection of the lower covering from external is
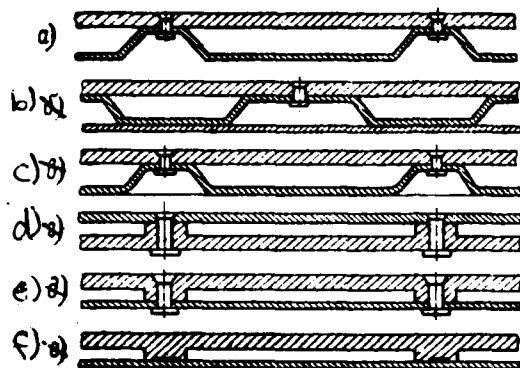accomplished/realized by roller or spot welding.

Fig. 3.18. The versions cf the construction/design of the transverse air ducts:

a) channel with the single corrugation; b) channel with the dual corrugation; c) channel in the form of dual skin/sheathing with punch-out under riveted joints; d) the milled channel in the lower covering, riveted with the outer covering; e) the milled channel in the outer covering, riveted with the lower covering; f) the milled channel in the outer covering, to which is welded the lower covering.

Page 70.

Besides the air-heat systems of permanent action, in a number of cases can be used cyclic air-heat deicers. The necessary condition for the effective operation of this system, as it was already said above, is the presence of the permanent effective "thermal knife" and the high rate of heating surface, which requires the increased flow

rate of hot air in heating-up period. Fig. 3.19 shows the versions of the construction/design or "thermal knives" for the air-heat deicers of cyclic action. In the first of them (see Fig. 3.19a), "thermal knife" it is made in the form of the longitudinal channel of small cross section along the leading edge of profile/airfoil. In the second version (see Fig. 3.19b) "thermal knife" it is made in form of tube "piccolo" established/installed near the outer covering. The third version (see Fig. 3.19c), is usual "thermoelectric knife".

The construction/design of the cyclically heated part of the air-heat deicer can be made differently, if we consider the possible combinations of the standard diagrams of the air-heat heaters of surfaces and versions "air-heat knives". Fundamental requirement when selecting of the diagram of cyclic deicer is the minimum thermal inertness of construction/design. Fig. 3.20 shows one of the possible diagrams of the air-heat deicer of cyclic action. It is obtained on the basis of the connection of the diagram, given in Fig. 3.17f, and "thermoelectric knife". For decreasing the thermal inertness of the construction/design of deicer pressure chamber A (see Fig. 3.17f) must be minimum space.
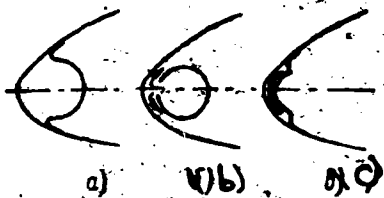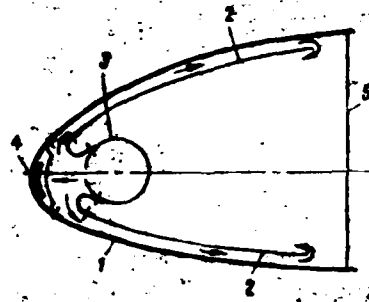
Fig. 3.19.   Fig. 3.20.

Fig. 3.19. Versions of construction/design of "thermal knives" for cyclic air-heat deicers.

Fig. 3.20. Possible diagram of cyclic air-heat heater of wing surface:

1 - skin/sheathing; 2 - corrugation; 3 - manifold; 4 - "thermoelectric knife"; 5 - wall or longeron/spar.

Page 71.

Jet-edge protection of frontal glasses.

A special question is the protection of frontal glasses of the pilot's cabin (helicopter) from icing with the aid of hot air. Fig. 3.21 gives the diagrams of two versions of the protection of frontal

glasses from icing with the use of hot air. In the first (see Fig. 3.21a) hot air is supplied into the flat duct between the external and internal panels of glass. However, this version of the heating of glass did not win acceptance as a result of the number of structural/design and operating shortcomings. More effective proved to be the method of the so-called jet-edge protection (or otherwise - "air barrage" (see Fig. 3.21b), which can be used both for the protection from icing and for an improvement in the visibility through glass with flights into rain. The principle of jet-edge protection lies in the fact that hot air is thrown out behind two-dimensional nozzle, arranged/located before the leading edge of glass, and is exerted on the settling water mechanical and thermal effect, in consequence of which it partially evaporates, partially it is blown away (for greater detail, see chapter V and VII).
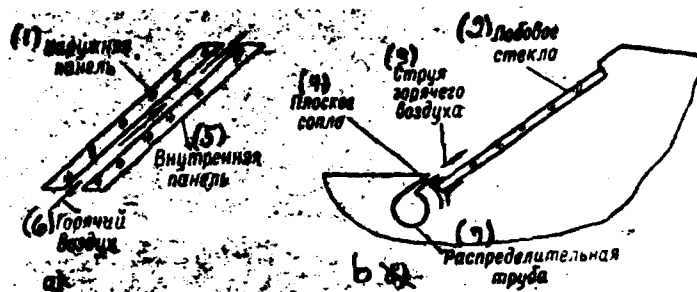
Fig. 3.21. Diagrams of the air-heat heaters of the frontal glasses:

a) the internal heating of the glasses; b) the jet-edge protection of glasses.

Key: (1). external panel. (2). front glass. (3). Jet of hot air. (4). Two-dimensional nozzle. (5). internal panel. (6). Hot air. (7). Manifold.
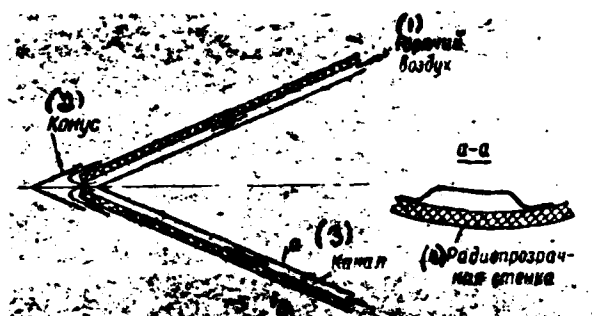
Fig. 3.22. Diagram of the use of air shields for anti-icing protection of the conical deflector of the radar antenna.

Key: (1). hot air. (2). cone. (3). channel. (4). radio-transparent wall.

Page 72.

Sometimes jet-edge protection can be used for the protection from icing and other aircraft components. For example, Fig. 3.22 shows its use/application for the protection of the conical radome. "air barrage" can serve also as means of defense from the icing of small air intakes or objectives of the optical instruments, established/installed towards the incident airflow (see Chapter X). Furthermore, jet-edge protection partially is utilized during the

combination of the boundary layer control system and de-icing system.

Deicers of gas turbine engines.

For the protection of the parts of the inlet duct of engines from all known methods widest application was obtained air-heat. In certain cases, as has already been mentioned, is applied more hotly oil, and also combination of the methods indicated. However, it should be noted that, in spite of comparative simplicity of the construction/design of the air-heat system and its sufficient reliability in operation, it has also shortcomings, characteristic to all air-heat systems with air bleed from compressor, i.e. the effectiveness of this system is found in direct dependence on engine power rating (besides TVD). Therefore under conditions of idling or close to it air-heat system is usually barely effective and it it is necessary to design with reserve or for the more economical utilization of hot air it is necessary to apply the automatic regulation of a quantity of selected/taken air depending on engine power rating.
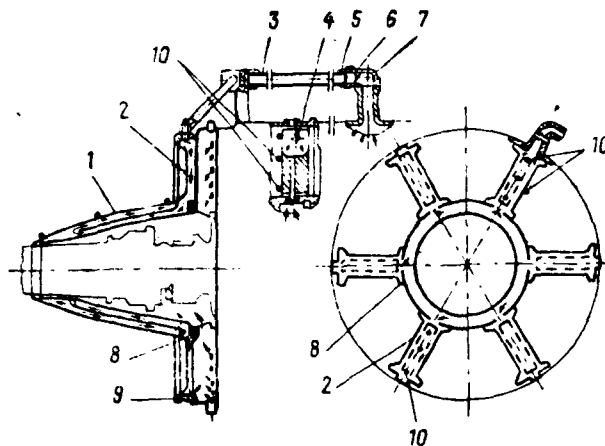
Fig. 3.23. The schematic of the de-icing system of the engine:

1 - fairing; 2 - applied spokes; 3 - tube of the supply of the air; 4 - blade directing apparatus; 5 - diaphragm; 6 - the throttle plate; 7 - tap/crane of air intake; 8 - adapter of the front/leading housing; 9 - adapter of the diffuser; 10 - thermocouple for measuring the temperature of surface during tests.

Page 73.

The diagrams of the distribution of hot air and the design of the heating of the shielded parts depend on the construction/design of the input parts of concrete/specific/actual engine and can be most diverse. For an example Fig. 3.23 and 3.24 give the typical patterns of air-heat POS of engines, and in Fig. 3.25 - schematic of the

combined (air and oil) system, used on engine AI-20 whose description
is, for example, in work [58].

During the development of the construction/design of air-heat
POS of engine it is necessary to focus attention on correct air
distribution according to all elements/cells of inlet duct, which
ensures the uniform heating of all shielded elements of
construction/design. For decreasing the heat losses should be
provided the necessary thermal insulation of supply lines and other
elements/cells in the line of hot air.

In certain cases it is expedient to apply the ejection of the
hot air, selected/taken from compressor. In particular, such ejection
is made in POS of engine D-20P. The ejection hot air is
selected/taken directly after the eighth step/stage of the second
cascade/stage. The ejected "cold" air is supplied from the
interlabyrinth cavity of the eighth step/stage of the second
cascade/stage of compressor [58].

Let us examine in more detail the construction/design of the
separate elements of de-icing system.

Struts (applied spokes). The heating of struts is
accomplished/realized usually at a distance from leading edge, equal

to approximately/exemplarily 300/o of its overall width. Heating is

accomplished/realized all over height/altitude of strut. With purpose

of an increase in the effectiveness of heating within the warmed part

of the strut usually it is established/installed deflector or

longitudinal corrugations (Fig. 3.26).
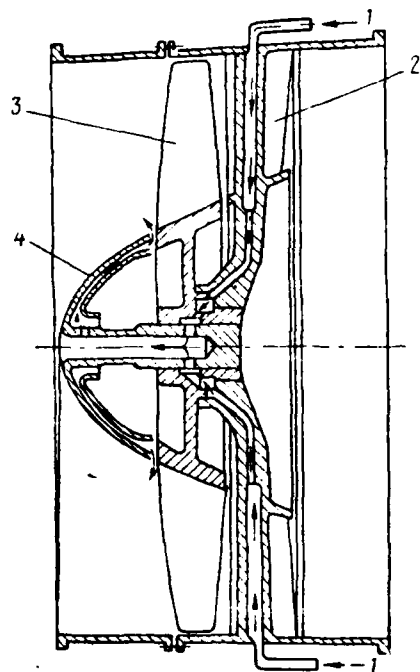
Fig. 3.24. The diagram of deicer with the heating of fairing and stator of I step/stage:

1 - supply of the hot air; 2 - stator blades; 3 - blade of the rotor; 4 - rotating fairing.

Page 74.

Fig. 3.25. Schematic of mixed type de-icing system:

1 - supply of hot air; 2 - blade VNA; 3 - shutter/valve; 4 - valve of bypass of hot air; 5 - ice-indicating equipment; 6 - supply of air to cartridge/ammunition of fuel automatic machine; 7 - air intake of fuel automatic machine; 8 - oil supply from pump; 9 - branch/removal of oil mixture to air separator; 10 - frontal crankcase.
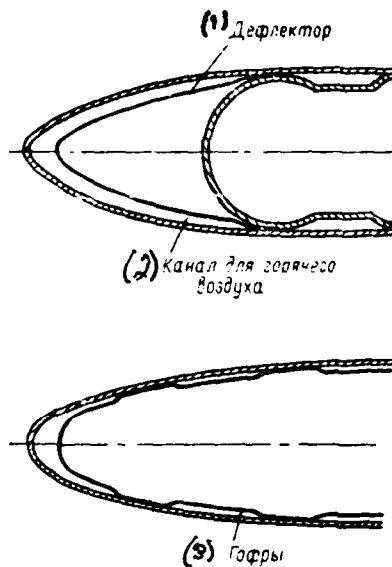
Fig. 3.26. Construction/design of the heating of struts.

Key: (1). Deflector. (2). Channel for hot air. (3). Corrugations.

Page 75.

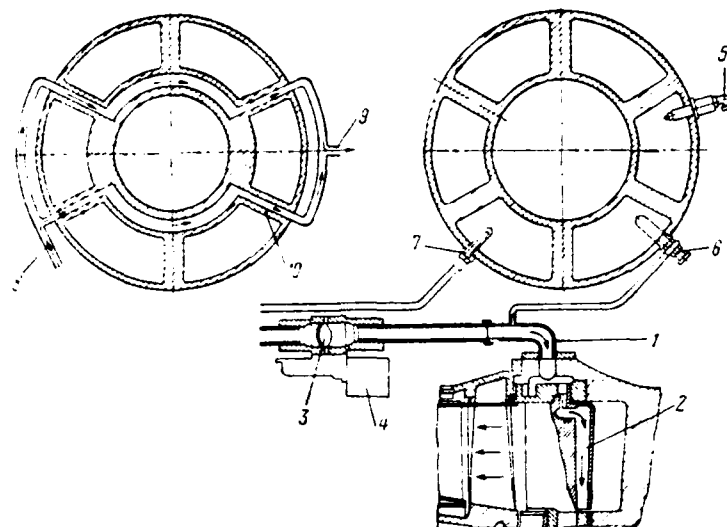Blades VNA. The heating of blades VNA must be examined taking into account the angle of their rotation and knee of trailing edge. When blade VNA fixed and the bend angle of trailing edge it is small, possible to accomplish/realize heating of its only leading edge at a distance of ~30o/o from the width of blade. If the knee of trailing edge is more than 8° or blade rotary, then it is necessary to provide the heating of the trailing edges of blades. The diverse variants of

the construction/design of heating are represented in Fig. 3.27.

Fig. 3.27a gives the schematic of the heating of blade VNA with
a deep slot/groove, in Fig. 3.27b - blade VNA with a deep slot/groove
and supplementary slots in the rear end of the blade. The hot air,
which comes out from supplementary slots, must provide protection of
trailing edge from icing.

Fig. 3.27c shows the version of the heating single-piece milled
blade VNA with special external thin-walled shell. Hot air enters
slot/groove on the leading edge of blade VNA and further on the
milled slots it emerges from the side of its trailing edge.

Fig. 3.27d gives the construction/design of the hollow skeleton
blade, in which is provided the heating of an entire surface of
blade.
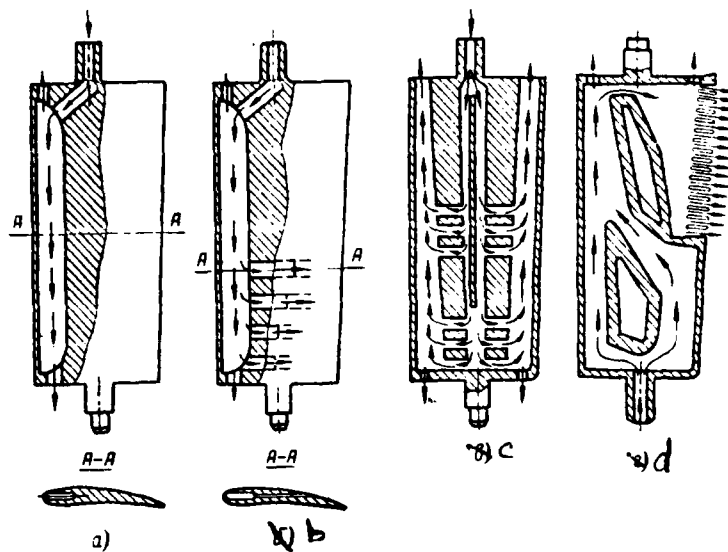
Fig. 3.27. Versions of the heating of blades VNA:

a) blade VNA with the deep slot/groove; b) blade VNA with a deep slot/groove and supplementary slots in the rear end of the profile/airfoil; c) the single-piece milled blade with the special thin-walled shell; d) hollow skeleton blade.

Page 76.

Fairing. For the effective heating of fairing hot air must be fed/conducted to its front/leading part, on which occurs most intens- ice formation. Hot air from struts or blades VNA is fed/conducted on tubes to its front/leading part and further on radial clearance,

formed by external wall and internal deflector, it passes along
fairing and it is thrown out through openings/apertures into the
inlet duct of engine. One of the versions of the
constructions/designs of fairing is given in Fig. 3.28.

3.6. Factors, which affect the selection of de-icing system.

As it was said in the beginning of this chapter, until today
most effective are thermal safety methods from icing. Therefore in
all cases when is required reliable protection in the sufficiently
broad band of the conditions of the icing; (to corresponding
international norms), should be applied thermal POS.

However, the use/application of other methods can be advisable
only when to the protection of flight vehicle from icing are
presented less stringent requirements, and the reserve of its power
is very limited (usually on light aircraft and helicopters with
piston engines), and also, when the use/application of thermal
methods either is impossible or it is extremely hindered/hampered
(radomes, sensors of some instruments, etc.).
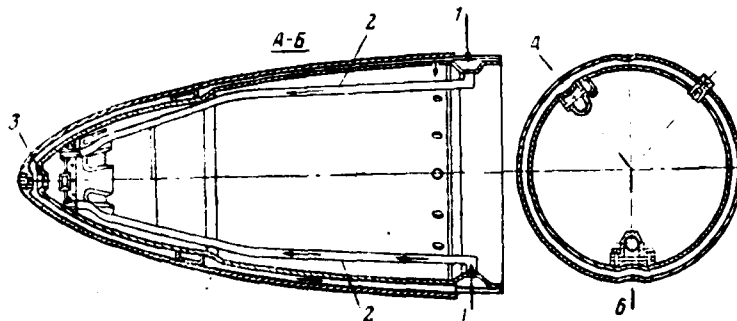
Fig. 3.28. The de-icing system of the fairing:

1 - supply of hot air to the fairing; 2 - tube of the supply of air to the nose/leading edge; 3 - air escape into nose/leading edge.

Page 77.

When selecting of one or the other type of thermal deicer it is necessary to consider the following factors:

a) the possibility of the most economical use of energy, selected/taken from aircraft engines. Here enter questions of the selection of the form of the source of thermal energy, its location of relatively heating surfaces, effect of the selection of energy input on the flight characteristics of flight vehicle, etc. The most complete response/answer to all these questions gives evaluation PCS (just as other systems) from the point of view of its equivalent

weight, as shown further;

b) the applicability of this deicer from the point of view of the

protection necessary for degree from icing, i.e. necessary whether

for the part of the flight vehicle in question the deicer of complete

evaporation or to admissibly utilize a deicer of incomplete

evaporation or the cyclic;

c) the possibility of the design or deicer on the shielded element of

construction/design, i.e. in essence this a question of the selection

of the air-heat or electrical deicer.

All these factors undoubtedly are tightly interlocked; therefore

before finally selecting one or another version POS, should be

rated/estimated it from different point of view.

Let us pause at separate moments/torques in more detail. Need in

the deicer of complete evaporation most frequently is connected with

the danger of the damage of the blades of compressor rotor of

aircraft engines in the case of incidence/impingement into the inlet

duct of the pieces of ice. In other words, if into engine is

inadmissible the incidence/impingement of ice, then all parts of

inlet duct, and also part of the flight vehicle, arranged/located

before the air intake, must be equipped with the deicers of complete

evaporation. In particular, this is related to the root sections of the upper surface of the wing of aircraft whose engines are arranged/located in the rear end of the fuselage. However, on the remaining shielded wing surface can be used either POS of incomplete evaporation or cyclic (Fig. 3.29). This layout of protective systems it has, for example, English aircraft "Trident".

But if compressor blades are made sufficiently durable, and small ice falling into compressor does not affect noticeably the operation of engine, then for the protection of the parts, arranged/located in inlet duct and before it, let us allow cyclic heating with sufficiently short cycle during intense heating. This system successfully is applied on the air intakes of some English aircraft (for example, "Argosy").

From the point of view of the savings of power the use/application of cyclic deicers is even more expediently for the air intakes of the supersonic aircraft, which have sharp edge. The fact is that the icing of the sharp edges of supersonic profiles/airfoils and air intakes differs from usual profiles/airfoils in terms of the larger difference between the value of the capture region and region of the spreading of the water film (see Chapter V).

Page 78.

Ice built-up edge is usually concentrated only on very the point of sharp edge, whereas the spreading of water it occurs many times further. As a result the zone of the capture/grip of ice is measured literally by millimeters, and the zone of the spreading of water during preheating of surface can reach several decimeters, as is evident, for example, in the photographs of Fig. 3.30, in which is shown the icing of the cold and heated sharp-lip inlet, which was being investigated on flying laboratory. For preventing barrier ice with permanent heating in this case it is necessary either to warm very large area, or to create the considerable superheating of surface in nose section.
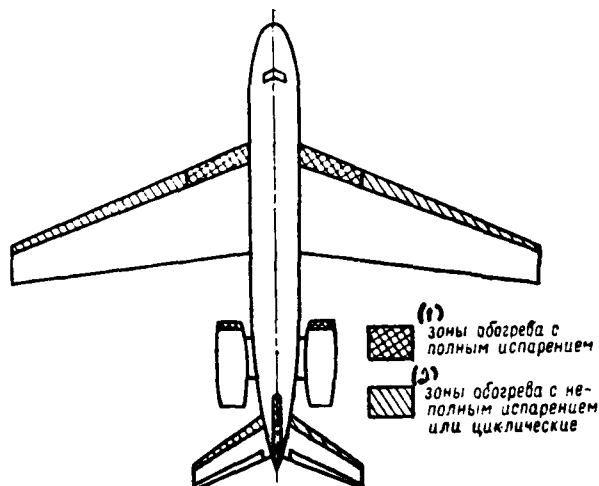
Fig. 3.29. Aircraft with the diverse variants of deicers.

Key: (1). zone heating with complete evaporation. (2). zone heating
with incomplete evaporation or cyclic.
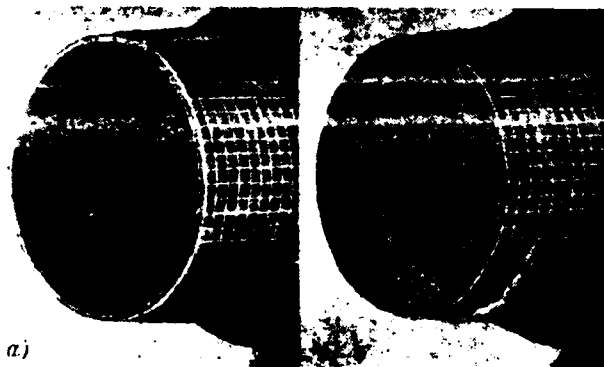
Fig. 3.30. Icing of sharp-lip inlet:

a) cold surface; b) heated surface.

Page 79.

However, the use of a cyclic deicer, which consists of the
combination of the continuous heating of sharpest edge (i.e. "thermal
knife") and cyclic heating of remaining surface (Fig. 3.31), makes it
possible to be restricted to the very small size/dimension (along
flow) of the latter. Consequently, this deicer will be considerably
more economical in comparison with permanent heating. However, the
duration of cycle in this case always can be selected sufficiently
low.

Generally, if on the shielded part is inadmissible the formation
of barrier ice, and the use of a deicer of complete evaporation is
difficult, then should be used POS of cyclic action.

Examining thermal de-icing systems as the user of energy, one
should consider that the different methods its selection differently
affect not these or other flight characteristics of flight vehicle,
either acting directly on the engine characteristics during the
selection from them of hot air or increasing the weight of apparatus.
Thus, for instance, the rate of climb of aircraft greatly strongly
affects air bleed from compressor [126].
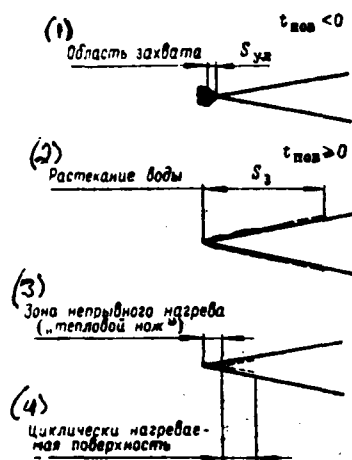
Fig. 3.31.
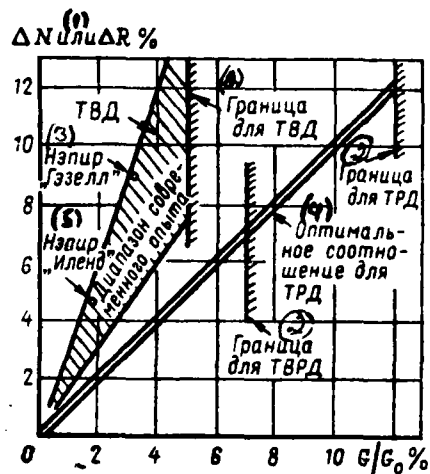
Fig. 3.32.

Fig. 3.31. Different size of warmed zone on sharp edge in cases of permanent and cyclic heating.

Key: (1). Capture region. (2). Spreading of water. (3). Zone of continuous heating ("thermal knife"). (4). Cyclically heated surface.

Fig. 3.32. Effect of air bleed from compressor on power or engine thrust:

G/G_0 - ratio of selected/taken air flow rate to general/common/total air flow rate through engine; ΔN, ΔR - change in thrust or power.

Key: (1). or. (2). Boundary for. (3). Nepir "Gazelle." (4). Optimum

relationship/ratio fcr. (b). Nepir "Island."

Page 80.

In turn, selection or one and the same quantity of air has different effect on the characteristics of the gas turbine engines of different diagrams. For TRD or usual diagram of expended power corresponds percentage decrease of the air flow rate through the turbine, as can be seen from rig. 3.32, borrowed from [107]. This TRD for protection from icing, and also for other needs can have selected to 12o/o of general/common/total air flow rate. More sensitive to air bleed from compressor is TVRD, ror which the air bleed must not exceed approximately/exemplarily 7o/o of the general/common/total air flow rate. Even more sensitive in this respect is TVD, in which it is lost by 2-3o/o of power by every 1o/o of selected/taken air; therefore permissible selection is limited only 5c/o of general/common/total air flow rate through the compressor.

3.7. Evaluation of the weight characteristics of de-icing system during design.

The weight of de-icing system has noticeable effect on the transport effectiveness of aircraft (helicopter) or its tactical flight data, for example, work [107] produces decrease of payload

approximately/exemplarily on 30/o for aircraft and on 60/o for helicopters.

In work [147] it is indicated that according to statistical data the weight of the structure POS or aircraft is approximately 0.8-1.0o/o of takeoff weight. There is given formula for the rough estimate of the weight FCS of the aircraft

$$G_\kappa = 225 + 0{,}003 G_0 \; \textit{кг}, \qquad (3.2)$$

where G_κ - a weight of structure POS;

G_0 - the takeoff weight of aircraft.

For a helicopter this weight relatively higher and even for most economical POS reaches 1.250/o of takeoff weight [107].

The given data are related to the adjusting weight of the structure of de-icing systems. However, the presence of protective system from icing on board aircraft or helicopter is connected with the expenditures of power for its work and with the expenditures of fuel/propellant, necessary for its "transport" by air. Furthermore, some elements/cells POS can cause an increase in the drag of flight vehicle, which will be also connected with the supplementary expenditures of power and fuel/propellant.

MICROCOPY RESOLUTION TEST CHART

NATIONAL BUREAU OF STANDARDS-1963-A
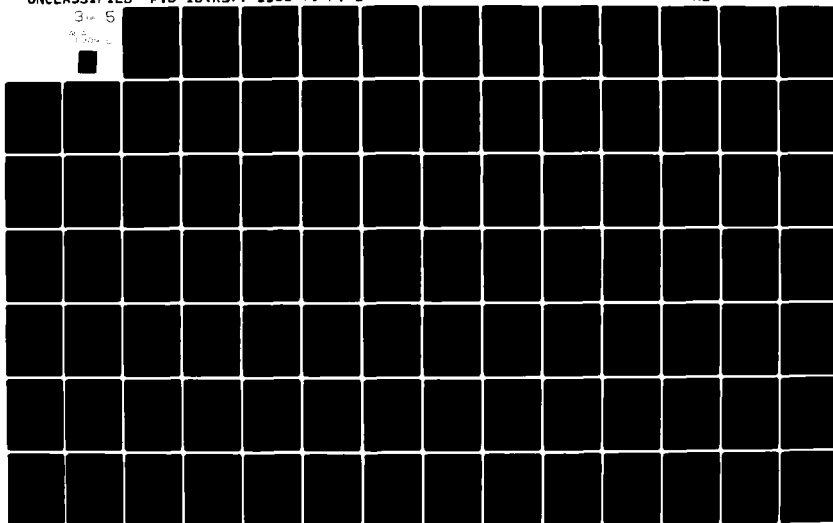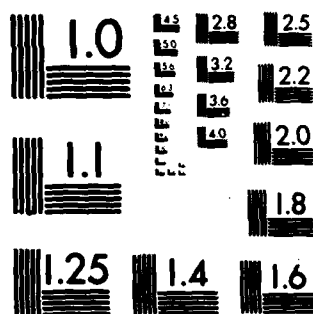
Page 81.

These expenditures can be presented in the form of the equivalent

weights which are added to the weight of structure POS:

$$G_{\text{пос}} = G_{\text{к}} + \Delta G_{\text{т}}^{\circ} + \Delta G_{\text{м}}^{\circ} + \Delta G_{\text{с}}^{\circ}, \qquad (3.3)$$

where $G_{\text{к}}$ - an adjusting weight of structure PCS;

$\Delta G_{\text{т}}^{\circ}$ - fuel load which is required for the "transportation" of de-icing

system with a weight of $G_{\text{к}}$;

$\Delta G_{\text{м}}^{\circ}$ - entire, equivalent horsepower, which is necessary for a work

POS;

$\Delta G_{\text{с}}^{\circ}$ - weight, equivalent to the drag which produces separate

elements/cells POS.

Adjusting weight POS is the total weight of the

construction/design of the deicers of the aircraft components or

helicopter, i.e.

$$G_{\text{к}} = \sum_{i=1}^{n} G_{\text{кi}} + \sum_{j=1}^{m} G_{\text{к. ист}j}, \qquad (3.4)$$

where $\sum_{i=1}^{n} G_{\text{кi}}$ - the total weight of the heaters of surface (wing, tail

assembly, air intakes of engines, glasses, screws/propellers, etc.),

including the weight of distributive, commutation and signalling

devices, and $\sum_{j=1}^{m} G_{\text{к. ист}j}$ - a weight of the structure of the sources of

powers which provide energy input into de-icing system. The weight of
the heaters of surface depends on the principle of their operation.
Thus, for instance, according to data [65] the weight of the
structure of the deicer of wing can be found from the equation

$$(G_{\text{я}})_{\text{кр}} = C_1 L_{\text{кр}}. \qquad (3.5)$$

where C_1 - a statistical coefficient in kG/m;

L - wingspan m.

Value C_1 composes approximately/exemplarily 5.8-6.0 for the
air-heat heaters and 3.8-4.1 for thermoelectric ones. But the more
precise evaluation of the weight of de-icing systems can be fulfilled
only on the basis of the data which can be accumulated during the
design of analogous devices/equipment.

The total weight of the sources of power for POS also depends on
the design features of system. Are possible the most varied
combinations with the use of sources indicated above of power. Let us
assume that the total number of heaters of surface in de-icing system
can be presented in the form of the sum

$$n = n_1 + n_2 + n_3 + n_4. \qquad (3.6)$$

where n_1 is the number of heaters to which is fed/conducted hot air
directly from the compressor of engine; n_2 - number of heaters,
connected with the special heat exchanger (in which are utilized, for

example, exhaust gases); n_3 - number of heaters with power supply from generators and n_4 - the number of heaters to which the required power is fed/conducted from auxiliary power unit (VSU).

Page 82.

Then the total weight of construction/design m of the sources of power or their parts, which ensure the operation of de-icing system as a whole, can be determined by the formula

$$\sum_{j=1}^{m} G_{\text{ист}\, j} = G_{\text{т. о}} + \frac{G_{\text{т}}}{N_{\text{т}}} \sum_{i=1}^{n_3} \frac{Q_i}{\eta_i} + \frac{G_{\text{BCY}}}{N_{\text{BCY}}} \sum_{i=1}^{n_4} \frac{Q_i}{\eta_i}, \qquad (3.7)$$

where $G_{\text{т. о}}$ - all constructions/designs of the special heat exchanger;

$G_{\text{т}}$ and $N_{\text{т}}$ - weight and power of the generators;

G_{BCY} and N_{BCY} - weight and power VSU;

Q_i and η_i - calorific requirement (required power) and thermal efficiency (coefficient of heat use) for the i deicer of wing, tail assembly of engine, glasses, etc.).

The values of the majority of the parameters, which stand in the right side of formula (3.7), either are known during the design of aircraft or it is possible to rate/estimate them according to statistics. In particular, the thermal efficiency of the air-heat

heaters lies/rests in the range 0.4-0.75, and the efficiency of

thermoelectric heaters is equal to approximately/exemplarily 0.8-0.9.

Values Q_i can be approximately calculated on the basis of

average/mean heat-flux density $\bar{q}_n$ from the formula

$$Q_i = \tilde{q}_n \cdot F_i. \qquad (3.8)$$

where F_i - surface area of the i heater to which is fed/conducted the

power. For the deicers of continuous action this area is equal to the

complete area of heater $F_{n \cdot нi}$, and in the case of cyclic deicer F_i it is

found from the expression

$$F_i = \frac{F_{n \cdot нi}}{n_c}, \qquad (3.9)$$

where n_c - a quantity of sections in the deicer in question.

As far as value is concerned of average/mean heat flux, then

approximately it is possible to consider that $\bar{q}_n \approx 1.0$ W/cm² for the

heaters of permanent action and approximately/exemplarily 1.5-2 times

more for cyclic heaters. More precision determination of external

heat flux is given in chapter V, VI and VII.

Page 83.

Unfortunately, there is insufficient information by the weights

of special heat exchangers for de-icing systems.

In the past on poston-engined aircraft sufficiently widely were

utilized benzine heaters. On aircraft with jet engines, besides air
bleed from compressors, it is expedient to utilize the heat
exchangers, which work on exhaust gases. One of the versions of such
heat exchangers successfully is applied, for example, on English
aircraft "Argosy" [58].

The quantity of fuel/propellant, which must be had during
takeoff directly for the "transportation" of the weight of structure
POS, can be determined as follows:

$$\Delta G_{\text{т}}^{\cdot} = G_{\text{к}} \frac{G_{\text{т}}}{G_{0}}, \qquad (3.10)$$

where $G_{\text{т}}$ - gross weight of fuel/propellant on takeoff.

The weight, equivalent to a quantity of heat which is
selected/taken with hot air directly from the compressor of engine or
with the aid of the generators, which have power drive, it is
possible to present in the form of this relationship/ratio:

$$\Delta G_{\text{м}}^{3} = \frac{G_{0}}{N_{\text{с. у}}} \sum_{i=1}^{n_{1}} \frac{G_{i}}{\eta_{i}}, \qquad (3.11)$$

where G_0 - complete complete takeoff weight of aircraft or
helicopter;

$N_{\text{с. у}}$ - installed power

In the case of turbojet and turbofan engines into formula (3.11)
must be substituted their equivalent horsepower, i.e.

$$N^\bullet_{\text{c. y}} = n_{\text{дв}} \cdot P_{\text{дв}} \ V_{\text{кр}} \ \ \kappa\Gamma \cdot \textit{м/сек}, \qquad (3.12)$$

where $n_{\text{дв}}$ – a quantity of engines on aircraft or helicopter;

$P_{\text{дв}}$ – thrust of one engine in the кчf:

$V_{\text{кр}}$ – Cruise speed of aircraft in m/s.

If on aircraft (helicopter) are autonomous air intakes for POS, then this can lead to an increase in the drag of aircraft. In this case effect POS on drag also it is possible to express by the equivalent weight

$$\Delta G^\cdot_c = (\Delta X_c)_{\text{пос}} \frac{G_\bullet}{X}, \qquad (3.13)$$

or

$$\Delta G^\cdot_c = K (\Delta X_c)_{\text{пос}}.$$

where X_c – the total drag of the aircraft;

K – quality coefficient of aircraft (in cruise).

Page 84.

An increase in the drag due to autonomous air intake is designed from the known formula

$$(\Delta X)_{\text{пос}} = (c_x)_{\text{заб}} \frac{\varrho V_0^2}{2} \ S_{\text{заб}}. \qquad (3.14)$$

Thus, complete equivalent weight POS on takeoff can be determined on the basis of the following formula:

$$G^{\cdot}_{\text{пос}} = G_{\text{к}} \left(1 + \frac{G_{\text{т}}}{G_{\text{o}}} \right) + \frac{G_{\text{o}}}{N_{\text{c. y}}} \sum_{i=1}^{n} \frac{Q_i}{n_i} + K(\Delta X)_{\text{пос}}, \quad (3.15)$$

in which the adjusting weight of structure $G_{\text{к}}$ is determined either from the statistical dependences of form (3.5), or by the direct calculation of weight after sketch design of one of the versions POS taking into account formulas (3.4) and (3.7).

The value of complete equivalent weight can serve as a comparative criterion of the efficiency/cost-effectiveness of the diverse variants of the de-icing systems which can be designed for this aircraft or helicopter. Physically this value indicates, to what extent is decreased payload weight during installation POS to aircraft. At the same time, knowing the equivalent weight of system, it is possible to rate/estimate its effect on the tactical flight data of aircraft.

chapter IV.

Methods of the definition of the zones of icing (zones of "catching")
on the surface of aircraft [1].

FOOTNOTE [1]. It is written to B. A. Stroganov. ENDFOOTNOTE.

Ice formation on the surface of aircraft can be represented as
the result of two phencmena:

- the collision of drops with the surface;

- spreading and freezing of these drops.

4.1. Collision of drops with the surface of the flying body.

In the majority of the works, dedicated to questions of aircraft
icing, instead of the term the collision of drops with surface is
used term catching or capture/grip of drops by surface. Althcugh
these terms are deprived of direct visual representation as concept
collision, in view of their general/commcn/total use and wide
acceptance subsequently we will use them.

Page 85.

The catching of drops by surface depends on the character of its aerodynamic flow, value and direction of the forces, which effect on drops and being determining the trajectories of their motion relative to surface.

The trajectories of the drops, which are contained in airflow, which encounters to surface, do not coincide with the flow lines of air, as a result of which the part of drops (it recovers by it), but another part passes it and is taken away by air flow (Fig. 4.1).

Quantitatively this phenomenon is characterized by the interception coefficient, which are the ratio of the mass of water, which contains in the incident flow, to the mass of water, by the recovered surface, in this interval of time. Are distinguished general/common/total and local interception coefficients.

The general/common/total, or integral interception coefficient, which relates to an entire zone of catching $S_{y\pi}$ is determined by the relation

$$E = \frac{G_{y\pi}}{w \cdot V_0 \cdot C_{max}},\qquad (4.1)$$

where $G_{y\pi}$ - a mass of the water, which caught into the unit of length (spread/scope of surface 1 s), in kg/s·m;

w - water content water content of clouds in kg/m^3;

C_{max} - thickness of midsection profile cross section m;

V_0 - flight speed in m/s.

Local interception coefficient e is analogous in sense, but it is related to the elementary section dS on the surface of catching about the point in question.
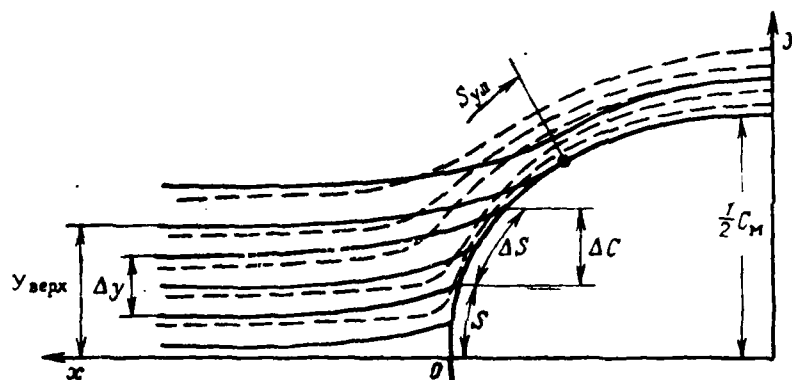
---- the trajectory of drops.

---- the flow line of air.

Fig. 4.1. Catching of drops on surface. System of coordinate axes.

Page 86.

With respect to the trajectories of the motion of drops
general/common/total interception coefficient can be presented as the
relation

$$E = \frac{(y_{\text{верх}} - y_{\text{нижн}})v_{\text{л}}}{C_{max}}, \qquad (4.2)$$

where $y_{\text{верх}}$ **and** $y_{\text{нижн}}$ - coordinates at infinity of the trajectories of
drops, tangents to upper and lower surface respectively.

Local interception coefficient also can be presented as

$$\varepsilon = \frac{dy}{dC} = \frac{\backslash y}{\Delta C}, \qquad (4.3)$$

where $\backslash y$ - difference of ordinates at infinity of the trajectories
of drops which fall to upper and lower boundaries of the area/site in
question; ΔC - projection of area/site ΔS is normal to flow. makes it
possible to also establish/install the zone of catching $(S_{\text{улл}})$, which is
area, prisoner between points on the upper and lower surface, in
which occurs the contact of trajectories with the surface (see Fig.
4.1). Zone and interception coefficient are the most important

parameters, which are determining intensity and ice hazard.

Spreading and freezing of drops from surface they are determined by the thermodynamic processes, which occur on surface, and first of all depend on the temperature of surface. If the temperature of surface is relatively high (it is close to 0°C), then the drop of water, after being hammered against surface, communicates to it certain energy content due liberation of latent heat of fusion with freezing. This leads to the fact that the drops, or are more precise a layer of moisture, they do not freeze immediately, but they spread up to certain distance. In this case occurs the partial loss of moisture due to evaporation and its blowing from surface into boundary layer (Ludlam's effect).

For the characteristic of this phenomenon is introduced the coefficient of freezing ξ_n, which gives the relationship/ratio between the mass of ice G_n, frozen in this section of surface, and the mass of the water, grasped in this section per unit time, $G_{\text{у}n}$:

$$\xi_n = \frac{G_n}{G_{\text{у}n}} = \frac{G_n}{\varepsilon \cdot \omega \cdot V_0 \cdot \Delta C}. \qquad (4.4)$$

4.2. Conclusion/output of the equations of motion of drop in air flow.

The majority of tasks regarding zones, coefficients and other

parameters of catching is solved by the construction of the
trajectories of the motion of drop in air flow, which flows around
about the body.

Page 87.

The determination of trajectories is produced on the basis of
equations of motion which link the real forces, which effect on drop,
and the inertial force. During motion the drops in air flow, if we
disregard/neglect gravitational force, to it acts only the
aerodynamic force, equal to

$$P_\kappa = \frac{1}{2} c_D \varrho |\vec{u}_\kappa|^2 F_\kappa, \qquad (4.3)$$

where c_D - a drag coefficient of the drop; ρ - air density; $\vec{u}_\kappa$ -
speed of drop relative to the air; F_κ - area of the lateral surface
of drop.

According to the second law of dynamics this force can be expressed
through mass and acceleration of the drop

$$P_\kappa = m_\kappa \cdot a_\kappa, \qquad (4.5a)$$

where m_κ - a mass of the drop; a_κ - acceleration of drop under the
action of force P_κ.

Counting the drop of spherical, this is expression, utilizing

radius (r_κ) and water density (ϱ_a), it is possible to convert as follows:

$$\frac{4}{3}\pi r_\kappa^3 \varrho_\mathrm{a} a_\kappa = \frac{1}{2} c_D \varrho |\vec{u}_\kappa|^2 4\pi r_\kappa^2 \qquad (4.5б)$$

or

$$\frac{d|\vec{u}_\kappa|}{dt} = \frac{3}{2}\frac{c_D\varrho}{r_\kappa\varrho_\mathrm{a}}|\vec{u}_\kappa|^2 = \frac{3}{2}\frac{c_D\varrho}{r_\kappa\varrho_\mathrm{a}}|\vec{v}-\vec{u}_\kappa|^2. \qquad (4.5в)$$

In this expression the relative speed of drop $\bar{u}_\kappa$ is represented as modulus of a difference in the vectors: to the speed of drop $\vec{u}_\kappa$ and air speed $\vec{v}$.

For convenience in the calculations equation (4.5) one should lead to the dimensionless form. A radius of drop and all other linear dimensions it is expedient to express with respect to the significant dimension of body and L (chord, length, radius, etc.), for which this equation is solved $\left(\bar{r} = \frac{r_\mathrm{м}}{L}; \bar{C} = \frac{C_{max}}{L}; \bar{x} = \frac{x_\mathrm{м}}{L}\right)$; the speed of drop u_κ and air flow v can be represented with respect to velocity of incident flow $V_0 : \bar{u} = \frac{u_\mathrm{ж}}{V_0}; \bar{v} = \frac{v}{V_0}$, and time t is represented in the form of dimensionless time $\bar{\tau} = \frac{t \cdot V_0}{L}$, unity of which is equal to the time, necessary in order to cover a distance of L with a a velocity of of V_0.

Page 88.

Furthermore, let us introduce the following designations:

$$Re_\bullet = \frac{2r_\kappa \cdot V_\bullet}{\nu}, \qquad (4.6)$$

$$\psi = \frac{9L\varrho}{r_\kappa \varrho_\bullet}, \qquad (4.7)$$

then by simple conversions equation (4.5) it is possible to lead to the form

$$\frac{du}{d\tau} = \frac{c_D \cdot Re_\kappa}{24} \frac{\psi}{Re_\bullet} |\vec{v} - \vec{u}|, \qquad (4.8)$$

where Re_κ - Reynolds number the drop

$$Re_\kappa = \frac{2r_\kappa |\vec{v} - \vec{u}|}{\nu}. \qquad (4.9)$$

The designations introduced above make specific physical sense and it is very convenient during calculation, since link the mode/conditions of flight with conditions icing and size/dimension of the body in question with the aid of the dimensionless parameters. Parameter Re_0 represents Reynolds number drop at the relative speed of drop, equal to velocity of incident flow. It characterizes initial conditions and does not depend on the position of drop in air flow and on the local velocity of air. Parameter ψ, which occasionally referred to as dimensional or scale parameter, characterizes the relationship/ratio between the sizes/dimensions of drop and the sizes/dimensions of body. As can be seen from equation (4.8), these parameters are criterial, since for guaranteeing the similarity of the trajectories of the motion of drops in geometrically similar bodies and airflow it

is necessary and it suffices to ensure their constancy.

The use/application of combination $\frac{c_D \text{Re}_\kappa}{24}$ is convenient to those

that for low ones Re_κ $\frac{c_D \text{Re}_\kappa}{24} = 1$ dependence $c_D = f(\text{Re}_\kappa)$ frequently represent

in the form $\frac{c_D \text{Re}_\kappa}{24} = \varphi(\text{Re}_\kappa)$.

Some authors [87] [89] instead of parameters indicated above Re_0

and ψ utilize parameter $k_* = \text{Re}_0/\psi$, which is called the parameter of

inertia, since it to some degree characterizes the force of inertia

of drop. Dormancy to our opinion, a shortcoming in this parameter in

the fact that is lost the literal and direct sense, which possess

parameters Re_0 and ψ. Furthermore, it does not eliminate the need

for the calculation of parameter Re_0, since, as will be shown below,

parameter Re_0 necessary in the majority of the cases for the

calculation of Reynolds number drop.

Page 89.

Passing to projections on axis of coordinates connected with

body, we will obtain the fundamental calculated equations of motion

of the drop:

$$\begin{aligned}
\frac{du_x}{d\tau} &= \frac{c_D \text{Re}_\kappa}{24} \cdot \frac{\psi}{\text{Re}_0}(v_x - u_x), \\
\frac{du_y}{d\tau} &= \frac{c_D \text{Re}_\kappa}{24} \cdot \frac{\psi}{\text{Re}_0}(v_y - u_y), \\
\frac{du_z}{d\tau} &= \frac{c_D \text{Re}_\kappa}{24} \cdot \frac{\psi}{\text{Re}_0}(v_z - u_z).
\end{aligned} \qquad (4.10)$$

These equations are initial during the determination of the
parameters of catching, since allow with one or the other
precision/accuracy to calculate trajectory the motions of drop of the
relatively considered/examined body. Between entering this equation
numbers $\dot{Re}_\kappa$ and Re_0 there is idle time the relationship/ratio

$$Re_\kappa = Re_0 \sqrt{(v_x - u_x)^2 + (v_y - u_y)^2 + (v_z - u_z)^2}, \quad (4.11)$$

which subsequently will ce frequently utilized instead of equation
(4.9).

Of that accepted is above assumptions the drop of water -
spherical in form and constant/invariable according to the
sizes/dimensions; gravitational force - is negligible; at the initial
moment of speed the drops and air - are equal, two first during
calculation de-icing systems practically always are satisfied, and
the third is correct, if the speed of flow is much more than the rate
of an incidence/drop in the drop, which for aircraft also is
provided.

4.3. The methods of the solutions of equations of motion.

Although mathematical equation of motion of special complexity
do not represent, their solution in practice is very labor-consuming
and it is usually connected with a whole series of simplifications.

In these equations enters a whole series of components, which often cannot be represented in an explicit form or in the form of the formulas, suitable for further solution. First of all this is related to the values of the drag coefficient c_D and local velocity of air v.

Drag coefficient c_D usually is taken according to the results of the experimental investigations of the resistance of spheres [ ] depending on number Re_κ (Fig. 4.2). For small Reynolds numbers $(Re_\kappa < 0,5)$ according to the law of Stokes $c_D Re_\kappa/24 = 1$. Utilizing this relationship/ratio, was made the series/row of the trajectory calculations and parameters of catching. Thus, for instance, L. M. Levin [31], examining a question about the precipitation of drops from flow to obstruction under condition $c_D Re_\kappa/24 = 1$, it established that the catching will occur only in such a case, when the relation of parameters ψ/Re_b will be more than certain specific (critical) value. The value of critical values $(\psi/Re_\sigma)_{\kappa\rho}$ for some different surfaces is given in Table 4.1.

Page 90.

Attempting to increase the range of the applicability of calculated formulas, Serafini [136] utilized the empirical dependence

$$c_D = \frac{24}{Re_\kappa}\left(1 - 0,158\cdot Re_\kappa^{\frac{2}{3}}\right).$$

With the aid of this relationship/ratio it derived the series/row of formulas for the catching of drops on wedge and double-wedge airfoil at supersonic speeds.

At present, when the solution of equations is fulfilled with the aid of high speed calculators, drag coefficient usually is assigned in the form of table $c_D Re_K/24 = \varphi_{\cdot}(Re_K)$, of datum in Table 3 of application/appendix.

The field of air speeds about the streamlined body is determined either from experiments via purgings, or by hydrodynamic computations.

The solution of the equations of motion of drop, if by any method they are prescribed/assigned drag coefficient c_D and the field of velocities $v(x, y, z)$, is fulfilled in by the aid of numerical methods in digital computers or on analogs.

One of the first installations for solving the task of catching was the mechanical differential analyzer of Lewis's laboratory (NACA).

However, calculaticn on mechanical analyzer remains very
labor-consuming. For conducting the calculaticn is continuously
necessary the participation of two-three operators and the cycle of
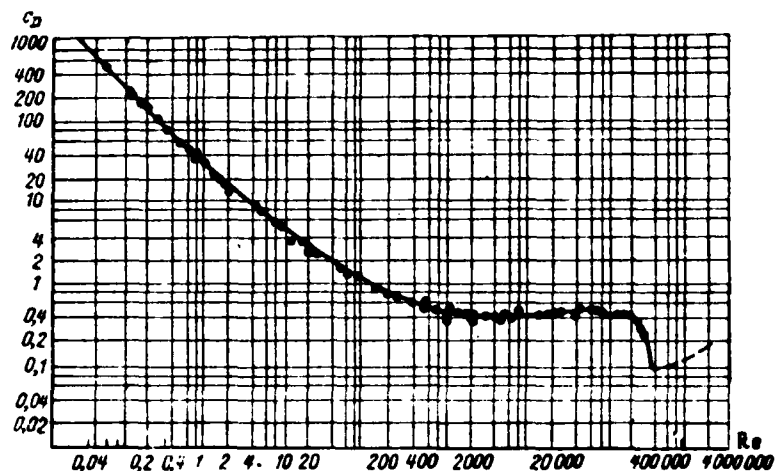calculation occupies sufficiently considerable time.

Fig. 4.2. Dependence of the drag coefficient of sphere on Reynolds number.

Page 91.

For the solutions of equations of motion from the point of view of the savings of time is very convenient the use/application of digital computers of the type "Urals", M-20 and so forth, etc. Programming for solving these equations is not characterized by special complexity and can be made by the programmer of average/mean qualification.

Especially showed well itself the use of calculators (for solving the equations of motion of drop) together with

electrohydrodynamic analogs (for determining of velocity fields about
the streamlined body) [71].

The use/application of electrohydrodynamic analogs for the
calculation of air-stream velocities is in detail presented in [55]
and [60]; therefore let us examine briefly only the essence of this
method.

The analogy between the motion, for example, of plane-parallel
air flow and electric current in two-dimensional conducting medium
directly d is visible from the comparison of their differential
equations.

Table 4.1. The minimum values of relation $\left(\frac{\psi}{Re_\theta}\right)_{\kappa\rho}$ with which occurs the catching of drops cn surface.

(1) Вид поверхностей	(2) Вид потока	$\left(\frac{\psi}{Re_\theta}\right)_{\kappa\rho}$
(3) Пластина	(4) Потенциальный, безотрывный	1
(4) Пластина	(5) Потенциальный с отрывом	$\frac{1}{\pi-4}$
(3) Пластина	(6) Удар плоской струи	$\frac{2}{\pi}$
(7) Пластинка в трубе при отношении ширины трубы к ширине пластинки, равном L	(4) Потенциальный, безотрывный	$\frac{1}{4}\cdot\frac{\sin\frac{\pi}{2l}}{\frac{\pi}{2L}}$
(8) Круговой цилиндр	(4) Потенциальный, безотрывный	$\frac{1}{8}$
(9) Эллиптический цилиндр при отношении осей, равном A	(10) То же	$\frac{1}{4(1-A)}$
(11) Шар	»	$\frac{1}{2}$
(12) Круглый диск	»	$\frac{\pi}{16}$

Key: (1). Type of surfaces. (2). Form of flow. (3). Plate. (4). Potential, nonseparable. (5). Potential with breakaway. (6). Impact/shock by flat/plane of drops. (7). Plate in pipe with ratio of width of tube to width of plate, equal. (8). Circular cylinder. (9). Elliptical cylinder in ratio of axes/axles, equal to A. (10). Then. (11). Sphere. (12). Circular disk.

Page 92.

For air flow. For the electric current

$$v_x = \frac{d\varphi}{dx}, \qquad\qquad i_x = \frac{dU}{dx},$$

$$v_y = \frac{d\varphi}{dy}, \qquad\qquad i_y = \frac{dU}{dy},$$

$$\frac{d^2\varphi}{dx^2} + \frac{d^2\varphi}{dy^2} = 0, \qquad \frac{d^2U}{dx^2} + \frac{d^2U}{dy^2} = 0,$$

v_x and v_y - components or the velocity vector of air along the axes x, y; φ - hydrodynamic potential; i_x; i_y - components of the vector of current density; U - electric potential.

For guaranteeing the similarity of the phenomena must be made the following conditions: a) electric analog must be geometrically similar to the object of study; b) the coefficients of electrical conductivity in model must be proportional to the density of air flow; c) boundary conditions for model and nature must be similar, i.e., they are connected with linear dependence.

Most frequently during the simulation of air flow are encountered the boundary conditions of this form: $d\varphi/dn = 0$ and φ=const. Condition $d\varphi/dn = 0$ is realized by installation into the electrically conducting medium of insulator. In this case the electric current can leak only along the isolated/insulated sections. This condition corresponds to the flow of the flow about the rigid surface or to flow at infinite distance from the streamlined body. The condition φ=const is realized with the aid of electric-conductive

tires, to which is fed/conducted direct/constant voltage.

For example, if the simulation of flow is fulfilled in electrolytic bath, then for the realization of the first condition it is established/installed the model of the streamlined body, made from insulator (paraffin, tree/wood, hardened paper, etc.). On the boundaries of bath, perpendicular to the incident flow, in electrolyte are dipped the electric-conductive tires, which simulate the conditions of the undisturbed flow.

The measurment of voltage U, which simulates hydrodynamic potential ϕ, is produced with the aid of probe and usually it is led to relative unity, i.e., the measured local potential difference is related to a voltage drop across busbars/tires. This is convenient to those that all results of measurements are obtained in portions from a voltage drop across busbars/tires and depend either on the absolute value of this potential difference or that its changes (in small limits) in resolving task. The measurment of the given voltage is accomplished/realized with the aid of bridge or compensating diagram.

Page 93.

The components of voltage U_x and U_y in directions x and y can be most simply determined with the aid of three-component tester. This

tester has three measuring probes, which give the values of voltage along the axes x and y. Then the corresponding components of velocity are approximately equal to

$$v_x \simeq \frac{\Delta U_x}{\Delta x}, \qquad v_y \simeq \frac{\Delta U_y}{\Delta y},$$

where ΔU_x and ΔU_y - a potential difference along the axes x and y, measured on the tester; Δx and Δy - distance between the measuring probes of tester.

Since distances Δx and Δy remain constant/invariable, then for calculation is necessary measurement only ΔU_x and ΔU_y. The values of measurments from tester, and also coordinates x and y are supplied into computer. In it is produced the calculation in accordance with the equations of motion of drops (4.10) and are determined the displacements of drop. If we connect the tester of electrolytic bath with the output of computer with servodrive, then the displacement of tester over electrolytic bath will correspond to the trajectory of the motion of drops. Fixing/recording this displacement on special plane table automatically, we obtain unknown trajectory.

The precision/accuracy of calculations depends on the error for electrolytic analog and error for the computing device/equipment.

According to the data of Abramson [71], accumulated error does

not exceed 2o/o. However, these questions exceed the scope of this
book and require more detailed examination.

The great advantage of electrolytic model is the fact that it
makes it possible to determine velocity field and to calculate the
trajectories of drops about the body of complex layout. This method
successfully can be used for the calculation both two-dimensional and
three-dimensional flow, in this case it is necessary only with
correspondingly to change the depth of bath. If we consider moreover
that the required precision/accuracy of calculations by the force of
the made assumptions (sphericity of drop, neglect of weight, etc.) is
small and is accompanied by usually experimental check under
conditions of icing, then this method must be recognized as one of
the most convenient methods for the calculation of the parameters of
the catching of drops.

4.4. Determination of the parameters, which characterize the process
of the catching of drops on the body surface of the simplest form.

The methods examined above of the trajectory calculations of
drops allow with one or the other precision/accuracy to determine the
following parameters of catching: interception coefficients, extent
of zone and mass flow rate of the catching of water.

Page 94.

However, unwieldiness of calculations and absence of sufficiently precise initial information (especially about velocity field about the bodies of intricate shape) led to the fact that such calculations were made only for that very limited in form of quantity of bodies.

Most completely the calculations of zones and interception coefficients were made for circular cylinders, ellipsoids of revolution and some profiles/airfoils. Although this information, naturally, do not exhaust all diverse cases, with which we encounter during the design of de-icing systems, they make it possible to come to light/detect/expose the general laws, which link the parameters of catching with flight conditions and meteorological conditions, and they give certain material which can be used in practice.

Circular cylinder.

The catching of drops by circular cylinders was examined in the series/row of works [87], [89], [150] it was initial stage during the solution of the tasks of catching. The calculation of the catching of drops on circular cylinder is fulfilled most simply, since the velocity field in circular cylinder in the uniform, potential, incompressible flow is described by the sufficiently simple

correlations:

$$v_r = 1 + \frac{y^2 - x^2}{(x^2 + y^2)^2},$$

$$v_y = -\frac{2xy}{(x^2 + y^2)^2}. \qquad (4.12)$$

These equations are analogously to equations (4.10) given in a dimensionless form, i.e., velocity is expressed relative to velocity of incident flow, and coordinates are given in the portions of a radius of cylinder.

The differential equations of motion of drops even in this simplest case can be solved only with the aid of computers. As a result of calculation are obtained trajectory of drops relative to cylinder as this shown in Fig. 4.3.

Fig. 4.4 shows the results of the calculations of the parameters of catching, made by different authors. The results of these calculations have certain disagreement, which depends on the method of calculation and made assumptions. In all cases the calculations began with the selection of "initial" conditions. As already mentioned higher, at "infinite" distance from the cylinder of the speed of drops and air flow they are accepted as identical ones. The examination of velocity fields about cylinder shows that it remains undisturbed approximately/exemplarily at a distance to five radii from the axis/axle of cylinder.

Page 95.

Noticeable changes in air circulation proceed only from $x=-5$ to the surface of cylinder; therefore with sufficient precision/accuracy it is possible to consider that at a distance of $x=-5$ of the speed of drops and air they drop and it is respectively equal to

$$v_x = u_x = V_\bullet,$$
$$v_y = u_y = 0.$$

After breaking distance from the axis/axle of cylinder to $x=-5$ to the series/row of the cuts (the more number it is selected cuts, the more precise the calculation), by numerical integration are solved equations (4.10) and are obtained the trajectories of motion. Upper trajectory, tangent to cylinder, determine the maximum extent of the zone of catching (angle $\theta_{y,n}$) for these conditions (ψ and Re_0). The drops, which move along trajectories arranged/located lower than tangential trajectories, recover by cylinder, while the drops, which move are higher than this of lines, they will pass past it.

General/common/total quantities of water, grasped by cylinder, is equal for a homogeneous cloud to the sum of the drops, which lie at band by the width, equal to $2y_{0y,n}$ since catching in the 3rd quadrant is analogous with the 4th ($y_{0y,n}$ — the ordinate of tangential

trajectory at infinity). Therefore the interception coefficient of cylinder E which is defined, as the relation of a quantity of water, which caught into cylinder, to a total quantity of water in the band of cloud by the width, equal to the diameter of cylinder, in this case is equal to $2y_{cyl}$.

A quantity of water, as this follows from (4.1), recovered by cylinder per unit time to linear meter, is equal

$$G_a = E \cdot D \cdot V_a w = 2y_{cyl} \cdot D \cdot V_a \cdot w \quad \text{кг/сек·м.} \qquad (4.13)$$
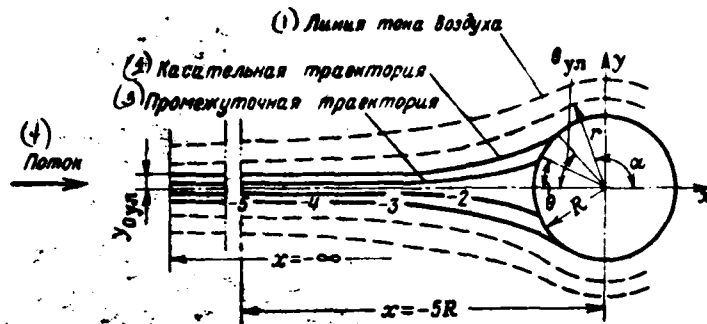
to Key: (1). Kg/S •m.

Fig. 4.3. Catching of drops on circular cylinder. Coordinate axes.

Key: (1). Flow line of air. (2). Tangential trajectory. (3). Intermediate trajectory. (4). Flow.
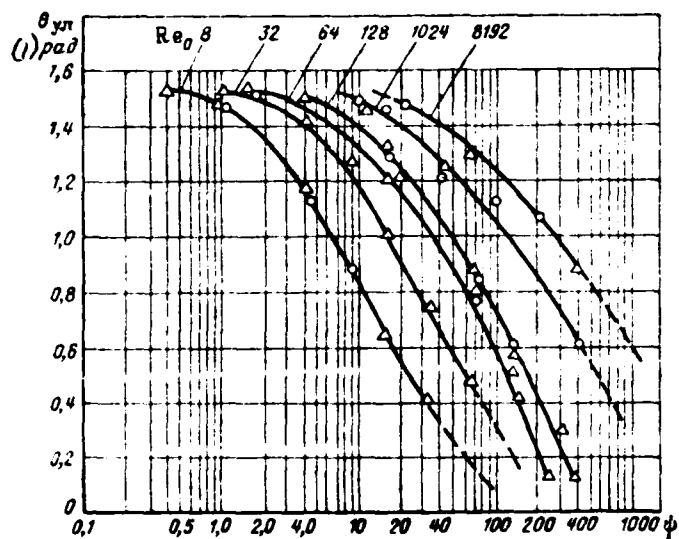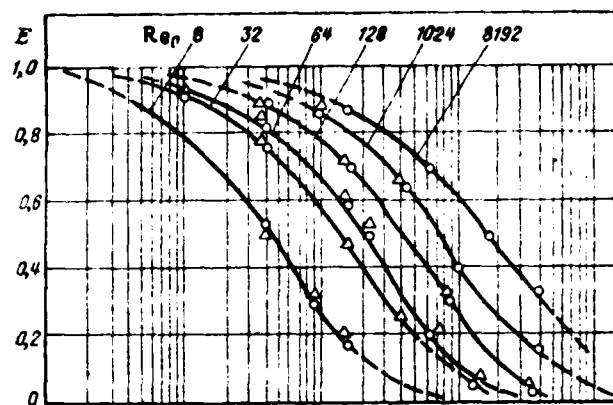
Page 96.

Fig. 4.4. Interception coefficient and maximum angle of catching for circular cylinder: o - according to data of Traybus; Δ - according to data of Bran, etc.

Key: (1). rad.

Page 97.

Local interception coefficient is defined as

$$\varepsilon = \frac{dy_0}{d\theta} \simeq \frac{\Delta y_0}{\Delta \theta},$$

where Δy_0 - distance at infinity between the upper and lower trajectories, which fall to the element/cell of surface ΔF selected about the point in question, and $\Delta \theta$ the central angle corresponding to emu.

Local interception coefficient for a cylinder depends on values of E and $\theta_{y,n}$ [89] and can be determined according to the formula

$$\varepsilon = \frac{\pi}{2} \frac{E}{\theta_{y,n}} \cos\left(\frac{\pi}{2} \frac{\theta}{\theta_{y,n}}\right). \qquad (4.14)$$

The data Given above show that a change in the water density and air (for heights/altitudes to 10000 m) and temperatures (in usual range) affects the interception coefficients and extent of the zone of catching to a lesser degree than dimensions of drops, speed of

flow and size/dimension of cylinder. Coefficient and zone of catching
increase with an increase in the size/dimension of drops and speed of
flow, since increase inertial forces, and a change in the trajectory
occurs in smaller measure. An increase in the size/dimension of
cylinder leads to the decrease of the parameters indicated, since
increases the absolute size/dimension of distance on which begins to
diverge the flow line of air, and this leads to the fact that at the
same values of speed and with size/dimension of drop the resisting
force acts on drop larger time and it more strongly bends its
trajectory.

As can be seen from formula (4.14), local interception
coefficient has great value at the critical point of cylinder $\theta=0$ and
it is numerically equal to

$$\varepsilon_{max} = \frac{\pi}{2} \frac{E}{\theta_{y_{\pi}}}.$$

If $\varepsilon \simeq 1$, the this means that the intensity of catching at the
particular point is maximally possible for these conditions of icing,
i.e., all drops, which are contained in air flow, in the vicinities
of this point they reccver on surface.

Ellipsoid of revolution.

The catching of drops in the surface of ellipsoids of revolution

is of large interest on the strength of the fact that a considerable
number of different elements/cells of the flight vehicles (beginning
with the forward fuselage and terminating with different suspensions)
it can be in the first approximation, represented in the form of
ellipsoids of revolution. Interest in the sizes/dimensions of ice
formation on these elements/cells is determined by the fact that
frequently in the nose parts of the fuselage it is arranged/located
the antenna and other elements/cells of radar equipment or guidance
equipment whose work deteriorates, if on the surface of nose fairing
is formed a layer of ice.

Page 98.

    Bringing these elements/cells whose form is very different, to
ellipsoid is convenient to those that for ellipsoids of revolution
are known the equations of the flow of their incompressible potential
flow thanks to which the determination of the parameters of icing is
reduced to the direct trajectory calculation of the motion of drops
by integrating equations (4.10). Since the ellipsoid flow of rotation
of the flow, directed along principal axis/axle, is axisymmetric, the
motion of drops can be examined only in one meridional plane in the
system of coordinates z and r (Fig. 4.5), equations of motion in
which (in dimensionless form) take the form

$$\frac{du_z}{d\tau} = \frac{c_D}{24} \frac{Re_\kappa}{Re_0} \frac{\psi}{Re_0} (v_z - u_z), \left.\begin{array}{c} \\ \\ \end{array}\right\}$$

$$\frac{du_r}{d\tau} = \frac{c_D}{24} \frac{Re_\kappa}{Re_0} \frac{\psi}{Re_0} (v_r - u_r), \left.\begin{array}{c} \\ \\ \end{array}\right\} \qquad (4.15)$$

where u_z and u_r - speeds of drops along the axes z and r; u_z and v_r - air speed along this same axes/axles.

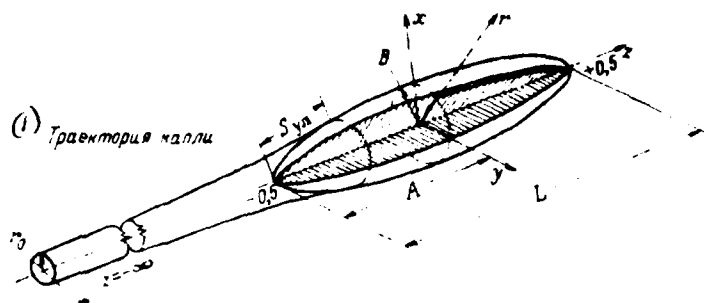As significant dimension is taken the transverse.

Fig. 4.5. Catching of drops on ellipsoid of revolution. Coordinate axes.

Key: (1). Trajectory of drop.

Page 99.

The components of the airspeed at any point of flow with coordinates z and r are equal to

$$v_z = 1 - c\left[\frac{1}{v_3}\ln\frac{\sqrt{M}+\sqrt{N}+v_3}{\sqrt{M}+\sqrt{N}-v_3} - \frac{1}{2}\left(\frac{1}{\sqrt{N}}+\frac{1}{\sqrt{M}}\right)\right], \quad (4.16a)$$

$$v_r = -\frac{r}{2}cr\left(\frac{1}{\sqrt{M}}-\frac{1}{\sqrt{N}}\right)\frac{1}{z^2+r^2+\sqrt{M}\sqrt{N}-\frac{v_3^2}{4}}, \quad (4.16b)$$

where

$$|\overline{M} = \sqrt{\left(z + \frac{\overline{e}_3}{2}\right)^2 + r^2},$$

$$|\overline{N} = \sqrt{\left(z - \frac{\overline{e}_3}{2}\right)^2 + r^2},$$

$$c = \frac{-\frac{1}{2}}{\frac{1}{2e}\ln\frac{1 + e_3}{1 - e_3} - \frac{1}{1 - e_3^2}},$$

$\overline{e}_3$ - eccentricity of the ellipse, which lies at meridional plane.

The procedure of the trajectory calculation of the motion of drops and determination of the parameters of the icing of ellipsoids is completely analogous to the procedure of calculation of catching on circular cylinder. Differential equations (4.15) also are solved with the aid of digital computers or with the aid of the differential analyzers.

Are given below the results of the calculations, made with the aid of the differential analyzers for ellipsoids of revolution with a thickness ratio of 10 and 200/o, during the flow of their air flow, directed along principal axis/axle [88].

Maximum extent $(S_{y,n})$ the zones of the catching of drops over the surface of ellipsoid of revolution and according to interception coefficient (E) are represented in Fig. 4.6 and 4.7 depending on parameters $\dot{\psi}$ and Re_0.

The effect of the fundamental characteristics of the flight conditions (speed and height/altitude) and size/dimension of drops to these parameters let us examine based on specific example. Let us determine zone and interception coefficient for a 10o/o ellipsoid in flight in a velocity of 360 km/u at the height/altitude of 1000 m in the cloud, which is of the drops with a diameter of 20 μ. The semimajor axis of ellipsoid is equal to 1 m. In this case of $Re_0 = 129$; $\psi = 1000$ and $S_{y,n} = 0.11$ (see Fig. 4.6b), and E=0.39 (see Fig. 4.6a). With an increase in the speed to 500 km/h ($Re_0 = 180$), $S_{y,n} = 0.14$, and E=0.42. With an increase in altitude to 7000 m at speed 360 km/h ($Re_0 = 79$) they will be respectively equal to 0.08 and 0.35. If flight occurred of the cloud, which is of the drops with a diameter of 40 μ, then for the height/altitude of 1000 m and velocity 360 km/h ($Re_0 = 258$; $\psi = 500$) $S_{v,n} = 0.25$ and E=0.62.

There is a definite interest in the examination of the icing of ellipsoids of revolution in the presence on the surface of the so-called "shaded zones" (Fig. 4.8). This zone is limited on the one hand to the surface of ellipsoid from the end/lead of the zone of catching along flow, but from other side by the trajectories of drops, very close to tangential trajectories, but no longer recovered by ellipsoid.
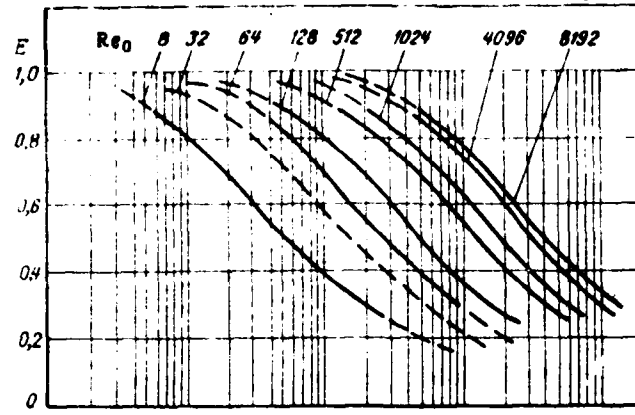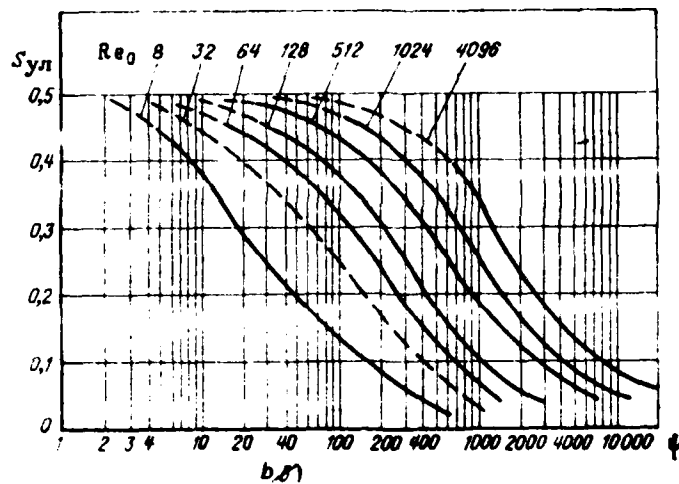
Page 100.

Within this zone the drops are absent, and it means, icing does not occur, then on the boundary of the "shaded zone" is observed the local increase (2-4 times) in the concentration of water d. s, connected with the "condensation" of their trajectories.

Fig. 4.6. Interception coefficient and extent of the zone of the catching of 10o/o ellipsoid of revolution. Air flow is directed along large axis/axle.

Page 101.

This phenomenon must be considered, in the first place, when selecting of the site of installation of ice-indicating equipment on board aircraft, for which it is necessary to ascertain that it does not fall into the "shaded zone", is otherwise knowingly unavoidable its ineffective work; in of the second, during the arrangement/position different external installations: antennas, branch connections, sensors, etc., since on the boundary of the "shaded zone" in places with the increased concentration of drops they will undergo intense icing, which can bring about a deterioration in their work or their even mechanical damages.
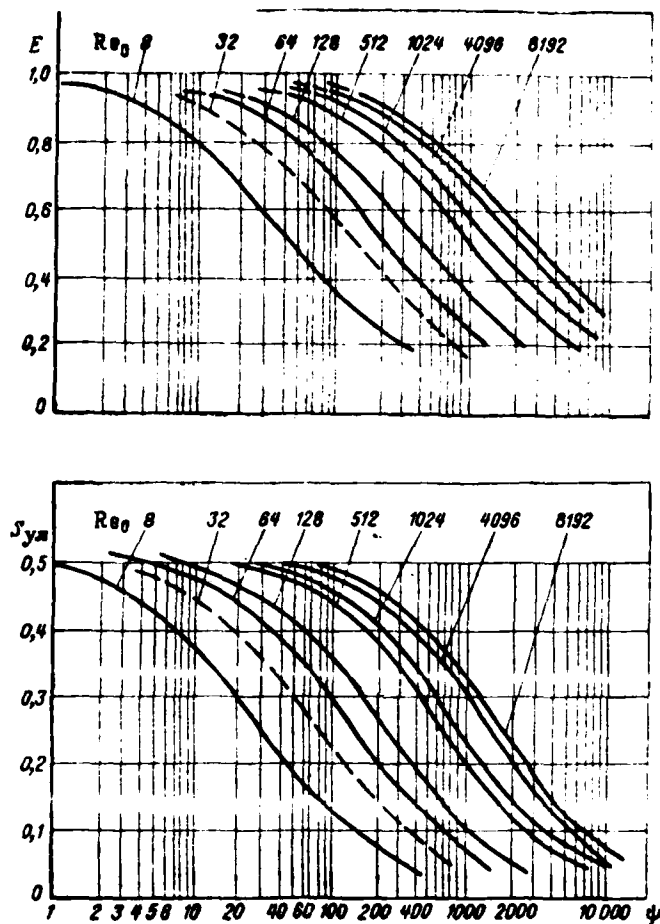
Fig. 4.7. Interception coefficient and extent of the zone of the catching of 20o/o ellipsoid of revolution.
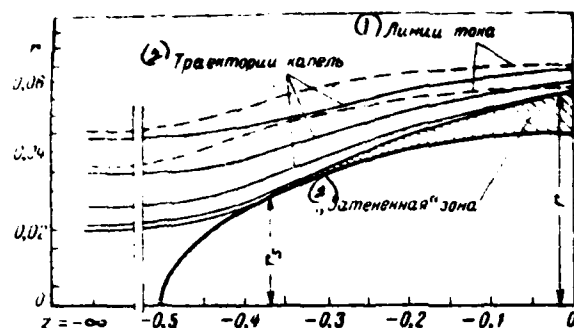
Page 102.

Fig. 4.8. Trajectory of drops and shaded zone in ellipsoid of revolution.

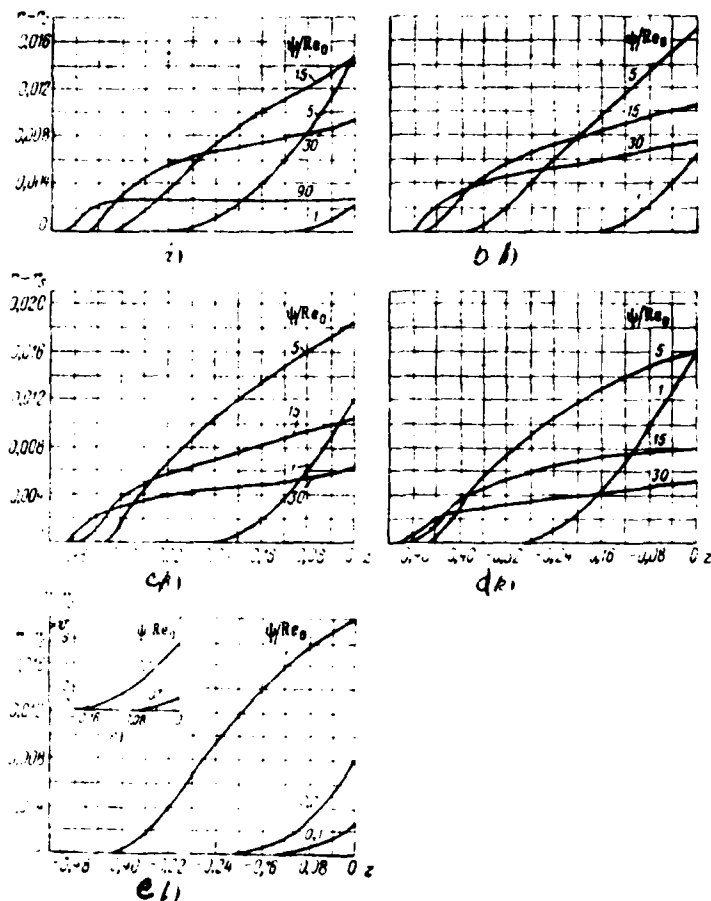Key: (1). Flow lines. (2). Trajectories of drops. (3). Shaded zone.

Fig. 4.9. Thickness of shaded zone on 20o/o ellipsoid of revolution (in fractions of semimajor axis); a) $Re_0=8$; b) $Re_0=128$; c) $Re_0=152$; d) $Re_0=1024$; e) $Re_0=4096$; f) $Re_0=8192$.

Page 103.

Location of the "shaded zones" and their dimensions for some-

conditions of icing (Re_0 from 8 to 1 8192) for ellipsoids of
revolution with a thickness ratio of 10 and 20o/o are given in Fig.
4.9 and 4.10 [88]. These data can be used when the design of de-icing
systems or selecting of the site of installation of signal of icing
on forepart/nose aircraft components or other elements of structures,
close in form to ellipscids of revolution.

4.5. Calculation of the zones of catching on wing profiles/airfoils.

In principle the order 1 of the calculation of the zones of
catching on wing profiles/airfoils does not differ from the
calculation methods examined earlier for circular cylinders or
ellipscids 1 of rotation. On 1 to the basis of that determined
according to purgings in aerodynamic ones to tubes or according to
velocity field calculations of air flow, which flows around about the
profile/airfoil, by numerical integration are determined the
trajectories of the drops of water, then from them are defined the
zones of catching on profile/airfoil during the flight conditions in
question, general/common/total and local coefficients of catching and
so forth, etc. At the same time calculation for wing
profiles/airfoils considerably becomes complicated because the
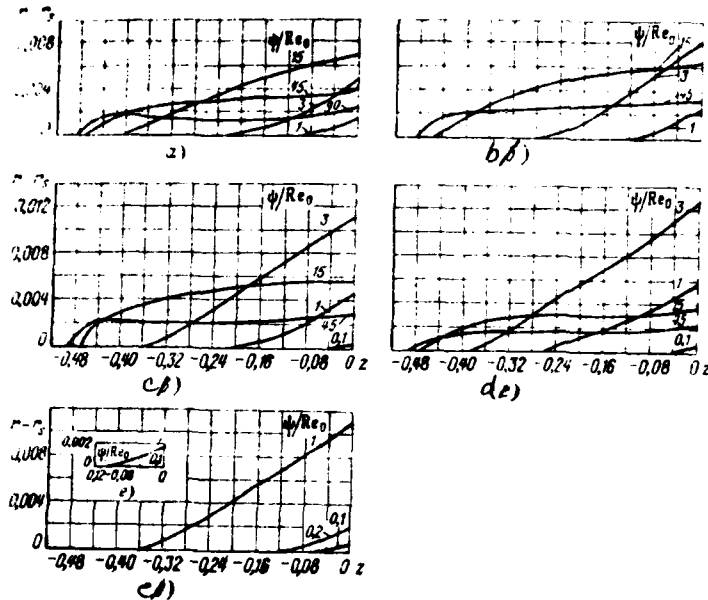velocity field of air flow, as a rule, it is not known.

Fig. 4.10. Thickness of the shaded zone on 10o/o ellipsoid of revolution (in fractions large semi-axis): a) $Re_0 = 8$; b) $Re_0 = 128$; c) $Re_0 = 152$; d) $Re_0 = 1024$; e) $Re_0 = 4096$; f) $Re_0 = 8192$.

Page 104.

While conducting of the wind-tunnel tests are usually limited to construction the diagrams/curves of pressures on profile, which makes it possible to determine local velocities on profile/airfoil, but it is insufficient for determining the speeds in air flow before it, which us interests to considerably larger degree. Is sufficiently accurate velocity field known only for some types of the

profiles/airfoils: the Zhukovskiy profile, some profiles/airfoils NACA, for which were made by a number of the authors "precise" calculations of the parameters of catching [36], [81].

The results of these calculations for convenience in their use in practice are rebuilt in the form of graphs and are given in Fig. 1-4 applications/appendices. These data can be directly used during calculations for the one-type profiles/airfoils or for profiles/airfoils, close in their aerodynamic characteristics, and in the first approximation, and for the profiles/airfoils of other types with estimate calculations. In this case also one should attempt to fit the cases, close from the point of view of aerodynamic flow pattern. During this selection as reference point for a comparison it is possible to accept coincidence or proximity of the diagrams/curves of pressure on the compared profiles/airfoils.

For the short-cut calculation of the zones of catching and interception coefficients Bergrun proposed semi-empirical method [81], special feature/peculiarity which is the fact that it is produced on the basis only of the form of profile/airfoil and distribution of local velocities according to its surface, i.e., on the base of those data which usually are as a result of the wind-tunnel tests.

Calculation according to this method is produced in reverse order, i.e., after assigning the position of any point on profile/airfoil are determined the conditions under which it will be the boundary of the zone of catching, or, to in other words are determined the conditions, under which the trajectory of the motion of drop, which passes through this point, will be tangential to surface.

As it was shown above, trajectories of the motion of drops in general form depend on the relationship/ratio of two parameters Re_0 and ψ. characterizing the conditions of icing and flight conditions; however, to each point of surface correspond many combinations ψ and Re_0. Therefore one of them must be accept or it is determined by any method, then second is possible to find by the aid of equations of motion. It is usually more convenient to be assigned by number Re_0, then from equations (4.10) we obtain

$$\psi = \frac{a_{\kappa} Re_0}{\left(\frac{c_n}{24} \frac{Re_{\kappa}}{}\right)\left(\frac{Re_{\kappa}}{Re_0}\right)}, \qquad (4.17)$$

where

$$a_{\kappa} = \sqrt{\left(\frac{du_x}{d\tau}\right)^2 + \left(\frac{du_y}{d\tau}\right)^2}.$$

Page 105.

This relationship/ratio is correct for any point in the trajectory of

the motion of drop, and it means, can be examined 1, also, at the

points, which correspond to the contact of trajectory with surface.

Thus, for any point on profile/airfoil and datum Re_0 it is necessary

to know how to determine values $\frac{c_D Re_\kappa}{24}$, $\frac{Re_\kappa}{Re_0}$ and a_κ or more precise

a_κ and Re_κ. since $\frac{c_D Re_\kappa}{24}$ is function Re_κ.

Relation $\frac{Re_\kappa}{Re_0}$ is determined approximately from the hodographs of

the speeds of drops and air in profile/airfoil. Examining the

hodographs of the air speeds and drops on Zhukovskiy profiles,

Vergran noticed, which independent of values ψ and Re_0 between them

is maintained/withstood the sufficiently specific relationship. Fig.

4.11 shows a typical example of the hodographs of the air speeds and

drops for a Zhukovskiy profile. As is evident, the hodographs of the

speeds of drops and air have the common point u=v=0, the hodograph of

drops for upper and lower surfaces passes through point $u_x = \cos \alpha$ and

$u_y = \sin \alpha$, which corresponds to the contact of trajectories at the

point of maximum thickness (in midsection), when tangential

trajectories are straight lines and coincide in the direction with
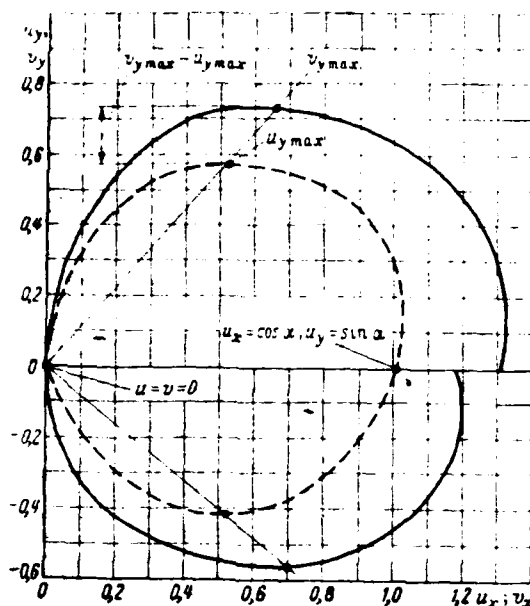
the incident flow.

Fig. 4.11. Typical hodographs of speeds (u_x; u_y) of drops, moving along tangential trajectories, and air speeds (v_x; v_y) on Zhukovskiy profile.

Page 106.

Furthermore, the maximum value of the vertical component of the speed of drop $u_{y\,max}$ occurs at the same point of the surface of the profile/airfoil where attains maximum the vertical component of air speed $v_{y\,max}$ or it is close to it, i.e., values $u_{y\,max}$ and $v_{y\,max}$ lie/rest on one straight line, passing through the origin of coordinates.

The hodograph of air speed easily can be constructed, if is

known the value of local velocities on profile/airfoil and its form.
The hodograph of the speeds of drops is constructed approximately on
characteristic points indicated above. Two of them (point $u=0$ and $v=0$
and $u_x = \cos\alpha$; $u_y = \sin\alpha$) are determined directly from physical flow
pattern, the third (point $u_{y\,max}$) is determined in a following manner.
As already mentioned higher, the position of points $u_{y\,max}$ and $v_{y\,max}$ on
profile/airfoil, but it means, also direction of the vectors of these
speeds coincides. Examining the hodographs of the air speeds and
drops in Zhukovskiy profiles, Bergran established that there is a
certain dependence between their values. This dependence in the form
of the relationship/ratio between $v_{y\,max} - u_{y\,max}$ and $v_{y\,max}$ is represented
in Fig. 4.12 with aid of which is located third point necessary for
the construction of hodograph.

The approximate construction of the hodograph of the speeds of
drop is fulfilled as follows (Fig. 4.13). On the hodograph of air
speed is noted point $v_{y\,max}$, which is connected by straight line since
the origin of the coordinates. With the aid of value $v_{y\,max} - u_{y\,max}$, of
that undertaken with Fig. 4.12, is plotted/deposited value $u_{y\,max}$ and
is determined $\left(\dfrac{Re_\kappa}{Re_0}\right)_{u_{y\,max}}$. In the first approximation, for the remaining
points of profile/airfoil it is accepted that

$$\frac{Re_\kappa}{Re_0} = \frac{v}{v_{u_{y\,max}}} \cdot \left(\frac{Re_\kappa}{Re_0} \right)_{u_{y\,max}}. \qquad (4.18)$$

With the aid of this relationship/ratio is constructed the curve A

(see Fig. 4.13) of the first approximation of hodograph. This curv
usually does not run through point $u_x = \cos \alpha$; $u_y = \sin \alpha$, which is the
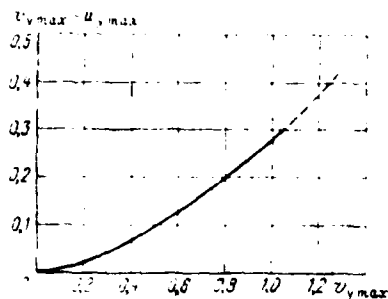third necessary point of the hodograph of the speed of drop.

Fig. 4.12. Dependence between the maximum vertical air speed $v_{y\,max}$ and a difference in the air speeds and drop.

Page 107.

For eliminating this shortcoming from point $u_x = \cos\alpha; u_y = \sin\alpha$ is carried out the curve B, tangential to by the curve A, and as a result is obtained the "final" hodograph of the speed of drop.

Error which is obtained during this approximate construction of the hodograph of the speeds of drop, according to Bergran's data, does not exceed 10-15o/o.

After constructing thus the hodographs of speeds for each point of profile/airfoil, is determined value Re_x/Re_0, necessary for determination φ from formula (4.17). entering this formula value a_x is computed according to the empirical dependence

$$a_\kappa = v \frac{dv}{dS} \, ,$$

(4. 19)

or

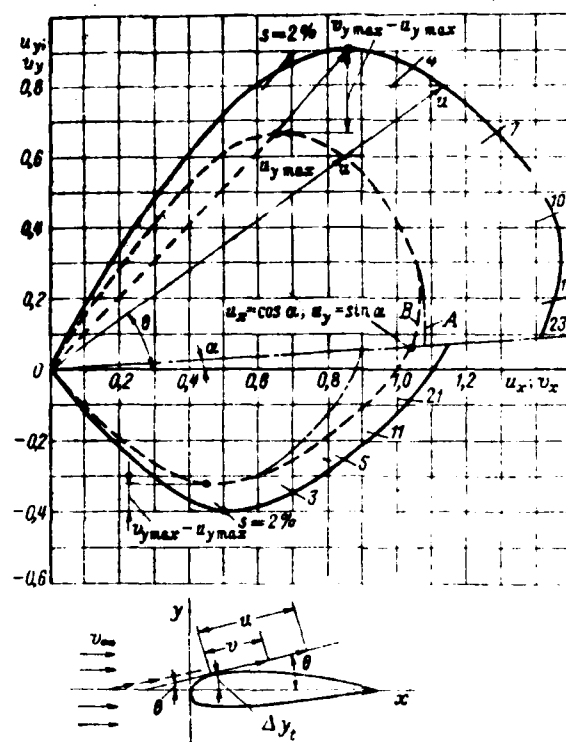$$a_\kappa = v_z \frac{dv_z}{dS} \, .$$

(4. 20)

Fig. 4.13. Approximate plot of the hodograph of the speeds of drops, which move along tangential trajectories (according to Bergran's method).

Page 108.

Entering into these equations the gradients of velocity dv/dS and
dv_r/dS easily can be obtained directly by construction v=f(S) or
$v_r = \varphi(S)$ depending on distance from profile/airfoil S and by
determination of the tangent of the inclination/slope of this curve
at the point in question.

Since previously it cannot be determined, which of formulas
(4.19) or (4.20) gives more exact solution, then for a control/check
it is necessary to utilize the fact that $a_\kappa = 0$ at the points at which
the straight lines, parallel to the incident flow, concern upper and
lower, surface of profile/airfoil. For calculation should be utilized
that of these formulas, that more accurately satisfies this
condition.

After determining thus value ψ on the basis of the surface of
profile/airfoil, they isolate the region of catching, i.e., that part
of the profile/airfoil on which these values satisfy the
prescribed/assigned conditions on flight conditions and the

sizes/dimensions of cloud drops.

For the very small/fine drops whose catching occurs only in the
vicinities of critical point, as this has already been noted earlier,
there exists specific value $\psi_{\text{кр}}$, beginning with which drop not at all
they fall to profile/airfoil, but they are taken away by flow. For
the vicinities of critical point value $\psi_{\text{кр}}$ can be determined by the
formula

$$\psi_{\text{кр}} = 4\text{Re}_0 \left(\cdot \frac{dv}{dS} \right)_{\text{кр}}, \qquad (4.21)$$

where $\left(\frac{dv}{dS} \right)_{\text{кр}}$ represents speed change along flow line near the
stagnant point whose values for Zhukovskiy profiles are represented
in Fig. 4.14. These graphs can be used for the calculation of the
minimum possible $(E=0)$ catching of drops only in the vicinities of
critical point.

Interception coefficient as distance ratio between tangential
trajectories at infinity to the distance between points of contact of
tangency on the surface of profile/airfoil $\Delta y_0 / \Delta y_t$ can be
approximately calculated, assuming that it linearly depends on ψ
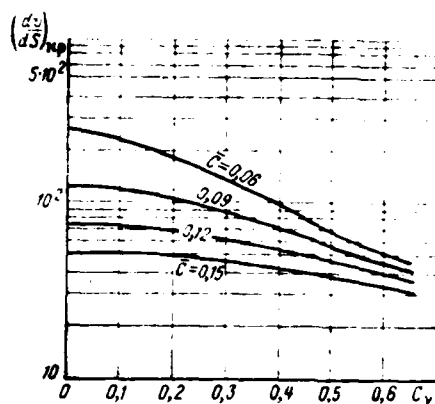with the permanent number Re_0.

Fig. 4.14. Dependence of the gradient of velocity $\left(\frac{dv}{dS}\right)_{\text{кр}}$ along stagnant flow line for a Zhukovskiy profile.

The data given above for Zhukovskiy profiles show that this assumption corresponds to reality in the range of the values of interception coefficients from 0 to 0.8. Thus, for any value of Re_0 easily can be constructed linear dependence Δy_n Δy_i on parameter ψ, if are known any their two values.

One of these values easily is determined from the presence of maximum $\psi_{\text{кр}}$, with which E=0. The second value is determined as follows. On the base of the calculation of the zones of catching $S_{\text{ул}} = f(\psi, Re_0)$ are constructed dependences $S = \varphi(\psi)$ with Re_0=const (Fig. 4.15a) which then are reconstructed dependence $\Delta y_i = \tau(\psi)$ (see Fig. 4.15b). Value Δy_i for each value of S is taken from the diagrams/curves of

profile/airfoil. Then on Fig. 4.16, in which is represented

dependence $\Delta y_t / C_{max}$ on angle of attack α for $\Delta y_0 / \Delta y_t = 0.8$ in Zhukovskiy

profile, is determined $\Delta y_t{}^{1}$ for that examined/considered α, and from

it on Fig. 4.15b is found value ψ, corresponding $\Delta y_0 / \Delta y_t - 0.8$ in our

specific case.

FOOTNOTE [1]. In chord. ENDFOOTNOTE.

This value is the second value, necessary for plotting of linear

dependence $\Delta y_0 / \Delta y_t$ on ψ with $Re_0 = const$ (see Fig. 4.15c).
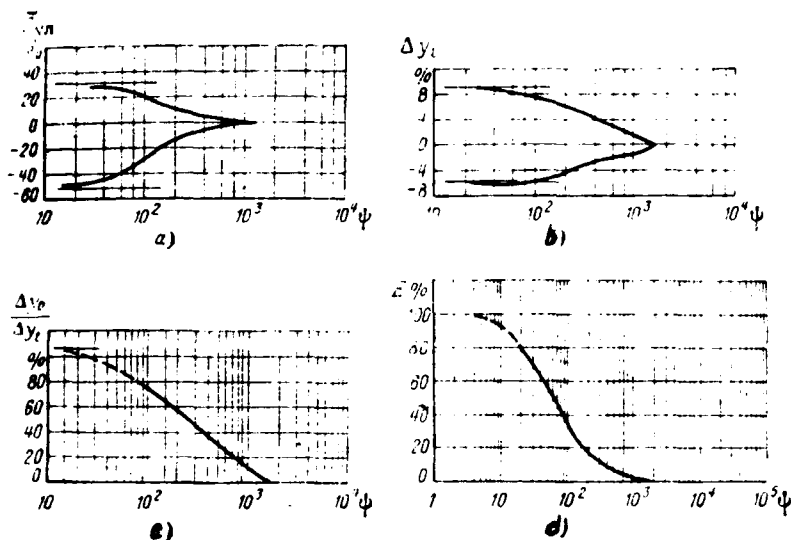
Fig. 4.15. Approximate determination of interception coefficient E (according to Bergran's method).

Page 110.

The general/common/total interception coefficient E of relatively maximum profile thickness C_{max} is determined with the aid of the relationship/ratic

$$E = \frac{\Delta y_0}{\Delta y_t} \frac{\Delta y_t}{C_{max}},$$ (4.22)

and then also it is represented in the form of curve $E - E(\psi)$ with $Re_0 = const$ (see Fig. 4.15d).

If is of interest distribution according to the zone of the

catching of local interception coefficient, then estimate calculation
can be made graphically by successive approximations as follows.

First is located the form of distribution, which corresponds to
the maximum catching of drops, i.e., to case $\psi = 0$. Is determined it
graphically very simply, since when $\psi = 0$ the trajectories of drops
will be straight lines, parallel to the incident flow. Therefore for
the determination of limiting distribution it suffices to conduct the
series/row of straight lines, parallel to the incident flow, and to
take ratio dy_0/dS on the duct/contour of profile/airfoil. Then for
those found earlier of the zone of catching and general/common/total
coefficient is accepted the linear distribution of drops. In this
case the distribution of local coefficients represents the triangle
whose base/root is equal to the zone of catching, and maximum value
ε'_{max} at apex/vertex at stagnant point is equal

$$v_{max} = \frac{2EC_{max}}{S_{ya}}. \qquad (4.23)$$

After this triangular distribution is modified in accordance
with limiting curve $\psi = 0$ in such a way that all values ε would
lie/rest within limiting curve, and the area of distribution was
equal to the area of triangular distribution.

Fig. 4.17 shows the sequence of the approximate construction of
the distribution of local interception coefficients by graphic
method. Dotted line plotted/applied the limiting curve of the

distribution (method of its determination is shown in Fig. 4.17a),
dot-dash line gave triangular distribution, and the final result of
the approximate distribution of local interception coefficients is
shown by solid line. In this case are possible two versions,
difference in which is clear from the figure (see Fig. 4.17b) and it
does not require special explanation. This construction is repeated
for several numbers Re_0. For a comparison Fig. 4.17c gives
distributing the local interception coefficients for profile/airfoil
$NACA65_2-0.15$. As is evident, the qualitative character of the local
distribution of catching, obtained to approximation/approach
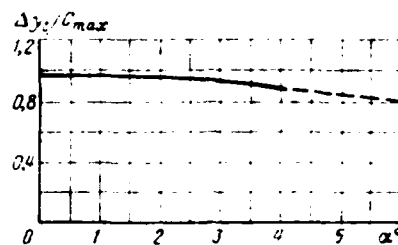graphically and "by accurately" calculation, it is very close.

Fig. 4.16. Dependence of relation $\Delta y_l / c_{y\,max}$ on angle of attack for a Zhukovskiy profile ($\Delta y_w / \Delta y_l = 0.8$)
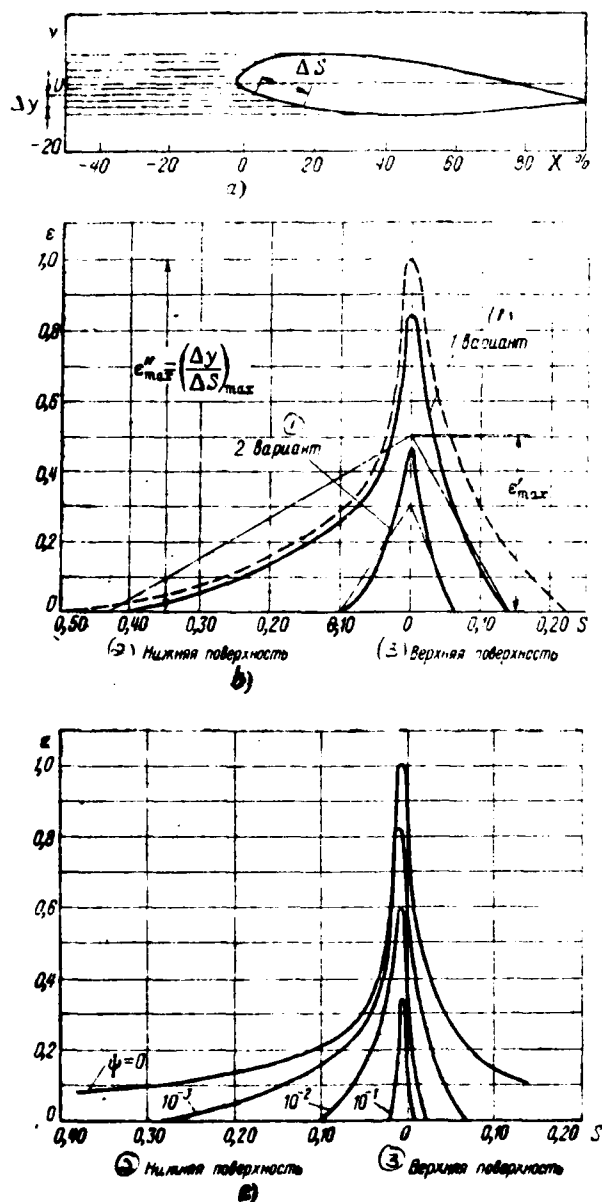
Page 111.

Fig. 4.17. Approximate determination of local interception
coefficient ε (according to Bergran's method).

Key: (1). version. (2). Lower surface. (3). Upper surface.

Page 112.

The method of approximate computation examined above gives good
results for profiles/airfoils, close to Zhukovskiy profile, since the
majority of empirical and semi-empirical relationships/ratios are
derived on his base. It is intended in essence for "thick"
profiles/airfoils (in thickness ratio 12-15o/o), for the
profiles/airfoils of small thickness (5-6o/o) used it should be with
large precaution. Error during calculation by this method in
comparison with "precise" calculations in calculators is
approximately 15o/o, the error in determination Re_K/Re_0 and a_K to
$\pm$10o/o leading to the error in zone and interception coefficients to
2-3o/o.

Another method which can be related to the approximation methods
of calculation, is the method, based on that, that even so the
trajectory calculation and other parameters of catching is produced
completely, but velocity field about the arbitrary profile/airfoil in
question is accepted as analogous velocity field about Zhukovskiy
profile. Thus, the trajectories of drops, designed for a Zhukovskiy

profile during identical modes/conditions and under meteorological conditions, are transferred to arbitrary profile/airfoil. The definition of the zones of catching, interception coefficients and other parameters in known trajectories is produced by the usual examined above methods.

It is necessary to say that the replacement arbitrary not only of the profiles/airfoils, but also other elements of construction/design (for example, the jaws of air intakes) by Zhukovskiy profile for obtaining the trajectories of the motion of drops is applied fairly often. The error in calculations, obtained during this replacement, as a rule, not on much exceeds error during the "precise" solution and frequently it can be permitted during designing calculation.

Example of 4.1. Let us conduct calculation according to Bergran process of the sizes/dimensions of zone and interception coefficient on profile/airfoil NACA-0012.

Initial data.

Flight speed on $V_0 = 150$ m/s.

Flight altitude on $H = 1000$ m.

Size/dimension of drops r. 10 $\mu = 10 \cdot 10^{-6}$ m.

Size/dimension of chord $b=3$ m.

Angle of attack of $\alpha = 6^0$.

The diagrams/curves of profile/airfoil and distribution of pressures on it are shown in Fig. 4.18a, b.

Calculation of the zone of catching.

1) On the base of the diagram/curve of pressures we compute local relative air speeds

$$\bar{v} = \frac{V_1}{V_0} = \sqrt{1 - \bar{p}}$$

and we construct their distribution according to the profile/airfoil (see Fig. 4.18c).

Page 112a.

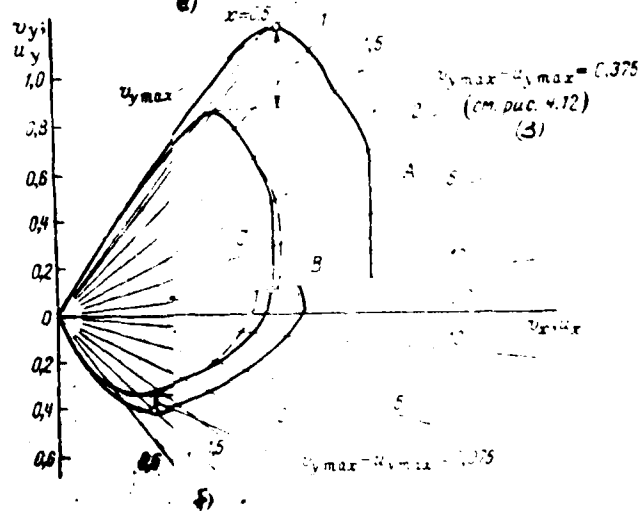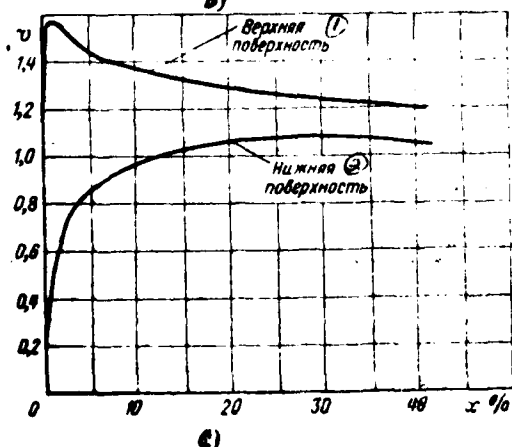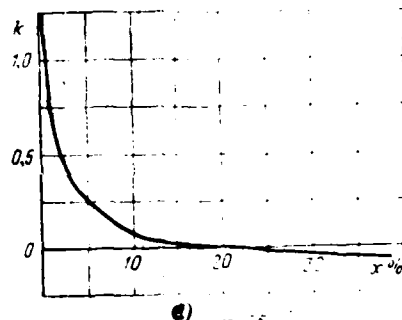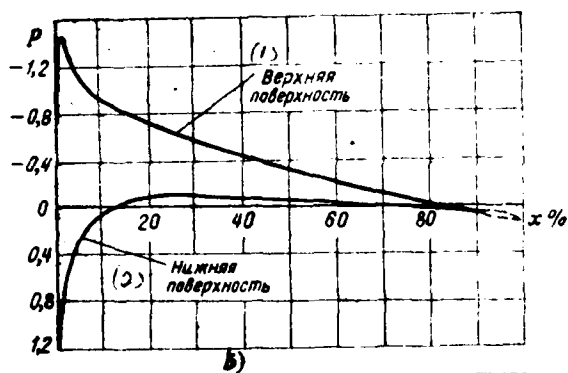*Fig. 4. 18*

Page 112b.

Верхняя поверхность

Нижняя поверхность

▲ ● по формуле (4.19)
△ ○ по формуле (4.20)
■ □ предельные точки с рис. 4.18а

а)

Верхняя поверхность

Нижняя поверхность

б)
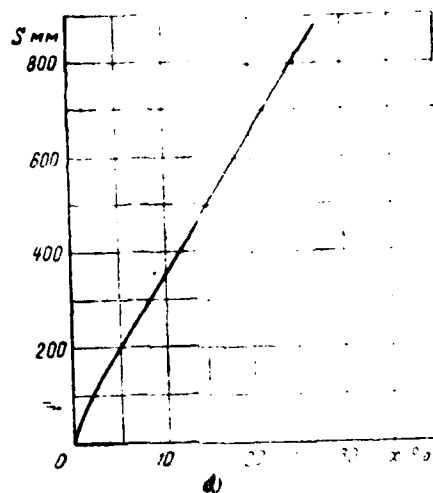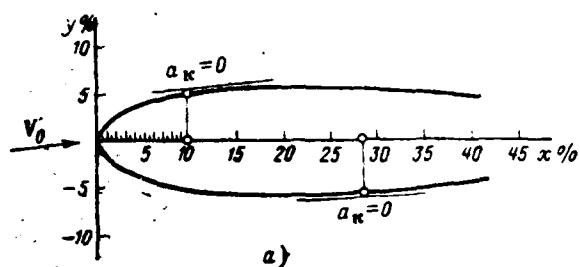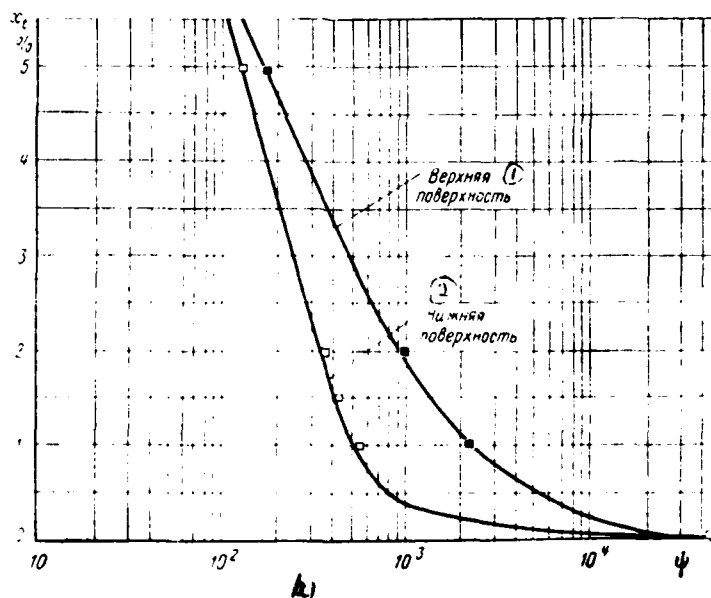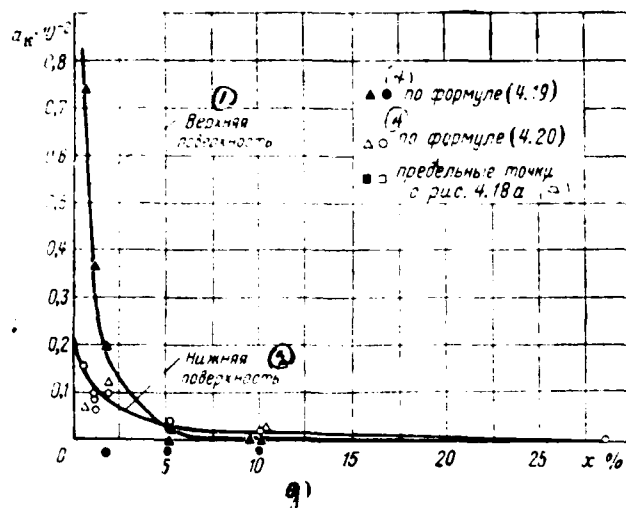
Fig 4.18 (Cont'd)
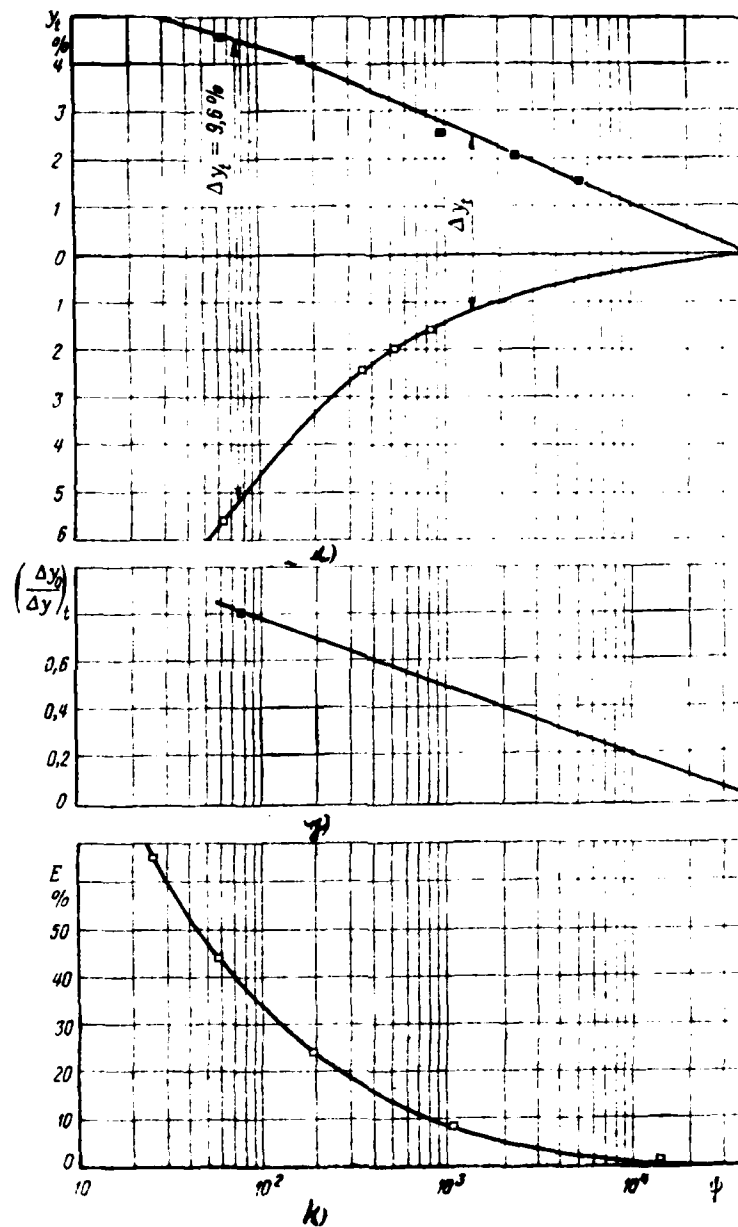
Page 112c.

Fig 4.18 (Cont'd)

Fig. 4.18. Calculation or zone and interception coefficient in Bergran's method for a profile/airfoil UASA-0012, α=6°.

Key: (1). Upper surface. (2). Lower surface. (3). see Fig. 4.12. (4). according to formula. (5). limit points with Fig. 4.18a.

Page 113.

Then we construct on the diagram/curve of profile/airfoil the curve $S = f(x)$ (see Fig. 4.18d) and curve of surface slope to axis/axle $\kappa = \varphi(x)$ (see Fig. 4.18e).

2) Utilizing Fig. 4.18c and 4.18e, we construct the hodograph of air speed, the curve A (see Fig. 4.18f). We construct in the first approximation, the hodograph of the speed of drops in surface, on the basis of the hodograph of air speed and utilizing Fig. 4.12 and equation (4.18), the curve B. Taking into account that the hodograph of the speed of drops must pass through points $u_x = \cos\alpha; u_y = -\sin\alpha$. We construct the second approximation/approach of hodograph, the curve C.

We compute according to formula (4.6) Reynolds number ($\nu = 1.5 \cdot 10^{-5}$ m²/s)

$$Re_0 = \frac{2 \cdot 150 \cdot 10 \cdot 10^{-6}}{1.5 \cdot 10^{-5}} = 200.$$

We determine on profile/airfoil the limit points of catching, which correspond to the motion of drops along straight paths when x_k = 0 (see Fig. 4.18a).

Using to equations (4.19) and (4.20), we calculate a value a_k in the series/row of the points of profile/airfoil. Values dv/dS and dv_x/dS we define as relations $\Delta v/\Delta S$ and $\Delta v_x/\Delta S$ on figures 4.18d and 4.18f.

We plot a curve $a_k = f(x)$ for an upper and lower surface, throwing/rejecting the clearly dropping out values, obtained during the calculation (see Fig. 4.18g).

3) We compute for different points of the profile/airfoil of the value of scale factor $\psi = f(x)$ in equation (4.17). Values $Re/Re_0; a_a$ and $\frac{c_D Re}{24}$ necessary for calculation are taken with Fig. 4.18f; 4.18g, also, from table 3 of application/appendix, respectively. The results of calculations we represent graphically in the form of dependence $\eta = f(\psi)$ for the prescribed/assigned value of $Re_0 = 200$ (see Fig. 4.18h).

We compute according to formula (4.7) value ψ corresponding to

the conditions of our task (**L=b**):

$$\psi = \frac{9 \cdot 1.11 \cdot 3}{1000 \cdot 10 \cdot 10^{-6}} = 3000.$$

For it on Fig. 4.18h we determine the zone of catching along profile/airfoil $r_{внутр} = 0.2\%$; $r_{верх} = 0.85\%$.

Calculation of interception coefficient.

Utilizing Fig. 4.18h and 4.18a, we construct dependence $y_l = f(\psi)$ (see Fig. 4.18i) we determine value ψ. which corresponds to ratio $\Delta y_0/\Delta y = 0.8$. For this of Fig. 4.10 for $\alpha = 6°$ we find appropriate value $\Delta y_l/C_{max} = 0.8$, whence $\Delta y_l = 0.8 \cdot C_{max} = 0.8 \cdot 12 = 9.6\%$ (in chord). Furthermore, we calculate a value $\psi_{кр}$ according to equation (4.21), appropriate $\left(\frac{u_n}{y}\right)_l = 0.$ Value $V_S^{\bullet} \cdot \left(\frac{dv}{dS}\right)_{кр}$ we determine from Fig. 4.14:

$$V_S^{\bullet} = 52; \quad \psi_{кр} = 4 \cdot 200 \cdot 52 = 42\,600.$$

On these two points we construct linear dependence $\left(\frac{u_n}{\Delta y}\right)_l$ on modulus/module ψ (see Fig. 4.18j).

We calculate a value general/common/total interception coefficient $E = \left(\frac{\Delta y_0}{\Delta y}\right)_l \times \frac{\Delta y_l}{C_{max}}$ and we construct dependence $E = f(\psi)$ (see Fig. 4.18j). Values $\left(\frac{\Delta y_0}{\Delta y}\right)_l$ and Δy_l necessary for calculation are taken from Fig. 4.18j and 4.18i.

For task $(\psi = 3000)$ $E = 9\%$. In question

Page 114.

4.6. Catching of drops by the sweptback wings.

During the calculation of the aerodynamic parameters of
sweptback wings [98] velocity of incident flow V_0 they usually expand
to two components: the parallel to leading wing edge V_{0l} and
perpendicular to it V_{0n}. Component $V_{0l} = V_0 \cdot \sin \chi$ during the flow around
of the wing of nonviscous gas does not depend on a change in the
pressures and speeds in plane normal to it, but therefore remains
constant.

Thus, if we during swept-wing design of axis/axle select then so
that the Z-axis is passed along spread/scope (on the wing leading
edge) (Fig. 4.19), then the components of the speed of the
incompressible inviscid flow relative to Z-axis

$$V_{0z} = V_0 \cdot \sin \chi \qquad (4.24)$$

it will be constant. This leads to the fact that between the speed of
drop u_z and the speed of airflow V_z there will not be the
differences, i.e., $u_z = V_z$ and the equation of motion of drop will be

$$\frac{du_z}{d\tau} = 0 \qquad (4.25)$$

and

$$z = u_z \tau + c.$$

Further simplifying the dependence between Re_κ and Re_0 [see

equation (4.11], we will obtain

$$Re_{\kappa} \quad Re_0 | \overline{(v_x + u_x)^2 + (v_y - u_y)^2}. \qquad (4.11')$$
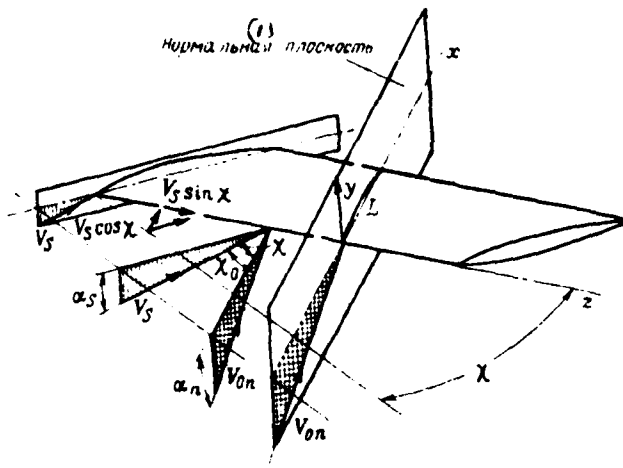
Fig. 4.19. System of coordinates of axes/axles on the sweptback wing.

Key: (1). Normal plane.

Page 115.

If we the right and left sides of equations (4.10) divide into
$\cos^2 \chi_0$, that all speeds will be expressed relative to the component
of the velocity of incident flow V_{on}, of that lying at the normal plane
(see Fig. 4.19) and equation of motion they will take the form

$$
\frac{du_x}{d\tau} = \frac{c_D}{24} \frac{Re_{\kappa n}}{Re_{on}} \Psi \, (v_{xn} - u_{xn}).
$$

where

$$
\frac{du_y}{d\tau} = \frac{c_D}{24} \frac{Re_{\kappa n}}{Re_{on}} \Psi \, (v_{yn} - u_{yn}).
$$

(1.10')

$$
Re_{on} = \frac{2rl_n \cos \chi_0}{\nu} = \frac{2rl_n}{\nu},
$$

$$
Re_{\kappa n} = Re_{on} \sqrt{(v_{xn} - u_{xn})^2 + (v_{yn} - u_{yn})^2}.
$$

Solution of equations (4.10') gives the trajectory of drops in normal plane without the account to sweepback. This conversion makes it possible to use the finished solutions and the calculation methods for the straight wings. Upon transfer to normal plane it is necessary to consider a change in the geometric parameters of profile/airfoil and stream conditions. So, if the angle of attack of wing of the relatively incident flow is equal to α, then in normal plane it will be $\alpha_n = \alpha \sec \chi_0$ and wing profile in normal plane also must be corrected via the multiplication of the ordinates of initial profile/airfoil on $\sec \chi_0$, furthermore, the thickness of the obtained profile/airfoil will always be more than initial. However, frequently during this conversion it is possible to consider that the obtained profile/airfoil is related to the same family, as initial.

As an example let us give calculation for a wing with profile/airfoil NACA 65_2-015 with the sweep angle of 45°. Chord length is equal to 2.5 m, the angle of attack of 4°.

Conditions of the icing: the diameter of drops $\bar{\lambda}$ 20 µ, temperatures of -20°C, heights/altitudes - 7000 m, flight speeds 500 km/h.

For the sweptback wing. For the straight wing

$$V_{on} = 350 \text{ км/час}^{(1)}, \qquad V_0 = 500 \text{ км/час},$$
$$Re_{on} = 70, \qquad Re_0 = 100,$$
$$\psi = 1455, \qquad \psi = 1455,$$
$$\alpha_n = 5°. \qquad \alpha = 4°.$$

Key: (1). km/h.

Then the zone of catching on the enclosure of profile/airfoil will

comprise on upper surface of 1.0o/o, on lower surface - 7o/o of chord

(see Fig. 2b applications/appendices), and interception coefficient

$R=15$o/o (see Fig. 4b application/appendix). For the straight wing

under the same conditions we will obtain the extent of the zone of

catching over upper surface of 1.5o/o, on lower - 9o/o, and the

interception coefficient $\varepsilon=200$/o.

Page 116.

Calculation method presented above does not consider the

displacement of drops in plane xz. However, usually this displacement

does not represent special interest, since it does not affect the

size/dimension of the zone of catching along chord. The displacement

of drops over spread/scope is of certain interest only when on wing

are some external parts (vortex generators, pressure units, etc.),

but in this case its effect is limited to the fact that in the

direction of downwash will occur somewhat larger ice formation, than

from of the "shaded" part.

4.7. Catching of drops at high velocities of flight.

For the evaluation of the compressibility effect of air on the trajectory of drops it is represented by advisable to examine several simple cases in order according to their results to draw the appropriate conclusions.

Compressibility effect on the catching of drops is caused by a change in the velocity fields in the compressed and incompressible flows. Fig. 4.20 depicts the distribution of local velocities on the surface of circular cylinder and Znukovskiy profile for the compressed and incompressible flows. As is evident, most are distinguished the speeds of the compressed and incompressible flows on cylinder, for a profile/airfoil this difference is less, moreover it is decreased with the decrease of thickness ratio (curves b and c).

The trajectory calculation of the motion of drops and parameters of catching for cylinders, made with the aid of simulators for the critical speed of the flow (for circular cylinder $M_{кр}$ 0.4) [89], showed that with the most varied sizes/dimensions of cylinders (from 12.5 to 750 mm) and drops (from 3 to 70 μ) the difference in

interception coefficients for the compressed and incompressible flows
is from 0.3 to 2.9o/o.

Thus, it is possible confidence to consider that for
contemporary thin profiles/airfoils the compressibility effect of air
on the parameters of the catching of drops at subsonic flight speeds
is negligibly small (in any case less than 3o/o) and in the majority
of the cases the calculation of the catching of drops can be made
without the account to compressibility.

During supersonic flights the icing as a result of the
aerodynamic heating of surface usually does not occur; however, the
series/row of theoretical and experimental works they show that the
icing in flight is possible to the speeds of order M=1.4. True, the
probability of this icing is very low, since it is possible at low
temperatures of surrounding air, but to examine, at least briefly, a
question about the catching of drops at supersonic speeds is
necessary.

Page 117.

Fundamental difference in physics of the catching of drops with
supersonic flow in comparison with subsonic consists in the
presence of the shock wave, in which occurs a velocity jump and all

other airstream data (temperature, density, etc.) and respectively
appears the aerodynamic force, which effects on drop.

The appearance of a shock wave, besides usual assumptions about
the constancy of the form of drop, neglect of the gravitational
force, etc. (see Section 4.2), makes it necessary to additionally
assume the following:

- the field of flow of air around the streamlined body does not
produce friction, with exception of shock wave;

- by imbalance of the forces, which effect on drop in transit
through the jump, it is possible to disregard.

The solution of the equations of motion of drops for the
supersonic flow most simply is fulfilled for the tasks, connected
with the flow around of plate [106] or clone [136], [151].
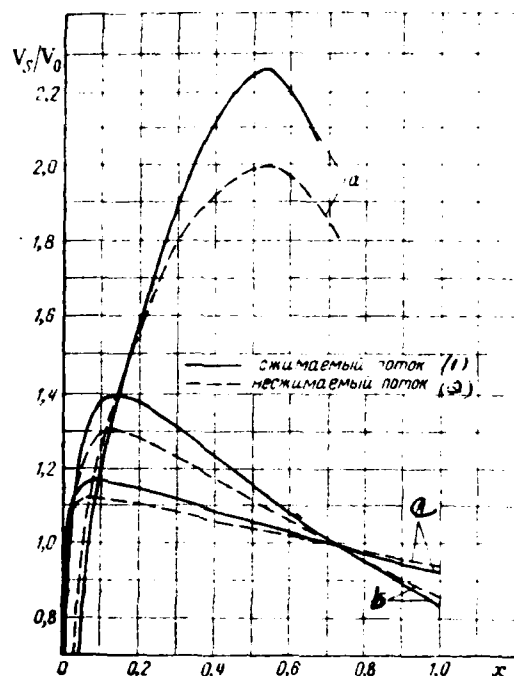
Fig. 4.20. Comparison of local velocities on the surface: a) circular cylinder, $M_{кр} = 0.4$; b) symmetrical profile/airfoil of Zhukovskiy $\bar{c} = 20\%$. $M_{кр} = 0.685$; c) symmetrical Zhukovskiy profile $\bar{c} = 6.5\%$; $M_{кр} = 0.835$, the angle of attack of $\alpha = 0°$.

Key: (1). compressible flow. (2). incompressible flow.

Pages 118-119.
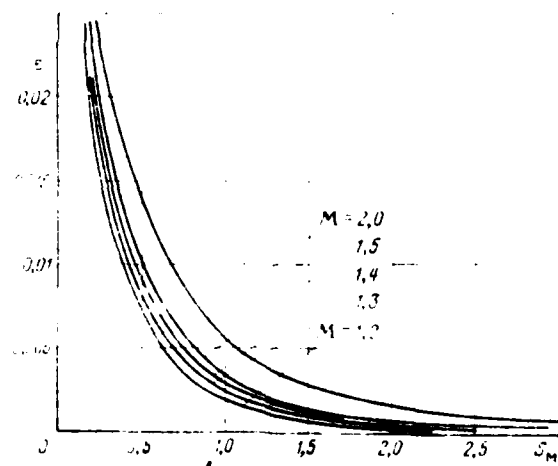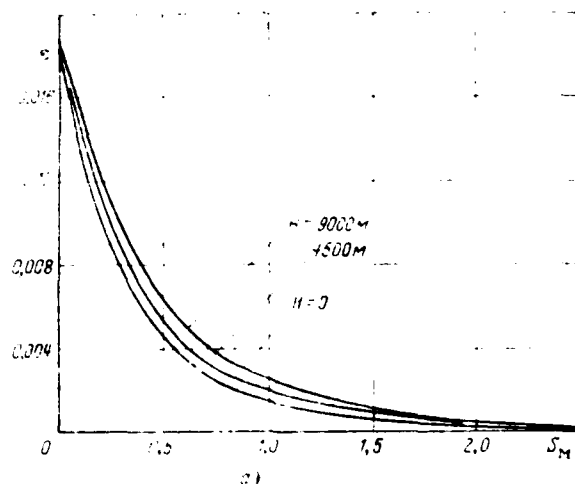
Fig 4.21.
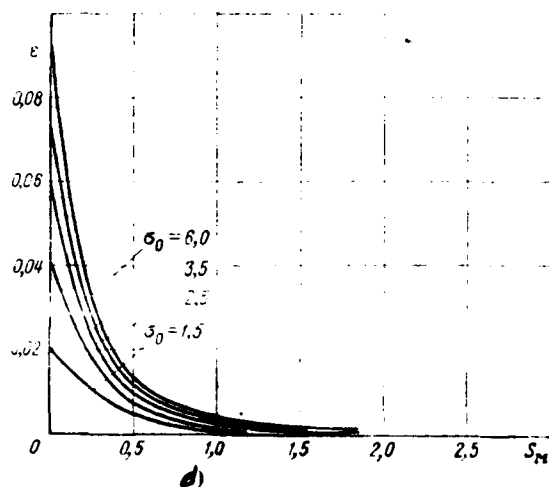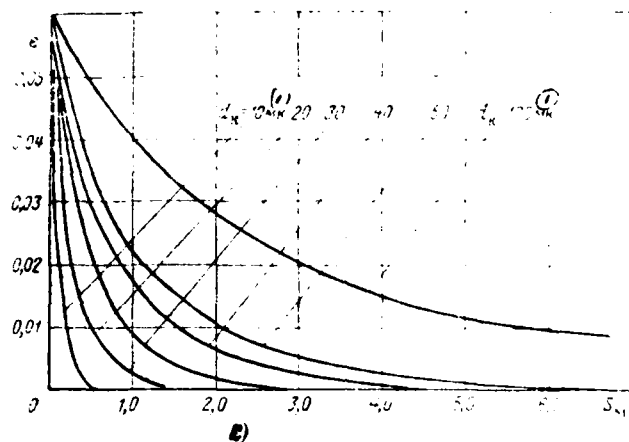
Fig. 4.21. Dependence of local interception coefficient on the surface of wedge on the flight conditions (H and M), size/dimension of drops ($d_к$) and wedge angle ($σ^0$): a) from height/altitude H; c) from the size/dimension of drops $d_к$; b) from speed M; d) from wedge angle $σ_0$.

Key: (1) M.

Pages 120-121.
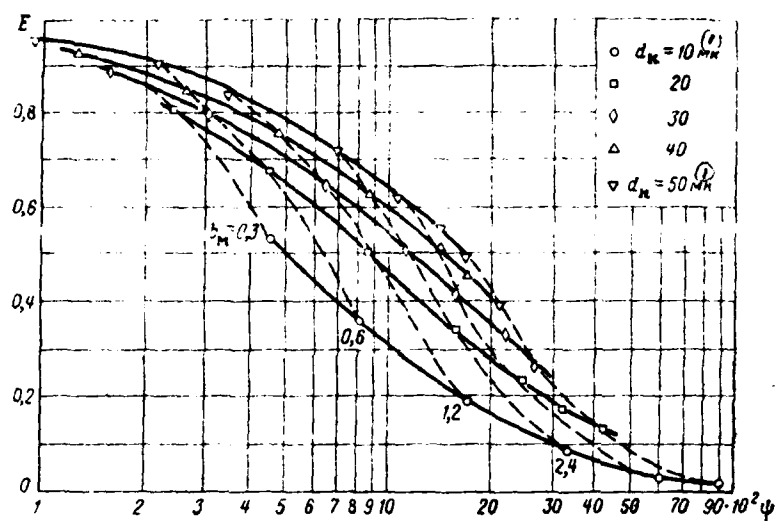
a)
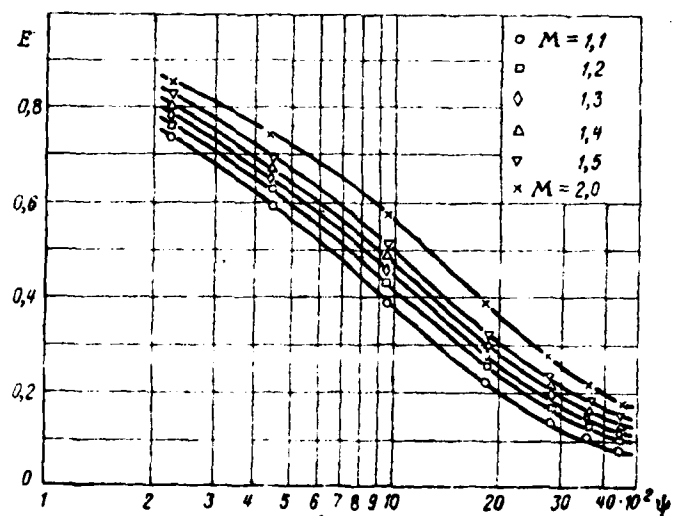
b)

Fig 4.22.
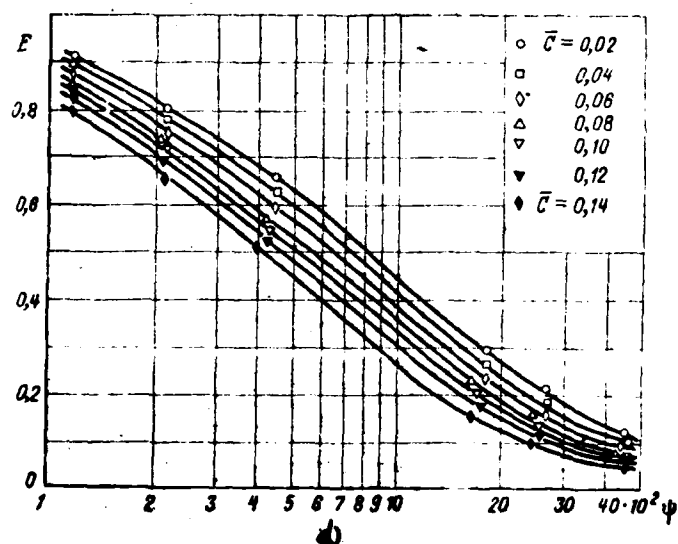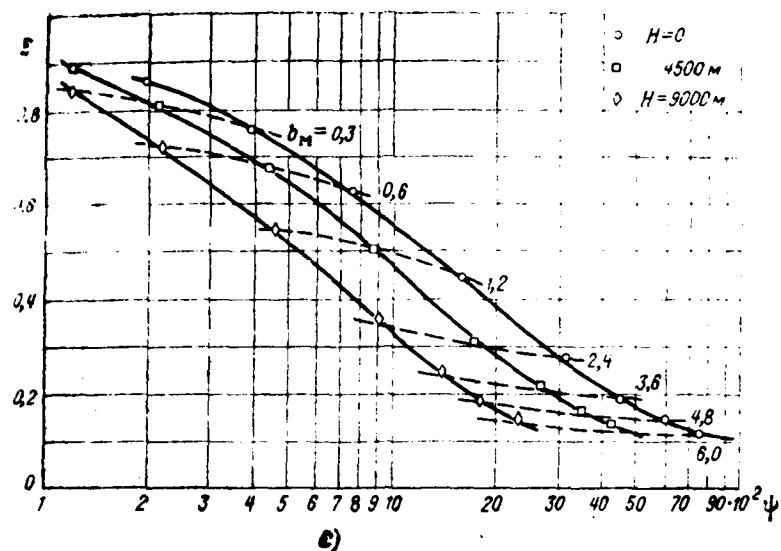
Fig. 4.22. Effect on the interception coefficient of the double wedge airfoil of the flight conditions (M, H), size/dimension of drops (d_k) and form of rhomb $\left(b_M; \bar{C} = \frac{c}{b_M}\right)$: a) M=1.4; H=4500 m; $\bar{C}$=0.02; α=0°; b) d_k= =20 μ; H=4500 m; $\bar{C}$=0.02; α=0°; c) d_k=20 μ; M=1.4; $\bar{C}$=0.02; α=0°; d)

$d_k = 20$ μ; M=1.4; H=4500 m; α=0°.

Key: (1). μ.

Page 122.

The integration of equation of motion for a wedge was made by Serafini [136] and the dependence obtained as a result of local interception coefficient ε on different flight conditions and conditions of icing was represented in Fig. 4.21.

The results of calculations for a wedge can be directly used for the calculation of double wedge airfoils, if angle of attack is not so great so that the catching of drops would occur not only on the leading edge of an airfoil profile, but also on its tail section. The results of the calculations of the general/common/total interception coefficient E of several double wedge airfoils are represented in Fig. 4.22.

4.8. Catching of drops by the air intakes of engines.

Due to complex geometric layout the theoretical calculation of the parameters of catching for air intakes is the task even of more complicated, than calculation for profiles/airfoils, and in the

majority of the cases it is not possible. If it is very rough to divide the air intakes of contemporary aircraft into two classes (subsonic and supersonic) and to give to them characteristic geometric layouts (Fig. 4.23), then it is possible to approximately/exemplarily show the procedure of calculation of the parameters of catching.

The inner body of the subsonic air inlets, as a rule, has a form of ellipsoid of revolution, and the field of inlet velocities into this air intake can be presented as the combination of velocity fields in ellipsoid and velocity field in the jaw of shell.

Velocity field about ellipsoid was examined earlier (see Section 4.4). The disturbances/perturbations, placed on velocity fields in ellipsoid by the shell of air intake, can be obtained, after accepting in the first approximation, the shell of air intake for the "Borda mouthpiece".
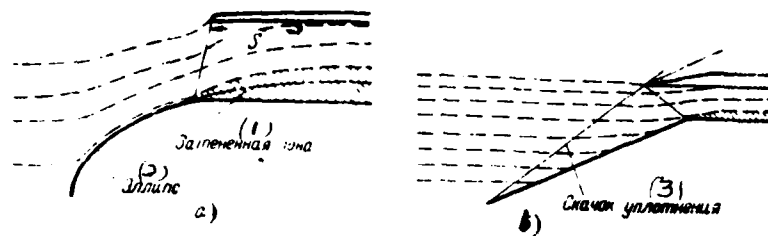
Fig. 4.23. Diagrammatic representation of the catching of drops in the air intakes: a) subsonic; b) supersonic.

Key: (1). Shaded zone. (2). Ellipse. (3). Shock wave.

Page 123.

The velocity field in the "borda mouthpiece" well known in aerodynamics is expressed by the complex function

$$\zeta = \theta + e^{\theta},\tag{4.26}$$

where

$$\theta = \varphi + i\psi.$$

Hence

$$\left.\begin{aligned} x &= \varphi + e^{\varphi}\cos\psi. \\ r &= \psi + e^{\varphi}\sin\psi \end{aligned}\right\}\tag{4.27}$$

and

$$\left.\begin{aligned} u_x &= \frac{\partial\psi}{\partial x} = \frac{\partial\varphi}{\partial r} = \frac{1 + e^{\varphi}\cos\psi}{1 + 2e^{\varphi}\cos\psi + e^{2\varphi}} \\ u_r &= \frac{\partial\varphi}{\partial r} = \frac{\partial\psi}{\partial x} = \frac{e^{\varphi}\sin\psi}{1 + 2e^{\varphi}\cos\psi + e^{2\varphi}} \end{aligned}\right\}\tag{4.28}$$

For final calculations it is necessary to fulfill
transition/transfer from the axes/axles, connected with shell, to the
axes/axles of ellipsoid, i.e., it is necessary to connect the value
of **speeds** u_x' and u_r' **with speeds** $u_{x,эл}$ and $u_{r,эл}$. **In this case** u_x' and u_r'
should be considered as the disturbances/perturbations, placed in the
velocity field of ellipsoid, i.e., finally the components of air
speed at **the entry into air intake** will be equal to

$$u_x = u_{x,эл} + u_x', \\ u_r = u_{r,эл} + u_r'. \quad\quad (4.29)$$

The calculations of the parameters of catching for the subsonic
air inlets with inner body in the form 10 and 20o/o ellipsoids were
made by Bran [88]. The parameters of catching on inner body in
practice do not differ from the cases examined above for ellipsoids
in the free flow. The parameters of catching on the internal surface
of shell are represented in Fig. 4.24 and can be used for the design
of de-icing systems for the subsonic air inlets, which have inner
body in the form of ellipsoid of revolution.

For the supersonic airs inlet characteristic geometric form
takes the form, represented in Fig. 4.23b. Inner body is formed by
cone or wedge, and shell is usually made with the undercut (it is
close to the flow line of air); the location of cone (wedge) and
shell   is such that in the normal modes of flight shock wave would
pass through the shear/section of air intake. The special

feature/peculiarity of shell is the very thin (2-3 mm) edge of jaw in shear/section, due to what they usually call sharp edge.

Ice formation on the jaw of shell (on sharp edge) is characterized by the fact that it occurs at very small (in comparison with "thick" edge) distance from the edge of shear/section.

Pages 124-125.

Ice formation at relatively high temperatures occurs   more in the direction, perpendicular to the lateral surface (it is analogous with horn-shaped ice on profiles/airfoils), but at low temperatures is more in the direction, parallel to the flow (it is analogous with tapered or lanceolate or ice on profiles/airfoils). Since area of the contact of ice with surface is small, it is frequently broken off by the incident flow, that can be attributed to the special feature/peculiarity of the icing of "sharp" edge in comparison with the profiles/airfoils and other bodies.
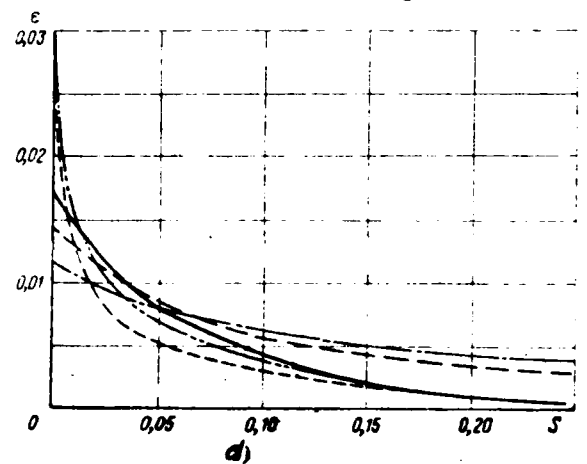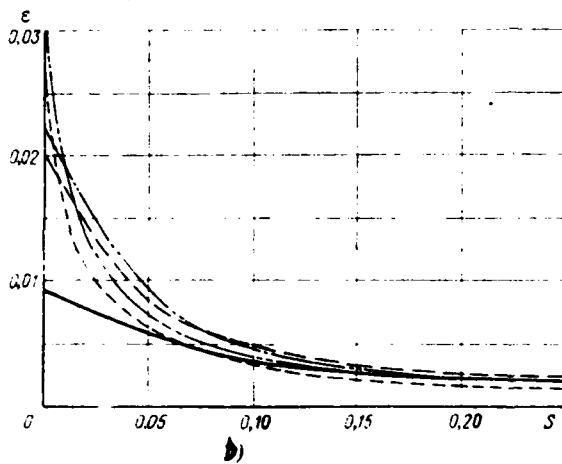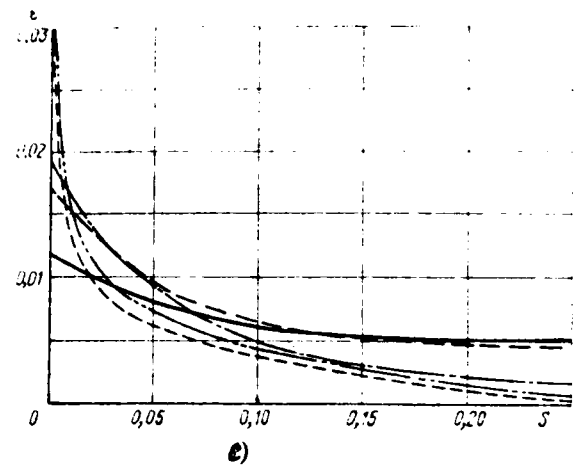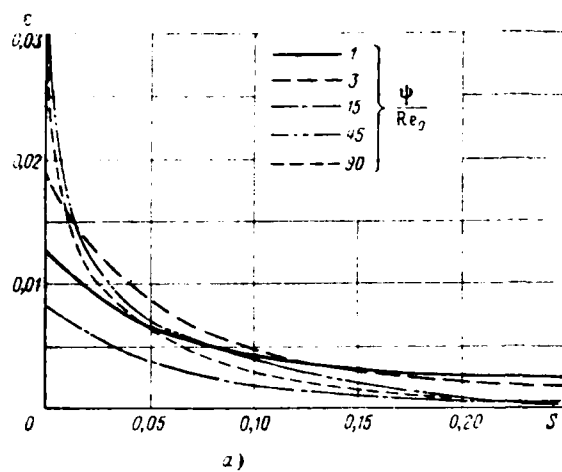
Fig. 4.24. The distribution of the local coefficient of the angle of the injection of drops on the jaw of the subscnic air inlet: a) $Re_0=8$; b) $Re_0=128$; c) $Re_0=512$; d) $Re_0=1024$ (size/dimension S is expressed in the portions of the large semi-axis of ellipse).

Page 126.

Chapter V.

Thermal design of deicers (exterior problem) [1].

FOOTNOTE [1]. Section 5. 1-5. 5 are written by R. Kh. Tenishev and V. S. Savin; Section 5. 6- by R. Kh. Tenishev, Section 5. 7 - by V. K. Kordinov. ENDFOOTNOTE.

5. 1. Heat exchange on surface under conditions of icing.

The calculation of thermal deicer is divided on the so-called "external" and "internal" tasks.

Exterior problem includes the calculation of the necessary heat-flux density, its distribution according to surface, determination of the extent of zone heating for the diverse variants of the systems of permanent and cyclic heating, determination of the relationship/ratio between the temperature of dry surface and its temperature under conditions of icing, etc., these questions can be examined independent of the means of utilized thermal energy and internal construction/design of heating devices/equipment.
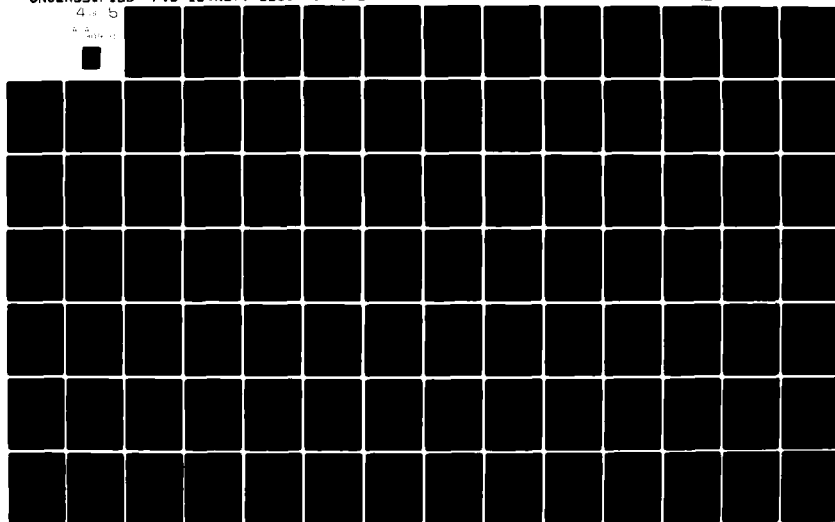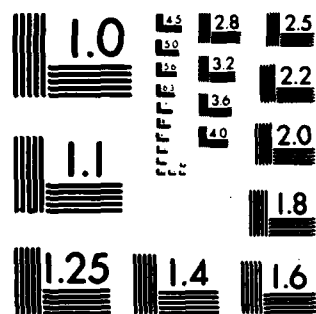
MICROCOPY RESOLUTION TEST CHART
NATIONAL BUREAU OF STANDARDS-1963-A

Internal task concerns the calculation of the internal parameters of deicer, heaters or surface directly connected with construction/design; therefore the methods of its solution for different types of deicers are different.

In present chapter is examined the exterior problem. To the calculation of the internal parameters of separately thermoelectric and air-heat systems are dedicated the subsequent two chapters.

Heat exchange on the surface, which undergoes icing or wetting due to the recovered drops, is characterized by more complicated processes, than on dry surface (in "dry" air) [2].

FOOTNOTE [2]. Term "dry" air very propagated in the literature on questions of icing indicates the absence in air of the weighed drops or crystals of ice. In the absence of the weighed water even close to saturation by water vapor air is considered in sense indicated above as "dry". ENDFOOTNOTE.

Let us examine the heat fluxes to the surfaces, shielded from icing, in reference to the unit of surface (i.e. density q of these flows, or heat transfer rates):

- convective heat flux q_{α};

- heat flux from the high-speed/velocity heating of surface due to air friction in boundary layer q^{*}_{1};

- heat flow, necessary for evaporating of water or ice from surface, $q_{\beta 1}$;

- the heat flow, emitted by the heated surface, $q_{...}$;

- the heat flux, which appears as a result of converting kinetic energy of drops during their collision with surface, $q_{\kappa\mu\mu}$.

Page 127.

All these heat flow are on surface independent of its temperature (t_{n}).

Besides them, when $t_{n} < 0$ appears supplementary heat flow, which is isolated during the crystallization of the supercooled drops on surface, $q_{\kappa p}$ and heat q_{n}, going for heating of a layer of ice during the heating to cold surface to $0°C$. Fig. 5.1, borrowed from [124],

clearly depicts the diagram or neat fluxes for this case.

When $t_n > 0$, besides q_α and q_β, is required small heat flux q_s to
the heating of water from the temperature of surrounding air to the
temperature of the heated surface. If heating surface (or air intake,
pressure unit of flow, etc.) recovers the crystals of ice, then is
required supplementary heat flow $q_{n\pi}$ for their melting.

Examining the equation of the heat balance of surface under
conditions of icing, there is no need for representing it in the form
of the sum of all enumerated above flows. Calculations show that such
components as q_α, q_β, $\dot{q}_{l}$, considerably exceed in absolute value others
components, portion of which usually composes several percentages of
general/common/total heat-flux density on surface. Therefore during
the calculation of the necessary heat output for the heating of the
majority of exteriors of the flight vehicles these secondary terms
can be disregarded/neglected. With this assumption the equation of
heat balance on surface takes the form

$$q_u = q_{uu} + q_{\beta u} - \dot{q}_l = q_\alpha + q_\beta.$$
(5. 1)
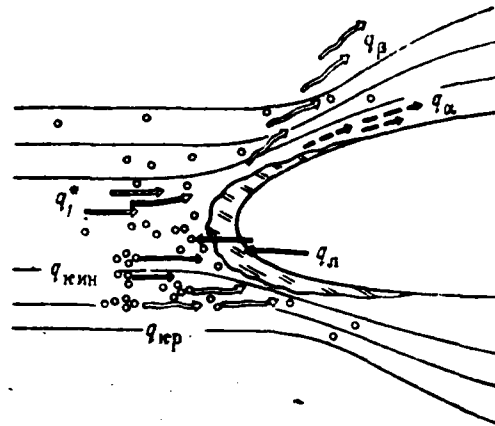
Fig. 5.1. Diagram of heat fluxes for an unheated surface under conditions of icing.

Page 128.

Sometimes (for example, during calculation of heaters of small nozzles, air intakes or pressure units which "are driven in" by the crystals of ice) should be considered also terms $q_{\text{в}}$ or $q_{\text{пл}}$:

or

$$q_{\text{п}} = q_{\alpha 1} + q_{\beta 1} - \overset{\bullet}{q_{\text{i}}} + q_{\text{в}}, \qquad (5.\,1\text{a})$$

$$q_{\text{п}} = q_{\alpha 1} + q_{\beta 1} - \overset{\bullet}{q_{\text{i}}} + q_{\text{пл}}. \qquad (5.\,1\text{б})$$

Value $q_{\text{п}}$ in these equations is the heat-flux density which must be conducted to the icing up surface in order to ensure its heating to the required temperature.

Let us examine fundamental component of this heat flux in more detail.

5.2. Calculation of convective heat emission.

As is known, convective heat flux from the unit of area of the heated dry surface can be represented in the form of the following equation:

$$q_n = \alpha\,(t_n - t_1) - \alpha\,(t_{1n}^* - t_1) = \alpha\,(t_n - t_1^*). \qquad (5.2)$$

For determination q_a with known or prescribed/assigned tc temperature surface t_n it is necessary to know heat-transfer coefficient α and the so-called equilibrium temperature of surface t_{1n}^*, which in the speed range which interests us of flight can be equated to the equilibrium temperature of boundary layer, the latter is equal to:

$$t_1^* = t_1 + \Delta t_1 = t_1 + r^* \frac{V_1^2}{2c_p}, \qquad (5.3)$$

where

t₁ - local temperature on boundary layer edge:

$$t_1 = t_0 + \frac{V_0^2 - V_1^2}{2c_p}; \qquad (5.4)$$

c_p - heat capacity of the air at a constant pressure in J/kg·deg.

Consequently, the resultant expression for the local equilibrium

temperature of surface will take the form

$$t'_{in} = t'_1 = t_0 + \frac{V_0^2}{2c_p}\left[1 - \left(\frac{V_1}{V_0}\right)^2(1 - r^*)\right]. \qquad (5.5)$$

The value, which stands in the bracket, is local recovery factor

$$r^*_1 = 1 - \left(\frac{V_1}{V_0}\right)^2(1 - r^*). \qquad (5.6)$$

Page 129.

On the basis of a large quantity of experiments it is
established/installed [69], that r*=0.85 in the case of the
stream-line conditions of the flow above the surface and r*=0.88 in
the case of turbulent flow conditions above the surface.

Calculation of local heat-transfer coefficients for aerodynamic
profiles/airfoils.

The repeatedly checked in practice formulas for local
heat-transfer coefficients are related to three well studied forms of
bodies, namely: flat/plane plate, circular cylinder and sphere. For
practical calculations aerodynamic profile/airfoil usually they
replace by equivalent cylinder in end connections and by flat/plane
plate on the remaining part of the profile/airfoil. Experiment shows
that this replacement, from the point of view of precision/accuracy,
is completely satisfactory[1].

FOOTNOTE [1]. Is known another approach and to the solution of this

task, based directly on boundary layer characteristics [140];
however, for practical use it is sufficiently bulky. ENDFOOTNOTE.

From the examination of local heat-transfer coefficients in the
perimeter of circular and elliptical cylinders and for a flat/plane
plate it follows that the dependence of the coefficient of heat
exchange in the perimeter of cylinder the nearer is suitable the
dependence for a flat/plane plate, the more eccentricity the cross
section of elliptical cylinder [68].

Local heat-transfer coefficients for a flat/plane plate during
laminar boundary-layer flow usually are designed from the formula of
Pol'gauzen

$$Nu = 0.332 Re^{0.5} Pr^{1/3}. \qquad (5.7)$$

During the calculation of local heat-transfer coefficient for a
flat/plane plate with turbulent boundary layer widest use found
Colburn's formula [69]

$$Nu = 0.0296 Re^{0.8} Pr^{1/3}. \qquad (5.8)$$

It is obvious that these formulas do not make it possible to
obtain the solution for the leading edge of profile/airfoil.
Therefore the leading edge of an airfoil profile is replaced by the
equivalent cylinder, for which is designed local heat-transfer
coefficient in the vicinity of frontal generatrix. From experimental
data it is known [96], [103], that the speed on the boundary of

boundary layer around the surface of circular cylinder changes in accordance with the equation

$$V_1 = 3.63 V_* \frac{S}{D}.$$ (5. 9)

Page 130.

Therefore local heat-transfer coefficient on the leading edge of profile/airfoil during the stream-line conditions of flow can be found from following criterial dependence [68]:

$$Nu_D = 1.06 (Re_D)^{0.5} Pr^{1/3}.$$ (5. 10)

Analogously during turbulent flow conditions let us have for the leading edge of profile/airfoil [17]

$$Nu_D = 0.063 Re_D^{0.8} Pr^{1/3}.$$ (5. 11)

The given formulas for the calculation of local heat-transfer coefficients are written in general form and therefore are somewhat inconvenient during practical calculations. In connection with this case these formulas can be considerably simplified and passed away depending on fundamental variable/alternating, namely: temperature, pressure, speed and extent of transfer surface.

The dependences, which are determining convective heat emission, contain such physical characteristics of air as density, viscosity/ductility/toughness, thermal conductivity and heat capacity, determined with so-called effective temperature of air T_*. So, air density is determined through T_* from equation of state

$\rho = \frac{p_0}{RT_{\flat\phi}}$. Heat capacity of the air c_p in the temperature range

(approximately/exemplarily from -50 to +50°C) which interests us

virtually does not depend on temperature, but its dynamic viscosity

and thermal conductivity can be determined according to the following

approximation formulas:

$$\mu = \mu_0 \left(\frac{T_{\flat\phi}}{273}\right)^{0.76}, \qquad (5.12$$

$$\lambda = \lambda_0 \left(\frac{T_{\flat\phi}}{273}\right), \qquad (5.13)$$

where μ_0 and λ_0 - value of coefficients with 0°C (273°K).

The best results during the calculation of heat-transfer

coefficients are obtained with $T_{\flat\phi}$ determined according to Eckert's

formula [69]:

$$T_{\flat\phi} = T_0 + 0.50 (T_n - T_0) - 0.22 (T_{1n} - T_0). \qquad (5.14)$$

After using the dependences given above, criterial equations

(5.7), (5.8) and (5.10), (5.11) can be presented in a simpler form.

Thus, for instance, heat-transfer coefficient for the leading edge of

profile/airfoil during the stream-line conditions of flow can be

found from the formula

$$\alpha = 1.06 \left(\frac{\lambda}{D}\right) \left(\frac{\rho V_0 D}{\mu}\right)^{0.5} \left(\frac{\mu c_p}{\lambda}\right)^{1/3} = 1.39 \cdot 10^{-2} T_{\flat\phi}^{0.04} \sqrt[]{\frac{\rho_0 V_0}{D}}, \qquad (5.15)$$

where D - the diameter of the equivalent cylinder of the leading edge

of an airfoil profile, determined graphically or according to the

method of least squares.

Page 131.

For the majority of usual subsonic aerodynamic profiles/airfoils
it is possible to consider that the diameter of equivalent cylinder
composes approximately/exemplarily 30o/o of maximum profile
thickness.

Further, as show calculations, in the range T_{ϕ} 273 ±   50K the
error during the determination of heat-transfer coefficients does not
exceed 3o/o during stream-line conditions and 10o/o with turbulent,
which is completely admissible for thermal designs.

Consequently, assuming/setting $T_{\phi} = 273$ K.   we obtain the
following calculation formulas for the local heat-transfer
coefficients of airfoil.

On the leading edge:

with the laminar boundary layer

$$\alpha = 1{,}74 \cdot 10^{-3} \sqrt{\frac{\rho_0 V_0}{D}} \; \text{вm/м}^2 \cdot \text{град}, \qquad (5.15a)$$

Key: (1). W/m²·deg.

with the turbulent boundary layer

$$\alpha = 9,35 \cdot 10^{-4} \frac{(\rho_0 V_0)^{0,8}}{D^{0,2}} \ \text{вm/м}^2 \cdot \text{град}. \qquad (5.16)$$

Key: (1). W/m²•deg.

On the remaining surface of the profile/airfoil:

with the laminar boundary layer

$$\alpha = 5,44 \cdot 10^{-3} \sqrt{\frac{\rho_0 V_1}{S}} \ \text{вm/м}^2 \cdot \text{град}, \qquad (5.17)$$

Key: (1). W/m²•deg.

with the turbulent boundary layer

$$\alpha = 4,4 \cdot 10^{-4} \frac{(\rho_0 V_1)^{0,8}}{S^{0,2}} \ \text{вm/м}^2 \cdot \text{град}, \qquad (5.18)$$

Key: (1). W/m²•deg.

where S - distance on the enclosure of profile/airfoil from leading

edge to the point of surface in question in m;

P_0 - air pressure at given height/altitude in N/m².

In order to use formulas (5. 15-5. 18) during the calculation of

local heat-transfer coefficients, it is necessary to know the

location of the points (more precise than regions) of

transition/transfer from laminar boundary-layer flow to turbulent

flow.

Flow conditions in the boundary layer above the arbitrary point of dry surface is determined by many factors, basic from which are the following: speed and turbulence level of the undisturbed flow, surface curvature and its roughness, sweep angle of surface, and also direction of the heat fluxes (preheating surface accelerates transition/transfer, and cooling - it slows down).

Page 132.

Transition point from laminar flow to turbulent on straight/direct and sweptback wings.

The phenomenon cf transition/transfer frcm stream-line conditions to turbulent can begin when local Reynolds number will exceed certain critical value. On the basis of investigations it is established/installed [125], that in the presence of the heating of surface on the straight wings the laminar boundary layer exists approximately/exemplarily to $Re=0.5 \cdot 10^6$ cr to the point of minimum pressure on profile/airfoil, moreover from these two points is selected outermost from the leading edge of profile/airfoil. Developed turbulent flow begins with Re numbers of order $2 \cdot 10^6$.

It is necessary to note that the numerical values of critical

Reynolds numbers oscillate in some limits depending on the turbulence

level of undisturbed flow, type or profile/airfoil, roughness of

surface, etc. However, in the majority of the cases the corrected

numerical values of the critical Re numbers can serve as computed

values during the determination of heat-transfer coefficients for the

straight wings in flight in "dry" air.

Fig. 5.2 shows an example of the typical distribution of local

heat-transfer coefficients in the enclosure of profile/airfoil

NACA-0012 with unswept wing.
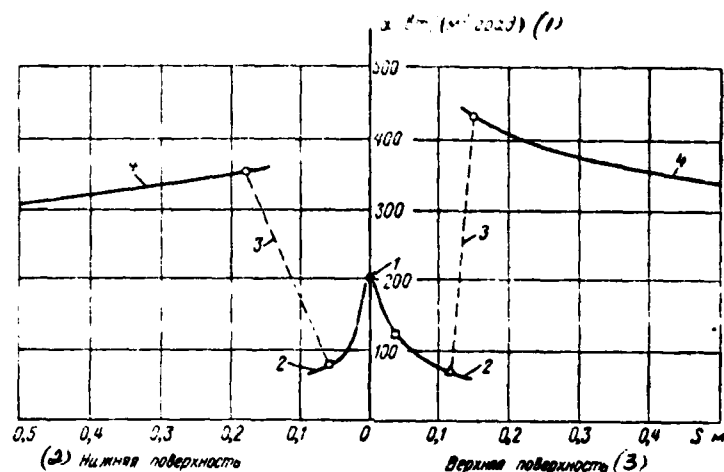
Fig. 5.2. A change in computed values of heat-transfer coefficients in the enclosure of the profile/airfoil of unswept wing in flight in "dry" air (profile/airfoil NACA-0012; b=3.0 m; c_y = 0.4; V_0=150 m/s; H=1000 m): 1 - according to formula (5.15a); 2 - according to formula (5.17); 3 - transient mode/conditions; 4 - according to formula (5.18); □ - corresponds Re=0.5•10⁶; ○ - corresponds Re=2•10⁶; Δ - point of the minimum of pressure.

Key: (1). W/(m²•deg). (2). Lower surface. (3). Upper surface.

Page 133.

Heat-transfer coefficients in transfer zone are conditionally represented the broken straight line, which connects the local

importance of heat-transfer coefficients into the end/lead of the
laminar zone and in the beginning of the steady turbulent flow.

The sweep angle of wing significantly affects the mechanism of
boundary-layer flow, especially in area of leading wing edge. The
experiments, carried out for circular cylinders, show that at the
sweep angles, which exceed 30°, the distribution of heat-transfer
coefficients in the enclosure of cylinder is located in accordance
with the theory of turbulent boundary layer [79]. The indirect
confirmation of this fact is the lowered/reduced value of the
temperature of the leading edge of the sweptback wing in comparison
with the temperature of the leading edge of the straight wing under
other identical conditions.

A change in the heat-transfer coefficients in the enclosure of
wing profile, which has sweep angle $\chi = 45°$, is shown in Fig. 5.3. The
calculation of heat-transfer coefficients was produced in formulas
(5.16) and (5.18). Heat-transfer coefficient has maximum value on
leading wing edge and then monotonically it decreases on the
enclosure of profile/airfoil. This distribution of local
heat-transfer coefficients is possible not only for the sweptback
wings.

α вт.(м² град) (1)

(2) Нижняя поверхность   (3) Верхняя поверхность
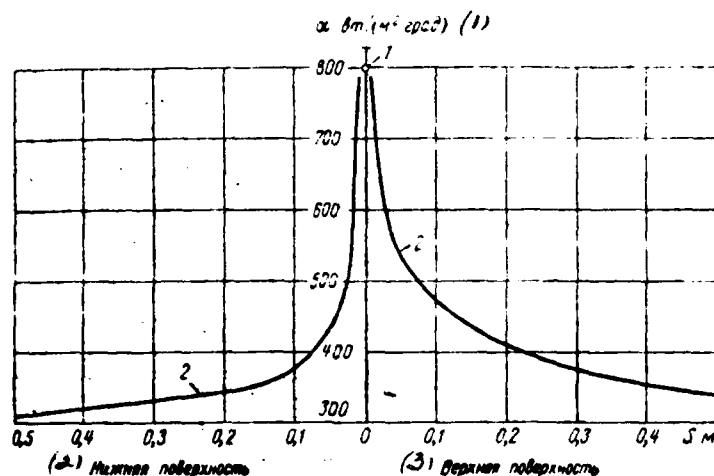
Fig. 5.3. A change in computed values of heat-transfer coefficients
in the enclosure of the profile/airfoil of the sweptback wing
(profile/airfoil NACA-0012; D=3.0 m; c_y = 0.2: V_0=150 m/s; H=1000 m; χ = 45°):

1 - according to formula (5. 16); 2 - according to formula (5.18).

Key: (1). W/(m²•deg). (2). Lower surface. (3). Upper surface.

Page 134.

For example, with the strong turbulence level and undisturbed flow,
caused by the tractor propellers (in the case of propeller-driven or
turboprop power plant), it can seem that even on the straight wings
flow conditions in boundary layer will be turbulent, beginning with

leading edge.

Heat emission under conditions of icing.

Icing exerts the strong turbulence influence on boundary layer;
therefore transition/transfer from laminar boundary layer to
turbulent occurs considerably earlier than this occurs with dry
surface.

Even at temperature of the surface higher than freezing point is
observed the acceleration of transition/transfer from the stream-line
conditions of flow to turbulent, since the wave formations of water
film which is accumulated/stored on surface in the zone of catching,
also prove to be perturbation source. Certain turbulence influence
exert, apparently, directly most recovered drops, passing through the
boundary layer and partially" spattering" with the impact/shock about
surface.

Consequently, heat-transfer coefficients for the deicers both of
cyclic and permanent action must be designed from formula (5.18),
which relates to turbulent boundary layer in the limits of entire
heating surface, except the leading edge for which the coefficient α
depends on sweep angle. For a leading edge it is possible to accept
the following design conditions:

- at the sweep angles of leading edge to 15-20° coefficient α (for cyclic POS on the width of "thermal knife") should be counted according to formula (5. 15a) - for the laminar layer:

- at the sweep angles or leading edge is more than 20° coefficient α must be counted in rormula (5. 16) - for a turbulent layer.

However, during processing ot the results of the tests POS, produced in "dry" air, it is necessary to use information on the location of the points of beginnings and end/lead of the transition/transfer from laminar boundary layer to turbulent which were given above.

Virtually, however, tne precision determination of heat-transfer coefficients in area of leading euge, as a rule, is required only during the calculation or the parameters of "thermal knives" (see examples   6.4 and 6.5). In other cases, especially with permanent heating, to completely admissibly take in the limits of the nose section of the profile/airfoil tne average/mean value of coefficient α.

FOOTNOTE ¹. As a result of the thermal conductivity of skin/sheathing (see Section 6.4) in this sufficiently narrow section occurs the temperature balance of surface, thanks to which this assumption significantly does not affect the final results of calculations. ENDFOOTNOTE.

Page 135.

Calculation of average heat-transfer coefficients for aerodynamic profiles/airfoils.

For the rapid evaluation of average value of the heat flux, which exits from surface by convection path, according to formula (5.2) it is necessary to know the values of average heat-transfer coefficients in the enclosure or profile/airfoil. It is obvious that the average heat-transfer coefficient is defined in general form as

$$\tilde{\alpha} = \frac{1}{S} \int_0^S \alpha \, dS. \qquad (5.19)$$

Moreover in each special case the value of average heat-transfer coefficient α is determined by the distribution of the local heat-transfer coefficient, obtained on the basis of formulas (5.15) -(5.18). However, calculations show that in the majority of the cases α it is possible to calculate with sufficient precision/accuracy, if we use the formula which determines local

heat-transfer coefficient with turbulent boundary layer. This
coincidence of average heat-transfer coefficients for a flat/plane
plate and average heat-transfer coefficients at the
prescribed/assigned distance in the enclosure of profile/airfoil from
stagnant point, apparently, is connected with the fact that the
extent of laminar and transfer zones has small   values in
comparison with the entire designed surface. It is completely obvious
that during the developed turbulent flow above the profile/airfoil
the coincidence of average/mean values α for a flat/plane plate and
for an aerodynamic profile/airfoil will be almost ideal. The laminar
boundary layer above the surface or the leading edge of an airfoil
profile is encountered comparatively rarely in design conditions of
the de-icing systems (this can take the place when local Reynolds
number in the warmed zone of profile/airfoil of unswept surface does
not exceed $0.5 \cdot 10^6$). But if nevertheless this occurs, then average
heat-transfer coefficient can be determined via the substitution of
formula (5. 17) into the integrand of equation (5. 19).

In general average heat-transfer coefficient is found from the
joint solution of equations (5. 18) and (5. 19). Assuming that in the
first approximation, the value of local velocity V_1 above the surface
of profile/airfoil is equal to the speed of undisturbed flow V_0, let
us have the following expression for an average heat-transfer
coefficient:

$$\tilde{\alpha} = 1,25\alpha,$$

or

$$\tilde{\alpha} = 5,5 \cdot 10^{-4} \frac{(\mu_0 r_0)^{0.8}}{S^{0.7}}. \qquad (5.20)$$

Page 136.

Fig. 5.4 as an example shows a change in the average heat-transfer coefficients of the examined above profile/airfoil in dependence on speed and flight altitude. Computed values $\tilde{\alpha}$ are given for a distance from stagnant point S=0.5 m, in this case was accept the assumption that $T_{\phi} = 273°$ K., It is easy to show that value $\tilde{\alpha}$ at other values of S and T_{ϕ} can be calculated on the basis of the relationship/ratio

$$\tilde{\alpha}_2 = \tilde{\alpha}_1 \left(\frac{0,5}{S_2} \right)^{0,2} \left(\frac{273}{T_{3\phi 2}} \right)^{0,5}, \qquad (5.21)$$

where $\tilde{\alpha}_1$ - a value of average heat-transfer coefficient at given speed and height/altitude with S=0.5 m and $T_{\phi} = 273°$ K.
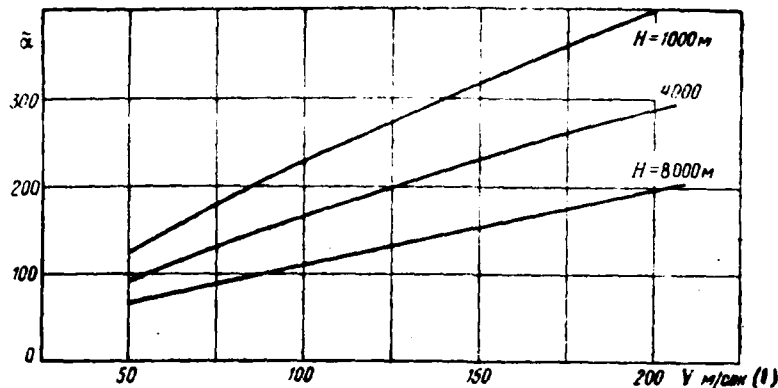
Fig. 5.4. Change in the average heat-transfer coefficients above the surface of the nose/leading edge or aerodynamic profile/airfoil in dependence on speed and flight altitude (S=0.5 m; $T_{sb} = 273°$ K).

Key: (1). m/s.

Calculation of heat-transfer coefficients for the parts of engine.

The fundamental parts of engine which require protection from icing, are the shells of air intake, fairings or spinners, struts and stator blades. Will be shown below the special features/peculiarities of the calculation of heat-transfer coefficients for these parts of the engine and are given calculation formulas.

If the shells of the air intake of engine are made in the form

of steady profiles/airfoils, then the calculation of heat-transfer
coefficients for the noses/leading edges of air intakes differs
little from the calculation of heat-transfer coefficients for lifting
surfaces.

Page 137.

Fundamental task consists in the selection of the equivalent
profile/airfoil, which replaces the nose/leading edge of air intake,
after which the procedure of calculation of heat-transfer
coefficients is reduced to the use of formulas (5.15)-(5.18) with all
observations which were made in the relation to the extent of the
zones of laminar and turbulent flow conditions. Mean heat-transfer
coefficients are designed from formula (5.20).

In work (69) it is shown that the dependences, obtained for
heat-transfer coefficients in the case of plane-parallel flow, can be
also used in connection with bodies of revolution. in particular, for
a cone the boundary layer thickness at any point of surface with
coordinate S is lower than the thickness on plate $1.1\sqrt{3}$ once. Therefore
the local coefficient of heat emission in the laminar zone of the
cone of the engine can be found from the formula

$$\alpha^{i} = 9{,}32 \cdot 10^{-3} \sqrt{\frac{p_0 V_1}{S}}. \qquad (5.22) \bullet$$

In the turbulent zone of the flow above the cone the coefficient of friction at length S from vertex corresponds to the coefficient of friction on flat/plane plate at length S/2 from leading edge, other conditions being equal, [117]. Consequently,

$$\alpha = 5.06 \cdot 10^{-4} \frac{(p_0 V_1)^{0.8}}{S^{0.2}}. \qquad (5.23)$$

In this case, as for a flat/plane plate, it is accepted that the laminar flow exists up to $Re=0.5 \cdot 10^6$, and developed turbulent flow occurs beginning with $Re=2 \cdot 10^6$. When the conditions of icing are present, flow conditions in boundary layer, beginning from the apex of the cone, should be considered turbulent and the local heat-transfer coefficients calculad in formula (5.18). Average heat-transfer coefficients for a cone in the limits of length S from apex/vertex will be equal to

$$\bar{\alpha} = 6.33 \cdot 10^{-4} \frac{(p_0 V_0)^{0.8}}{S^{0.2}}. \qquad (5.24)$$

Since such comparatively large engine components, as the struts of fastening inner body have usually aerodynamic profiles/airfoils, then the calculation of local heat-transfer coefficients for these parts of engine in no way differs from the calculation of local heat-transfer coefficients for the lifting surfaces of aircraft, i.e., it is necessary to use formulas (5.15) - (5.18) taking into account the observations of the relatively transfer zone of flow. For stator blades in view of their small geometric dimensions it suffices

to know only coefficients of heat emission the average/mean over
surface.

Page 138.

Work [69] gives the experimental data according to average
heat-transfer coefficients for blades, obtained by different
researchers with the purging of grids/cascades, i.e., the series/row
of vanes (for example, guiding device), on the basis of which was
obtained the following calculated formula:

$$\alpha = 5 \cdot 10^{-3} \frac{(\rho_0 \widetilde{V})^{0.57}}{l_\pi^{0.13}},\qquad\qquad (5.25)$$

where l_π - ratio of the perimeter of the profile/airfoil of blade to
a number π, and $\widetilde{V}$ - the average speed of airflow near blade.

Calculation of heat-transfer coefficients for propellers.

The screws/propellers of aircraft and helicopter work under
conditions of severe vibration and imposition of speeds (speed of
forward motion and the rotational speed). These conditions have the
same effect on flow conditions as the sweepback of the lifting
surfaces of aircraft.

Therefore the calculation of local heat-transfer coefficients

for propeller blades should be performed according to formulas (5.16) and (5.18) for turbulent flow conditions.

It is necessary to note that for aircraft screws/propellers the velocity, which must be substituted in formulas (5.16) and (5.18), is determined from the expression

$$V_{r0} = V \overline{V_0^2 + V_r^2}, \qquad (5.26)$$

where

$$V_r = \omega R = \frac{\pi n}{30} R \qquad (5.27)$$

there is the tangential speed, which appears in cross section of blade screw/propeller, distant at a distance of R from rotational axis, n - number of revolutions per minute. Respectively local velocity V_{r1} at the arbitrary point of the cross section profile of the screw/propeller of aircraft is found from the expression

$$V_{r1} = V_{r0} V \overline{1 - \overline{p}}.$$

For the screw/propeller of helicopter into formula (5.18) in place of V_0 is substituted directly the value of tangential speed V_r, since during one revolution the averaged speed of the flow, which encounters to screw/propeller, does not depend on the speed of forward motion and is determined only by rotary motion of screw/propeller.

Average heat-transfer coefficients in the cross section of the screws/propellers of aircraft and helicopter can be obtained in the

same manner as for for the lifting surfaces of aircraft.

In the validity of the proposed formulas for the calculation of heat-transfer coefficients it is not difficult to be convinced, if to use the experimental data according to average heat-transfer coefficients for the blades/vanes of helicopter, given in work [130].

Page 139.

Observations about the calculation of heat-transfer coefficients for cockpit windows.

The calculation formulas, given above, make it possible to calculate heat-transfer coefficients, also, for other aircraft components or helicopter which undergo icing in flight.

In particular, if the surface of glazing or fairing is correct cone, then local heat-transfer coefficients are designed from formulas (5.22) and (5.23), but average heat-transfer coefficients - according to formula (5.24). But if surface is made in the form of ellipsoid, then heat-transfer coefficient at the tip of ellipsoid [34] should be designed from the formula

$$\alpha = 2.46 \cdot 10^{-2} \sqrt{\frac{\rho_0 V_0}{D}}, \qquad (5.28)$$

where D - diameter of the equivalent sphere, inscribed into the
nose/leading edge of fuselage. On remaining surface of sight glasses
or radar antennas local heat-transfer coefficients are designed from
formulas (5.22) and (5.23), and average coefficients in formula
(5.24).

If sight glasses are made in the form of the flat surfaces,
tilted ϕ to the incident airflow, then, as it follows from work [5],
local heat-transfer coefficients for them can be calculated from the
formula

$$\alpha = 4.4 \cdot 10^{-4} \frac{(\rho_0 V_1)^{0.8}}{S^{0.2}} [1 + 0.4 (\text{tg}\,\varphi)^{1.75}]. \qquad (5.29)$$

It is necessary to indicate that during the determination of the
local heat-transfer coefficients and location of points the
beginnings and the end/lead of the transition/transfer from distance
laminar to turbulent mode/conditions must be counted off from the
stagnant (critical) point of body, into which are inscribed the
surfaces of glass in question, fairings, etc.), but not from the
beginning of these quite surfaces.

For the case of the cylindrical surface, established/installed
in parallel to incident airflow, on heat-transfer coefficients will
have effect the curvature of body in the plane, perpendicular to flow
direction. However, in the first approximation, heat-transfer

coefficients for this body can be designed as for a flat/plane plate,
i.e., by taking into account the possibility cf ice formation, from
formulas (5.18) or (5.20) for turbulent flow conditions.

Page 140.

5.3. Calculation of heat of vaporization and heating of water (ice)
on the surface, streamlined with flow.

Heat of vaporization of water (ice).

The heat-flux density for evaporation from the unit of the moist
surface of certain quantity of water G_n depends on the intensity of
evaporation, which in turn, is determined by the value of the
coefficient of mass transfer and by a concentration difference or by
a difference in the partial pressures (elasticity) of the saturated
water vapor[1] directly in moist surface e_n and at certain distance
from it, out of boundary layer e_1.

FOOTNOTE [1]. Under conditions of icing the air is usually saturated
(or it is close to saturation) by water vapor. Therefore in all
calculations is accepted saturation pressure. ENDFOOTNOTE.

First value e_n is determined by the temperature of moist surface

$t_{n.в.н.}$ the second e_1 - temperature of flow on boundary layer edge t_1.
(The same is related it is related also to the iced over surface, but
elasticity of vapor in this case should be, correspondingly, accepted
necessary ice $e_{n.л.}$).

Thus,

$$q_{\beta L} = G_{u}L_{u} = \beta_{P}L_{u}(e_{n} - e_{1}) \quad вm/м^{2}, \quad (1) \qquad (5..30)$$

Key: (1). W/m².

where β_{P} - coefficient of mass transfer, which relates to a
difference in partial pressures [2]:

L_{u} - heat of evaporation in the J/kg:

e - vapor pressure in N/m².

In the case in question, however, it is much more convenient
during calculations to use not the coefficient of mass transfer
directly, but to express it through the coefficient of heat emission,
being based on Reynolds's known approximate analogy between heat- and
mass exchange with their joint course:

$$\beta_{P} = \frac{\alpha}{\varrho_{в.в}c_{p\,в.в}R_{в.п}T} \cdot \qquad (5.31)$$

where the indices "vl" are related to humid air, " v.p" - to water
pair.

In view of relatively low concentration of vapor in the temperature range which interests us it is possible to accept: $\dot{\varrho}_{n.n} \approx \varrho$; $\dot{c}_{p\,n.n} \approx c_{p}$; $p-e_1 \approx p$. Then, taking into account, that $\frac{1}{R_{\text{B.n}}T} = \frac{\varrho_{\text{B.n}}}{p_{\text{B.n}}} \approx \frac{R}{R_{\text{B.n}}} \frac{p}{\varrho}$, where a relation of gas constants of air and water vapor $R/R_{n.n} = 0.622$, we have

$$\beta_p = \frac{0.622\alpha}{c_p p}.$$

(5.31a)

Page 141.

Consequently,

$$q_{\beta 1} = \frac{0.622\alpha L_n}{c_p} \cdot \frac{e_n - e_1}{p}.$$

(5.30a)

Further should be considered the part of the heat, compensated due to the high-speed/velocity heating:

$$q_{\beta}^{\cdot} = \frac{0.622\alpha L_n}{c_p} \cdot \frac{e_{1\text{B}n}^{\cdot} - e_1}{p}.$$

(5.32)

Here $e_{1\text{B}n}^{\cdot}$ - saturation pressure which corresponds to the equilibrium temperature of moist surface.

Elasticity of vapor on the boundary of boundary layer is determined approximately from the relationship/ratio

$$e_1 = e_0 \frac{p}{p_0},$$

(5.33)

where e_0 - saturation pressure at ambient temperature t_0.

Thus, the heat-flux density, which must be conducted to surface

for the compensation for heat of vaporization, must be equal to

$$q_\beta = q_{\beta 1} - q_\beta^\bullet = \frac{0.622 \alpha L_{\text{м}}}{c_p} \cdot \frac{e_\text{n} - e_{\text{\i{}вл}}}{p}.   (5.34)$$

Calculation of the heat of heating the absorbed by water and crystals

of ice.

During the steady heat exchange evaporating water from surface

is accompanied by its heating from ambient temperature to the

temperature surface. In this case one should consider, besides the

heat of high-speed/velocity heating, also preheating water due to the

heat of the conversion of kinetic energy into heat with the

impact/shock of drops about surface which will be equal in the first

approximation,

$$\Delta t_{\text{в. кин}} = \frac{V_0^2}{2 c_\text{в}},$$

where $c_\text{в}$ - specific heat of water.

Then, knowing the local intensity of the catching of water at the

particular point of surface $G_\text{в}$, we can determine the heat flux,

necessary for heating of water from its equilibrium temperature to
the temperature of the surface:

$$q_\text{в} = G_\text{в} c_\text{в} (t_\text{в. эн} - t_\text{пов} - \Delta t_\text{в. кип}).$$ (5.35)

Page 142.

For the case of heating the crystals of ice term $q_\text{л}$ is divided
by two: 1) during heating from $t_\text{л. кри} = t_0 + \dfrac{V_0^2}{2c_\text{л}}$ to 0°C, where $c_\text{л}$ —
specific heat of ice, and 2) during heating from 0°C to $t_\text{п. пт}$.
Furthermore, appears the term, which considers heat of fusion of ice,
$L_\text{л}$. Thus, for heating of the crystals of ice from $t_\text{л. кри}$ to $t_\text{п. кт}$ 0
the necessary heat-flux density is equal to

$$q_\text{л} = G_\text{е} [c_\text{л} (0 - t_\text{л. кри}) + c_\text{л} (t_\text{п. кт} - 0) + L_\text{л}].$$ (5.36)

5.4. Design conditions for an exterior problem.

Total density of thermal flow.

Utilizing formulas (5.2), (5.34), (5.35) and (5.36) the
preceding/previous sections, we obtain all values, necessary for the
calculations of total heat-flux density according to formulas (5.1):
$q_\text{п} = q_\text{α} + q_\text{β} + q_\text{β}$, or $q_\text{к} = q_\text{α} + q_\text{β} + q_\text{л}$. However, as it was said in Section
5.1, for calculation with the virtually real precision/accuracy of
the heating of the majority of the parts of the flight vehicles by
all right members of equality (5.1b), in comparison with first two,
it is possible to completely disregard. Furthermore, it is necessary

to keep in mind that under conditions of icing as the temperature of surface t_u and equilibrium temperature t_1 should be accepted the temperature, which corresponds to moist surface, i.e., $t_{n\ вл}$ and $t_{1вл}$. Then the total density of external heat flux is equal to

$$q_n \quad \alpha\,(t_{n\ вл} - t_{1вл}) + \frac{0.622\alpha L_u}{c_p}\cdot\frac{e_u - e_{1вл}}{p}. \qquad (5.37)$$

This equation contains two unknown values: $t_{1вл}$ and $e_{1вл}$.

Its solution, however, does not represent work, since with the aid of sufficiently simple conversion it can be given to such form, in which it is not contained unknowns. For this we find expression $t_{1вл}$ from condition $q_n = 0$ (taking into account, which in this case $t_{n\ вл}$ corresponds $t_{1вл}$ and $t_{1вл} - t_1$)

$$t_{1вл} \quad t_1 - \frac{0.622}{c_p}\cdot\frac{e_{1вл} - e_1}{p}. \qquad (5.38)$$

Substituting this expression in (5.37), after some conversions we obtain the equation given above in the following form:

$$q_n \quad \alpha\,(t_{n\ вл} - t_1)\left(1 + \frac{0.622 L_u}{c_p p}\cdot\frac{e_n - e_1}{t_{n\ вл} - t_1}\right). \qquad (5.37a)$$

Page 143.

This equality is solved already without difficulty, since $t_{n\ вл}$ and, consequently, e_n must be prescribed/assigned, and t_1 easily is determined from formula (5.5).

The factor

$$1 + \frac{0.622 L_н}{c_p p} \cdot \frac{e_n - e_{1вл}}{t_{н.вл} - t_1} = X, \qquad (5.39)$$

for the first time introduced of Hardy [111], [112], [113], consider
an increase in the density of total heat flow relative to the density
of the flow of convective heat emission.

It must be noted that for the small values of the
high-speed/velocity heating of surface, which correspond to rated
flight performances for POS, in the first approximation, it is
possible to accept $t*_1 = t_1$ or even (for estimate calculations) $t_1 = t_0$,
$e_1 = e_0$ and $p = p_0$.

Finally, taking into account, that in the **temperature** range
$c_p \approx 1000$ **J/kg•deg** which interests us and $L_н \approx 25 \cdot 10^5$ **J/kg**, we have
$\frac{0.622 L_н}{c_p} = 1550.$

Consequently,

$$X = 1 + \frac{1550}{p} \cdot \frac{e_n - e_1}{t_{н.вл} - t_1}. \qquad (5.39a)$$

**Dependence of heat-flux density on ambient conditions and flight
conditions.**

Let us examine how depends the density of external heat flux on the temperature of medium, flight speed (flow), height/altitude, and also local conditions for the flow around surface, in order to determine the severe (calculation) conditions under which value q_n will be maximum.

The effect of the range of the calculated temperatures of icing does not require the special explanations: both the convective heat emission and heat emission for evaporation grow/rise with an increase in the calculated range of temperatures of icing, i.e., than that lower prescribed/assigned $t_{орасч}$ by those is required high heat-flux density q_n.

Dependence q_n on the calculated value of the speed of flow is more complicated: to the larger speed of flow $V_{орасч}$ corresponds the high value of heat-transfer coefficient, but at the same time temperature drop (other conditions being equal,) $t_{n.вл} - t_1^*$ is decreased as a result of the increase Δt^*_1, which increases proportional to the square of speed, as that follows from formula (5.4). As a result their product $q_n = \alpha (t_{n.вл} - t_1^*)$ with certain value $V_{0\,орасч}^*$ has a maximum.

Page 144.

Dependence $q_\beta = \alpha \Delta t_\beta$ has the similar, but flatter character of
curve with the maximum, shifted to the right in comparison with curve
q_u. the location of this maximum along the axis V_0 somewhat depending
on prescribed/assigned flight altitude.

Altitude effect on the calculated value of heat-flux density is
expressed in the fact that the value of heat-transfer coefficient
and, consequently, also q_α, as this follows from Section 5.2, with
height/altitude is decreased, in the case of turbulent boundary layer
it is proportional to the degree of 0.8 ratios of pressure at the
heights/altitudes in question: $\alpha_{H2} = \alpha_{H1}\left(\frac{p_{02}}{p_{01}}\right)^{0.8}$, (where $H_2 > H_1$, whereas heat
of vaporization is inversely proportional to degree of 0.2 of this
sense $q_{\beta 1} = q_{\beta 2}\left(\frac{p_{01}}{p_{02}}\right)^{0.2}$. As a result with an increase in rated altitude
H_{pacq} the total quantity of heat-flux density q_n somewhat is
decreased, and maximum $q_n(V_{\bullet pacq})$ is shifted/sheared to the right (see
example of 5.1 and Fig. 5.8b).

From the given example it is evident that calculated value q_n
corresponds to minimum rated altitude of flight in the speed of flow
on the order of 150 m/s.

The distribution of the necessary heat-flux density according to

profile/airfoil $q_n(S)$ usually corresponds to the diagram/curve of the local pressures p. In fact, the local value of coefficient α and expression $\Delta t_\beta = \frac{0.622 L_n}{c_p} \cdot \frac{c_n - c_{1n,1}}{p_1}$ follow change V_1 (since $V_1 = V_0 \sqrt{1-\bar{p}}$).

It is logical that as the calculated distribution of the value of heat-flux density $q_n(S)_{\text{расч}}$ should be accepted the envelope for curves $q_n(S)$, obtained for several flight conditions.

Change $\tilde{q}_n(z)$ in the span of usual wing or tail assembly, as a rule, is small, it somewhat grows/rises from one root to in accordance with certain increase of average heat-transfer coefficient. For the delta wing or change $q_n(z)$ in spread/scope it can be considerably greater.

Distribution $q_n(R)$ according to a radius of propellers is obtained in accordance with a change in the circular/neighboring speed of the flow around blades/vanes. Since in this case dependence q_n examined above on V_0 remains valid then at the length of blade/vane usually is maximum $q_n(V)_{max}$, which corresponds to the cross section in which peripheral speed V_r has value on the order of 150 m/s.

Finally, one should again emphasize that everything said above is related to the density of external (surface) heat flux q_n. The

density of internal thermal flows and its distribution depend on type

and construction/design of deicer, thermal leakages and the like and

can considerably exceed q_n.

Page 145.

Heating the partially moistened surface. Concept about flowing the

water film.

The dependences examined above are related to the completely

moistened surface. However, the specific sections of the surface

shielded from icing in the zone of flowing in are wet only partially,

in this case the temperature or dry sections proves to be, naturally,

higher than moist. As a result mean temperature of the heated surface

will be between t_n and $t_{n.вл}$ (for a metal covering it will correspond

to certain averaged temperature which will be established/installed

due to the thermal conductivity of metal). In other words, in order

to heat to the prescribed/assigned temperature the partially

moistened surface, is required less heat-flux density. This decrease

in the first approximation, is proportional to the relation to the

surface of moist sections to an entire surface, which can be taken

into consideration in calculations by the introduction of the

corresponding coefficient.

Let us examine flowing the water film, which is formed as a result of the catching of the drops of water by the surface, heated to positive temperature. On it it is possible to isolate two zones: the zone of the catching of drops $S_{y,n}$ (examined in chapter IV) and the zone of the flowing in of water S_1. For the deicer, designed for complete drainage, these two zones, determined for heaviest design conditions, must in sum compose extent of the zone of heating $S_{\text{H}} \geqslant (S_{y,n} + S_3)_{\text{рас}}$ (Fig. 5.5a). But if value S_{H} proves to be less, then will be formed barrier ice.

The fundamental parameter, which characterizes flowing the film, is the flow rate of the water through the cross section of film $G_{n,n}$ on 1 m of the length (spread/scope) of the surface:

$$G_{n,n} = \varrho_{\text{B}} \delta_{n,n} \bar{V}_{n,n}, \qquad (5.40)$$

where ϱ_{B} - water density;

$\delta_{n,n}$ - thickness;

$\bar{V}_{n,n}$ - speed of film average/mean over cross section.

If they was not the losses of water as a result of evaporation and blowing, then local rate of discharge $G_{n,n}(S)$, beginning from leading edge and to the end/lead of the region of catching, would grow/rise (curve 1, Fig. 5.5b). As a result of evaporation $G_{n,n}(S)$ it

decreases (curve 2), and when blowing off of the part of the water is present, this decrease will be even more considerable (curve 3). The flow of film continues until $G_{n,a}(S)$ decreases to zero or until water will achieve the **boundary of heating**. In the latter case this boundary flow rate $G_{n,a}(S_a)$ characterizes the possible initial intensity of the formation/education of barrier of ice[1].

FOOTNOTE [1]. In proportion to the increase of barrier ice it itself can become the object of the direct catching of drops, as a result of which the intensity of its formation/education grows/rises. ENDFOOTNOTE.

Page 146.

As is known [20]. there are three flow conditions fluid films over rigid surface depending on Reynolds number:

$$Re_{n,a} = \frac{\delta_{n,a} v_{n,a} \delta}{v_a} = \frac{G_{n,a}}{\varrho_a v_a}. \qquad (5.41)$$

When $Re_{n,a}$ to 20-30 - flow laminar, when $Re_{n,a} > 30$ - the flow has wave laminar (pseudo-laminar) character, when $Re_{n,a}$ order 1500 and more - a flow becomes turbulent.

a)

b)
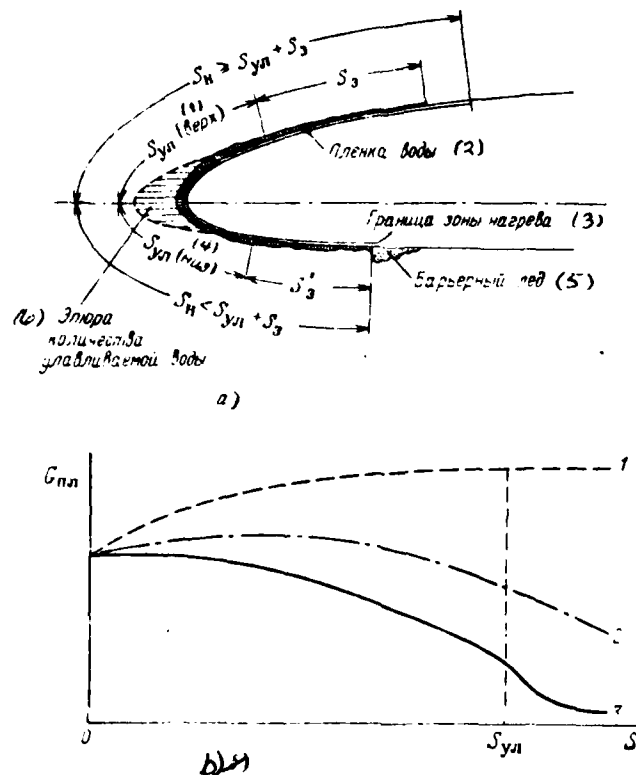
Fig. 5.5. The diagram of the process of the spreading of the water, recovered by the profile/airfoil: a) the zone of catching and spreading of the water; b) a quantity of the water: 1 - without taking into account the losses; 2 - taking into account the evaporation; 3 - taking into account evaporation and escape.

Key: (1). top. (2). Film of water. (3). Boundary of heating zone. (4). base. (5). Barrier ice. (6). Diagram/curve of quantity of absorbed by water.

Page 147.

It is easy to ascertain that with icing even under conditions of the greatest calculated **water content** and even without taking into account the losses of **water** $Re_{n.n}$ it has a value which completely corresponds to the region of **stream-line** conditions (for example, for **the quantity** of absorbed by water, obtained in example of 4.1, number $Re_{n.n}$ **of the** account of losses it composes a total of about $2 \cdot 10^{-6}$) .

For approximate solution of the equation of motion of film let us accept the following assumptions: in view of the small thickness of film surface we consider flat/plane; by the speed of film in comparison with air speed, and also gravitational forces and inertia of film in comparison with the frictional force of airflow negligible. In this case the equation of motion of Navier-Stokes for a thin film will take the form

$$v_a = \frac{\partial^2 \tilde{v}_{n.n}(y)}{\partial y^2} = 0 \qquad (5.42)$$

under the following boundary conditions:

on body surface

$$y = 0, \quad v_{n.n}(0) = 0, \qquad (5.43a)$$

on the outer edge cf the film

$$y = \delta_{n.n}, \quad \mu_{B} \frac{\partial v_{n.n}(\delta_{n.n})}{\partial y} = f_{\text{тр}}, \qquad (5.~136~6)$$

where μ_{B} - dynamic viscosity of water,

$f_{\text{тр}}$ - stress of friction of airflow.

Its solution

$$v_{n.n}(y) = f_{\text{тр}} \frac{y}{\mu_{B}} \qquad (5.44)$$

corresponds to the linear law of speed change in the thickness of film. Consequently, speed on the outer edge of film is equal to

$$v_{n.n}(\delta_{n.n}) = f_{\text{тр}} \frac{\delta_{n.n}}{\mu_{B}} \qquad (5.44a)$$

and the speed

$$\tilde{v}_{n.n}(\delta_{n.n}) = \frac{f_{\text{тр}}}{2} \cdot \frac{\delta_{n.n}}{\mu_{B}}. \qquad (5.446)$$

average/mean over cross section.

Taking into account equality (5.40), express is speed and thickness of the film through the flow rate:

$$v_{n.n}(\delta) = \sqrt{\frac{G_{n.n} f_{\text{тр}}}{2\mu_{B}\rho_{B}}} \qquad (5.45)$$

and respectively

$$\delta_{n.n} = \sqrt{\frac{2G_{n.n}\mu_{B}}{\rho_{B}f_{\text{тр}}}}. \qquad (5.46)$$

Page 148.

The obtained parameters to a considerable extent depend on the speed of flow and temperature of the film of water. So, the thickness of film decreasesinversely proportional to the local velocity of airflow V_1, since friction stress is equal to:

$$f_{тр} = c_f \varrho \frac{V_1^2}{2},\qquad (5.47)$$

where c_f - the coefficient of friction. It is decreased also with an increase in the temperature of film, since the viscosity of water depends substantially on the temperature (see Table 5.1).

Experiments which were being carried out by the authors of present chapter on the special installation (Fig. 5.6), which made it possible over wide limits to assign $G_{пл}$, initial thickness $\delta_{пл}$, temperature of surface and the speed of airflow, confirmed sufficiently well the validity of the obtained approximate dependences.
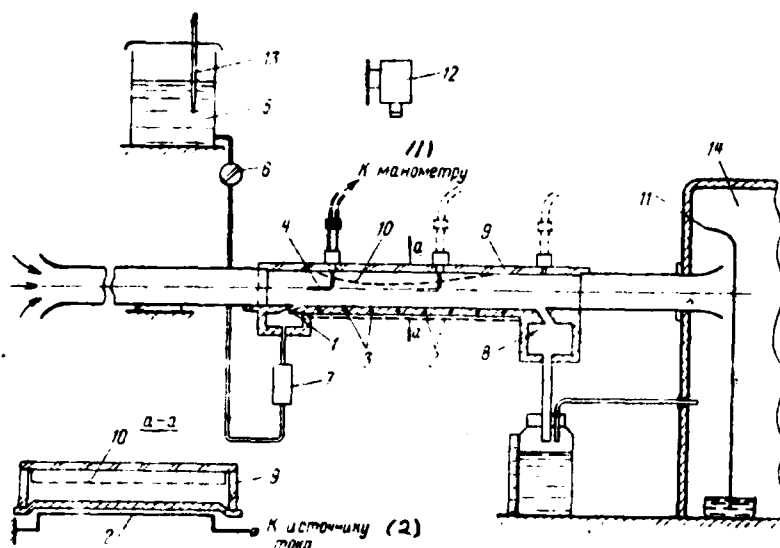
Fig. 5.6. The installation diagram for the investigation of flow of water on the surface: 1 - adjustable slot; 2 - section of the heating; 3 - thermocouple; 4 - air-pressure head; 5 - tank with the water; 6 - tap/crane, which controls water supply; 7 - flow meter; 8 - header; 9 - Plexiglas duct; 10 - interchangeable shaped insert/bushing; 11 - panel for the catching of the spray of the water; 12 - motion-picture camera; 13 - thermometer; 14 - pressure chamber.

Key: (1). To manometer. (2). To current source.

Table 5.1. Viscosity of water at different temperatures.

(1) Температура в °C	0	10	20	30	40	50	60	70	80	90
(2) Вязкость н·сек/м³ в	1790	1310	1000	800	650	550	470	405	355	315

Key: (1). Temperature in °C. (2). Viscosity N•s/m².

Page 149.

Experiments made it possible to also have representation about the effect of the wettability or surface on the flow of film and about phenomenon of blowing water in dependence on factors indicated above. As a result of these investigations was obtained the picture, familiar to many researchers, carrying out by questions of the catching of drops (Fig. 5.7a): in the nose section of the body film continuous, then it is disrupted to separate bands, separate of them can apply to considerable distances.

This decrease of quantity of water due to blowing it would be possible to consider with the aid of certain coefficient $\xi_в$, then the local flow rate of water in film in the presence of blowing is equal to

$$G_{пл}(S) = \xi_в G_{пл}(S)_{max},$$
$$(5.48)$$

where $G_{пл}(S)_{max}$ – an expenditure without taking into account losses for blowing.

Thus, qualitatively character $\varepsilon(S)$ will take the form, shown in Fig. 5.7b (twisting $\underline{\xi_в}$). However, to quantitatively estimate value $\xi_в$ is very difficult, since very is difficultly to experimentally determine separately losses from evaporation and blowing, in to the same value of blowing to a considerable extent depends on particular factors (wettability and temperature of surface, the form of body, flight conditions, the conditions for flow, etc.).
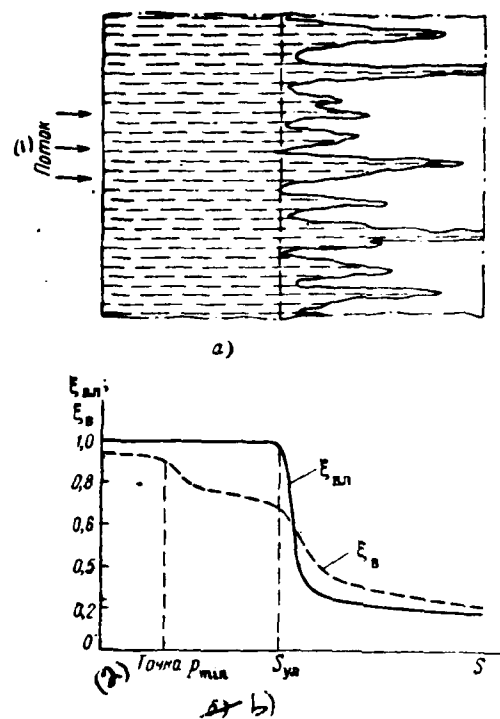
Fig. 5.7. Character of the wettability of the heated surface under conditions of the icing: a) the visual picture of the course of the film of the water; b) tentative values of the coefficient of humidity on the surface of metal covering.

Key: (1). Flow. (2). Point.

Page 150.

Relative value of the moist sections of surface yields to

quantitative evaluation considerably more easily, since it is
determined by direct observation and can be expressed through another
coefficient which can be named/called the coefficient of the humidity
(or wetting) of surface $\xi_{s,n}$ (it is equal to the ratio of moist
sections $\Delta S_{s,n,i}$ in the zone in question to an entire area of this zone
ΔS_i):

$$\frac{\Delta S_{s,n,i}}{\Delta S_i} = \xi_{s,n}. \qquad (5.49)$$

Of the picture described above of the flow of film it follows
that in the nose section of the body, approximately/exemplarily in
the limits of the region of catching $\xi_{s,n}$ 1. then, beginning from the
boundary of the region of catching and further, its value sharply
decreases (curve $\xi_{s,n}$).

Quantitatively this decrease $\xi_{s,n}(S)$, as coefficient ξ_s it depends
on many factors. For example, in connection with lifting surfaces
with metal covering it is possible to accept value $\xi_{s,n}$ beyond the
limits of the region of catching in average/mean order 0. 2-0. 3.

Consequently, during the calculation of surface density [1] of
heat flux q_n beyond the limits of the region of catching it is
necessary value q_β to multiply by $\xi_{s,n}$.

FOOTNOTE 1. With the calculation of that applied of from within heat

it is necessary to consider that at the end of the zone heating th-
density of internal flow can be substantially higher than surface
one, as a result of the leakages of heat beyond the limits of the
warmed casing (see Section 6.4). ENDFOOTNOTE.

After designating it q_β', let us have

$$q_\beta' = \alpha \xi_{в.л} \frac{0.622 L_i}{c_p} \frac{e_п - e_{1в.л}'}{p}. \qquad (5.50)$$

Should be focused attention on the fact that the convective term
in this case does not change, since calculated temperature drop
$\Delta t_{п.в.л} = t_{п.в.л} - t_{1в.л}'$ will remain the same as when $\xi_{в.л} = 1$. As a result the
necessary density of heat in the zone of flowing in will be equal to

$$q_{п.з} = q_\alpha + \xi_{в.л} q_в = q_\alpha + q_\beta. \qquad (5.51)$$

Opening the expressions of values, entering this formula, it it
is possible to represent in other form

$$q_{п.з} = \alpha (t_{п.в.л} - t_1') \left[1 - \xi_{в.л} \frac{1550}{p} \cdot \frac{e_п - e_1}{t_{п.в.л} - t_1'} \right] =$$
$$= \alpha (t_{п.в.л} - t_1') X', \qquad (5.51a)$$

where $X' = 1 - \xi_{в.л} \frac{1550}{p} \cdot \frac{e_п - e_1}{t_{п.в.л} - t_1'}$ - this the same factor (5.39), but with
consideration the coefficient of the humidity of surface.

Example   5.1. To obtain the dependence of heat-flux density on
profile of the wing, examined in example of 4.1 with the following
data: H=1000 m, V_0=150 m/s, $t_{0 расч} = -30°C$, $|t_{п.в.л}|_{расч} = 0°C$.

Page 151.

Let us examine q_n for the zone of catching S_{y_n} and zone of flowing in S_3.. In limits $S_{y_1} = 0.06$ of m we accept roundedly $\widetilde{\alpha} = 500$ W/m²deg. From Fig. 4.18b and $\frac{C}{m}$ we have $\bar{p} = -1.4$ and $V_1 = 230$ m/s, further according to formula (5.5) we determine $t*_1 = -30 + 150/2000$ $[1 - 0.12(230/150)^2]$ ■ $= -22°C$. Local pressure $p = p_0 - \bar{p} q_{ck}$, where $q_{ck} = \varrho \frac{V_0^2}{2} = 1.1 \frac{150^2}{2} = 12\,400$ N/m², consequently p=90•10³-12.4•10³x1.4=72,600 N/m². According to formula (5.39) $c_1 = 38$ 72,600/90,000=30.7 N/m² and according to formula (5.39a) $\chi = 1 + 1550/72,600 • 610 - 31/0 - 22 = 1.57$.

Thus, the average flux density of heat in the limits of the region in question is equal (formula 5.37a) $q_n = 500$ [0-(-22)] 1.57=17,300 W/m².

Heat-flux density in the region of flowing in q'_n we determine taking into account the fact that the surface will not be completely wet, i.e., according to formulas (5.51) or (5.51a), accepting $\xi_n = 0.3$.
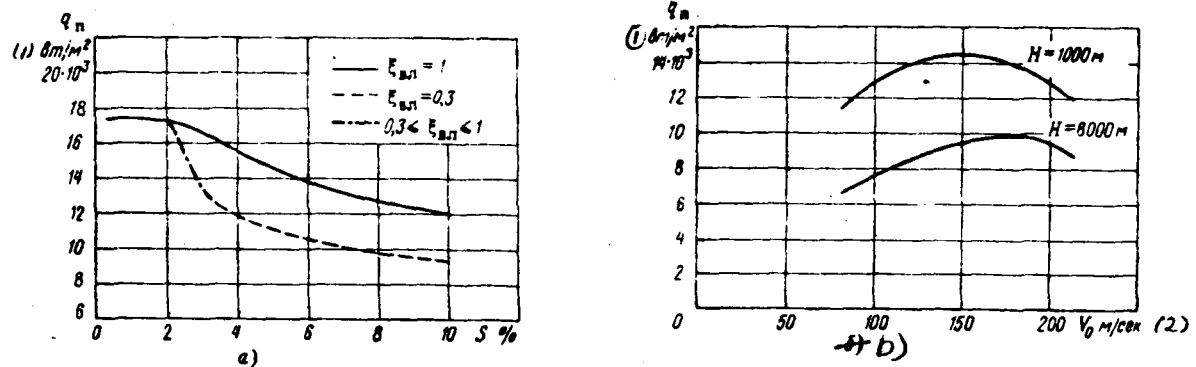
Fig. 5.8. Necessary density of the surface heat flux: a) density distribution according to the enclosure of profile/airfoil (along chord); b) the dependence of the average density of heat on speed and flight altitude.

Key: (1). W/m^2. (2). m/s.

Page 152.

The placenta of accomplishing calculations we will obtain density distribution heat flow according to profile/airfoil $q_n(S)$, shown in Fig. 5.8a.

For a comparison on it is given curve q_n for the case of complete wetting ($\xi_{B.\Pi} = 1$).

Example of 5.2. To calculate for the conditions, examined in the preceding/previous example, average/mean heat-flux density $\tilde{q}_n$ in limits of S=10o/o for H=1000 m and 8000 m, accepting conditionally $\tilde{S}_{a,\pi} = 1$

The results of calculations (for H=1000 m) are brought to table.

V_0 м/сек (1)	100	150	200		
$\tilde{\alpha}$ вm/м² град (2)	310	430	490	По 5.21	формуле
$\tilde{V}_1$ м сек (1)	168	209	259		(3)
$\tilde{t}_1$ °C	—26,4	—21,6	—14	По 5.5	формуле
$\tilde{\lambda}$	1,43	1,54	1,85	По 5.39	формуле
$\tilde{q}_n$ вm/м² (4)	12 900	14 300	12 700	По 5.37a	формуле

Key: (1). m/s. (2). W/m² deg. (3). According to formula. (4). W/m².

They are analogous calculation we make for H=8000 m. Dependence $\tilde{q}_n$ for this example on flight speed with H=1000 m and H=8000 m is given in Fig. 5.8b.

5.5. Calculation of the temperature of moist and dry surfaces.

Temperature of moist surface.

Equality (5.37) makes it possible to obtain the dependence between the temperature of moist and dry surfaces, which, as shown

below, considerably facilitates calculation, and testing de-icing
systems. With dry surface, as it follows from (5.2), $q_n = \alpha(t_{11} - t_1^{\cdot})$.
Substituting this expression into equality (5.37), we have

$$\alpha(t_{11} - t_1^{\cdot}) = \varkappa(t_{11.\,\text{в.л}} - t_{1\text{в.л}}^{\cdot}) + \frac{0.622\alpha L_н}{c_p} \frac{e_n^{\sim} - e_{1\text{в.л}}^{\cdot}}{p} \qquad (5.52)$$

also, after elementary conversions, taking into account (5.38):

$$t_{n.\,\text{в.л}} = t_{11} - \frac{0.622 L_н}{c_p} \frac{e_n - e_1}{p} = t_n - \Delta t_{1\beta}. \qquad (5.53)$$

Equations (5.38) and (5.53), that contain in terms of two
interdependent variable/alternating, are solved by the method of
successive approximations. For example, as first approximation it is
possible to accept: for $t_{1\text{в.л}}^{\cdot} = \frac{t_n - t_1}{2}$, and for $t_{n.\,\text{в.л}}^{\prime} = \frac{t_n + t_1}{2}$.

Page 153.

Substituting them in initial equations, we find appropriate values
$e_{1\text{в.л}}^{\cdot}$ or e_n, through them we determine the temperature in second
approximation/approach and i.e., until the results of the subsequent
solutions coincide between themselves with the required
precision/accuracy.

The temperature of moist surface both $t_{n.\,\text{в.л}}$ and $t_{1\text{в.л}}^{\cdot}$ can be
computed also according to the following formula, obtained on the
base of approximation by parabola $(A + Bt + Bt^2)$ cf the dependence of

vapor pressure on the temperature:

$$t_{\text{n. вл}} = \frac{1}{2B}\left[\sqrt{(65\rho_1 \cdot 10^{-5} + Б)^2 - 4ВД} - 65\rho \cdot 10^{-5}\right] - \frac{Б}{2B}, \quad (5.54)$$

where $Д = 610 - e_1 - 65\rho \cdot 10^{-5} t_n$ (for equilibrium temperature respectively $t_{\text{n. вл}} = t^*_{1\text{ вл}}$ and $t_n = t^*_1$). Remaining coefficients somewhat depend on the range of temperatures. For example, for $t_{\text{n. вл}}$ from -20 to 0°C B=46.7 and V=0.97; for $t_{\text{n. вл}}$ from -15 to +15°C B=50.5 and V=1.5.

Temperature drop in the dry surface.

The solution of the reverse problem, i.e., the determination of temperature or a temperature drop is dry in the surface through the value of the temperature drop, which occurs under conditions of icing, is convenient to fulfill with the aid of the coefficient, analogous the coefficient X examined above, expression (5.39). For this we convert equation (5.53) to the following form:

$$\Delta t_n = t_n - t^*_1 = (t_{\text{n. вл}} - t_1)\left(1 + \frac{0.622 L_n}{c_p} \frac{e_n - e_1}{t_{\text{n. вл}} - t_1}\right) =$$
$$= (t_{\text{n. вл}} - t_1) \cdot X_1, \quad (5.53a)$$

where the coefficient

$$X_1 = 1 + \frac{0.622 L_n}{c_p} \frac{e_n - e_1}{t_{\text{n. вл}} - t_1}. \quad (5.55)$$

Coefficient X_1 is characterized by from X fact that the temperature drop in it is related not to the equilibrium temperature t^*_1, but to

the temperature of flow t_4. Coefficient of X_1 is shown, in how often a temperature drop in the dry surface must be the more than appropriate temperature drop/jump in the moist surface.

Example of 5.3. To determine the (see example of 5.1) temperature drops/jumps maximum in the limits of heating surface of wing profile with $t_{o\,вех} = -30°C$. $t_{n.\,вл} = 0°C$. $V_0 = 150$ m/s, $H = 1000$ m. From Fig. 4.18 we see that the maximum $V_1 = 230$ m/s corresponds $\bar{S} \sim 2o/o$ chord, at this point $\bar{p} \sim -1.1$, according to formula (5.3) we determine $t_1 = -45.3°C$. We further find through formula (5.55) coefficient

$$X_1 = 1 + \frac{1560}{12\,600} \cdot \frac{610 - 25}{0 - 45,3} = 1,28.$$ Consequently, a maximum temperature drop in the dry surface at the point of profile/airfoil in question must be

$$\Delta t_{1n} = 45,3 \cdot 1,28 = 57°C.$$

Page 154.

The maximum speed of flight (flow), at which is possible the icing of surface.

Utilizing equation (5.38) in connection with the equilibrium temperature of the iced over surface, it is possible to rate/estimate the maximum speed of flight (airflow) $V_{л.\,пр}$, at which ceases the icing of unheated surface due to high-speed/velocity heating, i.e., temperature $t_{1л}$ reaches 0°C. Substituting in (5.38) expression t_1,

for $t_{1,a,1}^{*}$ and equalizing its 0, and also accepting for simplification $V_1 = V_0$, we have the approximate equality

$$0 = t_1 + \frac{V_{a,\,np}^2}{2c_p}r^* - \frac{0.622L_a}{c_p}\frac{e_n - e_1}{p}. \qquad (5.56)$$
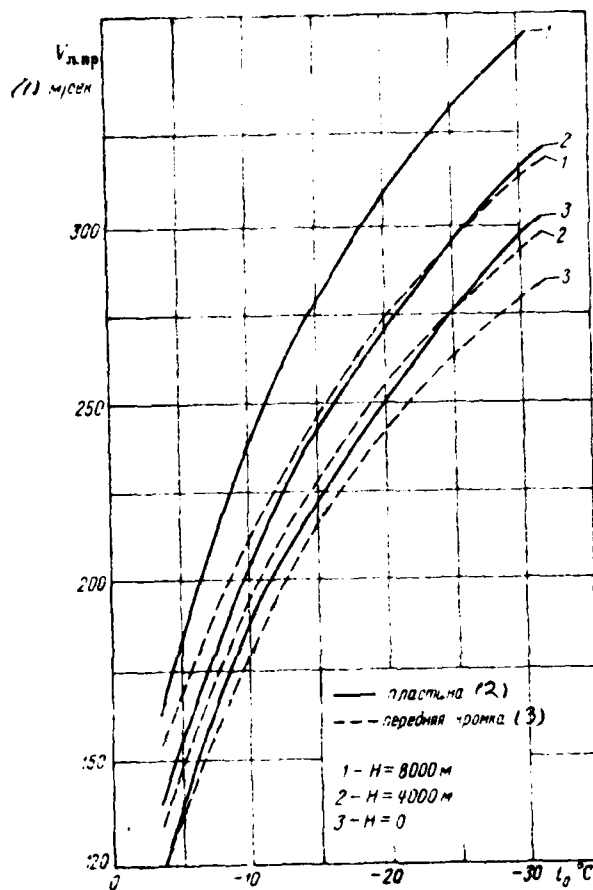
Fig. 5.9. Dependence of flight speed maximum for icing on temperature of medium and flight altitude.

Key: (1). m/s. (2). plate. (3). leading edge.

Page 155.

Taking into account, that in this case $e_n = 610$ N/m², we
obtain

$$V_{\text{л. пр}} = \frac{2c_p}{r^2} \sqrt{\frac{0.622 L_н}{c_p} \frac{610 - e_1}{p} - t_1}. \qquad (5.57)$$

As can be seen from this expression, value $V_{\text{л. пр}}$ for different
sections of the iced over surface is different. Minimum value $V_{\text{л. пр}}'$
is obtained for the leading edge where p and t_1 have the greatest
values, and vice versa, for preventing ice at the points, which hav-
minimum p, is required considerably high maximum speed, especially at
high altitudes.

Formula (5.57) makes it possible to determine maximum radius
$R_{\text{л. пр}}$ of the icing of screw/propeller at one or the other temperature
of the air:

$$R_{\text{л. пр}} = \frac{V_{\text{л. пр}}}{\omega}, \qquad (5.58)$$

where ω - angular velocity of rotation of screw/propeller.

In fig 5.9 is given dependence $V_{\text{л. пр}}$ on ambient temperature at
different flight altitudes for a leading wing edge and for the
surface, in parallel streamlined with flow (plate); while in Fig.
5.10 - dependence $R_{\text{л. пр}}$ on t_0 for the helicopter rotor blades of
Mi -4.
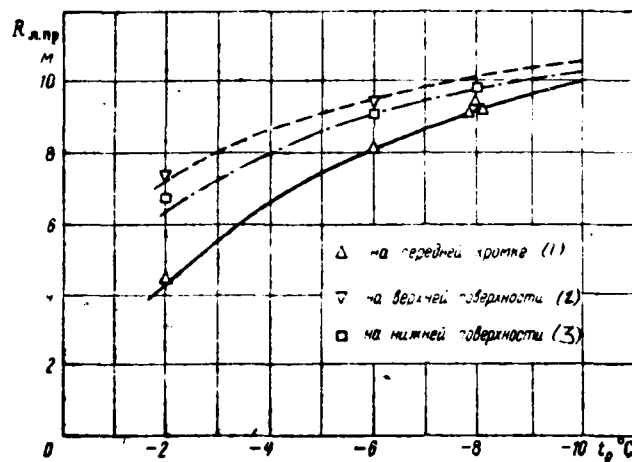
Fig. 5.10. The maximum radius of the icing of the blade/vane of carrying propeller of the helicopter of Mi-4 while hovering under conditions of the artificial icing (are shown experimental points).

Key: (1). on leading edge. (2). on upper surface. (3). on lower surface.

Page 156.

Temperature of the surface of glass with jet-edge protection.

As has already been mentioned in chapter III, the principle of jet-edge were sew glasses it consists in the joint thermal and mechanical effect of external hot jet on the film water, which is formed on surface as a result of settling to it the drops in flight under conditions of icing or rain. Effectiveness of the jet-edge protection is determined by the temperature and by jet velocity.

With the heating of surface by external jet a quantity of water, evaporated from the unit of surface per second, is determined by the dependence

$$G_{\text{в}} = \frac{0.622\alpha}{c_p} \frac{e_{\text{п. с}} - p_{\text{в. п. стр}}}{p}, \qquad (5.59)$$

where $e_{\text{п. с}}$ — saturation pressure at temperature of the moist surface of glass $t'_{\text{с. вл}}$;

$p_{\text{в. п. стр}}$ — elasticity of vapor at temperature of hot jet $t_{\text{стр}}$.

determined from the relationship/ratio, which escape/ensues from
(1.9) and (1.10) : $p_{\text{в. п}} = \varphi e_{\text{стр}} = e_0.$ remains equal to elasticity of vapor,
that saturates surrounding air.

Consequently, with an increase in the temperature of jet
grows/rises difference $e_{\text{п. с}} - e_0.$ Furthermore, an increase in the
temperature of most water film favors its blowing as a result of the
decrease of viscosity/ductility/toughness. Analogous effect gives the
increase of jet velocity - in this case grows/rises the heat emission
and, consequently, also the intensity of evaporation and increases
mechanical effect on film and, consequently, also its blowing. in
particular, under the joint influence of the parameters indicated is
decreased the thickness of the film [see expression (5.45)], thanks
to which it more rapidly is displaced into separate brooks (i.e. it
is decreased the coefficient of the humidity of surface $\xi_{\text{в,п}}$). which
already by itself leads to an improvement in the visibility.

The relationship/ratio between the temperature of the dry and
moist surface of glass is determined by the equation, analogous
(5.53):

$$t_{\text{с. в,п}} = t_{\text{с}}^{\bullet} - \frac{0.622 L_{\text{п}}}{c_p} \frac{e_{\text{п. с}} - e_0}{p},\qquad (5.53\text{б})$$

where $t_{\text{с}}^{\bullet}$ — temperature of the surface of dry glass.

Speed and temperature of jet as is known ▮▮[1], they are connected with specific relationship and depend from distance of S to nozzle edge. In this case for determining the local importance of speed $V_{\text{стр}}(S)$ and temperature $t_{\text{стр}}(S)$ of jet can be in the first approximation, used the dependence [1]

$$\frac{t_{\text{стр}}(S) - t_1}{t_{\text{стр}}(0) - t_1} = 0{,}72 \frac{V_{\text{стр}}(S) - V_1}{V_{\text{стр}}(0) - V_1} = \frac{0{,}86}{\sqrt{\dfrac{a_c S}{h} + 0{,}4}}, \quad (5.60)$$

where t_1 - temperature and V_1 - velocity of incident flow of the air above the surface of the glass; $t_{\text{стр}}(0)$ and $V_{\text{стр}}(0)$ — temperature and jet velocity in nozzle edge; h - height/altitude of the slot of nozzle.

FOOTNOTE applied from by the limits of the initial section of jet [1]. ENDFOOTNOTE.

Page 157.

Coefficient a_c can be accepted for a slot jet equal to 0.1.

from formula (5.60) it follows that surplus speed $\Delta V_{\text{стр}}(S) = V_{\text{стр}}(S) - V_1$, temperature drop in jet $\Delta t_{\text{стр}}(S) = t_{\text{стр}}(S) - t_1$ is higher, the greater surplus discharge velocity behind nozzle $\Delta V_{\text{стр}}(0) = V_{\text{стр}}(0) - V_1$, which will be in complete agreement with the physical representation about the picture of flow, confirmed

experimentally. Consequently, the effectiveness of jet-edge
protection is most high during critical outflow (for a usual nozzle),
and the zone of the action ("range") of jet depends in this case on
the flow rate of hot air, i.e., on value h.

Fig. 5.11 gives the temperature slopes of surface along the
jets, calculated by formulas (5.60) and (5.53b). For a comparison are
given also the experimental points, obtained on laboratory
installation [1].

FOOTNOTE [1]. Experiment was carried out by engineer V. V. Lonasov.
ENDFOOTNOTE.
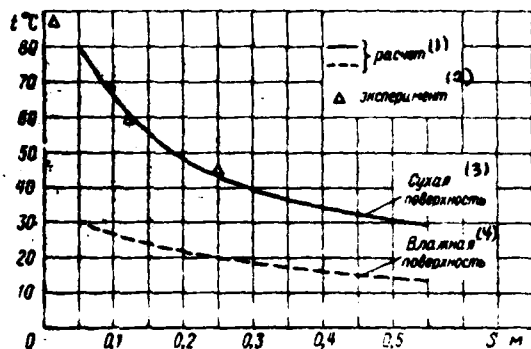
Fig. 5.11. Temperature of the surface of glass with jet-edge protection $(t_{\text{тр}} = 150^6 C; \; t_1 = t_0 = 0^\circ C; \; V_0 = 80$ м/s.

Key: (1). calculation. (2). experiment. (3). Dry surface. (4). Moist surface.

Page 158.

5.6. Estimate of the magnitude of the zone of heating, necessary for complete evaporation of water.

The value of heating surface, as it was shown above, consists of the zone of catching S_y' and zone of flowing in S_j of water. The first of them is determined by the ambient conditions for the flow around body and does not depend on type or construction/design of

deicer. The second depends both on the conditions for flow and on the construction/design of the heater of surface, in this case the determining parameter is the temperature of surface and, therefore, the corresponding value of the density of the heat flow applied to it. In other words, the zone of heating of the deicer of complete evaporation and the density of the heat applied to surface are inseparably interconnected values.

The methods of calculation of the parameters of thermal deicers taking into account the special features/peculiarities of internal heat supply are examined in the following two chapters. Nevertheless, for preliminary analysis and selection of one or the other version POS is very desirable to compare the systems in question with respect to the fundamental parameters. As such parameters for POS of permanent action can serve the size of zone heating and surface heat flux Q_n^- on 1 m of spread/scope.

The quantity of heat applied to the surface, which must be expended on the evaporation of the water spreading on it, is determined from the relationship/ratio

$$Q_\beta - Q_n \quad Q_\alpha \geqslant \xi_u G_{y,\jmath} L_u,   (5.61)$$

where Q_n — total heat flux in the W/m;

Q_α — portion of heat flux, expended to convective heat emission,

in the W/m;

   ξ_B — coefficient of quantity of water on the surface(see
      section 5.4)

   $G_{v_{.a}}$ — **quantity of water** on 1 m of spread/scope, recovered 1 s, in

kg/m•sek.

The heat flux Q is the sum of the products of heat-flux

densities in appropriate sections

$$Q_n - Q_a \quad \sum_{1}^{n} (q_n - q_a)_i \cdot S_i. \qquad (5.62)$$

During the preliminary (estimate) calculations, for which is

intended the method in question, it suffices to be restricted two to

the sections indicated above: $S_{y,n}$ and S_i, taking within the limits of

these sections the average/mean values of the densities of the heat

and other entering the calculation values. in this case on the basis

of (5.61) and (5.62) we obtain the following expression for

determining the size of the zone of the flowing in:

$$S_i = \frac{\xi_B G_{v,a} L_{_{\text{H}}} - (q_n - q_a)_{y,n} S_{y,n}}{(q_n - q_a)_a}, \qquad (5.63)$$

where the value with the index of "ul" - they are related to the zone

of catching, with the index of "z" - to the zone of flowing in.

Page 159.

The deicer of complete evaporation must ensure protection from

ice at lowest prescribed/assigned (i.e. calculation) temperature of
air and, on the other hand, prevent the formation of barrier ice with
the maximum calculated water content (which occurs with temperature,
close to 0°C). Consequently, in formula (5.63) total heat-flux
density q_n is determined from formula (5.37) for the calculated
temperature of air $t_{0\,pacч}$ and prescribed/assigned temperature of moist
surface $t_{n.в.т}$. A quantity of absorbed by water $G_{y.л}$ must correspond to
maximum calculated water content at such temperature of air
with which ceases the icing of surface (due to the $t_{0(л.пр)}$,
high-speed/velocity heating, which corresponds to the rated speed of
flight:

$$t_{0(л.пр)} = 0 - \Delta t'_{18.т}. \qquad (5.64)$$

For this same temperature $t_{0(л.пр)}$ in formula (5.63) must be
determined convective component of heat-flux density q_α. It it is
possible to determine via the conversion of the temperature of dry
surface $t_n = t_{0(л.пр)} - \Delta t_{n.вл} + \dfrac{q_n}{\tau}$ to the temperature of moist surface
$t_{n.вл}$ according to equation (5.38) or (5.54). Then $q_\alpha = \alpha\,(t_{1вл} - t'_{n.\,вл})$.

During the calculation of total heat-flux density for the zone
of flowing in should be considered the coefficient of the humidity of
surface, i.e., $q_{n-з}$ one should determine from formulas (5.51).

It is obvious that the calculated heat-flux density cannot be
less than this value, which provides (at a calculated temperature of

air, for example, $[t_{0\,pacu} = -30^\circ C]$ the temperature of surface under conditions of icing, equal to 0°C, i.e.., $[t_{a.\,sa}]_{pacu} = 0^\circ C$. If in this case zone S_j comes out undesirably high sizes/dimensions, it is possible to decrease it, after raising the intensity of heating surface. This can be fulfilled, as can be seen from expression (5.63), increasing q_n either simultaneously all over heating surface or in one or the other its zone when the quantity of heat, spent on the evaporation of water from surface, will remain constant

$$Q_{\beta\,II} = Q_{\beta\,I}. \qquad (5.65)$$

In general value S_j can vary from certain maximum value, which corresponds $[t_{a.\,sa}]_{pacu} = 0,$ and in limit to zero. The decrease of zone is convenient to consider, after introducing the ratio of the size/dimension of reduced zone $S_{j\,II}$ to initial $S_{j\,I}$ in the form: $n_S = \frac{S_{j\,II}}{S_{j\,I}}.$ It is obvious that $0 < n_S \le 1.$

Increased heat-flux density $q_{n\,II}$ necessary in this case with respect to initial density $q_{n\,I}$ can be calculated as follows.

Page 160.

From condition (5.65) we have

$$\frac{q_{\beta I}}{q_{\beta II}} = \frac{S_{II}}{S_I} = n_s, \qquad (5.65a)$$

taking into account expression (5.34), and also indicated above agree

$e_{i \, \text{в.л}}^{\cdot} = 610$ **Н/м², we determine value**

$$e_{n11} = \frac{q_{\beta1} p}{\alpha} \frac{c_p}{0.622 L_\text{и}} \frac{S_{\text{э1}}}{S_{\text{э11}}} = \frac{q_{\beta1}}{n_\text{s}} \frac{p}{1550 \alpha} + 610 \ \text{н/м².} \qquad (5.66)$$

(1)

Key: (1). N/m².

Further, on table or graph/diagram of dependence e=f(t) we find temperature e_{n11} corresponding to elasticity $t_{\text{n. в.л11}}$ and we obtain finally (accepting $t_{\text{n. п.л}}^{\cdot} = 0°$)

$$q_{n11} = \alpha \, (t_{\text{1вл 11}} - 0) + q_{\beta11}. \qquad (5.67)$$

It is obvious that **the heat flux (on 1 m of spread/scope)** in the second case is equal to $Q_{n11} = q_{n11} \cdot S_{\text{э1}}$, **as shown below,** $Q_{n11} < Q_{n1}$. **Since** the heat flux for evaporation in this case is not changed [condition (5.65)], this decrease can occur only due to convective component of heat flux Q_α. **Let us** look how changes this component with the decrease of zone heating. The relation of the convection currents for the zone of flowing in will be equal

$$\bar{Q}_\alpha = \frac{(Q_{\text{аз})11}}{(Q_{\text{аз})1}} = \frac{(t_{\text{n. вл11}} - t_{\text{1вл}}^{\cdot}) \, n_\text{s}}{(t_{\text{n. вл1}} - t_{\text{1вл}}^{\cdot})}. \qquad (5.68)$$

Approximating curve $e_n(t)$ **by exponential curve** $e_n = 610 \exp \ (k t_{\text{n. вл}})$, where k=0.7 in the range $t_{\text{n. вл}} = 0 \div +20° C$, **we have**

$$t_{\text{n. вл}} = \frac{1}{k} \, (\ln e_n - \ln 610). \qquad (5.69)$$

Further, after using (5.65a) and (5.34), **we express** e_{n11} **in** function n_s:

$$e_{n11} = \frac{e_{n1} - e_{\text{1вл}}^{\cdot}}{n_\text{s}} + e_{\text{1вл}}^{\cdot}$$

and we substitute in (5.69):

$$t_{\text{п. вл}} = \frac{1}{k} \ln \frac{e_{\text{пл}} - e^{\cdot}_{\text{1вл}}(1 - n_s)}{610 n_s}.$$

Thus, the relation of the convection currents, expressed through the reduction factor of zone, will be equal

$$\bar{Q}_\alpha = \frac{n_s^{\cdot}}{t_{\text{п. вл}} - t^{\cdot}_{\text{1вл}}} \left[\frac{1}{k} \ln \frac{e_{\text{пл}} - e^{\cdot}_{\text{1вл}}(1 - n_s)}{610 n_s} - t^{\cdot}_{\text{1вл}} \right]. \quad (5.68a)$$

This expression, equal to one when $n_s = 1$, in proportion to decrease n_s monotonically is decreased to zero (Fig. 5.12). The obtained conclusion/output proves the advantage of heating with an enhanced intensity of: with the contraction of zone heating, in spite of the appropriate increase in the heat-flux density, required heat flux (by unity of the spread/scope of surface) is decreased.

Page 161.

It is necessary, however, to keep in mind that too intense a heating can prove to be inadmissible from the point of view of structural strength, furthermore, in this case grow/rise heat losses into unheated parts, which, decreases the effect of heat economy. Therefore raised heat-flux density should be in reasonable limits.

The more clearly described calculation methods let us show based
on examples.

Example   5.4. To determine (approximately) the size of the
warmed zone, necessary for the complete evaporation of water on
profile/airfoil NACA-0012, b=3 m under conditions of icing, given in
examples of 4.1 and 5.1.

The temperature of air maximum for the icing of surface in the
flight conditions (V_0=150 m/s, H=1000 m) in question for the upper
small arc of profile/airfoil on the average is equal to $t_{0(л. пр)} \approx -3°C.$
Consequently, calculated value $w \sim 0.8 \cdot 10^{-3}$ kg/m^3. Let us examine
the upper surface of profile/airfoil. In accordance with example
4.1 we have $S_{ул. верх} = 0,06$ m, $S_{ул. нижн} = 0,02$ m, E=0.09; therefore in the first
approximation, we can accept

$$G_{vл. u} = \frac{S_{ул. верх} + G_{ул}}{S_{ул. верх} + S_{ул. нижн}} = \frac{S_{ул. верх}}{S_{ул}} \cdot E w V_0 C_u =$$
$$= \frac{60}{80} \cdot 0,09 \cdot 0,8 \cdot 10^{-3} \cdot 150 \cdot 0,12 \cdot 3 = 2,9 \cdot 10^{-3} \ кг/сек \cdot м. \quad (1)$$

Key: (1). kg/s•m.

The calculation of remaining values we fulfill separately for the
zone of catching and zone of flowing in, taking the average/mean
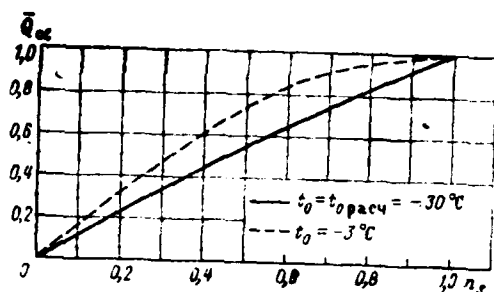values of these values.

Fig. 5.12. Dependence of the convective heat emission of surface on the degree of the decrease of the width of the warmed zone.

Page 162.

Zone of catching.

According to formula (5.5) $t_1^* = -3 + \frac{150}{2000}\left[1 - 0,12\left(\frac{230}{150}\right)^3\right] = 5°C$; according to formula (5.33) $e_1 = 490\frac{72\,600}{90\,000} = 395$ W/m². From equation (5.38) or according to formula (5.54) we find $t_{1.м} = 0,2°C$. From example 5.1 we have $\tilde{q}_{к.уд} = 17\,300$ W/m², $a_{уд} = 500$ W/m²·deg, hence we determine

$t_n - t_1^* \quad \frac{q_n}{\alpha} = 5 + \frac{17\,300}{500} = 40°$ and from equation (5.53) we find $t_{n.в.1} = 14°C$.

Consequently, $q_{а.уд} = 500\,(14 - 0,2) = 6900$ W/m², $q_{в.уд} = 17\,300 - 6900 = 10\,400$ W/m². The value of the coefficient of a quantity of water in the limits of the zone of catching we take $\xi_1 = 1$.

Zone of flowing in.

In a similar manner we find $t*_1 = -3 + (150/2000) [1 - 0.12(217/150)^2]$
$= 8.4 - 3 = 5.4°C$; $c_1 = 490 \frac{76\,400}{90\,000} = 415$ W/m²; $t'_{1.м} = 0.9°C$. The value of heat-flux density in the zone of flowing in we accept on the average (see Fig. 5.8) $\tilde{q}_{n.\,з} = 11\,000$ W/m² and value $\alpha = 430$ W/m²·deg (see Fig. 5.2), thus, $t_n = 0.9 + \frac{11\,000}{430} = 31°C$ and, therefore, $t_{n.\,м} = 11.7°C$. As a result we obtain $q_{aз} = (11.7 - 0.9) \cdot 430 = 4650$ W/m² and $q_{\beta з} = 11\,000 - 4650 = 6350$ W/m². In the zone of flowing in we accept $\zeta_з = 0.3$.

By formula (5.63) we determine the necessary size of the zone of the flowing in

$$S_3 = \frac{0.3 \cdot 2.9 \cdot 10^{-3} \cdot 25 \cdot 10^5 - 10\,400 \cdot 0.06}{6350} = 0.25 \text{ м}.$$

Thus, the size of the warmed zone on the upper surface of profile/airfoil must be equal to $S_н = S_{уn} - S_3 = 0.25 + 0.06 = 0.31$ m $(\overline{S}_н \approx 10\%$ of chord), and the corresponding value of heat flux (on 1 m of spread/scope)

$$Q_н = 17\,300 \cdot 0.06 + 11\,000 \cdot 0.25 = 3790 \text{ вm/м}. [1]$$

Key: (1). W/m.

Example   5.5. To determine the necessary heat-flux density, if it is required to decrease the zone heating from 10o/o (see example 5.4) to 7o/o.

The zone of flowing in in this case will be equal to

$S_3 = 0,07 \cdot 3 - 0,06 = 0,15$ м; i.e., $n_s = \dfrac{0,15}{0,25} = 0,6$ and $q_{\beta \, 11} = \dfrac{6350}{0,6} = 10\,600$ W/m².

According to formula (5.66) we determine $e_{n \, 11} = \dfrac{6350 \cdot 76\,400}{0,6 \cdot 1550 \cdot 430} + 610 = 1820$ W/m².

To this value of elasticity corresponds $t_{n.\, nn} = 15,7°$ C. Consequently,

$q_{n \, 11} = (15,7 - 0) \cdot 430 + \dfrac{6350}{0,6} = 17\,350$ W/m².

Since for the air-heat deicer to fulfill required density distribution of heat according to the enclosure of profile/airfoil is difficult, then in this case it is expedient to raise the density of heat in the zone of catching, due to what the density of heat in the zone of flowing in decreases. Let us assign, for example, value $q_{\beta_3} = 8000$ W/m². Solving expression (5.63) relative to value $q_{\beta \, yn}$, we have

$$q_{\beta \, yn} = \frac{-S_3 q_{\beta_3} + \frac{1}{3} \cdot G_{yn} L_n}{S_{yn}} = \frac{2180 - 8000 \cdot 0,15}{0,06} = 13\,400 \; вm/м^2. \; (1)$$

Key: (1). W/m².

←— According to formula (5.66)

$$e_n = \frac{13\,400 \cdot 72\,600}{1550 \cdot 500} + 610 = 1900 \; н/м^2, \; (1)$$

Key: (1). N/m².

hence $t_{n.\, nn} = 17°$ C. Consequently, $\tilde{q}_{n.\, yn} = 16,8 \cdot 500 + 13\,400 = 21\,800$ W/m² and

$$\tilde{q}_{n.\,3} = 13.3 \cdot 430 + 8000 = 13\ 700 \quad W/m^2.$$

Page 163.

The heat fluxes, which correspond to the examined versions of heating, will be equal to:

$$\begin{aligned}
&1)\ Q_n = 17\ 300 \cdot 0.06 + 17\ 350 \cdot 0.15 = 3640\ sm/m. \\
&2)\ Q_n = 21\ 900 \cdot 0.06 + 13\ 700 \cdot 0.15 = 3370\ sm/m.
\end{aligned} \Big\} (1)$$

Key: (1). W/m.

Comparing them with value Q_n obtained in example 5.4, we see that at the enhanced intensity of heating, especially in the second version, the required heat flux somewhat decreased. The decrease of heat flux occurred due to a reduction/descent in its convective component due to the decrease of surface heating.

Example 5.6. Let us compare the deicer of complete evaporation, designed in example 5.4 on $t_{\text{поач}} = -30°C$, with the same deicer, but by that designed on $t_{\text{поач}} = -20°C$.

Fulfilling calculation analogous with example 5.4, we will obtain the following data: $\tilde{q}_{n.\,yn} = 11\ 600$ W/m², $\tilde{q}_{\alpha\,yn} = 5000$ W/m², $\tilde{q}_{n.\,3} - 6300$ W/m² (when ε_n 0.3) and $\tilde{q}_{as} = 3270$ W/m². Since the calculated water content remained the same as in the preceding/previous example

(appropriate $t_{0(\text{п. пр})} = -3°C$).   then term $\bar{s}_{\text{п}} \cdot G_{1,1} \cdot L_{\text{п}} = 2180$ W/m² also remained

without change. Thus, we obtain $S_3 = \dfrac{2180 - (11\,600 - 5000) \cdot 0.06}{6300 - 3270} \approx 0.59$ m and

$S_{\text{п}} = 0.06 + 0.59 = 0.65$ m, which corresponds $\bar{S}_{\text{п}} \approx 22\%$ chord. Consequently, in

this case the size of the zone necessary for complete evaporation

increased in comparison with example 5.4 more than twice. This is

completely logical, since the calculated density of heat in this case

is considerably lower. In this case in contrast to the version

examined above with the reduced width of heating (example   5.5)

should respectively increase the value of heat flux (on 1 m of span):

$Q_{\text{n}} = 11\,600 \cdot 0.06 + 6300 \cdot 0.59 = 4420$ W/m.

An increase in the heat flux in comparison with the

preceding/previous case occurred due to the increase of convective

component in connection with an increase in the area of the heating

(since heat flux by evaporation did not change). In fact

here $Q_{\text{a}} = 500 \cdot 0.06 + 3270 \cdot 0.59 = 2220$ W/m against $Q_{\text{a}} = 1580$ W/m in example

5.4.

From the comparison of the examined examples it is necessary

that the deicer complete evaporation, designed for the temperature

range of air to -30°C, together with the considerably smaller size of

zone heating is more economical, to say nothing of the fact that by

the second of them at temperatures lower than -20°C will be generally

ineffective.

5.7. Calculation of the parameters of humid air in the inlet duct of engine.

The calculation of the deicers of the intake parts of the engine is characterized by the fact that the temperature of air in inlet duct can be different relative to external.

Before examining the method of determining airstream data at the engine inlet, let us examine the following positions.

Page 164.

From theory of similitude for TRD [ТРД — turbojet engine] it is known that actual flow rates of the air through the inlet duct can be expressed as

$$G_{\text{в}} = \frac{G_{\text{пр}} p_1^{\cdot} \sqrt{T_{H0}^{\cdot}}}{p_\text{в} \sqrt{T_1^{\cdot}}},\qquad (5.70\text{а})$$

where $G_{\text{пр}}$ - the given air flow rate in the kg/s;

$p_1^{\cdot}, T_1^{\cdot}$ - pressure in N/m² and temperature in °K of stagnation air flow before the entry into the compressor;

p_{Ha}, T_{Ho} - **pressure** in N/m^2 and temperature in °K of air under terrestrial conditions.

The given flow rate of air G_{np} is the function of the given number of revolutions, flight mach number and area of jet nozzle.

During the calculation of de-icing systems design conditions are the flight speeds, which correspond to flight Mach number up to 0.5. In this range of Mach numbers the given flow rate of air (in the subcritical modes/conditions of the outflow of gas) changes insignificantly and the effect of flight Mach number on G_{np} can be disregarded/neglected.

Therefore as the basis of the determination of airstream data at the engine inlet it is possible to place the dependence of the given air flow rate through the engine on the given number of its revolutions, obtained during bench tests or by calculation in accordance with prescribed/assigned engine power rating.

The actual consumption of the air through the engine can be expressed also through airstream data in the compressor with the aid of gas-dynamic functions:

$$G_{\text{к}} = m \frac{p_1^{\cdot}}{\sqrt{T_1}} F_i q\left(\lambda_i\right) \ \textit{кг/сек,} \qquad (5.70\text{б})$$

Key: (1). kg/s.

where F_i - cross-sectional area of inlet duct in the m²;

$q\left(\lambda_i\right)$ - coefficient of the flow rate of air, which is the function of the velocity coefficient the table of values of which is given in work [1]:

$$m = \sqrt{k\left(\frac{2}{k+1}\right)^{\frac{k-1}{k}}} \sqrt{\frac{1}{R}} .$$

For air m=0.0403 s•deg⁰·⁵/m.

Equalizing expressions (5.70a) and (5.70b), after conversion and substitution of prescribed/assigned values p_{H0} and T_{H0} we will obtain dependence for determining the coefficient of the flow rate of air

$$q\left(\lambda_i\right) = 0,00415 \frac{G_{\text{пр}}}{F_i}, \qquad (5.71)$$

which considerably simplifies the calculation of the actual air-stream velocities in the intake part of the engine at different speeds and flight altitudes.

The calculation of the parameters for "dry" air is produced in the following sequence.

Page 165.

We find the value of the given numbers of revolutions for the flight
conditions in question from the expression

$$n_{пр} = \frac{n\sqrt{T_{H0}}}{\sqrt{T_к^{\cdot}}} = \frac{n\sqrt{288}}{\sqrt{T_к^{\cdot}}} \approx \frac{17n}{\sqrt{T_к^{\cdot}}},$$

where n - an engine speed in r/min;

$T_к^{\cdot}$ - temperature of the stagnation airflow in inlet duct in °K.

Values $T_к^{\cdot}$ and $p_к^{\cdot}$ we determine from the relationships/ratios:

$$T_к^{\cdot} = \frac{T_0}{\tau(M)} \qquad\qquad (5.73)$$

and

$$p_к^{\cdot} = \frac{p_0}{\pi(M)}, \qquad\qquad (5.74)$$

where r(M) - a value of the quantity of the ratio of the absolute
temperature of air at flight altitude to the absolute temperature of
the stagnated airflow in the inlet duct of engine, depending on
flight mach number and determined on the tables of the gas-dynamic
functions;

$p_{\kappa}^{\cdot}$ - pressure of the stagnation airflow before the entry into the inlet duct of the engine;

$\pi(M)$ - the ratio of the pressure of atmospheric air to the pressure of the stagnation airflow at the engine inlet, which depends on Mach number of flight and determined on the tables of the gas-dynamic functions;

p_0 and T_0 - pressure and temperature of the undisturbed flow of air at given height/altitude.

Having a value of the given number of revolutions on curve $G_{np} = f(n_{np})$ for this engine, we determine the given flow rate of air by which we further compute the coefficient of expenditure/consumption $q(\lambda)$, and in the tables of gas-dynamic functions we find the values of velocity coefficients λ_i. It should be noted that coefficient of speed λ_i in each cross section of inlet duct, for each flight conditions and engine power rating it depends only on the given flow rate of air and area of the cross section indicated.

The values of the air-stream velocity in inlet duct we determine from the expression

$$V_i = \lambda_i \cdot a_{\kappa p} = 18,3 \cdot \lambda_i \sqrt{T_i^*}, \qquad (5.75)$$

where $T_i^* = T_0^*$.

Page 166.

Static pressure $p_{i\kappa}$ and temperature $T_{i\kappa}$ of "dry" air in each

cross section of the inlet duct of engine are determined with the aid

of the tables of gas-dynamic functions for appropriate values

λ_i, i.e. $p_{i\kappa} = \pi p_0^* \sigma_\kappa$ and $T_{i\kappa} = \tau T_0^*$,

where σ_κ - a coefficient of losses of pressure in the inlet duct

which can be taken as equal to 0.95-0.85.

Everything said is correct only in the case of "dry" air.

However, Under conditions of icing surrounding air is not "dry", but

it is saturated by water vapors and contains the supercooled drops of

water. This moisture, falling into the inlet duct of engine, changes

the parameters of intake air. At the flight speed, smaller air-stream

velocity in the inlet duct of engine, temperature of air in channel

there will be always less than the temperature of air of the

environment due to rarefaction/evacuation, which produces the

condensation of water vapors in channel. This excess moisture will be

determined by the difference

$$\Delta M_{\text{в. п. к}} = M_{\text{в. п.}} - M_{\text{в. п. к}}, \qquad (5.76)$$

where $M_{\text{в. п. к}}$ - a moisture content of air in inlet duct in kg vapor/kg

of the air;

$M_{a.n}$ - moisture-content of surrounding air in kg/kg.

But if the temperature of air in the inlet duct higher than ambient temperature, then occurs the evaporation of the drops of water in channel. Because of this there appears a shortcoming in the moisture, necessary before saturation. This shortcoming by absolute value is determined by the same difference [see expression (5.76)]. Having placed the corresponding values for $M_{a.n}$ and $M_{a.n.\kappa}$, after some conversions we will obtain

$$\Delta M_{a.n.\kappa} = 0{,}622 \frac{e_0 - e_i \frac{p_0}{p_{i\kappa}}}{p_0} , \qquad (5.76a)$$

where e_i - vapor pressure, which corresponds to the temperature in this section of the channel;

$p_{i\kappa}$ - pressure in this cross section.

To directly solve this equation is not impossible, since is unknown the actual temperature of air in the inlet duct of engine, and consequently, is unknown value e_i.

During calculations it is accepted that the supersaturation of air by water vapors does not occur, but is obtained condensate in the

form of the water drops which increase the water content of air in intake channel of engine, or with an increase in the temperature occurs the evaporation of water drops, which leads to decrease of the water content of air in this channel.

The value of a change in the temperature of air during condensation or evaporation in it of moisture for 1 kg of air will be determined by the following dependence:

Page 167.

$$\Delta t = \frac{\Delta M_{\text{н. п. к}} L_{\text{н}}}{c_p}. \qquad (5.77)$$

The hence true value of the temperature of air in this cross section of inlet duct can be defined as

$$t_{i\,\text{ист}} = t_i + \Delta t, \qquad (5.78)$$

or, after substituting the appropriate values, we will obtain

$$t_{i\,\text{ист}} = t_i + 0.622 \frac{L_{\text{н}}}{c_p} \frac{e_0 - e_i \frac{p_0}{p_{1\text{к}}}}{p_0}, \qquad (5.78a)$$

where t_i - temperature in this cross section without taking into account of evaporation or condensation of water in channel.

This is the equation, which contains two unknowns: $t_{i\,\text{ист}}$ and e_i. is solved by the method of successive approximation analogously with equations (5.38) and (5.53), moreover the initial temperature of air

in the inlet duct of engine can be taken as equal to t_a and after finding for this value (from Table 1 of application/appendix) value e_a further we determine t_i in second approximation, etc. as long as the subsequent value of the temperature of air will not be equal with the prescribed/assigned precision/accuracy preceding/previous.

Chapter VI.

Thermal design of electrical deicers [1].

FOOTNOTE [1]. Written by R. Kh. Tenishev. ENDFOOTNOTE.

In chapter III was noted that the electrical heating of the
fundamental elements of airframe structure virtually attain only by
cyclic method; therefore in present chapter the primary attention is
given to the calculation of the unsteady thermal processes in
heaters.

The thermal design of the electrical heaters of permanent action
in the case of one-dimensional problem (i.e. without taking into
account the leakages of heat) presents no difficulties. However,
calculations by two- and three-dimensional thermal fields even during
steady process can be sufficiently complicated, but these problems
easily are solved with the aid of comparatively simple electric
analogs, examined in Section 6.5.

As far as calculation is concerned electrical POS, then it does
not differ in terms of special specific character from the
calculation of other thermal users of current and difficulty it does

not represent.

6.1. Cyclic heating of surface.

The cycle of the work of the deicer of cyclic action consists of the time of heating $\tau_{\text{к}}$ and time of cooling $\tau_{\text{охл}}$, which in sum compose the duration of cycle $\tau_{\text{ц}} = \tau_{\text{н}} + \tau_{\text{охл}}$.

Page 168.

Fig. 6.1 shows the typical form of the temperature curve of cyclic heating, which is change in the time of the temperature differential of heater of relatively equilibrium temperature $t'_{1\text{в.л}}$ of boundary layer at the point of surface in question. Since $t'_{1\text{в.л}}$, as this follows from chapter V, can be equated to the temperature of surface before the inclusion/connection of heating, then it is obvious that $\Delta t_{\text{п}} (\tau = 0) = 0$.

A temperature drop in surface $\Delta t_{\text{п}}$ relative to the temperature of the external flow t_1 easily is computed if necessary according to formula (5.5). When in text is encountered drop/jump $\Delta t_{1\text{п}}$, it specially is specified, in all remaining cases is implied $\Delta t_{\text{п}}$ in the relatively equilibrium temperature differential.

Entire dependences, obtained in present chapter, are related to temperature gradient of dry surface, what is on the basis of formulas (5.53) completely legitimate and simplifies the form of the calculations of dependences.

As is known, heat propagation in solid body is described by equation of Fourier's thermal conductivity.   In general considered/examined task it is necessary to solve the system at least of the two-dimensional equations of Fourier, comprised for each layer of heated bundle or each part of the heated construction/design. This system of the acceptable analytical solution does not have, but its solution in digital computers also is sufficiently labor-consuming, since it requires the examination of a large quantity of points of variable thermal field, usually for several versions of heaters. For these purposes are more convenient special integrators [44], intended for the tasks, described by equations in partial derivatives, including - thermal. However, such integrators are not always available to the designer.
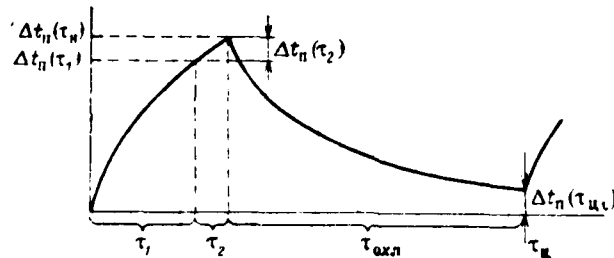
Fig. 6.1. The temperature curve of the cyclic heating of surface.

Page 169.

Therefore in this chapter (Section 6.5) is briefly presented the method of the construction of sufficiently simple electric analogs, thermal processes specially fitted out for simulation in surface heaters. These models which can be assembled in any instrument laboratory they make it possible to determine all necessary thermal parameters of electrical deicer. Nevertheless, are of interest and some simplified particular analytical solutions, since they give the possibility more clearly to present and to analyze the interdependence of the separate parameters.

6.2. Calculation of the heaters of thin-walled constructions/designs.

Solution of the approximate equation of heat exchange.

As a result of the fact that thin walls rapidly are warmed thoroughly all their over thickness, thermal process in them with sufficient precision/accuracy is described by the approximate equation of heat exchange. It is based on the fact that the transient process in thin wall (or bundle) is replaced by a continuous series/row of the stationary processes following after each other by duration $d\tau$, that differ from each other by the value of temperature dt.

We will be restricted to the solution of the one-dimensional task (question about the thermal leakages along the skin/sheathing is examined especially in Section 6.4), after taking the heating bundle, which consists of four layers (Fig. 6.2) (number of layers can be arbitrary, but their overall thickness must not exceed 2-3 mm).
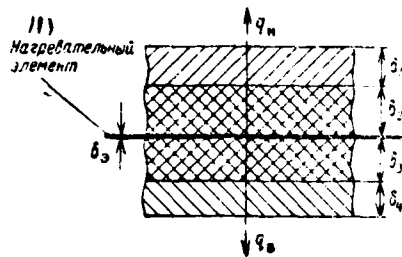
Fig. 6.2. Diagram of heating bundle.

Key: (1). Heating element.

Page 170.

In this case the approximate equation takes the form

$$q\,d\tau = K_{\text{и}}\Delta t_{\text{,}}\,d\tau + K_{\text{в}}\,\Delta t_{\text{,}}\,d\tau + (c_{\text{э}}\varrho_{\text{э}}\delta_{\text{э}} + c_1\varrho_1\delta_1 + c_2\varrho_2\delta_2$$
$$+ c_3\varrho_3\delta_3)\,dt, \qquad (6.1)$$

where

$$K_{\text{и}} = \frac{1}{\dfrac{1}{\alpha} + \dfrac{\delta_1}{\lambda_1} + \dfrac{\delta_2}{\lambda_2}}\;\;\textit{вm/м·град}, \qquad (6.2a)$$

$$K_{\text{в}} = \frac{1}{\dfrac{1}{\alpha_{\text{в}}} + \dfrac{\delta_3}{\lambda_3} + \dfrac{\delta_4}{\lambda_4}}\;\;\textit{вm/м·град}, \qquad (6.2b)$$

Key: (1). W/m·deg.

q - heat-flux density (the specific power), isolated by heating

element, in W/m^2;

Δt_s — a temperature drop in the heating element;

c, ϱ, δ — specific heat into $J/kg \cdot deg$, density in kg/m^3 and thickness of the layer in m;

K_a — coefficient of internal and

K_u — the coefficient of external heat transfer.

The sum of these coefficients is equal to over-all heat-transfer coefficient from heating element to the external and internal surfaces:

$$K_s = K_u + K_a. \qquad (6.2\text{в})$$

By dividing variable and integrating by time from 0 to preset time of heating τ_H and by the temperature from initial temperature drop Δt_n $(\tau=0)$ to current value $\Delta t_n(\tau)$, we obtain the solution of equation relative to τ:

$$\tau = \frac{c_1\varrho_1\delta_1 + c_2\varrho_2\delta_2 + c_3\varrho_3\delta_3 + c_4\varrho_4\delta_4}{K_s} \ln(q - K_s\Delta t_s). \qquad (6.3)$$

As a result of involution and some conversions we have simple expression for determining the temperature drop in the heating element in dependence on the heating time:

$$\Delta t_s(\tau) = \frac{q}{K_s}(1 - e^{-m\tau}) + \Delta t_s(\tau_{\text{ш}})e^{-m\tau}, \qquad (6.4)$$

where

$$m = \frac{K_s}{c_1 \varrho_1 \delta_1 + c_2 \varrho_2 \delta_2 + c_3 \varrho_3 \delta_3 + c_4 \varrho_4 \delta_4} \qquad (6.5)$$

- rate of heating, which has dimensionality 1/s;

$\Delta t_s(\tau_{\text{ш}})$ - residual/remanent temperature drop in the heating element at the end of the time of cooling next cycle (before beginning 1st cycle $\Delta t_s(\tau_{\text{ш0}}) = 0$).

In order to obtain temperature drop on external surface, we will use equality $K_{\text{н}} \Delta t_s = \alpha \Delta t_{\text{n}}$, from which we have

$$\Delta t_{\text{n}}(\tau) = \frac{q}{\alpha} \frac{K_{\text{н}}}{K_s}(1 - e^{-m\tau}) + \frac{K_{\text{н}}}{\alpha} \Delta t_s(\tau_{\text{ш}}) e^{-m\tau}. \qquad (6.6)$$

The nearer value $\Delta t_{\text{n}}(\tau)$ to $\Delta t_s(\tau)$, the less the temperature drop in exterior layers of heating bundle and thereby, therefore, it is more modern in thermal sense.

Solving equation (6.1) for the case of cooling when q=0, we obtain the even simpler dependence

$$\Delta t_{\text{n}}(\tau') = \Delta t_s(\tau_{\text{н}}) \frac{K_{\text{н}}}{\alpha} e^{-m\tau'}, \qquad (6.7)$$

where $\Delta t_s(\tau_{\text{н}})$ - a temperature drop in the heating element at end point of heating (at the cutoff of heating); τ' - time, calculated off the

1.0

1.1

1.25 1.4 1.6

45
50
56
36
40

2.8 2.5

3.2 2.2

36

2.0
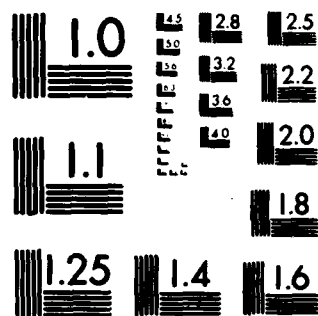
1.8
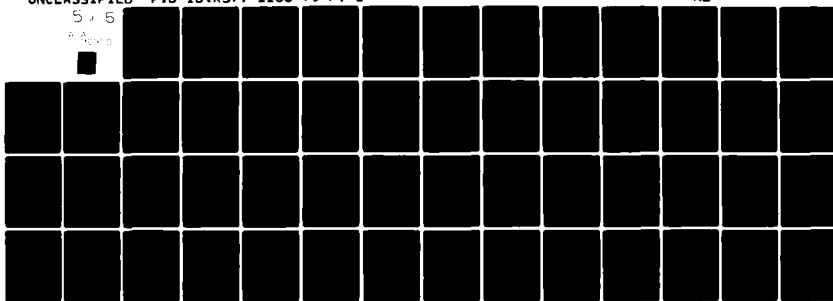
MICROCOPY RESOLUTION TEST CHART
NATIONAL BUREAU OF STANDARDS 1963-A

beginning of cooling.

Page 171.

When selecting of constructing/designing the heater for
thin-walled construction/design it is necessary to focus attention on
the following. From the comparison of expressions (6.2) and (6.5) it
is possible to see that the rate of heating is found in inverse
dependence on the square of the thickness of the layer of heater,
i.e., even a small increase in the thickness of the layer
significantly depresses the rate of heating and, correspondingly, the
temperature of the heating to surface. The aforesaid is related both
to the external ones and to interior layers of heating element.

In spite of this, designers frequently unjustifiably overstate
the thickness of the internal insulation/isolation (discussion deals
with thin-walled heater), considering that this must decrease the
losses of heat inside. In actuality they are usually small and then
in many instances can be disregarded/neglected (as shown in example 6./
given below)   . whereas since the value of the internal coefficient
of heat emission usually of the order by two of less than the
external, the rate of heating with increase of internal
insulation/isolation noticeable are decreased which makes the quality
worse of cyclic deicer. Consequently, the thicknesses both external

and of interior layers of the insulation/isolation of thin-walled
heater must be selected only from the condition of necessary
dielectric strength. Only with the thicknesses of lower covering on
the order of 2 mm and more makes sense to somewhat increase the
thickness of internal insulation/isolation. However, this heater will
be sufficiently heat-inertial.

The sign/criterion of the increased inertness of heater, besides
the low rate of heating, is also the high value of residual/remanent
temperature drop Δt, (τ_w), which contributes to the formation of barrier
ice as a result of the fact that the surface longer time is in the
heated state, i.e., the increase of temperature from one cycle to the
next is not the positive property of cyclic heater, as sometimes they
count. However, on the contrary,   effective deicer must
provide jettisoning of ice from next section during the first cycle.
Therefore subsequently during the determination of the parameters of
cyclic deicer let us examine only one first cycle of its work.

Specific power, heating time and temperature drop in the cyclic
deicer.

These three parameters are tightly interlocked; therefore they should
be examined   together.

Solving expression (6.6) relative to the specific power (after being restricted, as it is said above, by the first cycle), we have

$$q = \alpha \, \Delta t_n \frac{K_o}{K_n} \frac{1}{1 - e^{-m\tau_k}} = \alpha \, \Delta t_n \frac{1}{\theta} \frac{K_o}{K_n},\qquad (6.8)$$

here $\tau_н$ - the heating time and $\Delta t_n (\tau_u)$ - the necessary temperature drop of cyclic deicer, about which the speech will go below.

Page 172.

Value $\theta = 1 - e^{-m\tau_н}$, which can be named/called the function of the relative (dimensionless) temperature of heating surface, characterizes the speed of the build-up/growth (form of curve) of the temperature of surface, and ratio $1/\theta$ is shown, in how often the specific power during cyclic heating must be more than with constant. In other words, this sense is the coefficient of heat efficiency or the coefficient of an increase in the specific power of heater during cyclic heating in comparison with permanent heating.

Fig. 6.3 gives dependence $1/\theta$ on time at different rates of heating. From graph it is evident that in proportion to the decrease of time, beginning with some values τ, value $1/\theta$ begins sharply to grow/rise. Consequently, to assign the heating time it is less than these, critical ones with respect to $1/\theta$ values $\tau_{кр}$ it is inexpedient, since this leads to sharp increase of the necessary

specific power. Value $\tau_{кр}$ depends also on the rate of the heating: the higher the rate, that $\tau_{кр}$ it is less, as can be seen from the same figure.

The time of heating $\tau_н$ cyclic deicer must be assigned on the basis of the permissible duration of a cycle, quantity of sections and available power.
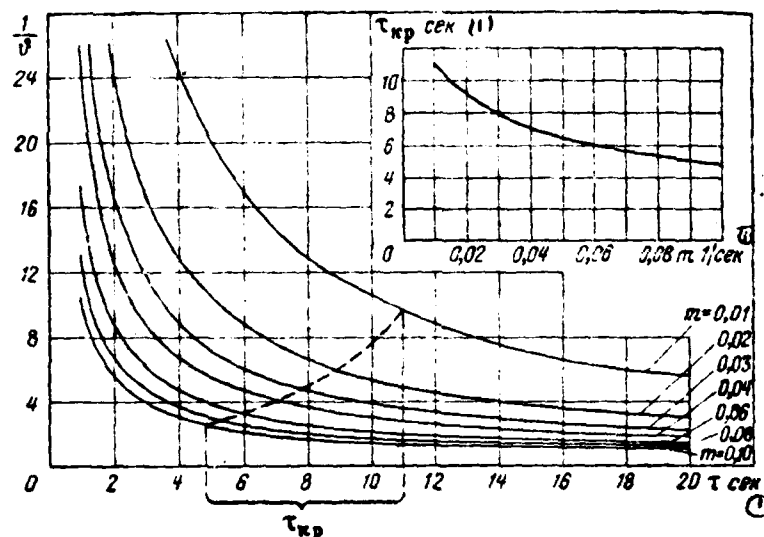

Fig. 6.3. Coefficient of the specific power and critical time of cyclic heating of thin-walled construction/design.

Key: (1). s.

Page 173.

For clarity the heating time is convenient to divide into two phases: the first - time τ_1, necessary for the heating to surface from $t_{in.1}$ to 0°C; the second - time τ_2, required for slight melting of the small layer of ice, which is contacted with surface. The thickness of this layer δ_1 depends on amounts of the external forces, which affect ice, and the surface roughness. Time τ_2 can be approximately determined by the formula

$$\tau_2 = \frac{\delta_n \rho_n L_n}{q}. \qquad (6.9)$$

The root-mean-square roughness of the lifting surfaces of subsonic aircraft is within the limits of two-three tenth's of a micron, separate

inequalities reach the tenth of millimeter and more. Therefore for the nonrotating surfaces it is possible to accept δ_n' order 0.2 mm; for the rotating parts is permitted considerably smaller value (because of centrifugal force), for example, for helicopter rotors δ_n' it can be accept in average/mean 0.1 mm, for tailed and aircraft screws/propellers - order 0.03-0.05 mm. Fig. 6.4 gives dependence τ_2 on the specific power of heating element with different ones δ_n'.

Thus, the total time of heating

$$\tau_n = \tau_1 + \tau_2. \qquad (6.10)$$

Time τ_1 is determined with prescribed/assigned q from the formula

$$\tau_1 = -\frac{1}{m} \ln\left(1 - \Delta t_n(\tau_1)\frac{\alpha}{q} \cdot \frac{K_2}{K_n}\right), \qquad (6.11)$$

where $\Delta t_n(\tau_1)$ - the minimally necessary temperature drop in the dry surface, which ensures under conditions of icing $t_{n.n.n} = 0$.

If expression under logarithm proves to be negative, then this means that during given power and construction/design of heater necessary drop/jump $\Delta t_n(\tau_1)$ cannot be achieved/reached during how conveniently prolonged heating.
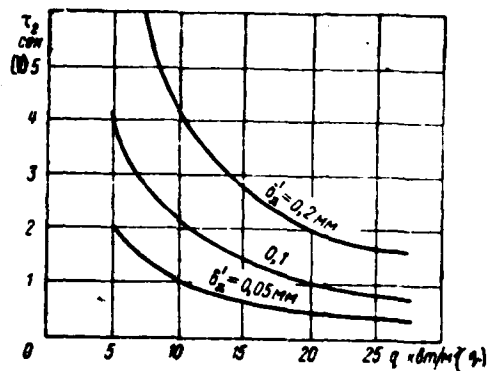
Fig. 6.4. Dependence of the time of slight melting ice on the specific power.

Key: (1). s. (2). kW/m².

Page 174.

During calculations of cyclic deicer frequently is introduced unjustified complication, actually connected with the determination of drop/jump indicated above $\Delta t_n(\tau_1)$. Therefore this value requires more detailed examination.

It would seem that during the calculation of cyclic deicer it is without fail necessary to take into consideration a layer of ice, possessing, as is known, sufficiently good thermal insulation

properties. However, in this case immediately arises question, what thickness and thermophysical constants of ice should be been assigned, since the form, the sizes/dimensions of ice built-up edges and their physical properties are very diverse. In this case it is obvious that the condition for jettisoning of ice is heavier, the less its thickness. However, with small thickness a temperature drop in a layer of ice becomes insignificant (of which it is easy to be convinced during calculation) and itself it is rapidly warmed thoroughly all over thickness following the surface. This leads to an increase in the intensity of its evaporation (as a result of an increase in difference $e_n - e_1$, see chapter V), which in turn, slows down the heating to surface, just as this occurs in the case of heating moist surface.

In other words, the surface covered with ice is warmed up least of all, where the thickness of ice comes to naught. Specifically, this zone of the descent of ice corresponds to the heaviest, design conditions on surface. The location of this zone, naturally, changes in dependence on the sizes/dimensions of ice built-up edge. Since the sizes/dimensions of ice under varied conditions of icing can be most varied, then it is obvious that in totality this calculated zone must encompass the entire surface from leading edge (or from the zone of action of "thermal knife"), also, to the end/lead of the prescribed/assigned zone heating.

Virtually this means that the calculation of the temperature of surface during cyclic heating can be fulfilled according to the same formulas, that also for a moist surface (see Section 5.5), i.e., without taking into account the thermal resistance of a layer of ice.

The validity of this assignment of external design conditions for a cyclic deicer (being physically obvious) is confirmed by the practice of numerous calculations of POS, repeatedly checked experimentally. However, attempts at the account of a layer of ice, besides the complication of calculations themselves, frequently lead to the erroneous results, usually occupying the amount of the specific power, as a result of which the required effectiveness at a calculated temperature of air is not provided.

The total quantity of temperature drop for a cyclic deicer in dry air for the complete time of heating τ_n will be equal to

$$\Delta t_n(\tau_n) = \Delta t_n(\tau_1) + \Delta t_n(\tau_2). \qquad (6.12)$$

where $\Delta t_n(\tau_2)$ - supplementary temperature to value of which will have time to warm up the surface for time τ_2.

Page 175.

From the graph in Fig. 6.4 it is evident, for example, that for the majority of the cyclic deicers of the lifting surfaces, which have specific power on the order of 15000-20000 W/m^2, at the average speed of the build-up/growth of the temperature of 2-3 deg/s value $\Delta t_n(\tau_s)$ must be located approximately/exemplarily within limits of 5-10°C.

During the calculation of cyclic deicer only value $\Delta t_n(\tau_1)$ is determined unambiguously on the basis of the prescribed/assigned calculated temperature of icing $t_{\text{орасч}}$. From the remaining two parameters - the specific power and heating time - one must be known, then another can be determined. In connection with this it is expedient to examine the following calculated cases.

1) The heating time is prescribed/assigned approximately. Accepting it for time τ_1, according to formula (6.8) we determine by q, then through the graph/curve of Fig. 6.4 we find $\tau_2(q)$, the total heating time will be equal to their sum $\tau_H = \tau_1 + \tau_2$.

This case can occur for a system with the automatically adjustable cycle when to previously assign a precise value of time is not required, or for a system with the fixed/recorded cycle, if there is a possibility within some limits to change the speed of the action of commutator.

2) The heating time is prescribed/assigned strictly (for example, for a system with the fixed/recorded cycle). In this case at first we determine the specific power approximately, without the account to power for slight melting of ice: $q-r_2(q)$, through we do not find $r_2 \approx \tau_2(q)$, then we determine $\tau_1 = \tau_u - \tau$, and finally we obtain the refined value $q=q(r_1)$.

3) Is prescribed/assigned specific power q. According to formula (6.11) we determine r_1, while on the graph/curve of Fig. 6.4 - a time r_2 and, therefore, $\tau_H = r_1+r_2$. For a system with the fixed/recorded cycle obtained time τ_u they usually round to the large side to values, which can be provided with the aid of the available of designer switchboards.

During the determination of time heating it is necessary to keep in mind that the duration of entire cycle (determined by the product of the time of heating and quantity of sections of deicer) in the prescribed/assigned range of the design conditions of icing must not be more than permissible value $n\tau_u < \tau_{u.don}$. Otherwise it is necessary to decrease either a heating time or a quantity of sections (or and that, etc.). On the other hand, one ought not the heating time to establish/install less $\tau_{u.p}$, as has already been spoken, this will lead

to irrational expenditure of energy.

Example 6.1. Calculate the temperature drops on the surface of
heating bundle for the time of heating $\tau_n = 40$ s with the following
data: $q=15000$ W/m²; $\delta_1 = \delta_4 = 0.5 \cdot 10^{-1}$ m (Duralumin); $\lambda_1 = \lambda_4 = 120$ W/(m·deg);
$c_1 = c_4 = 0.88 \cdot 10^3$ J/(kg·deg); $\rho_1 = \rho_4 = 2700$ kg/m³; $\delta_2 = \delta_3 = 0.5 \cdot 10^{-3}$ m (pasted
BF-2 fiber glass fabric); $\lambda_2 = \lambda_3 = 0.5$ W/(m·deg), $c_2 = c_3 = 1.26 \times 10^3$
J/(kg·deg); $\rho_2 = \rho_3 = 1400$ kg/m³.

Page 176.

Average heat-transfer coefficient we accept $\tilde{\alpha}$=300 W/m²·deg.
During the calculation of the coefficients of heat transfer we see
that by ratio δ/λ for metallic layers it is possible to disregard
completely in comparison with other terms in the denominators of
expressions (6.2). Furthermore, when $\alpha_{\text{в}}$ to 20-25 W/m²·deg with error
not more than 10o/o it is possible to disregard $K_{\text{в}}$ in comparison with
$K_{\text{н}}$. This precision/accuracy of designing calculation is completely
sufficient, since physical constants themselves and other reference
data hardly can be previously known with larger precision/accuracy.
According to formula (6.5) we determine m - 0.0417 1/s and further
according to formula (6.6) we find Δt_{n} (τ=40) =41° C. The results of
calculation Δt_{n} in the function of time are given in the form of graph
in Fig. 6.5a. There is given the curve of the heating of the same
heater, but with δ_1=2 mm, and also for a comparison - curves,
obtained for these examples on electric analog. Graph in Fig. 6.5b
shows that with the thickness of internal wall 6 mm the
precision/accuracy of calculation according to formula (6.6) is
already clearly insufficient and more precise formula (6.21),
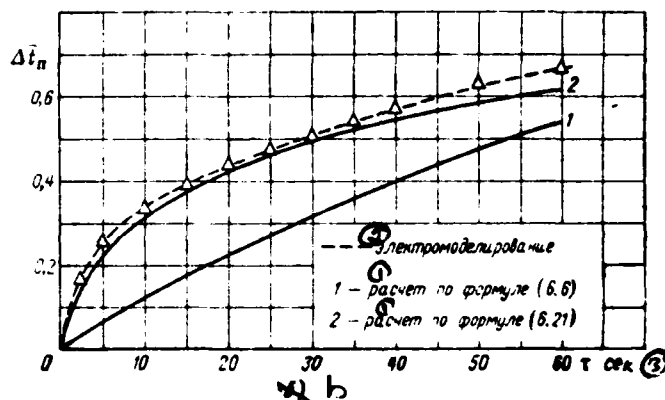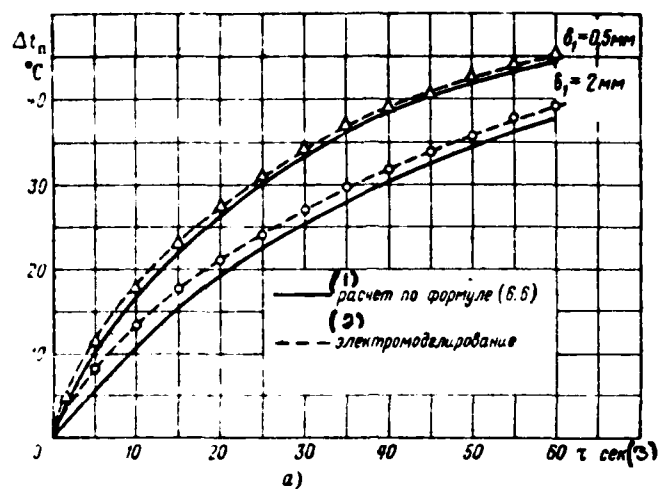examined in the following section.

Fig. 6.5. Curves of the heating to the surface:

a) with different thicknesses of the outer covering (δ_4=0.5 mm); b) with the thickness of the lower covering by δ_4=6 mm (δ_1=0.5 mm).

Key: (1). calculation according to formula. (2). electric modeling. (3). s.

Page 177.

6.3. Calculation of the heaters of thick-walled and continuous constructions/designs.

Solution of the system of equations of thermal conductivity.

For solving the task we will use somewhat simplified network, in which instead of the separate skins (Fig. 6.6a) is examined seemingly uniform layer with the equivalent values of thermal constants, identical for external and interior layers of the insulation/isolation (see Fig. 6.6b).

The equivalent (conditional) values of indicated constant can be calculated according to the following formulas:

$$a_1 = \frac{\lambda_1}{cQ_1} \quad (6.13a)$$

and

$$a_2 = \frac{\lambda_2}{cQ_2}, \quad (6.13б)$$

where

$$\lambda_1 = \frac{\delta_м + \delta_{из1}}{\frac{\delta_м}{\lambda_м} + \frac{\delta_{из1}}{\lambda_{из1}}}, \quad (6.14a)$$

$$\lambda_2 = \frac{\delta_{из2} + \delta'_м}{\frac{\delta_{из2}}{\lambda_{из2}} + \frac{\delta'_м}{\lambda_м}}, \quad (6.14б)$$

and

$$cQ_1 = \frac{cQ_м \delta_м + cQ_{из1}\delta_{из1}}{\delta_м + \delta_{из1}}, \quad (6.15a)$$

$$cQ_2 = \frac{cQ_{из2}\delta_{из2} + cQ_м\delta'_м}{\delta_{из2} + \delta'_м}. \quad (6.15б)$$

$$\lambda_H \quad \lambda_{H31} \quad \lambda_{H32} \quad \lambda_M$$
$$c_H \quad c_{H31} \quad c_{H32} \quad c_M$$
$$\varrho_H \quad \varrho_{H31} \quad \varrho_{H32} \quad \varrho_M$$
$$\delta_H \quad \delta_{H31} \quad \delta_{H32} \quad \delta_M$$
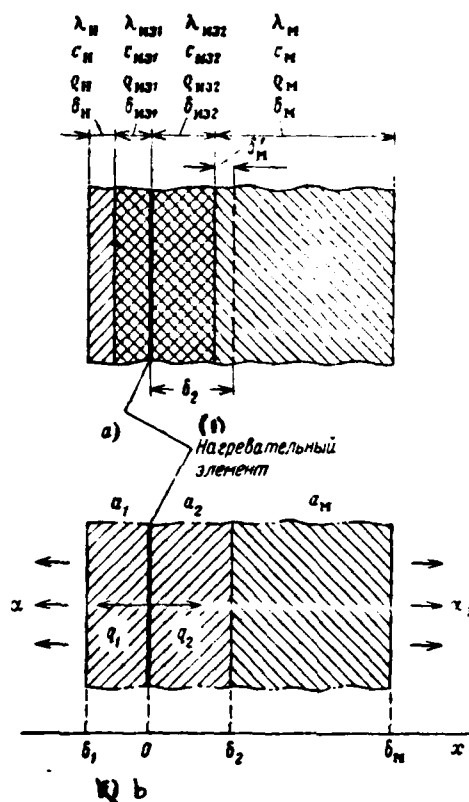
(1)
Нагревательный элемент

Fig. 6.6. Network of the heater of the thick-walled construction/design:

a) the diagram of the construction/design; b) equivalent diagram.

Key: (1). Heating element.

Page 178.

The thickness of the layer δ_v, which we conditionally "occupy" in

metallic body, always it is possible to fit such that $a_1 = a_2$. The origin of coordinates we accept in the plane of the heating element of Fig. 6.6b.

In the case of one-dimensional task for the accepted by us diagram we have a system of three equations:

$$\frac{\partial \Delta t_1(x, \tau)}{\partial \tau} = a \frac{\partial \Delta t_1(x, \tau)}{\partial x^2},$$
$$\frac{\partial \Delta t_2(x, \tau)}{\partial \tau} = a \frac{\partial \Delta t_2(x, \tau)}{\partial x^2}, \qquad (6.16)$$
$$\frac{\partial \Delta t_{\text{м}}(x, \tau)}{\partial \tau} = a_{\text{м}} \frac{\partial \Delta t_{\text{м}}(x, \tau)}{\partial x^2}$$

under the following initial and boundary conditions:

$$\tau = 0$$
$$1) \ \Delta t_1(x, 0) \quad \Delta t_2(x, 0) = \Delta t_{\text{м}}(x, 0) = 0,$$
$$x = 0$$
$$2) \ \Delta t_1(0, \tau) - \Delta t_2(0, \tau) = 0,$$
$$3) \ -\lambda \frac{\partial \Delta t_1(0, \tau)}{\partial x} - \lambda \frac{\partial \Delta t_2(0, \tau)}{\partial x} = q,$$
$$x = \delta_1 \qquad (6.17)$$
$$4) \ \frac{\partial \Delta t_1(\delta_1, \tau)}{\partial x} + \frac{a}{\lambda} \Delta t_1(\delta_1, \tau) = 0,$$
$$x = \delta_2$$
$$5) \ \Delta t_2(\delta_2, \tau) - \Delta t_{\text{м}}(\delta_2, \tau) = 0,$$
$$6) \ -\lambda \frac{\partial \Delta t_2(\delta_2, \tau)}{\partial x} - \lambda_{\text{м}} \frac{\partial \Delta t_{\text{м}}(\delta_2, \tau)}{\partial x} = 0.$$

The solution of system (6.16) is expedient to fulfill by the method of the transform of Laplace [35], introducing for this the following image:

$$L[\Delta t(x, \tau)] = [T(x, p)] \rightarrow \Delta t(x, \tau). \qquad (6.18)$$

where p - operator of Laplace (i.e. L [Δt(x, τ)] it is the image of function Δt(x, τ)).

Derivative of image on the coordinate:

$$\frac{\partial [T(x, p)]}{\partial x} = [T'(x, p)] \rightarrow \frac{\partial \Delta t (x, \tau)}{\partial x} = \Delta t'(x, \tau). \qquad (6.19)$$

Page 179.

Without setting forth course of solution, let us give the results of determining the temperature of external surface (i.e. with $x = \delta_1$) for some particular tasks. Relative to image the solution will be equal

$$[T_1(\delta_1 p)] = \frac{q(-E)}{\lambda p \left(\sqrt{\frac{p}{a}} - x \right)}$$

$$\frac{1 - h(-2E_2) - h(\bar{x}_M)(-2E_{\Lambda}) - (\bar{x}_M)(-2E_2)(-2E_M)}{1 - h(\bar{x})(-2E_1)(-2E_2) - h(\bar{x}_M)(-2E_M) - (x)(\bar{z}_M)(-2F_1)(-2E_2)(-2F_M)},$$

$$(6.20)$$

where are accepted the following designations:

$$(E_1) = \exp\left(\sqrt{\frac{p}{a}} \delta_1 \right); \quad (-E_1) = \exp\left(-\sqrt{\frac{p}{a}} \delta_1 \right);$$

$$(2E) = \exp\left(2\sqrt{\frac{p}{a}} \right) \text{ и т. д.};$$

$$(\bar{x}) = \frac{\sqrt{\frac{p}{a}} - x}{\sqrt{\frac{p}{a}} + x}; \quad (x_M) = \frac{\sqrt{\frac{p}{a}} - x_M}{\sqrt{\frac{p}{a}} - x_M};$$

$$x = \frac{\alpha}{\lambda}; \quad x_M = \frac{\alpha_B}{\lambda_M}; \quad h = \frac{1 - \Lambda}{1 + \Lambda}.$$

value $\Lambda = \frac{\lambda}{\lambda_M} \sqrt{\frac{a_M}{a}} = \frac{\sqrt{\lambda c \rho}}{\sqrt{\lambda_M c_M \rho_M}}$, being the ratio of the coefficients of the heatswellof insulation and metal, characterizes the degree of the diversity of their thermal properties.

The simplest solution is obtained for the case of heating the semi-restricted body whose thermophysical properties are close to the properties of the thermal insulation layers of heater, i.e. virtually, when heater is established/installed to thick-walled nonmetallic body, since in this case the terms, which contain $\exp\left(-2\sqrt{\frac{p}{a_u}}\,\delta_u\right)$, and also coefficient h will be equal to zero. As a result, passing to original [13], we obtain for this case the

following solution of a relatively temperature drop in the surface:

$$\Delta t_n(\tau) = \frac{q}{\alpha}\left[\operatorname{erfc}\left(\frac{\delta_1}{2\sqrt{\alpha\tau}}\right) - \exp\left(x\delta_1 + x^2 a\tau\right) \times\right.$$

$$\left.\times \operatorname{erfc}\left(\frac{\delta_1}{2\sqrt{a\tau}} + x\sqrt{a\tau}\right)\right]. \qquad (6.21)$$

Page 180.

This formula can be presented also into somewhat other form through the fourier numbers $Fo=a\tau/\delta^2{}_1$, and Biot $Bi_1=\alpha\delta_1/\lambda$:

$$\Delta t_n(\tau) = \frac{q}{\alpha}\left[\operatorname{erfc}\left(\frac{1}{2\sqrt{Fo_1}}\right) - \exp\left(Bi_1 + Bi_1^2 Fo_1\right) \times\right.$$

$$\left.\times \operatorname{erfc}\left(\frac{1}{2\sqrt{Fo_1}} + Bi\sqrt{Fo_1}\right)\right]. \qquad (6.21a)$$

The figuring here function $\operatorname{erfc}(z) = 1 - \operatorname{erf}(z)$, where $\operatorname{erf}(z) = \frac{2}{\sqrt{\pi}}\int_0^z e^{-t^2}dt$ — probability integral (error function for Gauss), known that into somewhat other form [6]: $\Phi(z) = \frac{2}{\sqrt{2\pi}}\int_0^z e^{-\frac{t^2}{2}}dt$, which is connected with $\operatorname{erf}(z)$ with the dependence

$$\operatorname{erf}(z) = \Phi(z\sqrt{2}).$$

The tables of one or the other form of integral are given usually in many manuals on mathematics (for example, [6]), and also in specialized literature, in particular, in [51].

Expression (6.21) contains the uncertainty/indeterminancy of form $\infty\cdot 0$ (with $z\to\infty$, $\exp(z)\to\infty$, $\operatorname{erfc}(z)\to\infty$), which easily is opened[1], namely: the second term in brackets approaches 0 with $\tau\to\infty$.

FOOTNOTE 1. For example, according to l'Hopital's rule. ENDFOOTNOTE.

The solution for the semi-bounded metallic body is obtained already much more complicated - in the form of the infinite converging series. Being limited, for example, in image by two members of series/row, we have in original the following solution:

$$\Delta t_n(\tau) = \frac{q}{\alpha} \left\{ \left[\text{erfc}\left(\frac{\delta}{2\sqrt{a\tau}}\right) - \exp(\varkappa\delta_t + \varkappa^2 a\tau) \times \right. \right.$$
$$\left. \text{erfc}\left(\frac{\delta}{2\sqrt{a\tau}} + \varkappa\sqrt{a\tau}\right) \right] - h\left[\text{erfc}\left(\frac{\delta_1 + 2\delta_2}{2\sqrt{a\tau}}\right) - \right.$$
$$\left. \left. \exp(\varkappa\delta_1 + \varkappa 2\delta_2 + \varkappa^2 a\tau) \text{erfc}\left(\frac{\delta_1 + 2\delta_2}{2\sqrt{a\tau}} + \varkappa\sqrt{a\tau}\right) \right] + \cdots \right\}. \quad (6.22)$$

It is easy to note that the first member of this expression is preceding/previous solution (6.21) for nonmetallic construction/design, whereas second with factor h - characterizes the decrease of the temperature of surface due to the supplementary leakage of heat in metal. In order to explain the legitimacy of the obtained solutions conformably for one or the other practical task, it is necessary the thickness of body to compare with the length of thermal wave for the time interval in question.

Page 181.

The temperature of heating (in our case temperature drop relative to the initial temperature) the uniform semi-restricted body at a distance of x from heat source is determined by the dependence

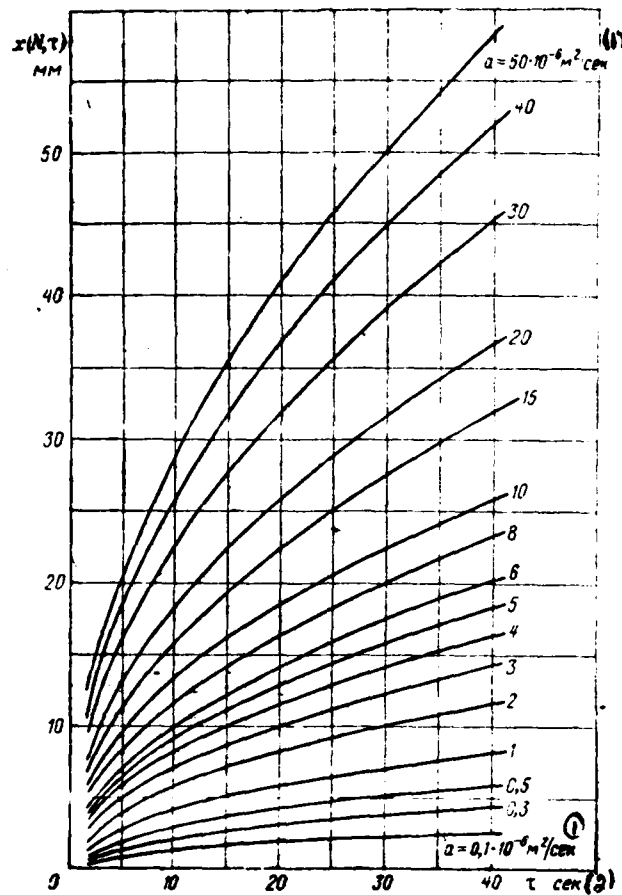$$\Delta t(x, \tau) = \Delta t_{\text{нач}} \exp\left(x\sqrt{\frac{\pi}{a\tau}}\right). \quad (6.23)$$

Fig. 6.7. Dependence of the length of thermal wave (with N=10o/o) in materials with different thermal diffusivity.

Key: (1). m²/s. (2). s.

Page 182.

Since the thermal wave does not have clearly expressed leading

edge, then its length can be determined only with some
prescribed/assigned precision/accuracy, i.e.

$$x(N, \tau) = \frac{a\tau}{\pi} \ln \frac{100}{N}, \qquad (6.24)$$

where $N = \frac{\Delta t(x, \tau)}{\Delta t_{\text{исm}}} \cdot 100\%$ - **the required precision/accuracy.**

If the thickness of the body of one order or more than
wavelength for the estimated time of heating, then body can be
considered semi-bounded and, therefore, the obtained solutions for it
are valid.

Fig. 6.7 shows the dependence of wavelength from N=10o/o in
materials with different coefficients of thermal diffusivity.

Taking into account that the time of cyclic heating does not
usually exceed 30-40 it is rare 60 s, from graph it is possible to
see that in nonmetallic materials (which have coefficient a of order
$0.3 \cdot 10^{-6}$ m²/s) thermal wave for this time is propagated in all to
several millimeters. This means that solution (6.21) is applicable
for the calculation of heating virtually all nonmetallic
constructions/designs, moreover its precision/accuracy the higher,
the less the heating time.

Formula (6.22) gives the considerably understated temperature of
surface, which is explained by two reasons: first, for the exact

solution are insufficient two members of the series/row whereas (with
a larger number of terms formula becomes very bulky); in the second
place, with the real for flight vehicles the warmed wall thicknesses
their temperature as a result of rapid warm-up grows considerably
more rapid than this would take place with semi-restricted body.
Therefore, as show calculations, for metallic wall thicknesses on the
order of 5-20 mm it is possible in the first approximation, to also
use formula (6.21). For intermediate thicknesses it is possible to
tentatively take the average value of temperature, calculated by
formulas (6.6) and (6.21).

Internal heat flow.

For the evaluation of the heat losses inside construction/design
it is necessary to determine flow exitting from a heating layer
toward internal insulation/isolation. This flow is equal to

$$q_2 = -\lambda \frac{\partial t_2(x, \tau)}{\partial x}.$$ (6. 25)

Temperature field $t_2(x, \tau)$ is determined by the method of
solution of system of equations (6.16) relative to interior layer of
insulation/isolation analogous with the preceding/previous case.

Page 183.

As a result, being limited by two members of series/row (after

unity), we have

$$q_2(0, \tau) = \frac{q}{2} \left\{ 1 - \left[\mathrm{erfc}\left(\frac{2\delta_1}{\sqrt{a\tau}}\right) - \right. \right.$$
$$\left. - 2\exp(2\varkappa\delta_1 + \varkappa a\tau)\,\mathrm{erfc}\left(-\frac{2\delta_1}{\sqrt{a\tau}} + \varkappa\sqrt{a\tau}\right) \right] +$$
$$\left. + h\,\mathrm{erfc}\left(\frac{\delta_2}{\sqrt{a\tau}}\right) + \cdots \right\}. \qquad (6.\ 26)$$

The obtained dependence has very peculiar curve in time (Fig. 6.8). At the first moment/torque, until the heat flux q_1 still achieves surface, both flows were symmetrical and equal to $q_2 = q_1 = q2$. Further increase q_2 is explained by the fact that in the beginning of heating the quantity of heat, removed from surface, $\dot{q}_a = \alpha \Delta t_a$ small (thus far is low Δt_a), therefore the large part of the heat is fixed inside.
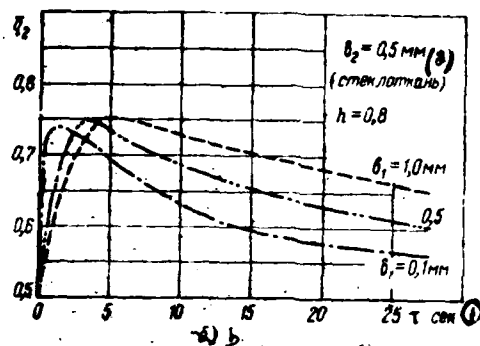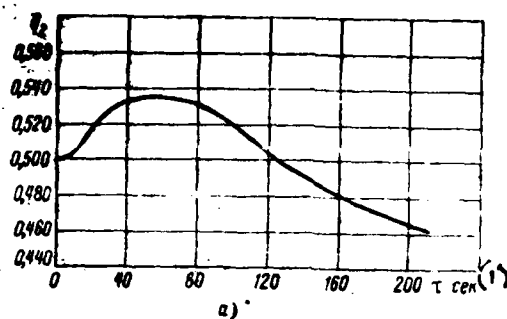
Fig. 6.8. Curve of a change in the internal heat flow in the time:

a) in the electrically heated glass; b) in heater, established/installed to metal blade/vane.

Key: (1). s. (2). (glass cloth).

Page 184.

In proportion to the heating to surface occurs the redistribution of flows and value q_2, in passing by through the maximum, subsequently is decreased (theoretically to zero). Virtually due to the presence

of the end leakages of heat internal flow, of course, always remains more than zero. But end losses begin noticeably to manifest itself during more prolonged heating. Therefore during the calculation of cyclic heating them in the first approximation, it is possible not to consider, with exception of points, close to the boundary of heating. The task of heating surface taking into account the end leakages of heat can be sufficiently simply solved with the aid of the electrical simulation (see Section 6.5).

It is obvious that the smallest value q_2 occurs in the nonmetallic construction/design (see Fig. 6.8a). In this case the solution contains only one member after unity, since h=0.

It is interesting to focus attention on the fact that the internal heat flux depends not only on the thickness of internal isolation δ_2, but also from ratio δ_2/δ_1 (see Fig. 6.8b). The value of internal losses depends also on the ratio of the coefficients of thermal diffusivity of external and interior layers, if they are made from different materials, namely: q_2 is inversely proportional $\sqrt{\dfrac{a_1}{a_2}}$.

Determination of the specific power and heating time.

During heating of thick-walled construction/design the specific power also is determined on the basis of temperature drop $\Delta t_\text{п}(\tau_1)$ and

corresponding to it time of the first phase of heating τ_1 (see the preceding/previous section). Thus, for the nonmetallic construction/design

$$q = \alpha \Delta t_n(\tau_1) \frac{1}{\mathrm{erfc}\left(\frac{\delta_1}{\sqrt{a\tau}}\right) - \exp(\varkappa\delta_1 + \varkappa^2 a^2\tau)\,\mathrm{erfc}\left(\frac{\delta_1}{2\sqrt{a\tau}} + \varkappa\sqrt{a\tau}\right)} =$$

$$= \frac{\alpha \Delta t_n(\tau_1)}{\theta_1}, \qquad (6.27)$$

where θ_1 - dimensionless function of the heating temperature, and ratio $1/\theta_1$ - coefficient of an increase in the specific power during the cyclic heating of thick-walled nonmetallic construction/design.

The graph/diagram of the dependence of this coefficient on number $Fo = a\tau/\delta^2_1$ with different $Bi = \alpha\delta_1\,\lambda$ is represented in Fig. 6.9a. As in the case of thin-walled construction/design, function has some critical values of numbers Fo, lower than which curves $1/\theta_1$ sharply grow upward. Fig. 6.9b gives the dependence of the critical time of heating τ_{kp} on ratio δ^2_1/a with different values of number Bi.

Page 185.

As already mentioned above, the first member of expression (6.22) is nothing else but function θ_1. Designating value in the brackets of the second term through θ_2, in the case of metal construction we have

$$q = \alpha \Delta t_n(\tau_1) \frac{1}{\theta_1 - \delta\theta_2}. \qquad (6.28)$$

Of the given above expressions it is possible to see that the rate of heating surface and, consequently, also the heat availability factor are located in of the reverse/inverse dependence on the square thickness of skin.
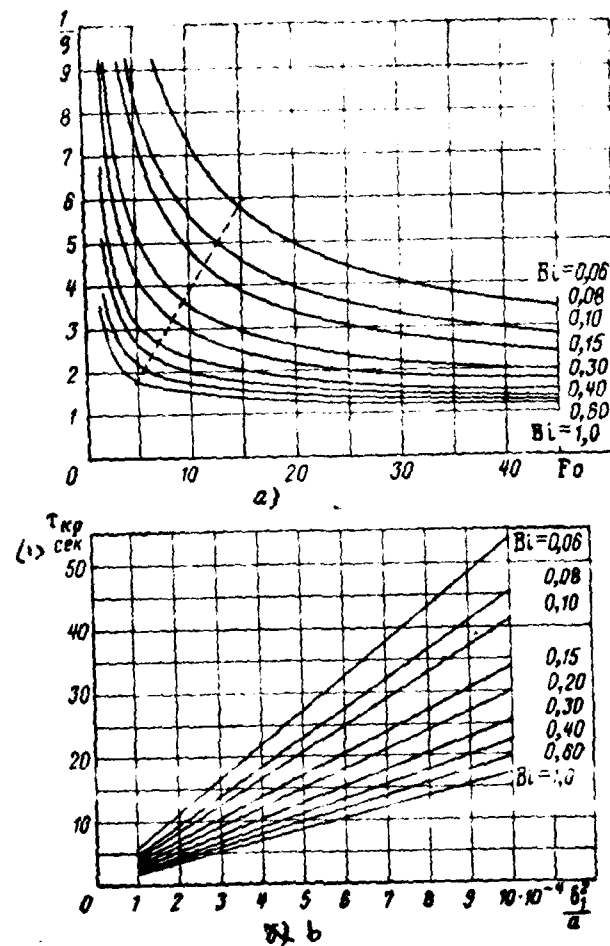
Fig. 6.9. Coefficient of the specific power and critical time of heating thick-walled construction/design.

Key: (1). s.

Page 186.

Example of 6.2. To calculate temperature drop relative to the temperature of flow Δt_{in} of the electrically heated glass: $q=5000$ W/m^2; $\delta_1=4 \cdot 10^{-3}$ m; $\delta_2=20 \cdot 10^{-3}$ m; $\lambda_{cT} =0.75$ W/m·deg; $a_{cT} =0.41 \cdot 10^{-6}$ m^2/s; $\tau_H =$ $=10$ s; $V_0=150$ m/s; $\alpha=120$ W/m^2·deg.

We find erfc $\dfrac{4 \cdot 10^{-3}}{2\sqrt{0.41 \cdot 10^{-6} \cdot 10}}$ =erfc $0.988=1-$erf 0.988.

For determining this value we will use table $\Phi_{(z)}$ from [6]: erf $0.988= \Phi(0.988\sqrt{2})=0.838$, therefore, erfc $0.988=0.162$. Analogously we find erfc $\left(\dfrac{\delta_1}{2\sqrt{a\tau}} + x\sqrt{a\tau}\right) = 0.0635$, where $x = \dfrac{\alpha}{\lambda} = 160$, then $\exp(x\delta + x^2 a\tau) = 2.117$.

Thus Δt_n ($\tau=10$)$=1.2$°C. Finally temperature drop relative to the temperature of airflow will be equal to $\Delta t_{in} = \Delta t_n + 0.88 \dfrac{V_0^2}{2000}$ to $=11.1$° C.

The curve of heating $\Delta t_n (\tau)$ (relative to equilibrium temperature) is given in Fig. 6.10a.
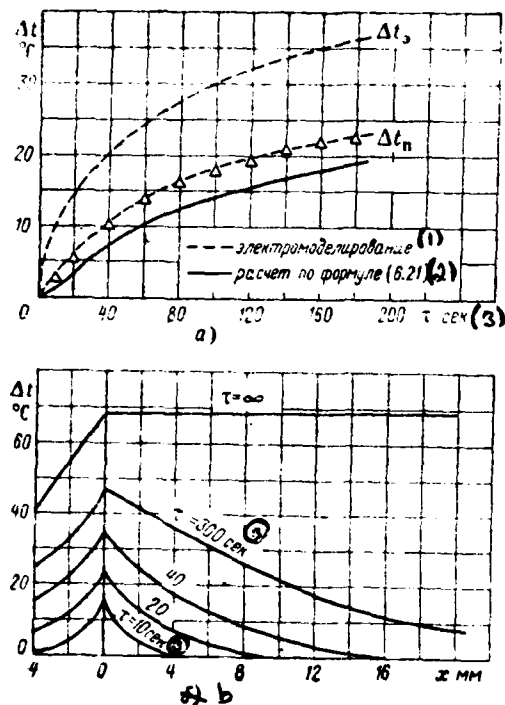
Fig. 6.10. Heating of the electrically heated glass:

a) the curve of the heating to the surface; b) temperature field according to the thickness of glass at different moment of time.

Key: (1). electrical simulation. (2). calculation according to formula. (3). s.

Page 187.

Example of 6.3. To calculate $\Delta t_n(\tau)$ for the heater, examined in

example 6.1, from that established/installed to thick duralumin wall.
According to formulas (6.13) and (6.14) we determine $a_2 = 0.48$ m²/s
and $\lambda_1 = 1.0$ W/m·deg.

In other respects the calculation is analogous
preceding/previous. The results of calculation $\lambda_{1,(T)}$ according to
formula (6.21) are given in Fig. 6.5b.

6.4. Account of the effect of thermal leakages, determination of the
parameters of "thermal knives".

Effect of thermal leakages.

The above-examined methods of calculation of heaters, as it was
stipulated, do not consider the leakages of heat beyond the limits of
heating surface. With the large width of heating element the value of
leakages on the average is actually/really small, but near boundary
of heating it becomes very essential. Therefore the less the width of
heating element, the stronger affects the effect of leakages heating
of an entire surface.

It is logical that the thermal leakages depend also on the
construction/design of heater and thermal conductivity of its layers,
first of all - outer covering (tipping). Therefore for different

heaters the effect of leakages will be different.

As an example Fig. 6.11 shows the distribution of the temperature of surface (in relative unity) taking into account the leakage of heat for several versions of the outer covering of heating bundle. For a comparison is shown the version without the outer covering, in which the leakages occur only on the lower covering. Curves are obtained on the electric analog whose diagram is shown in Fig. 6.14.
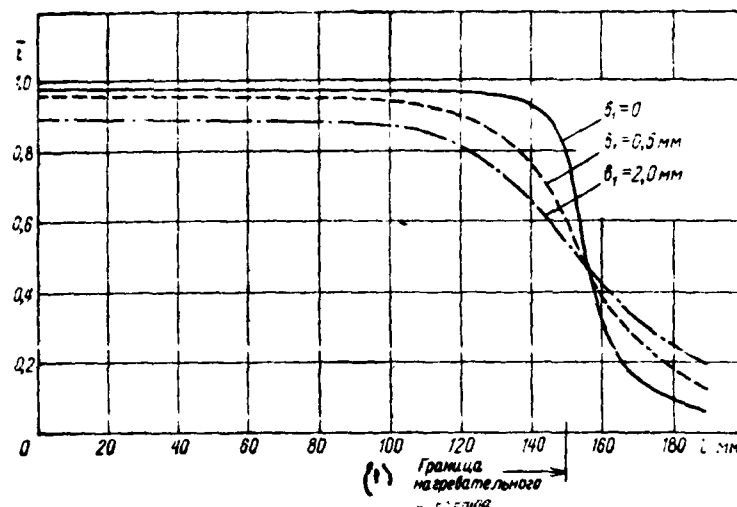
Fig. 6.11. Temperature of surface taking into account the leakages of heat along skin/sheathing.

Key: (1). Boundary of heating element.

Page 188.

For increasing the temperature of surface near the boundary of the warmed zone it is necessary thermal leakages to compensate by the appropriate increase of the specific power on certain width in the boundary of heating element, moreover the width of this section[1] and its specific power are interlocked, which in more detail shown below, in the examination of "thermal knife".

FOOTNOTE [1]. This section with the increased specific power on the boundary of the cyclically effective heater sometimes is completely erroneously also called "thermal knife". ENDFOOTNOTE.

From the aforesaid it also follows that if according to the calculation (see Section 5.3) the distribution curve of the surfaces of heat-flux density q_n (S) it will have more or less sharp bend, then in the presence of the heat-conducting outer covering there is no need to reproduce this bending for q(S) in heating element, and it is possible to be restricted by the considerably rougher, stepped distribution of the specific power. But if we accept the even distribution of power as most simple, then its value must be determined for the section of surface, located under severe conditions heating; therefore heat on remaining surface will be expended completely rationally.

Determination of the parameters of "thermal knives".

Thermal leakages are the decisive factor, which are determining skin heating in the zone of "thermal knife" - in the limits of this zone they are commensurated with external heat flux and even they can considerably exceed it. Therefore the parameters of "thermal knife" even in larger measure depend on the specific construction/design of heater.

General considerations are here such: specific power $q_{T.H}$ of the heating belt of "knife" and its width $b_{T.H}$ are found in the definite dependence - the less the width, the the the specific power must be above, and vice versa. Furthermore, the less the width of belt, the less "knife" consumes powers, in spite of increase of the specific power, since $Q_{T.H} = q_{T.H}b_{T.H}$ is decreased in proportion to decrease $b_{T.H}$. However, the amount of the specific power should not be allowed/assumed very large, otherwise even small technological defect with the cementing of heating bundle it can lead to its hot spot. Usually the specific power of "knife" must not exceed 2.5-3 W/cm². On the other hand, to apply the width of belt is more than 30-40 mm also inexpediently.

Page 189.

Fig. 6.12 gives the curves of the relative temperature of surface in the zone of "thermal knife" depending on the width of belt and thickness of skin/sheathing. As in the preceding/previous example, curves are obtained on the electric analog (see example of 6.6).
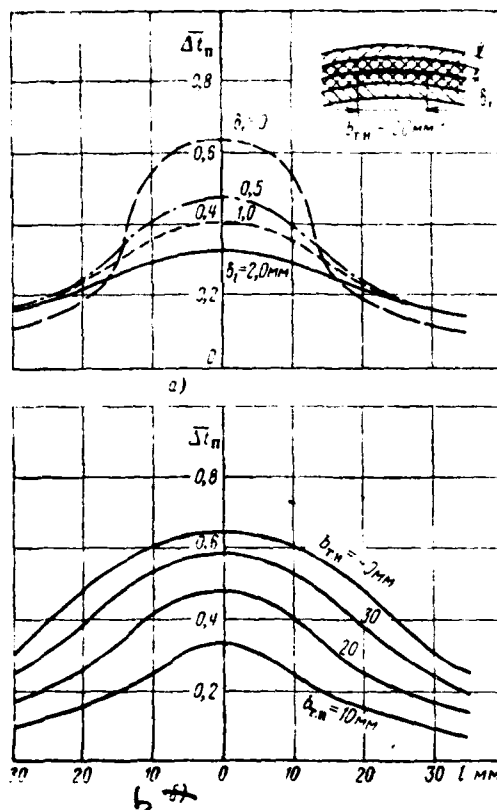
Fig. 6.12. Curves of relative temperature drops in the surface in the zone of "thermal knife":

a) depending on the thickness of skins/sheathings (with $b_{т.н}$ =20 mm);

b) depending on the width of belt $b_{т.н}$ (with $δ_1$=0.5 mm).

Page 190.

6.5. Use/application of electrical simulation for the thermal design of surface heaters.

To electrical simulation is devoted sufficiently much literature
[12], [21], [44], [57], [121], [131], [153], [155], etc.; therefore
here there is no need for stopping on the theory of this question and
the general methods of simulation. From known electric analogs for
our purposes most convenient and accessible are the grid models which
can be assembled usually from finished standard resistance and
capacities/capacitances. For simulation can be utilized also the
grids of the existing electro-integrators, as for instance, EI-12,
etc.

As is known, electrical simulation with the aid of such models
is based on the analogy of the equations, which describe, on one
hand, thermal processes in solid bodies and, with another, electrical
processes in the circuits, which contain resistance and
capacities/capacitances. The fundamental condition of analogy is the
equality of the criteria of similarity of the thermal and electrical
tasks:

$$\frac{c \varrho l}{\lambda \tau} = \frac{R C_{эл} n^2}{\tau_{эл}},\qquad (6.29)$$

where c, ϱ, λ, l - respectively specific heat capacity, density, thermal
conductivity and determining size/dimension of each part of the
heated body;

τ - the preset time of the heating;

$R, C_{э,л}$ - resistance and capacity/capacitance of the electrical circuit;

$\tau_{э,л}$ - time of the course of the electrical process;

n - factor which in the majority of the cases can be accepted equal to unity.

The preparation of model begins with the laying out of heating bundle in the sections whose space is selected on the basis of the required precision/accuracy of the solution (precision/accuracy the higher, the less the space), moreover it is desirable to select the relation of space L toward the thickness of fundamental skin/sheathing δ_1 not more than 10 (Fig. 6.13).

As the determining size/dimension depending on the specific conditions of task can be selected any of the sizes/dimensions (thickness of skin/sheathing or another layer, space of laying out, etc.).

Calculation of the resistance of model.

Depending on that, such as size/dimension is undertaken that

being determining, there can be the following cases:

1. As the determining size/dimension is accepted the thickness
of skin/sheathing δ_1 and the corresponding to it resistance is equal
to R_1, then the resistance, which correspond to remaining layers, is
determined from the relationships/ratios:

$$R_2 = R_1 \frac{\lambda_1}{\lambda_2} \cdot \frac{\delta_2}{\delta_1}.$$

$$R_3 = R_1 \frac{\lambda_1}{\lambda_3} \cdot \frac{\delta_3}{\delta_1}.$$

(6. 30)

Page 191.

Each subsequent resistance can be computed also, on the basis of
preceding/previous:

$$R_3 = R_2 \frac{\lambda_2}{\lambda_3} \cdot \frac{\delta_3}{\delta_2}.$$ (6. 30a)

2. As determining size/dimension is accepted space ΔL, then
corresponding to it resistance is equally

$$R_{\Delta L1} = R_1 \left(\frac{\Delta L_1}{\delta_1} \right)^2.$$ (6. 31)

3. If as determining size/dimension is accepted space ΔL and to
it corresponds resistance R_{L1}, then

$$R_1 = R_{\Delta L1} \left(\frac{\delta_1}{\Delta L_1} \right)^2.$$ (6. 32)

Latter/last two formulas are valid it goes without saying and
for remaining layers.

Resistance R_a, which corresponds to the thermal resistance of

boundary layer (value, inversely proportional to heat-transfer coefficient *a*), is determined through the resistance of the surface layer; if the latter is equal to R_a, then

$$R_a = R_1 \frac{\lambda_1}{\alpha \delta_1},$$
(6. 33a)

and vice versa

$$R_1 = R_a \frac{\alpha \delta_1}{\lambda_1}.$$
(6. 33b)

Calculation of electrical capacitances.

The value of the determining electrical capacitance, which corresponds to the heat capacity of a layer in question, is located through the formula

$$C_{_{3,7}} = \frac{\tau_{_{3,7}}}{Fo \cdot R} = \frac{l^2}{aR} \cdot \frac{\tau_{_{3,7}}}{\tau},$$
(6. 34)

where $Fo = \frac{a\tau}{l^2}$ – the fourier number, in reference to the determining size/dimension of the layer in question;

R – resistance, which corresponds to the determining size/dimension;

$\tau_{_{3,7}}$ – time of the electrical simulation; it is selected on the basis of the available reserve of electrical capacitors/condensers and characteristics of measuring and registering apparatus. If the recording equipment is low-inertia and moving rapidly, then time $\tau_{_{3,7}}$ can be little, therefore, will be required small amounts of capacitance. Usually for models $\tau_{_{3,7}}$ in question it is accepted within the limits from tenths to several seconds.

Page 192.

Simulation of heat source.

Since the temperature of heating element in proportion to the decrease of heat emission can grow/rise to high values, then also in electric analog it is necessary to create the appropriate conditions. For this in the circuit of current source it is necessary to include/connect the supplementary of resistance $R_{ист}$ of the largest possible value. But since, on the other hand, it is limited to the allowable voltage of feed/supply or to the sensitivity of measuring equipment, then it should be accepted at least by an order more than the sum of all resistance of model from the point of the connection of source (afterward $R_{ист}$) to R_α inclusively. For example, for the diagram, shown in Fig. 6.13, $R_{ист} \geqslant 10\,(R_1 + R_2 + R_\alpha)$.
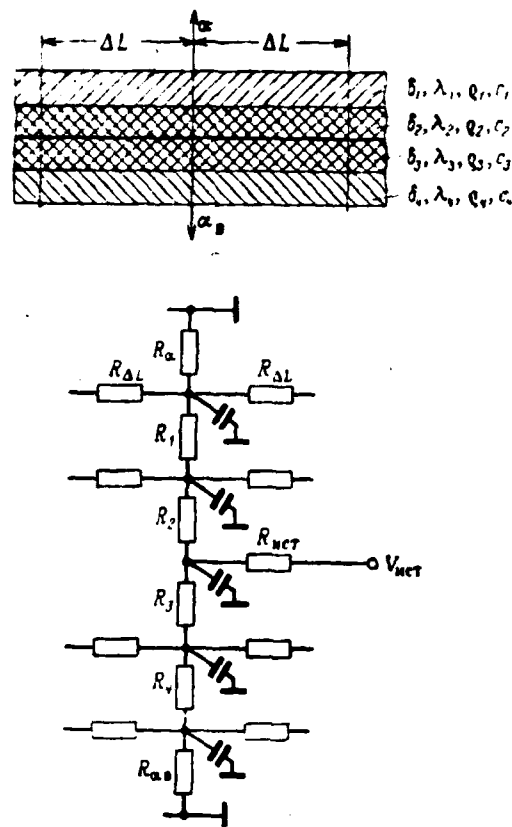
Fig. 6.13. Schematic of heating bundle and its electric analog.

Page 193.

If specific power q is permanent by the area of heating element, then $R_{мст}$ at all points must be equally. But if q is changed over surface, then maximum from these values, for example, q_1, should be accepted for basis, and to it must correspond $R_{мст1}$, obtained of the condition indicated above. Then at remaining points $R_{мст i}$ it is equally

$$R_{мст i} = R_{мст 1} \frac{q_1}{q_i}.$$ (6. 35)

Methods of simplification in the models.

In many instances it manages without the considerable decrease of the precision/accuracy of the solution to considerably simplify the schematic of electric analogs, which is very convenient for their practical use. Let us examine several examples.

To account for thermal leakages along skin/sheathing the unheated part of it also must be simulated. However, since the length of unheated part is sufficiently great (up to tail piece of the profile/airfoil), for its simulation is necessary a very large number of elements/cells of model. However, it proves to be that there is no need in a large number of such elements/cells which let us name/call cells (Fig. 6.14), since beginning with certain number of cells further elongation of diagram virtually does not increase the precision/accuracy of the solution. The quantity of cells, which must be taken for obtaining the prescribed/assigned precision/accuracy of simulation, depends on the relationship/ratio of resistance $R_{\perp L}$ and R_a (Fig. 6.15). From Fig. 6.15 and 6.16 it is evident that with an increase in the quantity of cells more than 5-8 resistance R_Σ with an accuracy to several percentages (in this case of approximately 5o/o) remain constant/invariable.

Moreover, if the temperature distribution on unheated part is
not examined, but it is required to only consider its effect, then
all cells, beginning with point K, it is possible to replace with one
equivalent resistance $R_{экв}$ (see Fig. 6.14). The value of this
resistance can be calculated according to the usual formulas of
electrical engineering for series-parallel circuits or determined
preliminarily experimentally on the model being investigated.

For an example following table gives $R_{экв}$ for several values R_a
and $R_{\Delta L}$ in anyone.

Table 6.1.

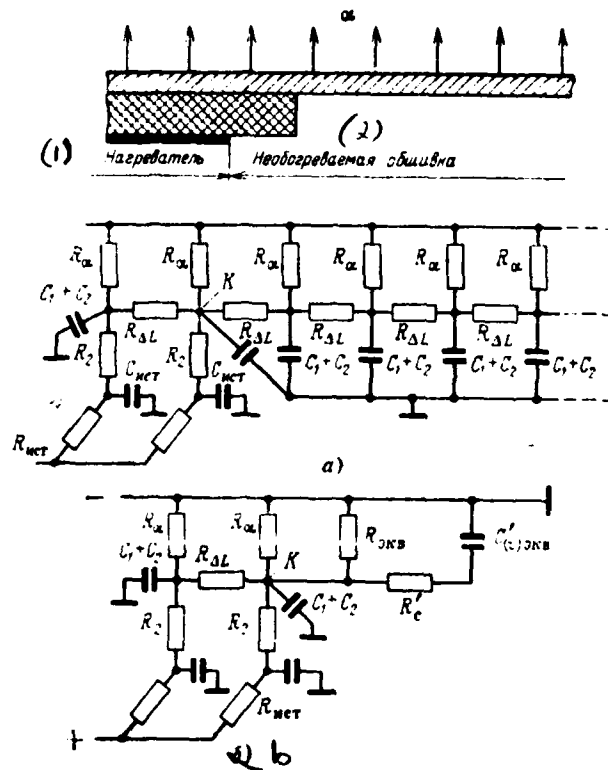| R_a	50	20	10	10	10	5	1
$R_{\Delta L}$	10	1	10	20	1	1	2
$R_{экв}$	27,8	5,2	16,3	27,2	2,8	2,7	2,6

Page 194.

Fig. 6.14. Simulation of fringe area of heating element:

a) schematic of electric analog of fringe area; b) simplified (it is equivalent) diagram.

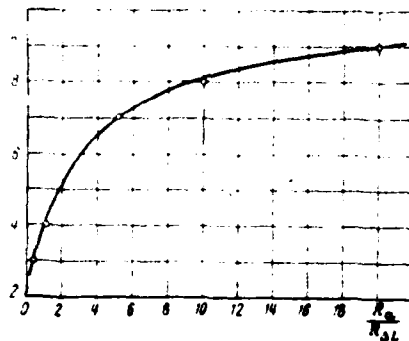Key: (1). Heater. (2). Unheated skin/sheathing.

Fig. 6.15. Minimum quantity of "equivalent" cells of model depending on relationship/ratio of their resistance.

Page 195.

During the calculation of capacities/capacitances for the unheated part of the skin/sheathing as the determining size/dimension should be taken ΔL and respectively resistance $R_{\jmath L}$, then

$$C'_{\jmath \eta} = \frac{\Delta L^2}{a\tau} \cdot \frac{\tau_{\jmath \eta}}{R_{\jmath L}} \, . \qquad (6.36)$$

The corresponding equivalent capacity/capacitance is determined from the condition

$$(R_{\jmath L} + 2R_{\jmath L} + 3R_{\jmath L} + \cdots + nR_{\jmath L})C_{\jmath \eta} = C'_{\jmath \eta \eta}R_{\varsigma}. \qquad (6.37)$$

where n - a number of cells, necessary for simulation of unheated skin/sheathing (see Fig. 6.15);

R_{ς} - supplementary resistance in the circuit of capacitor/condenser.

Values $C'_{экв}$ and R'_c can be selected any in the limits of the condition

$$C'_{экв}R'_c = \text{const.}$$

Usually thermal resistance and, consequently, also corresponding to it resistance R_1 of electric analog is more than to two systems lower than resistance of insulating layer R_2. Therefore in the majority of the cases it can be disregarded/neglected or, at the worst, it is simple to add it to R_2. However, the heat capacity of skin/sheathing it is not possible to disregard/neglect, and it is possible only corresponding to it electrical capacitance C_1 to add to capacity/capacitance C_2. It is analogous for remaining layers.
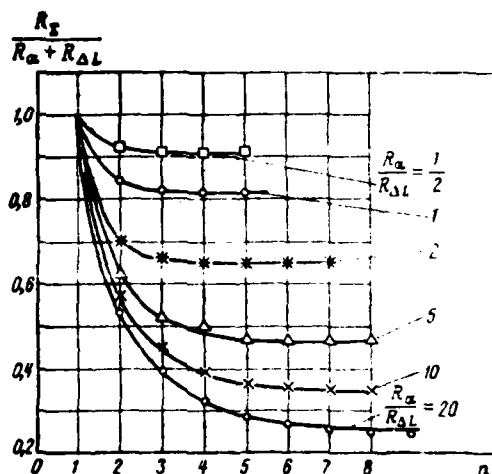
Fig. 6.16. Ratio of the value of "equivalent" resistance to the resistance of cell depending on a number of cells.

Page 196.

Further, with the more or less symmetrical conditions of heat emission on both sides from the middle of heater (usually passing approximately/exemplarily on leading edge) it is possible to simulate only the half of the width of heater element/cell. In this case the diagram from the side of the rejected/thrown half remains extended.

Bringing the results of simulation to the conditions of thermal task.

Determination of temperatures. The temperature of the surface (or temperature drop) of heating element is determined on the basis

of the following considerations. As is known, temperature drop on surface for the one-dimensional stationary heat flux (when the leakages of heat along skin/sheathing are absent) at each point of surface is equal to

$$\Delta t_n(\tau = 0) = \frac{q}{\alpha}.$$

Voltages at the points of model, which correspond to the surface of heater, are determined from the relationship/ratio

$$U_n(\tau = \infty) = \frac{R_\alpha}{R_{\text{нст}} + R_1 + R_2} \qquad (6.38)$$

(or directly are measured on model when $R_{\perp L} = \infty$).

Relative voltages at the arbitrary moment of the transient process

$$\overline{U}_n(\tau) = \frac{U_n(\tau)}{U_n(\tau = \infty)}, \qquad (6.39)$$

where $U_n(\tau)$ - measured stress level.

From the condition of the similarity of the electrical and simulatable thermal process we obtain the unknown value of the temperature at the point of surface in question at any moment of the time

$$\Delta t_n(\tau) = \Delta t_n(\tau = \infty) \cdot \overline{U}_n(\tau). \qquad (6.40)$$

The temperature of remaining layers is determined analogously.

During determination the temperatures of unheated skin/sheathing value Δt ($\tau = \infty$) and corresponding to it voltage U_n ($\tau = \infty$) are

determined for the latter/last point of heating element, which
adjoins directly the unheated part of the skin/sheathing, further
temperature is determined from formula (6.40).

Page 197.

Determination of heat fluxes. To heat fluxes correspond in
electric analog electric currents. To the total quantity of heat Q_s,
isolated by heating element, corresponds total current $I_м$, consumed by
model. Heat fluxes in separate structural parts Q_i are determined
from the relation

$$Q_i = Q_s \frac{I_i}{I_м},\qquad\qquad (6.41)$$

where I_i - a circuital current of that section of model which
corresponds to the part of nature in question.

Example of 6.4. To calculate electric analog and to determine
the necessary specific power of the "thermal knife",
established/installed on unswept wing in the heating bundle, examined
in example of 6.1, $b_{т.н}$ =20 mm, $t_{о рис}$ =-30° C. As design conditions (as
this follows from Section 5.4) we accept H=1000 m, V_0=150 m/s. For
determining the heat-transfer coefficient we will use graph in Fig.
5.2, from which we obtain the value of heat-transfer coefficient on
leading edge α=200 W/m²·deg. We accept: ΔL_1=10, δ_1=5 mm, $R_{\Delta L_1}$ =4
kilohm. We determine according to formula (6.32) R_1=40 ohms,

according to formula (6.30) R_2=16 kiloohm, R_3=16 kiloohm, R_4=40 ohms, $R_{5L.}$ =4 kiloohm, according to formula (6.33a) R_a =64 kiloohm, $R_{\text{исг}} \approx 10(R_a + R_1 + R_3)$= 800 kiloohm. Obtained on this model curves of relative temperature drops in the surface are shown in Fig. 6.12a. The required amount of the specific power of "knife" we determine from relationship/ratio $q_{\text{т. н}} = q_n \frac{1}{\overline{\Delta t_n}}$, where q_n =a(0-t*$_1$) X=6000 W/m^2 we determine according to formula (5.37), $t_{\text{н. кн}}$ =0° C and H=1000 m.

Consequently, for an example in question in accordance with Fig. 6.12 $q_{\text{т. н}}$ ≈12500 W/m^2.

Example of 6.5. To determine the specific power of the "thermal knife", analogous preceding/previous, but established/installed on delta wing at $t_{\text{о рас}}$ =-30° C and -20° C. Heat-transfer coefficient is determined on graph/curve in Fig. 5.3, moreover in this case one should consider that the zone of the increased value α is sufficiently narrow; therefore into calculation should be taken the average value of coefficient in the carrying which is equal order 600 W/(m^2·deg). Consequently, with t_0=-30° C the specific power of the "knife in question" must be equal to about 31000 W/m^2. With the width of belt $b_{\text{т.н}}$ =30 mm $q_{\text{т.н}}$ it can be reduced to 25000 W/m^2. Curves $\overline{\Delta t_n}$ in this case differ somewhat from preceding/previous see Fig. 6.12b). At $t_{\text{о рас}}$ =-20°C $q_{\text{т.н}}$ must be about 19500 W/m^2 with $b_{\text{т.н}}$ =20 mm and about 16000 W/m^2 with $b_{\text{т.н}}$ =30 mm. Logically (as it follows from Fig. 6.12), with

an increase in the thickness of skin/sheathing value Δt is decreased and, therefore, required value $q_{\text{т.н}}$ grows/rises. Comparing the results of the examined two examples, it is easy to explain, for example, then the fact that "thermal knife" of the stabilizer of An-10, which has $b_{\text{т.н}}$ =13 mm and $q_{\text{т.н}}$ =1.2 W/cm^2 [58], has approximately/exemplarily the same effectiveness of action as the "thermal knife" of the aircraft of Tu-114, which has $b_{\text{т.н}}$ =20 mm and $q_{\text{т.н}}$ =1.8 W/cm^2.

Example of 6.6. To calculate electric analog for the electrically heated glass, examined in example of 6.2. Negligible by heat flow along glass (i.e. we are limited to one-dimensional task). We accept: for determining size/dimension $\delta_1 = 4\cdot 10^{-3}$ m, for the determining time $\tau = 180$ s, $\tau_{\text{м}}$ =3 s, R_1=16 kiloohm, α=120 $W/(m^2\cdot deg)$. According to formulas (6.30) and (6.33) we find R_2=80 kiloohm, R_α =26 kiloohm. According to formula (6.34) $C_{\text{м1}} = \frac{(4\cdot 10^{-3})^3}{0.41\cdot 10^{-4}\cdot 180}\cdot\frac{3}{16\cdot 10^3}$ =42$\cdot$10^{-6} f=42 μF. With respect $C_{\text{м2}}$ =210 to μF. Additional resistance in the circuit of source $R_{\text{ист}}$ =400 kiloohm. For obtaining the temperature field by the thickness of glass (and also for increasing the precision/accuracy of the solution) we divide/mark off δ_1 into several layers, for example, δ_1 to 4 layers by 1 mm $\delta_1 = 4\Delta\delta_1$. Respectively $R_1 = 4\Delta R_1$, $C_{\text{м1}} = 4\Delta C_{\text{м1}}$; δ_2 we divide/mark off into 10 layers by 2 mm. The obtained as a result of simulation temperature field in glass is shown in Fig. 6.10b.